Energy Research and Development Division
FINAL PROJECT REPORT

BIRD AND BAT IMPACTS AND BEHAVIORS AT OLD WIND TURBINES AT FOREBAY, ALTAMONT PASS WIND RESOURCE AREA

Prepared for: California Energy Commission
Prepared by: K. Shawn Smallwood

NOVEMBER 2016
CEC-500-2016-066

PREPARED BY:

Primary Author(s):
K. Shawn Smallwood
Lee Neher

Shawn Smallwood
3108 Finch Street
Davis, CA 95616
Phone: 530-756-4598

Contract Number: PIR-11-022

Prepared for:

California Energy Commission

Joe O'Hagan
Lillian Mirviss
Contract Manager

Aleecia Gutierrez
Office Manager
Energy Generation Research Office

Laurie ten Hope
Deputy Director
ENERGY RESEARCH AND DEVELOPMENT DIVISION

Robert P. Oglesby
Executive Director

ACKNOWLEDGEMENTS

This study was funded by the California Energy Commission's Public Interest Energy Research program (PIER) and by Ogin, Inc. PIER staff provided valuable logistical support, especially Joe O'Hagan and Lillian Mirviss. John Howe of Ogin, Inc. was very helpful throughout the study. The study benefitted from review comments provided by the Alameda County Scientific Review Committee (Mike Morrison, Joanna Burger, Julie Yee, Sue Orloff, and Jim Estep), and was supported logistically by SeaWest personnel followed by EDF Renewables personnel. NextEra provided additional logistic support, in particular Loan Tran and Renee Culver. Lee Neher provided GIS support and GIS analysis, and spatial data were digitized by Daniel Funderburg, Sara Michehl, Leah Neher, and Sherrity Neher. Bird carcasses were provided for detection trials by Native Songbird Care, Wildlife Care Associates, Critter Creek Wildlife, Tim Schweizer, Doug Bell, and Lindsay Wildlife Hospital. Finally, the study could not have happened without excellent field support from Joanne Mount, Skye Standish, Elizabeth Leyvas, Brian Karas, Erika Walther and Douglas Bell. Brenda Nakamoto helped with report preparation.

PREFACE

The California Energy Commission Energy Research and Development Division supports public interest energy research and development that will help improve the quality of life in California by bringing environmentally safe, affordable, and reliable energy services and products to the marketplace.

The Energy Research and Development Division conducts public interest research, development, and demonstration (RD&D) projects to benefit California.

The Energy Research and Development Division strives to conduct the most promising public interest energy research by partnering with RD&D entities, including individuals, businesses, utilities, and public or private research institutions.

Energy Research and Development Division funding efforts are focused on the following RD&D program areas:

- Buildings End-Use Energy Efficiency
- Energy Innovations Small Grants
- Energy-Related Environmental Research
- Energy Systems Integration
- Environmentally Preferred Advanced Generation
- Industrial/Agricultural/Water End-Use Energy Efficiency
- Renewable Energy Technologies
- Transportation

Bird and Bat Impacts and Behaviors at Old Wind Turbines at Forebay, Altamont Pass Wind Resource Area is the final report for the Test of Avian Collision Risk of a Closed Bladed Wind Turbine project (agreement PIR 11-022) conducted by K. Shawn Smallwood. The information from this project contributes to Energy Research and Development Division's Energy-Related Environmental Research Program.

When the source of a table, figure, or photo is not otherwise credited, it is the work of the author of the report.

For more information about the Energy Research and Development Division, please visit the Energy Commission's website at www.energy.ca.gov/research/ or contact the Energy Commission at 916-327-1551.

ABSTRACT

Wind is a clean, renewable energy resource that is expanding rapidly in California and nationwide. However, high numbers of fatal bird and bat collisions with wind turbines have led to cancellations or permitting delays for many wind energy projects. Because the likelihood of such fatal collisions depends upon complex interactions between site characteristics, turbine design, and animal behavior, the two most promising approaches to reducing collisions risks are to carefully site new wind turbines and to develop new wind turbines designs that reduce collision risk.

The original goal of this study was to test whether a new shrouded wind turbine design would reduce avian and bat collisions; unfortunately, before installation of the new wind turbines could occur, the wind project was cancelled. Following this, the researchers then analyzed the collected data to explore whether variation in fatality rates can be explained by bird and bat flight patterns and avoidance behaviors. This information was then used to map collision hazards in the study portion of the Altamont Pass Wind Resource Area to inform the siting of new and repowered wind turbines. The researchers also sought to improve collision risk estimation methods by conducting integrated trials to determine bird and bat carcass detection probabilities, assessing whether body mass can serve as a predictor of detection rate variables, quantifying species identification, and reducing estimation errors when fatality rates occur. The results of this research improve current understanding of bird and bat mortality rates at wind turbine sites and provide a template for guiding the siting of new and repowered turbines to minimize wildlife fatalities throughout the state.

Keywords: Bats, behavior monitoring, birds, California, collision hazard models, fatality rates, nocturnal monitoring, repowering, siting, wind energy, Altamont Pass Wind Resource Area

Please use the following citation for this report:

Smallwood, K. S. and L. Neher. 2016. ***Bird and Bat Impacts and Behaviors at Old Wind Turbines at Forebay, Altamont Pass Wind Resource Area***. California Energy Commission. CEC-500-2016-066.

TABLE OF CONTENTS

LIST OF FIGURES

LIST OF TABLES

EXECUTIVE SUMMARY

Introduction

As wind energy has rapidly developed, industrial-scale wind turbines have been associated with large numbers of bird and bat fatalities; therefore, there is a need for new approaches to minimizing wildlife impacts as additional wind projects are constructed or repowered. Because the likelihood of collisions depends upon complex interactions among site characteristics, turbine characteristics, and animal behavior, the two most promising approaches to reducing fatal collisions are to carefully site new wind turbines to avoid locations where bird and bat flight behaviors make them most vulnerable to collision and to develop new wind turbines designs that reduce collision risk.

This study originally focused testing whether replacing older, open bladed turbines with new shrouded wind turbines would reduce bird and bat fatalities. After three years of monitoring existing wind turbines in four portions of the Altamont Pass Wind Resource Area (APWRA), collectively referred to as the Forebay project, the developers determined that the new shrouded turbines would not be installed in the study area. Despite this, there remained a large quantity of valuable data that could be used to improve wind turbine siting and fatality monitoring methodologies.

The goals of the project were revised to:

- Develop the predictive tools needed to safely and quickly site new wind turbines in the APWRA.
- Improve field methods to increase the accuracy of fatality rate estimates.
- Explore nocturnal flight patterns of birds and bats and mammalian scavenger activities that might bear on fatality rate estimates.

Integrated Detection Trials and Fatality Estimates

Once the goals of the project changed, the objectives were revised to improving field methods for estimating fatality rates. Carcass searches have often been used to quantify the impact of existing wind turbines on bats and birds. However, a number of studies have shown that carcass searches may vastly underestimate the actual number of animals killed when detection biases are not taken into account. These detection biases result from searchers not detecting some carcasses that are present for various reasons, such as dense vegetative cover and from not detecting some carcasses due to scavenging.

This study sought to detect most of the available fatalities by performing searches at five day intervals on average; this was the briefest search interval for any searches lasting longer than two months in the APWRA.

Based on fatality rates from monitoring performed at all Forebay turbines from 2005 through 2009, 60 clusters of wind turbines were identified as having the highest fatality rates among the 403 Forebay turbines. From these 60 clusters, a random subset of clusters was selected. For each randomly selected cluster, the nearest similar-sized cluster to the control treatment was assigned to ensure replication and interspersion of treatments.

Fatality monitoring was conducted for nearly three years. Personnel experienced in fatality searches walked parallel transects separated by 6—7m and out to 50m from wind turbine pads. Each wind turbine was searched an average of every five days. All found fatalities were left in place, and repeat detections were recorded.

To address detection bias, researchers developed and tested a new integrated detection method for analyzing bird caracasses. They placed fresh frozen carcasses of 79 different bird species, ranging in size from a hummingbird to a wild turkey, at random locations within the fatality search areas on random days Monday through Friday. Carcasses were marked and placed at a rate of two per week throughout the fatality monitoring period. This new method yielded an overall detection rate that better reflects realistic carcass deposits and the ecological factors that affect detection variability in fatality monitoring.

Body mass explained most of the variation in detection rates, and emerged as a continuous predictor variable that could be applied to the typical body masses of species found in routine fatality monitoring. Compared to the earlier approach of using separate trials for estimating carcass persistence and searcher detection rates, the integrated detection trial resulted in lower fatality estimates of birds, but higher fatality estimates of bats. The integrated trial method also revealed potential biases resulting from carcasses remaining unfound beyond a single search, errors in time since death estimates, and errors in species identifications.

Fatality rates at Forebay were generally highest at barely operable wind turbines, or those that were operable no more than a third of the time. The next highest fatality rates were at wind turbines that were never operable. In fact, all of the red-tailed hawk fatalities detected in this study were caused by collisions with non-operable wind turbines. Burrowing owl fatality rates were highest at nonoperational wind turbines and lowest at the most operated wind turbines. For some species, much of the collision risk is due to the structure of the turbine rather than the moving parts.

Topography strongly influenced fatality rates; fatalities tended to be highest at wind turbines located in ridge saddles and lowest on slopes of ravines or other concave, valley-like terrain structures.

Raptor Flight Behavior

Careful siting of wind turbines is one of the principal measures available to minimize raptor fatalities caused by collisions with the turbines. This portion of the study focused on golden eagles, red-tailed hawks, burrowing owls and American kestrels. The objective was to carefully site new wind turbines to minimize the frequencies at which raptors encounter wind turbines while flying, especially while raptors perform specific types of flight behaviors, such as golden eagles flying low across ridge-like topographic features, and red tailed hawks and American kestrels hovering or kiting. To investigate how these raptors react to wind turbines, the research team developed focused behavioral surveys.

Researchers collected flight behavior data and assessed it in the context of the local terrain to develop collision hazard models for golden eagles, American kestrels, and red-tailed hawks. They established sixteen flight behavior observation stations among the Forebay sites. Data from these stations were supplemented with data gathered from 45 stations across the rest of the APWRA. Each bird was recorded onto image-based maps of the survey area to depict the bird's flight path and summarize individual bird flight behaviors. Researchers paid special attention whenever a bird came within 50m of a wind turbine and recorded the bird's approach angle to the turbine, any changes in flight direction or height, behavior, interactions with other birds, and the wind turbine's operating status. For burrowing owls, burrow locations were recorded and later related to terrain. The terrain was measured using imagery, digital elevation models, and geoprocessing. The location of each raptor was characterized by aspect, slope, rate of change in slope, direction of change in slope, and elevation; then located on a digital grid of the terrain.

For all four raptor species, annual fatality rates were estimated among individual wind turbines monitored throughout the APWRA and over various time periods since 1998. All fatality rates were adjusted for search detection, carcass persistence rates, maximum search radius, and monitoring duration.

Models were developed to predict the likelihood each grid cell would be used by golden eagle, red-tailed hawk, and American kestrel. Four collision hazard classes were created from these models, ranging from terrain least likely to be associated with a collision to the terrain most likely to be associated with a collision. The models did not focus on low lying terrain because researchers assumed that it would be avoided for wind turbine siting.

To understand patterns of fatality rates in the APWRA, fatality rate models were also developed for golden eagle and red-tailed hawk (no model was predictive for American kestrel). For burrowing owls, burrow locations were recorded and later related to terrain.

As depicted on maps of recorded flights, terrain strongly influenced bird flight paths. Over 1,000 wind turbine encounter events were recorded, and these events served as a useful predictor variable for the golden eagle collision hazard model. Other useful predictor variables for golden eagle were the number of ridge crossings, the rate of interactions with other birds, and fatality rates. For red-tailed hawks, useful predictor data included kiting, hovering, surfing flights, and fatality rates. For American kestrels, useful predictor data included kiting, hovering, and surfing flights, but fatality data were not useful. For burrowing owls, burrow locations and fatality rates were the most useful predictor variables. Collision hazard maps generally corresponded well with the spatial distribution of fatality rates depicted in the maps.

Nocturnal Behavior of Birds, Bats and Scavengers

In the first study of its kind, three years of nocturnal surveys were conducted to identify the behavior of birds, bats, and mammalian scavengers near wind turbines. Before this study, observations of flying nocturnal wildlife around wind turbines were made mostly using radar and acoustic detectors. Several studies have used radar for nocturnal surveys of passage rates and flight height; however, radar requires clear weather, and in many cases researchers are unable to identify targets to species. Acoustic detectors have often been used to identify species of bats flying within the rotor zone of wind turbines and to quantify passage rates. However, passage rates measured by acoustic detectors have yet to correlate significantly with bat fatality rates.

Thermal cameras have also been used to view flying nocturnal wildlife, principally bats; however, no precedent existed for using thermal cameras to watch nocturnal birds or mammalian scavengers.

Researchers used a thermal camera to perform 214 hours of nocturnal surveys at quarterly intervals at 14 stations to monitor nocturnal bird and other animal behavior, which provided insight into behavior that could lead to fatalities.The camera was moved 360° to pan the ground and airspace for all signs of wildlife; pausing at intervals to examine candidate targets emitting sufficient heat to represent an animal. Since the feathers of some bird species dampen heat emission, live targets of scans also were identified by detecting dark silhouettes formed by the animal's body. While some owls only emitted enough heat to be detected when facing the camera, bats were highly visible and could be seen at great distances. Weather measurements such as wind speed and temperature were recorded at the state and end of each survey. All wildlife data was recorded onto maps of the survey area as either line or point features.

The investigators observed birds colliding into both operational and nonoperational turbine structures, and many birds and bats flying close to operational turbine blades. Bats appear to be attracted to wind turbines, possibly because insects may be attracted to the heat of the turbines. Nocturnal burrowing owl behavior at night is markedly different than during the day, with many of the owls hovering dangerously close to the spinning blade tips.

The investigators mapped nocturnal mammal movement and found that carnivores such as coyotes, skunks, and badgers purposely target turbine sites, including downwind areas, in search of food. Such carnivores may also flush birds during the night in close proximity to wind turbines. These observations show that carnivore behavior may cause underestimation of fatality rates.

Rate Payer Benefits

Wind energy is playing an important role in California achieving its greenhouse gas and renewable energy goals; it is a major source of low-cost, clean energy within the state, with nearly 6,000 MWs of installed capacity in 2014, and representing over 27 percent of California's in-state renewable energy generation capacity. Permitting of such projects, however, is often delayed due to concerns over wind turbine induced bird and bat mortality. Information from this research improves our ability to understand actual mortality rates; more importantly, this research provides a template for guiding the siting of new and repowered turbines to minimize such fatalities and improve wind turbine siting and permitting in California.

CHAPTER 1: Introduction

Wind energy has been developing rapidly and has emerged as a major source of renewable energy worldwide. However, industrial-scale wind turbines have been associated with large numbers of collision fatalities of birds and bats (Smallwood 2013). One challenge going forward is to find ways to minimize wildlife impacts as additional wind projects are constructed or repowered. A variety of approaches to minimizing such impacts has been considered and implemented. Two promising approaches to minimizing collision impacts are to (1) carefully site new wind turbines to avoid the locations where birds and bats perform flight behaviors most prone to collision and (2) test the safety of new wind turbine models that possess attributes hypothesized to reduce the risk of collision. This study was originally directed toward the second approach – the testing of a new wind turbine model in a before-after, control-impact (BACI) design (Anderson et al. 1999) – but, for a reason that will be explained in the following paragraph, later became more relevant to the first approach of carefully siting new wind turbines as part of repowering.

1.1 Mixer-Ejector Wind Turbine

The new wind turbine model was developed by FloDesign, which was later renamed to Ogin, Inc. (“Ogin”). This wind turbine was rated at 100 KW, but was expected to achieve higher capacity factors than conventional 100 KW, open-bladed turbines due to its higher output per swept area, improved off-axis performance, lower cut-in speeds, and higher cut-out speeds (http://www.youtube.com/watch?v=WB5CawKfE2M). Its rotor was to be surrounded by an ejector shroud designed to speed the incoming wind for increased power generation (Figure 1). It was hypothesized that the shroud would act as a shield against birds entering the rotor plane from a parallel axis to the plane, an angle of approach that vastly increases a bird’s exposure time to blade strike (Tucker 1996a, b). It was further hypothesized that the shroud would be more visible to birds, which would offset the effect of motion smear (Hodos 2003) and reduce the likelihood of birds flying through the rotor plane on a path that was perpendicular to the rotor plane. To test these hypotheses, Ogin agreed to install its new wind turbine, called a mixer-ejector wind turbine, or “MEWT”, in a BACI experimental design. However, after three years of monitoring of the existing wind turbines during the “before” phase of the experiment, Ogin determined that it was unable to install its wind turbine. Despite the incompletion of the BACI experiment, there remained a large quantity of data that were of high value to wind turbine siting and fatality monitoring methodology.

Figure 1: Ogin’s 100 KW Mixer-Ejector Wind Turbine (“MEWT”) on a Tubular Tower, as it Appeared in the Prototype Phase

Photo Credit: Ogin, Inc.

1.2 Report Organization

Following Ogin’s determination that it could not install its MEWT, the objectives were revised from those related to testing the avian safety of MEWTs to those related to improving field methods for estimating fatality rates and to behavior data needed for preparing map-based collision hazard models that are needed for guiding the siting of new wind turbines. The field methods related to estimating fatality rates were focused on the two factors that contribute most to accuracy, which would be: (1) Detecting as many of the available fatalities as possible; and, (2) Accurately estimating the proportion of fatalities not detected during routine fatality monitoring. This study sought to detect most of the available fatalities by performing searches at 5 day intervals on average. The search interval averaging 5 days was the briefest ever achieved over any searches lasting longer than two months in the Altamont Pass Wind Resource Area (“APWRA”), so the “before” phase of the Ogin study provided an opportunity to estimate fatality rates more accurately for small birds and bats at old-generation wind turbines. This study is summarized in Chapter 2 of this report.

To more accurately estimate the proportion of fatalities not detected during routine fatality monitoring, an integrated detection trial was used instead of the typical separate trials for carcass persistence and searcher detection. This integrated trial was initially developed in a brief study in the APWRA (Warren-Hicks et al. 2013), and then further designed and, for the first time, fully implemented as part of a monitoring effort in this study. The integrated trial was intended to more realistically simulate the carcass deposition and environmental exposure that carcasses of birds killed by wind turbines typically experience. It was intended to simultaneously account for carcasses persisting longer than the periodic search interval and carcass detection probabilities changing through time due to environmental exposure, i.e., wind, rain, sun, arthropods, bacteria, growing vegetation. Related to the issue of carcasses persisting through the periodic search interval, the new approach was also intended to account for shorter search intervals providing more opportunities for searchers to find persisting carcasses. The approach consisted of placing two carcasses per week on random days of the week at random locations within the search areas, and the trial carcasses, as well as non-trial carcasses, were left in the field indefinitely.

Leaving all found carcasses in the field, whether trial carcasses or wind turbine fatalities, was another novel study method. After reviewing many reports of fatality monitoring, there emerged a concern that the ecological relationships between the scavenger community and carcasses deposited by wind turbines might be altered by the practice of removing carcasses that had been found by searchers (Smallwood 2013, Smallwood et al. 2013a). Any practice that changes the availability of carcasses to the scavenger community can also change searcher detection probabilities, and can therefore bias the results of monitoring. Another concern over the common practice of removing found carcasses was the claim that clearing searches at the beginning of monitoring periods truly cleared the search area of available carcasses, or whether it succeeded only in removing useful data while not clearing all of the available carcasses. In this study, all found carcasses were left in the field as they were found, and all subsequent discoveries were recorded as if they were found for the first time. This new practice was assessed for potential confusion caused by double-counting and for workload. It also allowed long-term monitoring of carcasses to learn under which circumstances they persisted or were found in new locations.

Due to the greater fatality detection achieved using a 5 day interval; this study provided the opportunity to compare fatality rates between wind turbines of different operability. The latter comparison bears on curtailment strategies, and whether shutting down wind turbines over prescribed periods of time might reduce or minimize avian fatality rates. Curtailment strategies have been documented to reduce bat fatalities (Baerwald et al. 2009, Arnett et al. 2011), but except for one study involving birds (de Lucas et al. 2012), evidence has been lacking on whether curtailment can effectively reduce or minimize bird fatalities. The condition of the wind turbines at Forebay were declining rapidly and an increasing number could not be repaired due to the unavailability of replacement parts. Some non-operating wind turbines were brought back into service by scavenging parts from other non-operating turbines that had not been selected for the BACI study. Thus, some wind turbines never operated, some operated in sufficient winds during all times other than the annual winter shutdown (November through February), and most operated over a portion of the non-winter periods. In this study, the wind turbines selected for the BACI experiment were monitored for operability, and for this reason fatality rates could be compared to levels of turbine operability to test whether a curtailment strategy might reduce or minimize avian fatalities.

Additional study objectives were related to the diurnal and nocturnal behavior surveys that were performed during the three years of the BACI experiment's "before" phase. Weekly diurnal behavior surveys were completed at 15 stations (Figure 2), where wind and temperature conditions were also measured. During diurnal surveys, flying birds were tracked by the observer and attributes of each flight were recorded at points that were written on handheld maps. Reported attributes included species, behavior (e.g., contouring, kiting, hovering, gliding, diving), height above ground, social associations (number of other birds flying with target bird), age class if golden eagle, and interactions with wind turbines. Since it was determined that the new turbines would not be installed, the primary objective of these behavior surveys changed to guiding the siting of new wind turbines, should new wind turbines be installed in this portion of the APWRA. This study is summarized in Chapter 3 of this report.

Smallwood performed 214 hours of nocturnal surveys at a quarterly interval at 14 stations, including 2 stations that were added to Santa Clara in April 2014. The surveys lasted 3 hours each. Smallwood recorded bats, owls, and migratory songbirds flying by wind turbines, and he recorded mammalian scavengers searching for wind turbine victims. This was the first study of its kind. This study is summarized in Chapter 4 of this report.

1.3 Study Area

The Altamont Pass Wind Resource Area (APWRA) is located approximately 56 miles (90 kilometers) east of San Francisco in the Diablo Range of Central California and covers portions of Alameda and Contra Costa Counties. See Figure 2. In 2014, there were over 3,300 turbines with an installed capacity of 462 MW in the 37,000 acre area. One of the earliest industrial scale wind energy developments in the United States, multiple studies in the APWRA have documented that substantial numbers of bts, golden eagles, red-tailed hawks, American kestrels, burrowing owls, barn owls, as well as other non-raptor species are killed each year in collisions with wind turbines (Orloff and Flannery 1992; Smallwood and Thelander 2004; ICF International 2015; Brown et al. 2013, 2014, 2015). Many of these species are protected by both federal and state wildlife legislation. Because many of the search intervals in earlier studies were too long, substantial numbers of bat fatalities were not documented until Brown et al. (2013, 2014, 2015).

There are several resasons for these high collision mortality rates at the APWRA, including, the high density of older, low power turbines, which are mounted on short towers that inadvertently positioned the blades of the turbine rotors at the height domains of most flights of golden eagle, redtailed hawk, American kestrel, and other species often killed by wind turbines, and are sited along low portions of ridge tops crests and on the slopes of canyons, which may increase the likelihood that raptors will collide with turbines. Examples of some of these older wind turbines are shown in Figure 3.

Figure 2. Map of the Altamont Pass Wind Resource Area

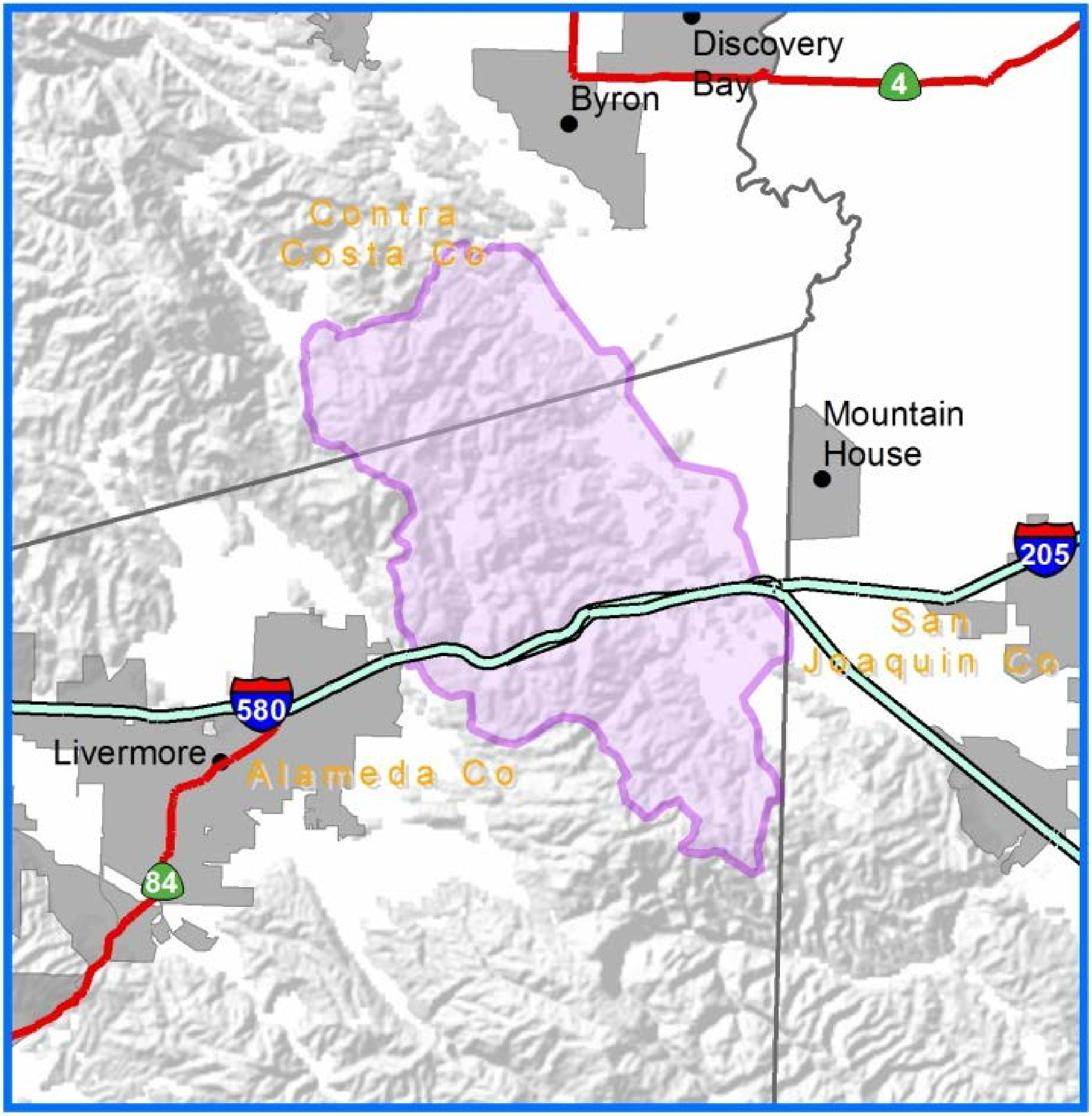

Figure 3: Wind Turbines in the Ogin Study Area Including 65 KW Micon Turbines (Top Left), 40 KW Enertech Turbine (Top Right), 95 KW Vestas Turbines (Bottom Left), and 65 KW Windmatic Turbines (Bottom Right)

CHAPTER 2:
Integrated Detection Trials and Fatality Estimates

2.1 Estimating Bird Fatalities

Since the earliest fatality monitoring at wind projects, investigators have debated field and analytical methods needed to adjust fatality estimates for the portion of fatalities that were not detected. Winkelman (1989) was likely the first to place bird carcasses in fatality search areas around wind turbines for the purpose of estimating searcher detection rates and carcass persistence rates. Orloff and Flannery (1992) placed bird carcasses in fatality search areas for the same purpose. Both Winkelman (1989) and Orloff and Flannery (1992) used a modified version of the Horvitz and Thompson (1952) estimator, which divides the number of found fatalities by the proportion of placed carcasses persisting to the next search and the proportion of placed carcasses found by searchers (of those available to be found). Gauthreaux (1995) suggested that fatality monitoring should be standardized so that results are comparable across projects. Morrison (1998) also advocated for standardization, and he recommended picking up found carcasses (a recommendation followed universally until this study). Many fatality monitoring projects ensued, along with trials to estimate searcher detection and carcass persistence rates. Smallwood (2007) identified many likely sources of error and bias in trials performed to estimate searcher detection error and carcass persistence. Smallwood et al. (2010), using remotely-triggered camera traps and fresh-frozen and thawed trial carcasses began field research into potential biases and sources of error. Investigators began in earnest to rectify the problems of bias using statistical methods (Shoenfeld 2004, Huso 2010, Bispo et al. 2010, Korner-Nievergelt et al. 2011, Péron et al. 2013, Huso et al. 2015), while Warren-Hicks et al. (2013), Smallwood (2013), and Smallwood et al. (2013) looked into improving study design and field methods. The study design that emerged has been characterized as integrated trials for estimating overall detection rates, which are then used to adjust the number of fatalities found for those not found during routine fatality monitoring.

Estimating the number of fatalities caused by a wind energy project begins with a true number of fatalities, F_T, caused by wind turbines (Figure 4). Presently, lacking remote detection of all collision events, investigators cannot know F_T, because some portion of the fatalities will not be detected by fatality monitoring. Efforts are therefore made to estimate F_T by adjusting the number of fatalities, F_A, by the number of fatalities found, F_U, and the proportion of fatalities found in carcass detection trials for which the number of trial placements, P_T, is known. The carcass detection trials are conducted in parallel to the fatality monitoring to simulate the detection probabilities associated with fatalities caused by wind turbines. Because the results of the detection trials can substantially affect the adjusted number of fatalities, F_A, it is critical that the detection trials be designed and implemented to realistically simulate the detection probabilities of wind turbine fatalities. Figure 4 depicts the steps performed in the conventional approach to simulating fatality detection probabilities (top), as well as the steps in the new integrated trials to estimate overall detection rates (bottom).

Figure 4: Comparison of Conventional Carcass Detection Trials and the New Integrated Trials for Estimating Overall Detection Rates in the Ogin Study

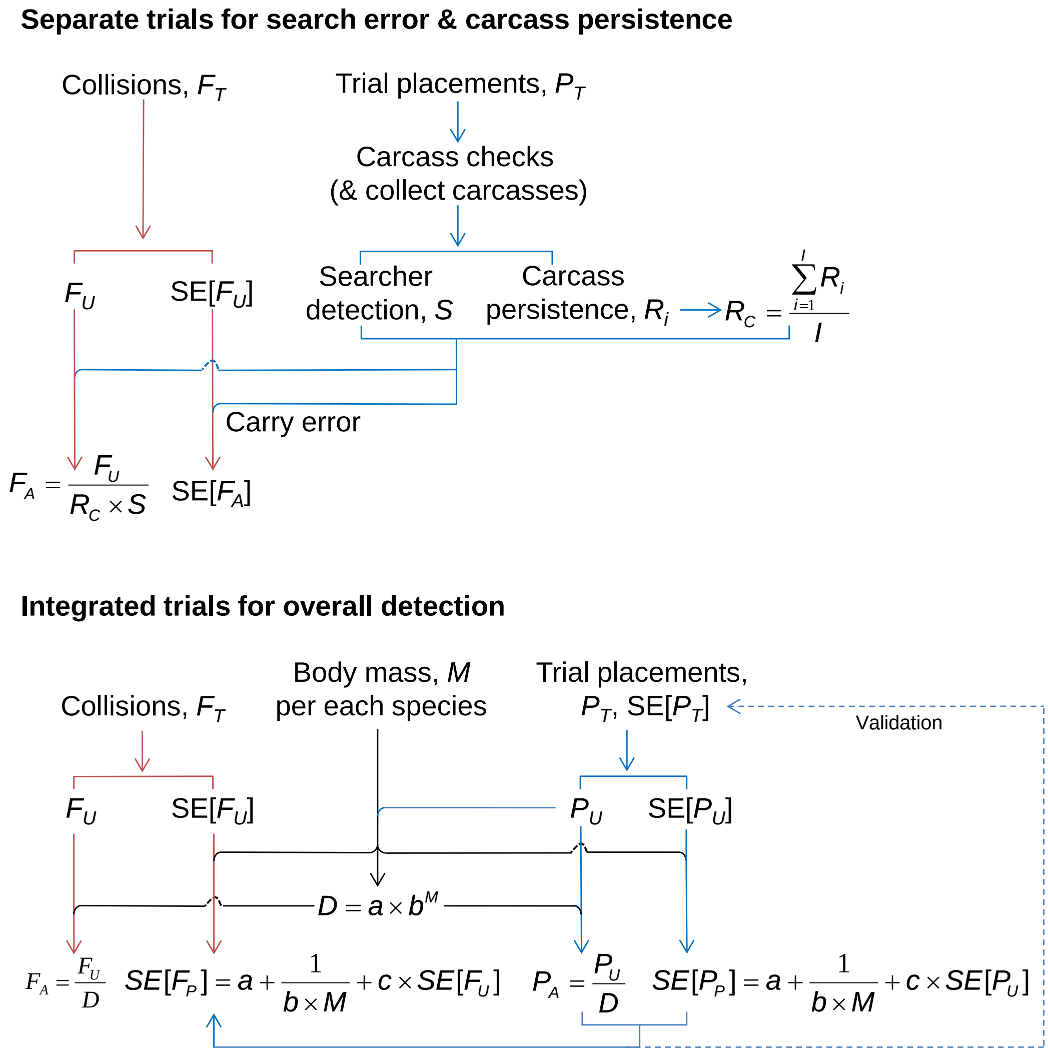

The conventional approach involves two separate trials, each with its own P_T, to estimate searcher detection rates and carcass persistence rates, where the rates are really proportions of P_T found and measured as S and R_i, respectively. Carcass persistence measured on the ith day into the persistence trial needs further treatment to account for carcasses deposited by wind turbines on additional days between the day of placements and the ith day into the trial that corresponds with the average search interval of monitoring. To do this, it is assumed that carcasses are deposited at a steady rate through a season, year, or whichever time period corresponds with the intended scope of inference of the trial. The mean daily carcass persistence rate is measured as R_C, and this proportion of P_T on the ith day into the trial that corresponds with the average search interval, I, is carried forward with S to adjust the number of fatalities found, F_U to obtain F_A. Because the detectability of carcasses changes through time due to scavenging, bacterial action, vegetation growth, and weathering, the searcher detection rate, *S*, should be treated in a similar manner as R_i leading to R_C, so in other words there should be an S_C. However, conventional trials have not attempted to estimate S_C (other than Howe and Atwater 1999), and it remains a neglected component of detection probabilities in fatality rate estimates based on the conventional approach (Smallwood 2013).

A significant challenge related to estimating fatalities is accounting for the error associated with each of the terms used to calculate F_A. There is error associated with the number of fatalities found, F_U, among the wind turbines, SE[F_U], and there is error associated with searcher detection and carcass persistence. Because the adjustment factors are proportions, error estimates are not readily available, but they can be estimated by fitting appropriate distributions to the measured proportions representing *S* and R_C and performing variance exhaustion methods such as Monte Carlo simulations. Smallwood (2013) also used the root mean square error (RMSE) of the nonlinear regression model that best fit the data representing R_i, and he used the SE of the mean among searcher detection trials conducted at wind projects with similar ground visibility. Smallwood et al. (2013) proposed treating trials as experimental units (rather than the individual carcasses intended to measure proportion found), the collection of which would yield means and standard errors going forward. Various methods have been available and tried to obtain representative measures of variance associated with R_C and *S*, but none have proven entirely satisfactory. Estimating the error associated with adjusted fatality rates has been awkward under the conventional approach.

Another significant challenge related to estimating fatalities is executing detection trials to realistically simulate the detection probabilities associated with wind turbine fatalities (Smallwood 2007). A few of the factors likely to be most influential to realistically simulating detection probabilities include (1) fatality search interval, (2) species composition, (3) lumping of species into broad size categories, (4) use of surrogate species, (5) frequency of carcass visits, (6) whether carcasses are left in the field, (7) scavenger swamping, (8) trial duration, (9) state of decomposition when deployed, and (10) the spatial distribution of trial carcasses. These factors are discussed in more detail below:

1. The fatality search interval greatly affects detection outcomes, and its affect is influenced by size of carcass. Because most bat and small bird carcasses are removed within 2 or 3 days, the longer the search interval, the greater the proportion of F_T that cannot be detected. On the other hand, the shorter the search interval, the more carcasses that are not found upon the first search since death will be available to be found during the second search or some later search. The shorter the interval, the more searches might miss a carcass that is eventually found, and this error violates the assumption that carcasses are not detected during searches subsequent to one search interval of the average associated with R_C (Korner-Nievergelt et al. 2011). In reality carcasses often persist through multiple searches, and some of these are eventually found and some are never found. Under the conventional approach, the search intervals also differ between the fatality monitoring and the detection trials, and so the detection probabilities differ. Searchers are typically tested for detection rates by placing carcasses in their search areas within 24 hours of their searches, thereby testing them on fresh carcasses even though they are routinely searching for carcasses that could have been in the field for a

week, a month, or several months. Carcass persistence trials typically involve a search interval of daily over the first week since placement, transitioning to weekly through the remainder of the trial. If the carcass remains available to be found, daily carcass checks are more likely to detect the carcass than would be a weekly or monthly interval being used by the fatality searchers (ignoring for the moment that the trial administrator also knows where the carcass was placed). In short, P_U, represented by S or R_C, poorly simulates F_U because the search intervals differ, and as search intervals lengthen, it will become increasingly difficult for P_U to simulate F_U because F_U will become increasingly unreliable and left-censored as species go undetected as fatalities.

2. The species of carcasses placed in trials should be the same species composing F_T, but the investigator will not know *a priori* the species composition of F_T, and will likely never know all of the species composing F_T because some species will go undetected throughout monitoring. One approach can be to predict which species likely fall victim to wind turbine collisions and then use carcasses of those species. The more common approaches have been to use species found as fatalities during monitoring or species readily available through research laboratories, pest control programs, or commercial vendors.

3. Lumping of species into broad categories introduces bias and uncertainty in several ways. If body size and conspicuousness influence detection outcomes, then searcher detection and carcass persistence rates can be biased high or low by placing carcasses of species on the low or high end of a size class. For example, small birds might consist of hummingbirds to mourning doves found during routine monitoring, but if the trial administrator places mourning doves, and then the trial detection outcomes will result in smaller adjustments to F_U. Similarly, it is typical to lump all bats together, even though bat species vary greatly in size and color. If bats falling victim to wind turbines range in size from a 3-g *Myotis* spp. to a 29-g hoary bat, and if the bat carcasses that are available for detection trials happen to be the more-often found hoary bats, then placing the hoary bat carcasses as trial bats will bias F_A low because the much larger hoary bats are easier to find than are the species of *Myotis*.

4. Use of surrogates to estimate detection rates of species for which trial carcasses were insufficiently available can also bias fatality rate adjustments. For the same body size, bats can be less detectable than birds because they shed no feathers and are dull in color.

5. Performing separate trials for searcher detection and carcass persistence requires extra visits to the carcasses as status checks. Not only do the carcasses need to be deployed in the trials, hence requiring a visit to the search areas, but the carcasses used in the searcher detection trial need to be checked by the administrator to confirm that they were available to be found by the searchers. Status checks must be performed on the carcasses placed in persistence trials, and these checks can number 14 or more visits, including daily checks over the first week and weekly checks thereafter (carcass check schedules have varied among studies). All of these extra visits can interfere with scavenger activity, and each increases the likelihood that the searchers will learn of the

trial or the locations of trial placements by seeing the carcass checker or by noticing sign of their visits such as tracks or depressed grass. Furthermore, the carcass checks themselves involve different detection probabilities than experienced by fatality searchers, because the administrator knows where the carcasses were placed and will search harder to find placed carcasses. Finally, extra visits for carcass checks and carcass collection will be imperfect, so they result in status outcomes associated with error that are never addressed in fatality estimation.

6. As part of monitoring that includes separate trials for searcher detection and carcass persistence, found carcasses have been collected from the field and trial carcasses have been collected at the conclusions of trials. This practice has been intended to minimize confusion between fatality finds and trial placements and to avoid double-counting of fatalities. However, collecting these carcasses can alter detection probabilities by interfering with the ecology of scavenging. In the absence of monitoring, it would be reasonable to assume that the scavenger community establishes routine search schedules and routine search patterns. These routines could be disrupted by removal of carcasses during monitoring.

7. Scavenger swamping results when too much biomass is placed at once in carcass persistence trials, thereby preventing the scavenger community from processing and removing all of the carcasses before the carcasses decompose to the point of being unattractive to the scavengers. Carcasses reaching this stage will more often last through the duration of the trial and will bias the persistence rate high.

8. Trial duration can also affect detection rates. Searcher detection trials typically expose searchers to fresh, whole carcasses, and usually only once. In reality, searchers can encounter carcasses that have been in the field since the last search or even since multiple past searches should carcasses have been missed previously. Searcher detection can change with the carcass's time in the field as vegetation grows around it and as scavenging and decomposition alter the profile and conspicuousness of the carcass. The duration of carcass persistence trials can alter mean days to removal (often used in other estimators) or proportion of carcasses remaining, because one or a few carcasses can persist over long periods.

9. Carcass condition at time of placement can also affect persistence rates, as a much greater proportion of fresh carcasses will be removed within the first few days of placement as compared to carcasses that have already decomposed over several or more days. Carcasses hosting maggots will be less attractive to most vertebrate scavengers, so the more of these types of carcasses that are placed; the more will persist over time periods that are much longer than the time periods between wind turbine collisions and removal of collision victims from the search areas.

10. Another factor that can affect trial results regardless of the type of trial used is the spatial distribution of the placements. Placements are typically randomized within the search areas, but it remains unknown how fatalities composing F_T are spatially distributed. If

wind turbine fatalities are nonrandom in their spatial deposition, then random carcass placements can result in bias. Until more is learned about the true spatial distribution of wind turbine fatalities, random placements will need to continue. A related source of bias is the practice of placing trial carcasses in special plots, outside the fatality search area. These types of placements not only inform the searchers that their special searches are tests of trial detections, thereby increasing their vigilance, but they also introduce a different suite of detection probabilities. For example, if the scavenger community routinely searches for food nearby the wind turbines, then it is less likely to do so in a special trial plot far from the wind turbines. Also, ground cover will differ.

To summarize, fatality monitoring is typically performed in parallel with detection trials, which are intended to simulate the detection probabilities associated with wind turbine fatalities. To the degree that the trials realistically simulate detection probabilities, they are used to adjust the number of found fatalities to estimate the true number of fatalities, and they are also used to estimate the error associated with the adjusted fatality estimates. This approach comes with multiple, substantial biases and sources of error, and these biases and error originate more from the design and execution of the studies than they do from the statistical treatment of the data.

The newer integrated trials for overall detection start from the same true number of collision fatalities, F_T, but diverge significantly from the conventional trials in design and execution of trial placements and carcass management. The newer approach involves three parallel series of steps, although these are integrated as part of the monitoring program. All carcasses are left in the field indefinitely, whether found as routine fatalities or as trial placements. Rather than performing separate trials for searcher detection and carcass persistence, only one set of trials is performed and trial carcasses are either found or not found by searchers. As part of this integrated trial approach for overall detection, it does not matter whether carcasses were missed due to searcher detection error or scavenger removal. Also, there is no trial duration, other than any maximum estimate of time since death that might be applied to fatality finds for inclusion in fatality estimates. To minimize the likelihood of scavenger swamping, trial carcasses are placed weekly to every two weeks in small groups, although more smaller-bodied carcasses can and should be placed than larger-bodied carcasses. At Forebay sites, 2 carcasses were placed each week on randomized days of the week.

For the newer trials, trial carcasses were obtained fresh-frozen from rehabilitation facilities and represented as many species as possible over a wide range of body sizes to better inform models of overall detection rates as functions of species' body mass within the given maximum search radius and average search interval. Prior to placement at randomized locations within the search areas, carcasses were weighed so that detection rates could be related to body mass. The resulting functions of overall detection rates on body mass were then projected to a data base on typical body mass attributed to each species occurring in the region. These overall detection rates could then be attributed to species found as fatalities by merging the data sets on species membership. (Note that this step is necessary because reliable measurements of body mass cannot be made from found fatalities, which often consist of decomposed or scavenged remains or feather piles.) This use of body mass to adjust both F_U and P_U serves as an axis of similitude between the processing of collision fatalities and trial placements, similar to the axis of similitude in the allometry of animal density, in which body mass links variation in morphometric variables to variation in ecological patterns related to species' distribution and abundance (Smallwood 2001).

Integrated trials for overall detection rates are more realistic than separate trials for searcher detection and carcass persistence. Carcasses placed in integrated trials need no additional carcass visits by the trial administrator, unless the administrator is interested in collecting additional information for hypothesis-testing in research. Furthermore, the placed carcasses in integrated trials can be treated as if they are wind turbine fatalities, including the estimation of error and in adjusting the found carcasses by overall detection rate, D. Because the number of true placements, P_T, is known and can be treated like fatality finds, the adjusted estimate of trial fatality finds can be related to the true placement rate as a validation. If the adjusted estimate of placements, P_A, correlates strongly with P_T across species, then the standard error of P_A, SE[P_A] can be predicted from D and SE[P_U], and represented as SE[P_P]. And as P_A could be related to P_T for validation, so too can SE[P_P] be related to SE[P_T]. A strong correlation between the predicted standard error and the known standard error of trial placements would justify expansion of the model to predict the standard error of the adjusted fatality rate, SE[F_P] from D and SE[F_U].

To summarize, the methods used in the integrated trials for overall detection are more likely to use fresh carcasses representing the full suite of species affected by the wind project and placed at a rate that is less likely to result in scavenger swamping. No carcass checks are required, although some carcass checks can facilitate research objectives, but regardless there are no additional detection probabilities introduced to the trials caused by administrator error, by administrators searching harder for placed carcasses than fatality searchers typically search for fatalities, or by administrators inadvertently alerting searchers to trial placements. Biases associated with trial duration are no longer factors, and the ecology of scavenging remains unaltered other than trial carcasses having been added to search areas (at least there are no removals of carcasses deposited by wind turbines).

Additional advantages of the integrated trials for overall detection include quantification of errors in searcher identification of carcasses to species and estimated time since death. The number of searches to carcass detection can be quantified, as well as the proportion and types of species never found. When well executed, these trials also account for variation in ground visibility due to vegetation cover, as well as any other variation in fatality detection encountered by the searchers, including shifts or variation in search interval. An integrated trial for estimating overall detection rates was the approach adopted for use at Forebay.

The fatality study at Forebay was originally designed to test the avian safety of Ogin's mixer-ejector wind turbine, otherwise referred to as the MEWT or shrouded turbine. Because Ogin determined that it could not install its shrouded turbine at Forebay, the study objectives shifted to testing hypotheses relevant to improving field methods for accurately estimating fatality rates. The original study design provided opportunities for testing certain hypotheses because it vastly increased detection rates of available fatalities by reducing the search interval from the typical 30 to 40 days in the APWRA (Smallwood and Karas 2009) to only 5 days, and because it employed a new integrated detection trial and left all found carcasses in place indefinitely.

These opportunities provided a much larger sample size of fatalities that could be used for hypothesis-testing and information about searcher detection that normally is not available in fatality monitoring, such as control of the variation related to time since death, estimates of time since death, species identification, and detection rates as functions of body mass. The objectives of this chapter were the following:

1. Compare fatality rates adjusted by an overall detection rate from an on-site detection trial against fatality rates adjusted by national average rates for carcass persistence and searcher detection;
2. Determine whether body mass of placed trial carcasses can explain most of the variation in detection rate, and whether body mass can serve as a useful predictor variable of detection rates;
3. Quantify error rates in species identification and estimates of time since death of placed trial carcasses; and,
4. Test in the field the feasibility of leaving all found carcasses in place, undisturbed.

2.2 Methods

2.2.1 Experimental Design

The fatality study was designed to maximize the likelihood of detecting an effect of the MEWT on avian collisions. To do this, four years of fatality monitoring data were used to identify the wind turbines associated with the highest rates of found bird carcasses. The fatality monitoring data had been collected by the Alameda County Avian Monitor from 2005 through 2009. The fatality rates calculated from this monitoring effort were not adjusted for searcher detection error or carcass persistence rates because they were only intended to characterize the numbers of bird carcasses actually found for the purpose of identifying the most hazardous wind turbines. The subset of turbines selected for the BACI study averaged 4.5 times more native bird fatalities/MW/year than at the rest of the turbines in the study area. These wind turbines were then assigned to a MEWT replacement treatment and a control treatment, and the treatments were replicated and interspersed (Figure 5A, 5B, 5C, Table 1). Based on these fatality rates, 60 clusters of wind turbines were identified as having the highest fatality rates among the 403 Forebay turbines. The highest fatality rates were desired for use in the experiment so that sample sizes would be large and the likelihood of detecting an effect would be greater. From these 60 clusters, a random subset of clusters were selected to be replaced by MEWTs following the "before" phase of the BACI monitoring. For each randomly selected cluster in the replacement treatment, the nearest, similar-sized cluster to the control treatment was assigned (Table 1). This approach ensured interspersion of treatments. Some adjustments were necessary due to wind turbines having been removed on the recommendations of the SRC. Where originally selected wind turbines had been lost, other turbines within the same turbine row and adjacent to the originally selected turbines were selected to replace the missing turbines. In one case, an entire row of wind turbines had been emoved, so the high-fatality cluster nearest to this string -- thenext string to the west – was selected. The turbines selected for replacement by

MEWTs totaled 4.04 MW, the turbines selected for the control treatment totaled 4.305 MW, and the remainder of the non-monitored turbine community totaled 14.25 MW.

Figure 5A: Study Turbines at Mountain House, Forebay

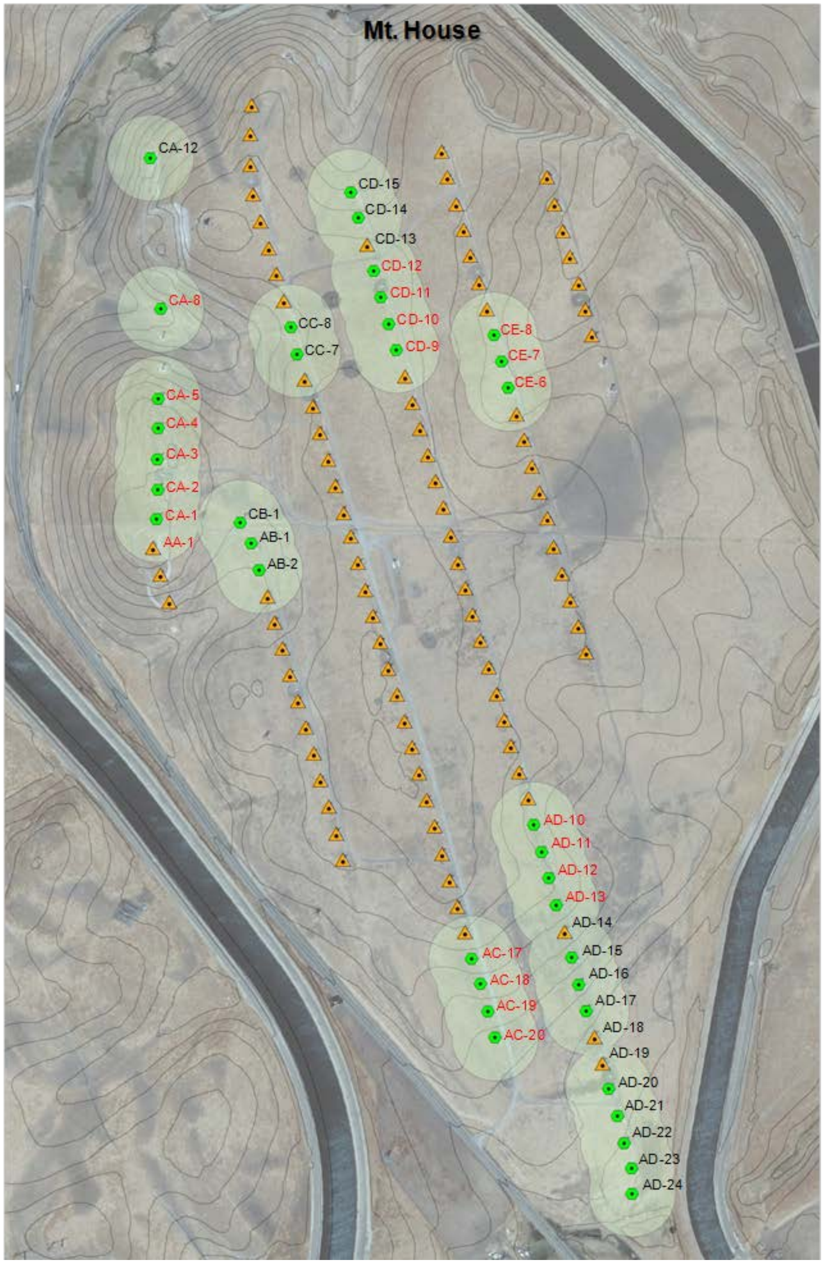

Study turbines with red labels = replacement; and black labels = control treatments at Taxvest project near Mountain House, Forebay

Figure 5B: Study Turbines at Midway Road, Forebay

Midway

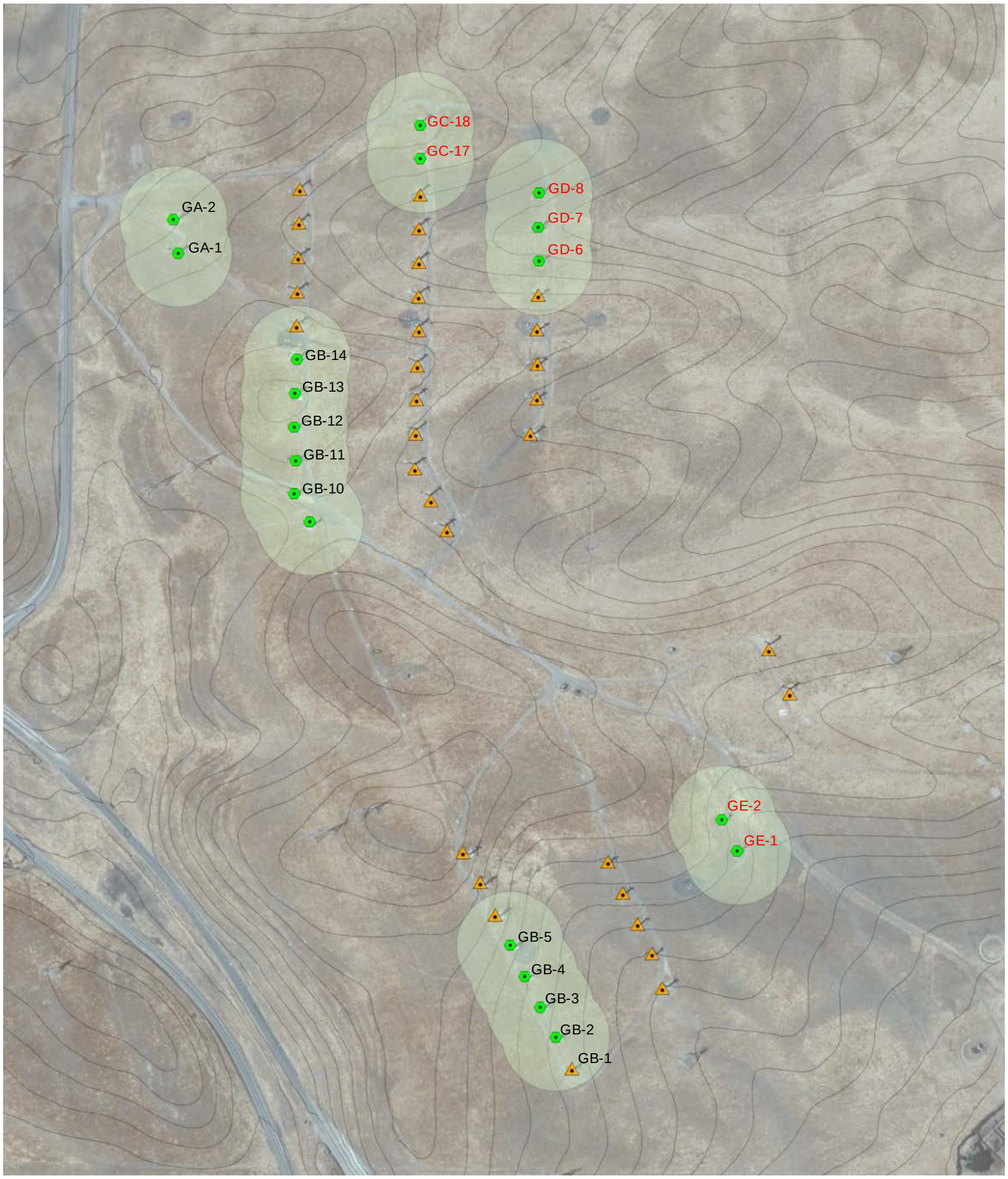

Study turbines with red labels = replacement and black labels = control treatments at Taxvest project off Midway Road, Forebay

Figure 5C: Study Turbines at Gate 11 and Venture, Forebay

Gate 11 and Venture

Study turbines with red labels = replacement; and black labels = control treatments at Altech 1, Viking, Swamp and Venture Wind projects composing Forebay

Table 1: Original Experimental Treatment Design at Forebay Sites

Random order	Treatment	String	Turbine addresses	MW	MEWTs	Notes
1	Replace	191	GE-1, GE-2	0.130	1	
2	Replace	204	WM-26, PO-33 to PO-38	0.455	5	
3	Replace	165	H-5, H-6	0.080	1	
4	Replace	199	WM-1, WM-2	0.130	1	
5	Replace	164	F-5, F-6	0.080	1	
6	Replace	182.2	CD-9 to CD-12	0.130	1	
7	Replace	170	K-3 to K-6	0.160	2	
8	Replace	201	WM-14 to WM-21	0.325	3	3 turbines removed
9	Replace	188	GD-6 to GD-8	0.195	2	
10	Replace	178.2	CA-6 to CA-8	0.195		2 turbines removed
10A	Replace	178.2	CA-3 to CA-8	0.260	3	Replaced group 10
11	Replace	182.1	AD-10 to AD-13	0.260	2	
12	Replace	168	J-3	0.040	1	
13	Replace	184	CF-6 and CF-7	0.130		Turbines removed
13A	Replace	183.2	CE-6 to CE-8	0.195	1	Replaced group 13
14	Replace	153	VK-15	0.065	1	
15	Replace	156	TV-1 to TV-5	0.325	3	
16	Replace	174	O-5, O-6, N-1 to N-3	0.160	2	1 turbine removed
17	Replace	161	D-1 to D-3	0.080	1	1 turbine removed
18	Replace	181.1	AC-17 to AC-20	0.260	3	
19	Replace	159	D-9 to D-12	0.160	2	
20	Replace	187	GC-17 to GC-18	0.130	1	
21	Replace	168	J-5 to J-6	0.080	1	
22	Replace	178.2	AA-1, CA-1, CA-2	0.195	2	
23	Replace	170	M-8 to M-10	0.120	1	
24	Replace	170	L-10 to L-12	0.120	1	
25	Replace	205	VK-1 to VK-2	0.130	1	

Random order	Treatment	String	Turbine addresses	MW	MEWTs	Notes
26	Replace	181.2	CC-11 to CC-13	0.195	2	
27	Replace	183.2	CE-1 to CE-3	0.195	2	
28	Replace	157	VTR-10 to VTR-11	0.130	1	
29	Replace	161	E-4 and E-5	0.080	1	
30	Replace	171	M-6, L-1, L-2	0.120	1	
1	Control	189	GB-2 to GB-5			
2	Control	203	WM-25, PO-27 to PO-32			1 turbine removed
3	Control	162	G-2 to G-6			
4	Control	162	F-7			
5	Control	162	G-11, G-12, F-12			
6	Control	182.2	CD-14, CD-15			
7	Control	171	N-9 to N-12			
8	Control	200	WM-3 to WM-10			1 turbine removed
9	Control	186	GB-9 to GB-14			1 turbine removed
10	Control	179	CA-12			
11	Control	182.1	AD-20 to AD-24			
12	Control	172	O-9 to O-12			
13	Control	181.2	CC-7 and CC-8			
14	Control	153	VK-7			
15	Control	175	O-1 and O-2			
16	Control	155	VK-24 to VK-26			
17	Control	161	D-6 to D-8, E-1			
18	Control	182.1	AD-15 to AD-17			
19	Control	171	N-4 to N-6			
20	Control	185	GA-1 and GA-2			
21	Control	164	F-1 and F-2			
22	Control	180.1	CB-1, AB-1, AB-2			
23	Control	169	I-1 to I-3			
24	Control	170	L-7 to L-9			

Random order	Treatment	String	Turbine addresses	MW	MEWTs	Notes
25	Control	153	VK-5 and VK-6			
26	Control	183.2	CE-6 to CE-8			
27	Control	183.2	CC-15 and CC-16			
28	Control	154	VK-22 and VK-23			
29	Control	160	E-6 and E-7			
30	Control	157	VTR-6			

The first 22 groups selected in random order would total 40 MEWT replacements, and the next 8 groups selected would total 50 MEWT replacements (It was planned to use 40 MEWTs).

2.2.2 Fatality Monitoring

Fatality monitoring began on 3 April 2012 at all of the replacement and control treatment sites and continued through 31 March 2015, although monitoring results reported herein were through 16 February 2015. On 21 April 2014 another 35 wind turbines (3.325 MW) were added to the search rotation in the Santa Clara project, and these were also monitored through 31 March 2015. Personnel experienced in fatality searches walked parallel transects separated by 6-7 m and out to 50 m from wind turbine pads. Each wind turbine was searched an average of every 5 days. All found fatalities were left in place, and repeat detections were recorded. Searchers recorded the species found, body parts, evidence of injury, estimated time since death, and position using a Trimble GeoXT GPS. Searchers took a photo of the carcass, and recorded the nearest wind turbine address. Searchers also recorded the dates of all fatality searches at all wind turbines involved in the study.

Searchers recorded fatalities found beyond the search radius whenever such fatalities were detected during routine searches. Fatalities found outside the search areas but not during a search were also recorded, but these were identified as incidentals. Incidental finds were included in fatality estimation when found at monitored wind turbines (few, if any, were found this way), but they were not included if found at non-monitored wind turbines.

Searchers estimated the number of days since death of each carcass, including a low and a high estimate. These estimates of days since death were later used to test the accuracy and precision of time-since-death estimates that were applied to detection trial carcasses, because thresholds of time since death are often established in fatality monitoring programs to decide whether fatality finds should be included in fatality estimates. There have also been proposals to develop fatality rate estimators around estimates of time since death, so it was useful to establish whether such estimates can be made with sufficient accuracy and precision.

Searchers identified carcasses to species when possible, and when not possible they identified the carcasses to the nearest possible taxonomic group or size class (small, medium, large). These identifications applied to detection trial carcasses enabled quantification of the accuracy of species identifications. Because all carcasses were left in the field as found, it was also possible to monitor the accuracy in species identifications through time, although some portion of the monitored trends in species identifications will have been influenced by the searchers' memory of which species was attributed to many of the carcasses, especially the larger or more charismatic species. With this potential bias in mind, the searchers were asked to identify the carcass as if they were seeing it for the first time. For example, had the carcass been identified as a red-shouldered hawk initially because the entire carcass was available and only a day since death, but two months later only matted body feathers remained, and then the searchers were expected to identify the carcass based on what they saw on the ground at the moment and not two months earlier. Given matted body feathers and nothing else to identify the remains, the searcher would record the fatality as a large raptor because the searcher would know that that level of identification would have been the best she could have done had she seen the remains for the first time. Often, however, the searcher would also record her memory of the species identification in the notes section of the Trimble GeoXT GPS data recorder.

2.2.3 Detection Trials

Two fresh frozen bird carcasses were placed each week on random days between Monday through Friday and at random locations within the search areas around wind turbines, averaging 2.3 g/ha/year of bird mass. The searchers were blind to these placements unless and until they found the carcasses. Carcasses of 79 species were placed, ranging in size from hummingbirds to wild turkey. The carcasses were obtained from rehabilitation centers, and were known to have been frozen immediately after death and to not pose any chemical or physical risk of injury to scavengers. Each carcass was marked by clipping wing and tail feathers and wrapping a small strip of black electrical tape or plastic zip-ties around each leg. Excess plastic was cut from the zip-ties and the cut edges filed to minimize risk of injury to scavengers. Similarly, only small strips of electrical tape were wrapped around legs, and excess tape trimmed away (Figure 6).

Figure 6: Red-Shouldered Hawk Carcass Marked and Placed in Integrated Detection Trial

Photo Credit: K. Shawn Smallwood

Trial carcasses were dropped from shoulder height and the disposition of each carcass was subsequently unaltered by study personnel. Data recorded for each carcass placement included date, time, turbine address, distance and bearing to turbine; species, body mass (g), age class, gender; whether slight, modest or no signs of desiccation; carcass source, transporter, and who placed it; whether partial, high, or no occlusion due to vegetation, rocks, burrows or other; whether the aspect facing upwards from the placement site was ventral, dorsal, or lateral; distances (m) in 3 directions (toward or away from turbine, and tangential to turbine in opposite directions) from placement site before carcass no longer recognizable as a carcass; whether placed in grassland, reclaimed turbine pad, gravel pad, gravel access road, cut bank, or other; and any relevant notes (Appendix 1).

All trial carcasses and all wind turbine-caused fatalities were left undisturbed where found, and their status was monitored as they were encountered during routine fatality monitoring. Searchers recorded the locations and attributes of all found carcasses using a Trimble GeoXT GPS, and they delivered the data to the trial administrator (Smallwood) weekly. Searchers described carcass remains and noted those marked as trial carcasses, and this information helped the trial administrator track all carcasses throughout the study. After 256 trial carcass placements over 2.5 years, logistic models were fit to detection rates, D, as functions of $\log_{10}$Body mass, X.

Also, placed trial carcasses were mapped by Smallwood using a Trimble GeoXT GPS as soon after placement as possible. The status of the placed carcasses was recorded at this time onto data sheets (Appendix 2). Status information included Date, time, trial carcass identification number, wind turbine address, distance and bearing to turbine, species, whether flight feathers were edged or frayed, whether body feathers were fluffy or matted, whether feathers were original, faded, or bleached in color, whether the remains were being visited by maggots, beetles, ants, flies, or grasshoppers, whether the remains were intact or the specific body parts were identified, and any notes that were relevant or that would help the trial administrator find the carcass for an additional status check.

2.2.4 Fatality Rate Adjustments

Prior to this study, the standard fatality rate estimator used in the Altamont Pass WRA was a variation of the Horvitz and Thompson (1952) estimator, which was the following (also see Figure 4):

$$F_A = \frac{F_U}{S \times R_C \times d},$$

where F_A and F_U were adjusted and unadjusted fatality-rate estimates (Fatalities/MW/year), respectively, S was the search detection rate expressed as the proportion of available carcasses that were found during a search detection trial, R_C was the carcass persistence rate expressed as the average proportion of carcasses remaining at the time of the next periodic search, and d was the average proportion of carcasses found beyond the maximum search radius among the carcasses predicted to be available based on a model fit to the cumulative number of carcasses found at increasing distances from wind turbines monitored across North America (Smallwood 2013). Averages from trials performed across North America typically represented S, R_C, and d to lessen the chance of deriving anomalous adjustment values from one study.

In this study, a new version of the Horvitz and Thompson (1952) estimator was used (also see Figure 4):

$$F_A = \frac{F_U}{D \times d \times A},$$

where A was the proportion of the search area that was actually searched (values <1 applied only to turbines occurring within the 50-m search radius of the experimental turbines selected for this study), D was the proportion of placed carcasses in the integrated detection trial that was predicted to be detected by searchers performing routine fatality searches, and all other terms were as defined above. The new term, D, was the overall detection rate and replaced R_C and S in the earlier version of the estimator. The source of the overall detection rate in this study was the 256 placed carcasses that were placed weekly throughout routine monitoring. These carcasses were divided into body mass classes so that detection rates could be related to body mass and a predictive model estimated for use against fatality finds that vary widely in body size. Several approaches for establishing the body mass classes were taken because no precedent was available for deciding which approach to use, and it needed to be established whether and to what degree the resulting models were robust to the classification of body mass.

In one approach for classifying carcasses into body sizes, natural breaks were used. In another approach, carcasses were sequentially ordered from lightest to heaviest, and every 16 carcasses in sequential order formed a body mass class. In the three other approaches, the size range of body size classes was increasingly doubled from starting ranges of 0-4 g, 0-6 g, and 0-10 g.

Based on all five approaches, the proportion of placed carcasses that were detected was related to the average $\log_{10}$-transformed body mass in each size class using least-squares regression analysis. The predicted proportions from this model, *D*, were then used to adjust the fatality rates of species found during routine fatality monitoring.

Fatality rate estimates were compared between the two estimators summarized above. The national averages that were used in this comparison were the following: searcher detection rates of 0.492 (SE = 0.060) for bats, 0.603 (SE = 0.037) for small birds, 0.800 (SE = 0.031) for medium-sized birds, and 0.886 (SE = 0.030) for large birds. National average carcass persistence rates were relied upon for the associated carcass size class at an average 5 day search interval in the BACI monitoring, which were 0.61 for bats and small birds, 0.73 for medium- and large-sized birds, 0.80 for rock pigeons, and 0.865 for birds larger than 1 kg. For the proportion of carcasses found within the search interval of 50 m at wind turbine tower heights ranging 18.5 m to 24.6 m, the national average of 0.92 (SE = 0.186) was used (Smallwood 2013).

2.2.5 Simulated Fatality Estimates from Trial Placements

The integrated detection trial approach offers an opportunity to examine fatality rate estimates at wind projects in a manner that never before existed (Figure 4). For the first time, fatality rate estimates can be simulated using the detection trial data intended for estimating the proportion of fatalities not found during routine monitoring. Detection trials are intended to simulate the detection probabilities associated with wind turbine fatalities so that one can estimate and adjust for the proportion of fatalities not found during routine monitoring. Detection probabilities are affected by species, carcass size, carcass persistence, time between placement and first subsequent search, carcass condition upon first and later subsequent searches, vegetation conditions, seasonality, inter-annual variation in scavenger activity, and potentially multiple additional factors. This study's integrated detection trial methodology more realistically simulates these probabilities than conventional trials by adding carcasses to the search area at frequent intervals throughout the monitoring period and by leaving the carcasses in the search areas as if they were fatalities that could be found upon the first search or upon a later search. This methodology not only allows one to estimate the proportion of undetected fatalities with a lower degree of pseudoreplication, but it also allows one to treat the placed carcasses as if they were actual fatalities. By pretending that the placed carcasses were actual fatalities, one can estimate a faux fatality rate, referred to as the true placement rate, P_T, the unadjusted placement finds, P_U, and the adjusted placement finds, P_A (Figure 4).

The placement rate is measured without error. Ideally, the only variation in the measured rate will be the variation in placements among wind turbines due to randomization, the trial administrator's decision about which trial bird (species, age class, size, condition) to place at each randomized location, and the degree to which days intervening searches are randomized for trial placements. The main point here is that, contrary to the true fatality rates, the placement rates are known and can be compared to the adjusted placement find rates as a validation of the accuracy of the estimates.

To simulate fatality estimates, placed birds served as the placement population from which was calculated the known placements/MW/year. The found placements were used for estimating the placement population by dividing the numbers of found placements by the overall detection rate (D) applied to the typical body mass of the species found. For this analysis, there was no need to adjust placement find rates for maximum search radius bias (d) because all placed carcasses were within the maximum search radius and there was no comparison being attempted between this project and other projects involving different maximum search radii or tower heights.

One of the goals of this analysis was to develop models to predict standard error of the mean placement rates, so that these models can be used to predict the SE of the adjusted fatality rates associated with wind turbines. After all, the detection trial was intended to simulate the detection probabilities associated with fatalities attributed to wind-turbines to enable estimation of the proportion of fatalities not found during monitoring. If the trial simulation is sufficiently realistic, then predictive models of the SE of trial fatality estimates ought to predict the SE of the fatality estimates.

As in Figure 4, the SE of the unadjusted trial fatality rate, SE[P_U], and body mass (g) typical of the species, M, were used to predict the SE of the adjusted trial fatality rate, SE[P_P] for birds placed at turbines searched every 5 days on average:

$$SE[P_P] = a + \frac{1}{b \times M} + c \times SE[\mathrm{P}_U]$$

Once the parameter values, a, b, and c, were optimized using simplex and quasi-Newton methods to search parameter space in nonlinear regression analysis (judged by minimizing root-mean square error, RMSE, and maximizing the coefficient of determination, r^2), and once it was confirmed that the predicted standard errors correlated strongly with the estimated standard errors among the trial data, then the models were applied to the wind turbine fatality data to predict the SE of the adjusted fatality rates:

$$SE[F_P] = a + \frac{1}{b \times M} + c \times SE[F_U]$$

So long as the integrated detection trial reasonably simulates actual fatality detection probabilities, the extension of the model to predict SE among the trial data should be suitable for projection to the wind turbine fatality rate. If SE of the adjusted fatality rate scales with body mass as expected, then body mass can serve as an axis of similitude between the two types of data (trial placement finds and wind turbine fatality finds). The pattern of finds among wind turbines should also influence SE, which is why SE of the unadjusted fatality finds is included in the models.

2.3 Results

2.3.1 Integrated Detection Trials

Body mass explained most of the variation in detection rates, no matter how detection rates were binned by body mass (Figure 7). All the models fit the data well enough for use in adjusting fatality rates, but the classification of carcasses based on doubling the size ranges achieved the largest coefficients of determination, and the doubling strategy that began from the 0-10 g size range achieved the smallest root mean square error (RMSE), so this was the model used in this study. Some of the remaining variation could be explained by the time between carcass placement and discovery, with longer times to discovery resulting in lower detection rates (Figure 8).

Figure 7: Number of Trial Carcasses Found

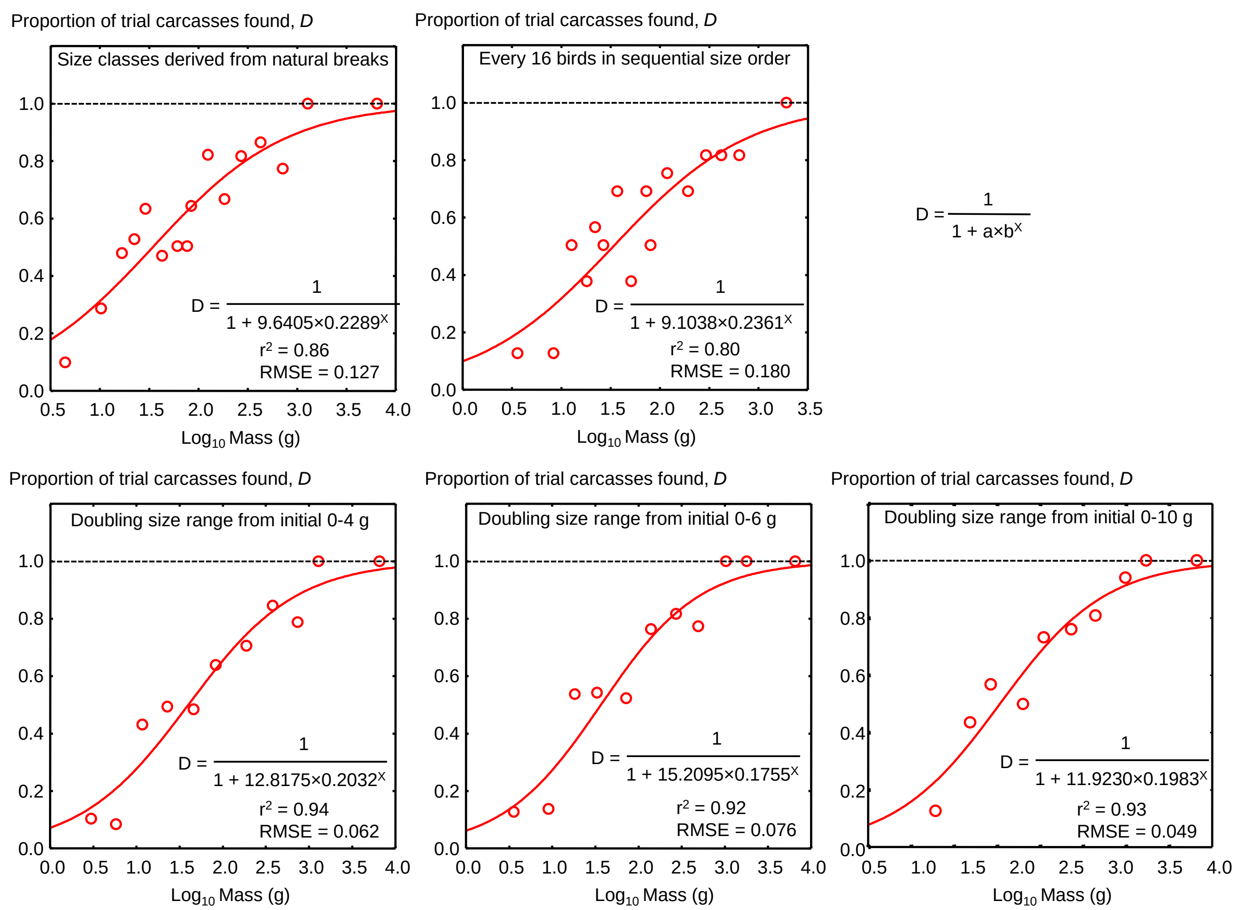

The proportion of trial carcasses found as logistic functions of log10 body mass, and whether body mass classes were derived from natural breaks (top left), every 16 trial carcasses in sequential order of body mass (top right), or doubling of size ranges from initial starting ranges of 0-4 g, 0-6 g, and 0-10 g (lower left, middle, and right, respectively).

Figure 8: Residuals of Overall Detection Rates

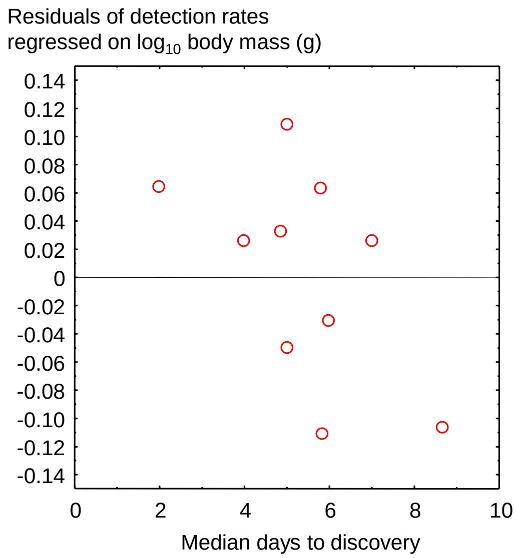

Regressed on log10 body mass (g) of 256 bird carcasses that were placed in integrated detection trials as part of the Ogin study and binned into 10 size ranges, which sequentially doubled in range from an initial range of 0-10g.

The residual variation in overall detection rates regressed on body mass was slight, but it did suggest a few meaningful patterns related to other variables (Figure 9). In relation to distance until the carcass was no longer visible, fewer trial birds tended to be detected when these distances were shortest, although detections also averaged fewer for carcasses that were visible for long distances. Detections tended to peak at 25 to 34 m from the turbine row (string) (Figure 9), perhaps because that distance range happened to more often overlap access roads. Detections tended to be lower in June as compared to other months of the year (Figure 9), probably due to tall grass falling over onto placed carcasses at this time of year. Detection rates also tended to peak when placed within a day of the next fatality search, and generally declined with number of days between placements and the next fatality search (Figure 9.)

Fifty-eight percent (n = 148) of placed birds were found, of which 57.4%, 15.5% and 9.5% were found upon 1st, 2nd, and 3rd searches following placement, respectively, and the remaining 17.6% were found upon the 4th through 121st searches (Figure 10). The average number of searches per 1st detection was 4.3, including 2.5 searches per 1st detection (median = 1.5) for birds weighing ≤10 g, 9.3 searches per 1st detection (median = 2) for birds weighing 10.1 to 20 g, and decreasing numbers of searches with increasing body mass.

The searchers found 57 (72%) of the 79 species placed, meaning that 28% of the species placed were never detected. Carcasses of another 25 species (32%) were found but misidentified. These misidentifications were made to Anna’s hummingbird, orange-crowned warbler, Wilson’s warbler, lesser goldfinch, black phoebe, western bluebird, dark-eyed junco, Black-headed grosbeak, pine siskin, fox sparrow, golden-crowned sparrow, Downy woodpecker, hermit thrush, Swainson's thrush, spotted towhee, California towhee, red-winged blackbird, western meadowlark, Brewer's blackbird, northern mockingbird, Eurasian collared-dove, northern saw-whet owl, green-winged teal, American coot, and peregrine falcon. Most of these misidentified species were very small. Found carcasses were also incorrectly identified to 6 species (8%) that were not placed, including violet-green swallow, yellow-rumped warbler, mountain bluebird, Say's phoebe, common poorwill, and burrowing owl. Another found carcass was misidentified as a fox sparrow, although this species had been placed but the found fox sparrow had been misidentified. In the end, and even though the fatality search interval averaged only 5 days, the fatality searchers were unable to detect 47 species, or 59% of the species placed in the integrated detection trial, and they added another 6 species that were not placed in the trial.

Of the 148 placed birds found, searchers correctly identified 56% to species, 9.5% to a larger taxonomic group, 24% to a size category, and 9.5% to a wrong species, and the average time preceding these errors were 7, 19, 23, and 47 days, respectively.

On average searchers overestimated time since death by 9 days (90% CI = 6 to 11 days) for 18 carcasses found 0-7 days since placed, by 12 days (90% CI = 7 to 18 days) for 101 carcasses found 8 to 14 days since placed, by 20 days (90% CI = -1 to 41 days) for 21 carcasses found 15 to 28 days since placed, by -1 days (90% CI = -22 to 19 days) for 7 carcasses found 29 to 90 days since placed, and by -74 days (90% CI = -211 to 63 days) for 5 carcasses found 140 to 595 days since placed (Figures 11 and 12). The negative values mean that time since death was underestimated.

2.3.2 Simulated fatality estimates from trial placements

Adjusted rates of found trial carcass placements, P_A, correlated strongly with known rate of trial carcass placements, P_T, although the regression slope was about 0.75 rather than the expected 1.00 (Figure 13). Adjusted detection rates of placed bird carcasses were less than proportional to the placement rates of bird carcasses, perhaps meaning that the more a species was placed in trials, the smaller the proportion of the species was found. Another possible reason for a regression slope of about 0.75 was that the adjustment factor introduced a bias. Even with a bias, the strong correlation between the adjusted rate of found placements and the known placement rate was encouraging. The slope of 0.75 needs further investigation, including whether it can be used to further adjust fatality rates.

The predicted standard errors associated with adjusted mean rates of found placements also correlated strongly with the known standard errors associated with placements (Figure 14), thereby justifying the projection of the model used to predict standard error of placed birds to also predict the standard error of fatality finds. The model used to predict SE[P_A] was the following (R^2 = 0.89, RMSE = 0.115):

$$\boldsymbol{SE[P_A] = -0.1313 + \frac{1}{1.0738 \times M} + 4.6431 \times SE[P_U]}$$

The model was based on the first two years of trial placement data, as the third year appeared to differ (Figure 14).

Figure 9: Patterns of Detection Residuals

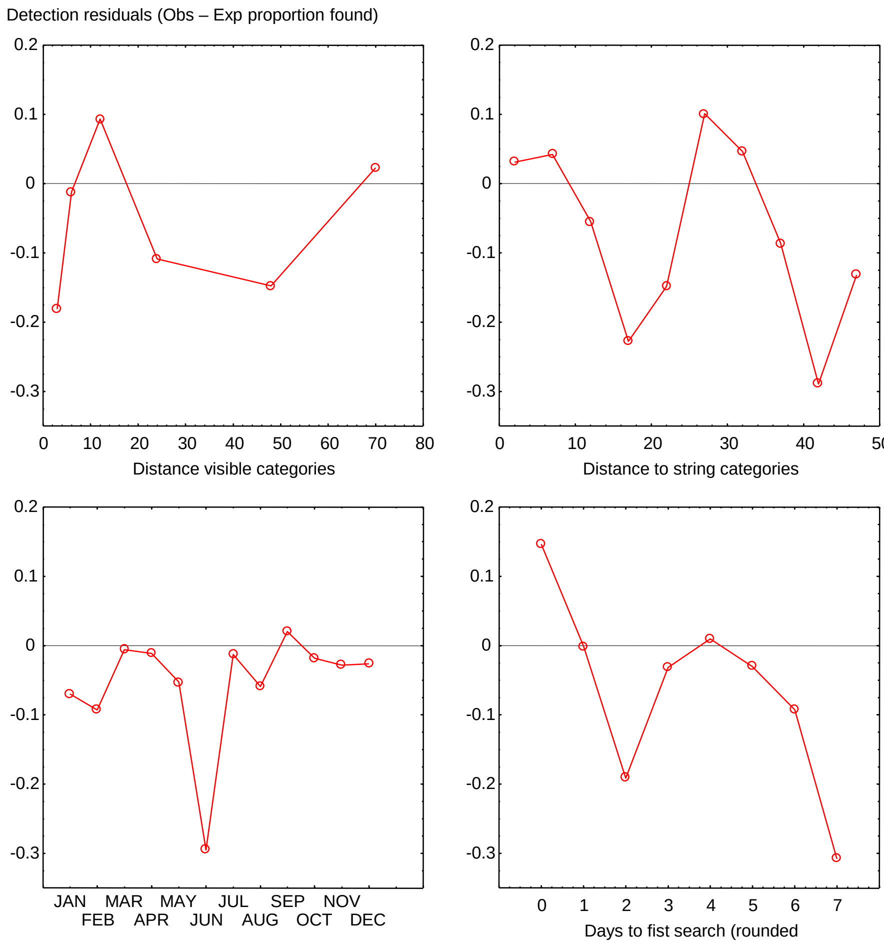

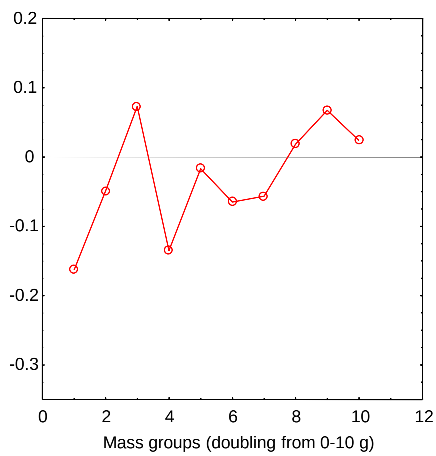

Category	Distance to string (m)
2	0-4
7	5-9
12	10-14
17	15-19
22	20-24
27	25-29
32	30-34
37	35-39
42	40-43
47	45-57

Category	Distance visible (m)
3	0.0-3.0
6	3.1-6.0
12	6.3-12.0
24	12.6-24.0
48	24.3-48.0
70	49.0-70.0

Measured as overall detection probability, D, minus fatality search outcomes among placed bird carcasses at Forebay, July 2012 through March 2015.

Figure 10: The Mean Number of Searches per Detection

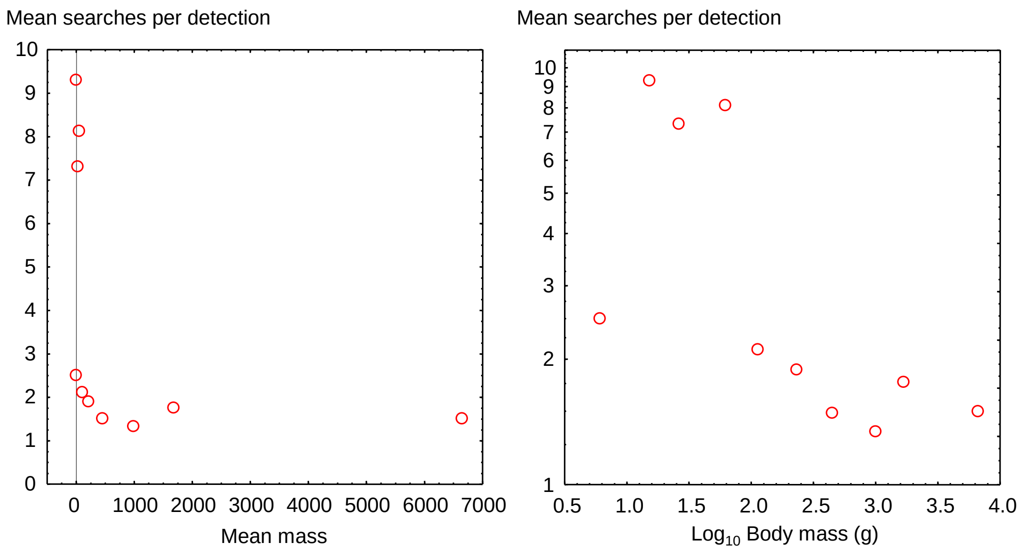

The number is related inversely to average body mass of trial birds within 10 ranges of body mass that increasingly doubled from an initial range of 0-10 g, based on 256 trial carcasses used in the Ogin study; Very small birds required many more searches to be discovered than did very large birds.

Figure 11: Searchers Over-Estimated Time Since Death

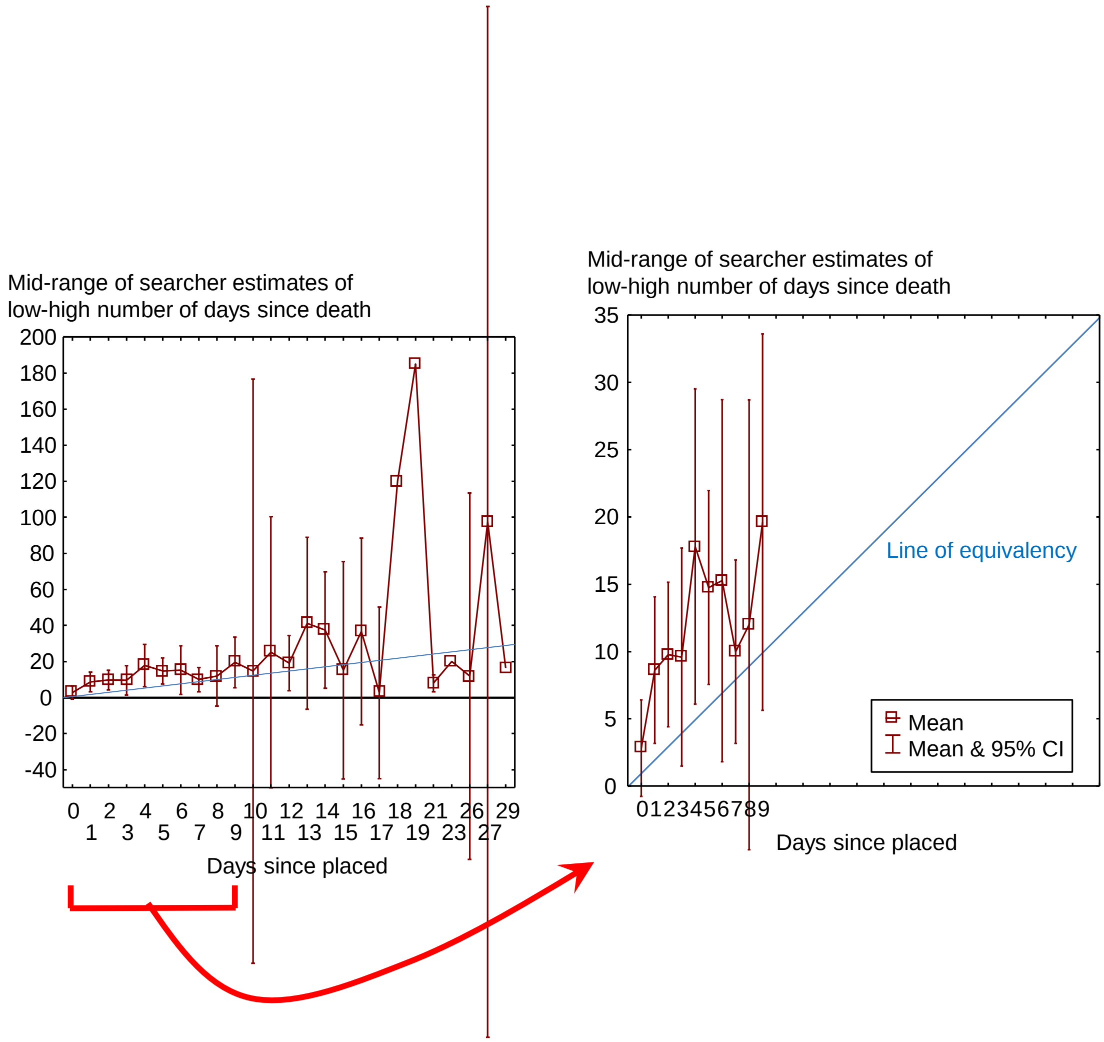

Found trial carcasses through 9 days and longer, and variation in time-since-death estimates increased greatly from 12 days.

Figure 12: Estimated Days of Time Since Death

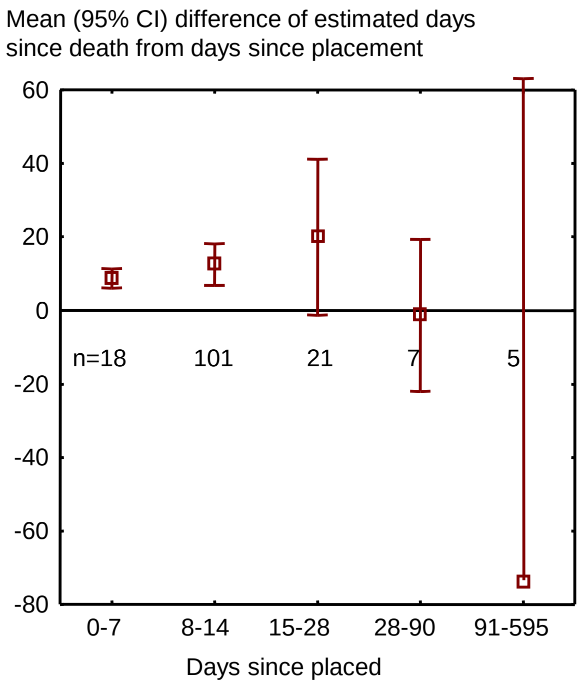

Searchers increasingly overestimated time since death of placed trial carcasses through 28 days since placement, after which time searchers tended to underestimate time since placement and the variation in errors increased substantially.

Figure 13: Adjusted Rates of Found Placements

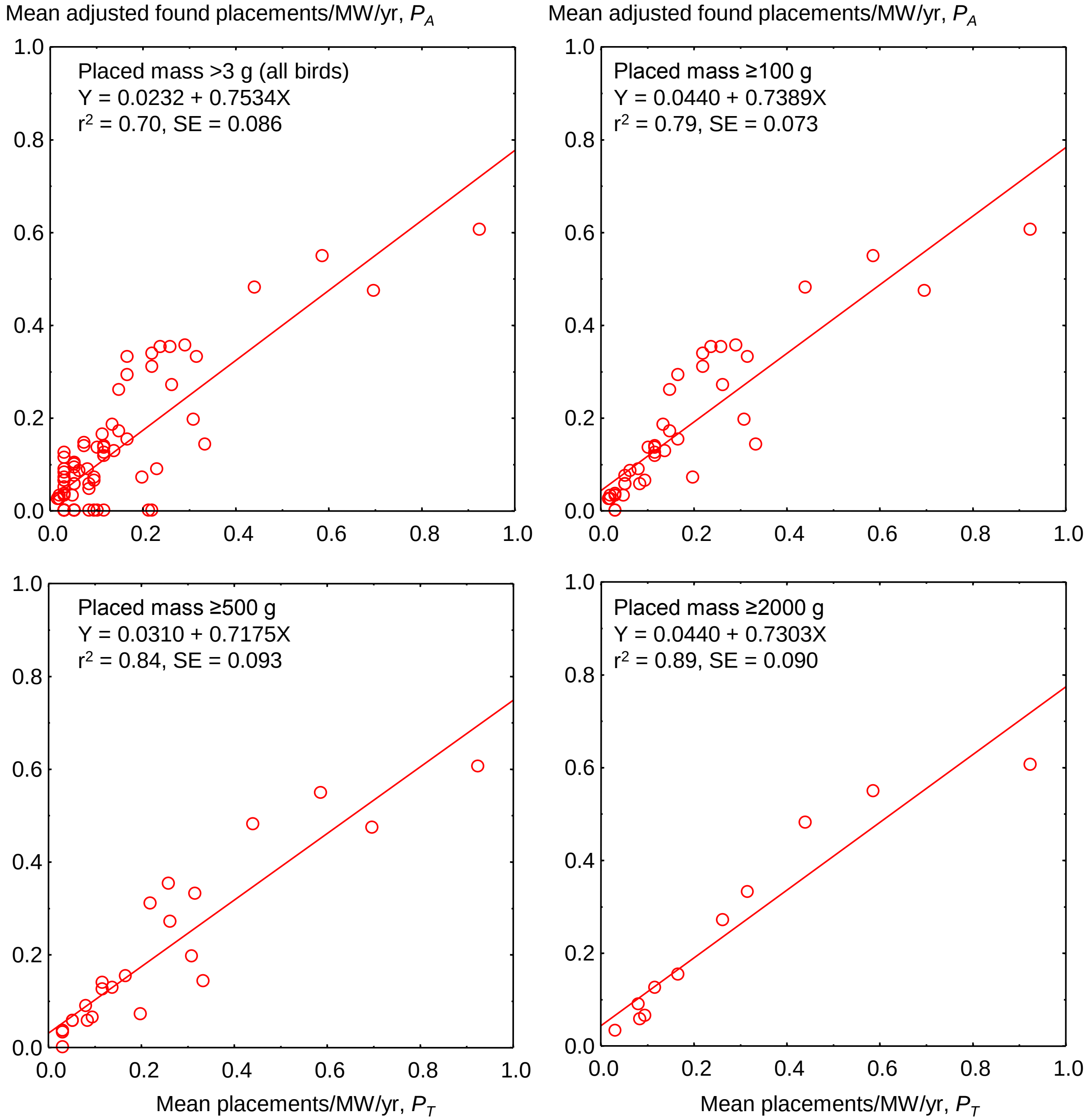

Adjusted rates of found placements regressed on known rates of trial placements averaged over all 3 years of monitoring at Forebay, including all placements (top left graph), placements of species totaling ⩾ 100 g (top right), totaling ⩾500 g (lower left), and totaling ⩾2,000 g (lower right).

Figure 14: Predicted Standard Error

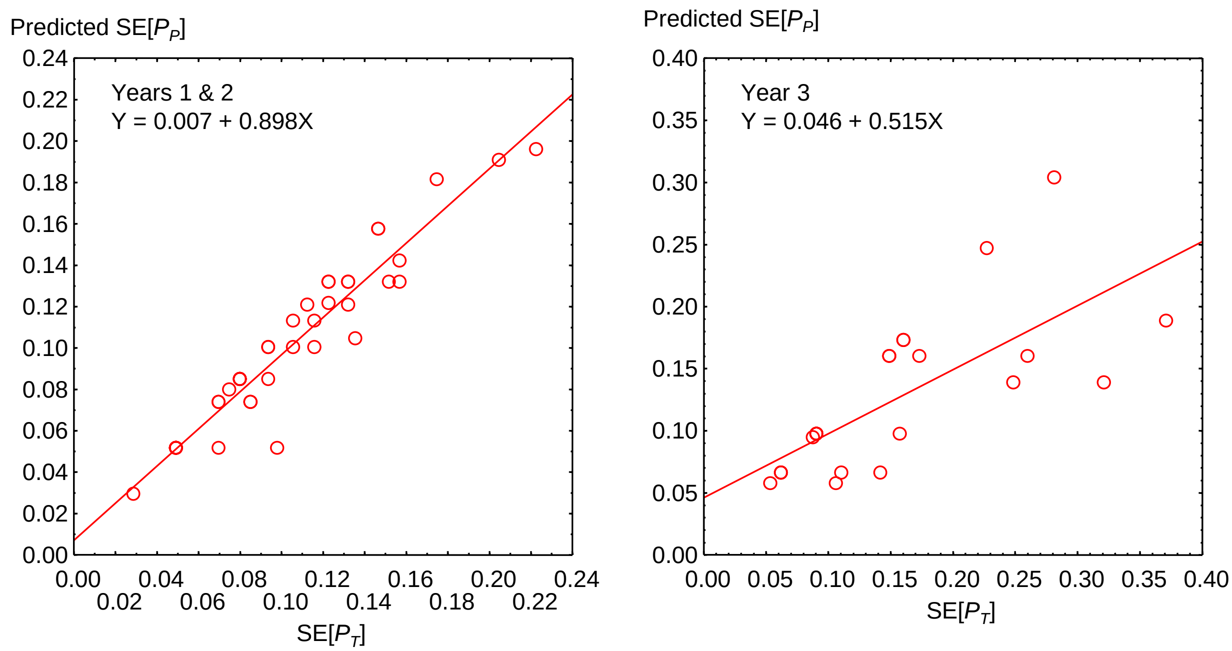

Standard error, SE[PP] predicted from body mass and the standard error of found trial carcasses, SE[PU], increased with increasing SE of known placements, SE[PT] for the first two years (left graph), but the relationship was weaker in the third year of monitoring (right graph) at Forebay, 2012-2015.

2.3.2.1 Fatality Estimates

Compared to fatality rates adjusted by national averages for carcass persistence, R_C, and searcher detection rates, p, fatality rates that were adjusted by overall detection rates from integrated detection trials, D, were 7 times greater for all bats as a group, half as great for all raptors as a group, and 69% of the estimate for all birds as a group (Table 2). The estimates based on D were about 79% of the estimates based on R_C and p were for golden eagle and other large-bodied birds, and the disparity was a bit greater for small birds (Table 2). In summary, the on-site integrated detection trial tended to yield lower bird fatality estimates but higher bat fatality estimates than did national average value for R_C and p.

Although it has long been thought that large raptors are more vulnerable to wind turbine collisions in the Santa Clara project than at Forebay, the results from a year of monitoring at Santa Clara did not support this belief (Table 3). Raptor fatality rates were higher among the selected turbines at Forebay, including for large raptors. However, the year of monitoring at Santa Clara was during a severe drought, and the wind turbines monitored at Forebay were selected for known high fatality rates in the past. The estimated bat fatality rate was much higher at Santa Clara, but that higher rate was likely an artifact of very small sample sizes (1 bat found at Santa Clara and 1 found at Forebay), a shorter monitoring period at Santa Clara, and fewer turbines to derive the average fatality rate.

Among Forebay turbines grouped by operability through the monitoring period, avian fatality rates were generally highest among turbines that were operable for at least some of the time but less than a third of the time (Table 4). The fatality rate for all birds as a group was 78% higher at this barely operable group of turbines compared to the fatality rate at the group of turbines that were operable at least 65% of the time, as well as compared to the group of turbines were operable between 33% and 65% of the time. None of the wind turbines were operable greater than 70% of the time due to the winter shutdown to mitigate wildlife impacts per SRC recommendations. Even at the group of Forebay turbines that were never operable during this study, the fatality rate of all birds as a group was 15% higher than at the two groups of turbines that were operable for more than 33% of the time.

Species found to have the highest fatality rates at the barely operable turbines included barn owl, rock pigeon, mourning dove, European starling, red-winged blackbird, and western meadowlark (Table 4). Species with the highest fatality rates at turbines that never operated include the red-tailed hawk, burrowing owl, killdeer, American coot, and rufous-crowned sparrow. All of the red-tailed hawk fatalities in this study were found at nonoperational wind turbines. Burrowing owl fatality rates were highest at turbines that never operated and declined with groups of turbines with decreasing operability. Contrary to red-tailed hawk and burrowing owl, American kestrel fatality rates were highest among wind turbines with intermediate operability. The most operable turbines caused the highest fatality rates amongst some species of songbird, including lesser goldfinch, Pacific-slope flycatcher, and ash-throated flycatcher, and for great-horned owl.

A review of the mapped distribution of fatality rates revealed strong clustering of fatalities and strong influences of topography. Fatality rates of all birds as a group were highest at Venture, followed by the northern aspect of the Taxvest project near Mountain House (Figures 15 to 18). Fatality rates of all birds as a group were highest at the ends of turbine rows were the rows descended into valley features (Figures 15-18). Omitting the rock pigeons and European starlings from the estimates, the fatality rates of native birds as a group revealed similar patterns, including the highest fatality rates at Venture and northern Taxvest, and at turbines on concave, valley-like topographic features (Figures 19 through 22). Note that the two turbines with relatively high fatality rates in the middle of the northern row in Figure 22 consisted of vacant towers, so no blade collision was possible.

The spatial distribution of red-tailed hawk fatality rates is shown in Figures 23 through 26. Not only were all red-tailed hawk fatalities found at nonoperational wind turbines, but all but two of these turbines were located in concave valley-like topographic structures.

The spatial distribution of American kestrel fatality rates was less clear (Figures 27 to 29). American kestrel fatality rates were not clustered, nor were they strongly associated with topography.

The spatial distribution of burrowing owl fatality rates revealed strong clustering at the Venture project and along an SW-NE band through the Altech project (Figure 30). Otherwise, the highest burrowing owl fatality rates corresponded with turbines within concave valley-like topographic structures (Figures 30 through 32).

Because so many rock pigeon fatalities were found during this study, maps were also produced to depict the spatial distribution of rock pigeon fatalities (Figures 33 through 35). Venture caused the highest fatality rates of rock pigeons, followed by the northern and southern aspects of the Taxvest project near Mountain House.

Estimated avian fatality rates were relatively high among the wind turbines monitored in this study. Across the 14.399 MW of monitored turbines, annual fatality estimates were 27 bats (90% CI: 25.1-28.9), 48.1 raptors (90% CI: 30-67), and 515.6 birds (90% CI: 398.4-633.9). The bat fatality estimate was only 11% of the national average among wind projects other than those in the APWRA, but the raptor estimate was 3.7 times the national average, and the bird estimate was 3.5 times the national average (Smallwood 2013). The monitored wind turbines caused the annual deaths of an estimated 9 American kestrels, 28 burrowing owls, 3 barn owls, 1 great-horned owl, 0.6 golden eagles, 0.7 ferruginous hawks, 5 red-tailed hawk, as well as 27 mourning doves, 203 rock pigeons (these pigeons were often found with leg-bands), 69 European starlings, 5 common ravens, 3 loggerhead shrikes, nearly 6 gulls, 17 western meadowlarks, and various numbers of other species.

Table 2: Comparison of Fatalities/MW/Year

Species/Taxa	Fatalities/MW/Year			
	On-site integrated detection trials, *D*		National averages, R_C and *p*	
	Mean	SE_P	Mean	SE
Mexican free-tailed bat	0.567	0.023	0.079	0.079
Bat	1.309	0.057	0.183	0.183
Grebe	0.058	0.034	0.101	0.071
American coot	0.096	0.057	0.132	0.093
Killdeer	0.139	0.053	0.258	0.153
Spotted sandpiper	0.048	0.023	0.071	0.071
Gull	0.246	0.074	0.342	0.120
California gull	0.029	0.023	0.040	0.040
Glaucous-winged gull	0.029	0.023	0.040	0.040
Herring gull	0.029	0.023	0.034	0.034
Turkey vulture	0.028	0.023	0.034	0.034
Golden eagle	0.044	0.040	0.056	0.056
Ferruginous hawk	0.045	0.040	0.056	0.056
Red-tailed hawk	0.357	0.117	0.428	0.157
Large raptor	0.057	0.034	0.068	0.048
American kestrel	0.616	0.123	1.190	0.344
Barn owl	0.191	0.064	0.255	0.105
Burrowing owl	1.920	0.313	3.858	0.864
Great-horned owl	0.084	0.042	0.103	0.059
Dove	0.794	0.160	1.561	0.446
Mourning dove	1.881	0.280	3.695	0.774
Rock pigeon	14.109	1.139	17.243	1.697
Common poorwill	0.068	0.035	0.103	0.103
White-throated swift	0.054	0.023	0.071	0.071
Acorn woodpecker	0.000	0.000	0.000	0.000

Species/Taxa	Fatalities/MW/Year			
	On-site integrated detection trials, *D*		National averages, R_C and *p*	
	Mean	SE_P	Mean	SE
Northern flicker	0.072	0.034	0.142	0.100
Ash-throated flycatcher	0.055	0.023	0.071	0.071
Black phoebe	0.108	0.040	0.116	0.116
Pacific-slope flycatcher	0.231	0.047	0.187	0.136
Say's phoebe	0.101	0.040	0.116	0.116
Horned lark	0.101	0.034	0.142	0.100
Corvid	0.035	0.023	0.042	0.042
Common raven	0.345	0.087	0.434	0.123
American robin	0.134	0.063	0.235	0.179
Loggerhead shrike	0.228	0.119	0.333	0.333
European starling	4.798	0.401	8.371	1.106
Yellow-rumped warbler	0.228	0.050	0.205	0.145
Sparrow	0.103	0.040	0.116	0.116
Lazuli bunting	0.143	0.049	0.142	0.142
Lincoln sparrow	0.058	0.020	0.061	0.061
Rufous-crowned sparrow	0.056	0.020	0.061	0.061
Song sparrow	0.053	0.023	0.071	0.071
Blackbird	0.251	0.064	0.400	0.182
Brown-headed cowbird	0.000	0.000	0.000	0.000
Red-winged blackbird	0.073	0.040	0.116	0.116
Tricolored blackbird	0.045	0.023	0.071	0.071
Western meadowlark	1.212	0.170	2.252	0.472
Finch	0.094	0.040	0.116	0.116
Goldfinch	0.075	0.023	0.071	0.071
House finch	0.278	0.060	0.338	0.172
Lesser goldfinch	0.073	0.023	0.071	0.071
Bird	0.000	0.000	0.000	0.000

Species/Taxa	Fatalities/MW/Year			
	On-site integrated detection trials, *D*		National averages, R_C and *p*	
	Mean	SE_P	Mean	SE
Large bird	0.420	0.129	0.501	0.174
Medium bird	0.660	0.147	0.884	0.244
Small bird	4.740	0.358	6.002	0.989
Thayer's gull	0.063	0.040	0.066	0.066
Northern oriole	0.052	0.023	0.071	0.071
All bats	1.876	0.081	0.263	0.263
All raptors	3.342	0.795	6.047	1.722
All birds	35.807	4.997	51.547	11.270

Adjusted by on-site integrated detection trials, D (left columns), or by national average values for carcass persistence, RC, and searcher detection, S (right columns), among all 224 wind turbines (14.399 MW) monitored as part of the Ogin study from 3 April 2012 through 16 February 2015. All estimates were also adjusted for search radius bias (Smallwood 2013) and proportion of the 50-m radius searched at some turbines partly included within the routine search areas, A. SEP was the predicted standard error based on body mass and SE of the unadjusted fatality finds.

Table 3: Comparison of Fatalities/MW/Year at 138 Forebay Wind Turbines

Species/Taxa	Fatalities/MW/Year			
	Selected turbines at Forebay		Santa Clara 95 KW Vestas	
	Mean	SE_P	Mean	SE_P
Mexican free-tailed bat	0.920	0.040	0.000	
Bat	0.000		8.377	0.381
Grebe	0.047	0.040	0.000	
American coot	0.156	0.094	0.000	
Killdeer	0.226	0.088	0.000	
Spotted sandpiper	0.078	0.040	0.000	
Gull	0.352	0.115	0.000	
California gull	0.047	0.040	0.000	
Glaucous-winged gull	0.000		0.000	
Herring gull	0.046	0.040	0.000	
Turkey vulture	0.045	0.040	0.000	
Golden eagle	0.000		0.000	
Ferruginous hawk	0.074	0.066	0.000	
Red-tailed hawk	0.334	0.150	0.421	0.381
Large raptor	0.046	0.040	0.000	
American kestrel	0.862	0.175	0.544	0.381
Barn owl	0.212	0.089	0.000	
Burrowing owl	2.584	0.450	0.000	
Great-horned owl	0.090	0.057	0.000	
Dove	0.860	0.173	0.535	0.381
Mourning dove	2.112	0.303	0.000	
Rock pigeon	19.400	1.692	0.467	0.381
Common poorwill	0.111	0.058	0.000	
White-throated swift	0.087	0.040	0.000	
Acorn woodpecker	0.000		0.000	
Northern flicker	0.117	0.057	0.000	

Species/Taxa	Fatalities/MW/Year			
	Selected turbines at Forebay		Santa Clara 95 KW Vestas	
	Mean	SE_P	Mean	SE_P
Ash-throated flycatcher	0.090	0.040	0.000	
Black phoebe	0.175	0.066	0.000	
Pacific-slope flycatcher	0.232	0.066	0.000	
Say's phoebe	0.164	0.066	0.000	
Horned lark	0.164	0.057	0.000	
Corvid	0.057	0.040	0.000	
Common raven	0.376	0.118	0.000	
American robin	0.066	0.040	0.597	0.381
Loggerhead shrike	0.000		0.000	
European starling	5.052	0.459	0.603	0.381
Yellow-rumped warbler	0.370	0.083	0.000	
Sparrow	0.167	0.066	0.000	
Lazuli bunting	0.000		0.000	
Lincoln sparrow	0.094	0.034	0.000	
Rufous-crowned sparrow	0.092	0.034	0.000	
Song sparrow	0.086	0.040	0.000	
Blackbird	0.408	0.105	0.000	
Brown-headed cowbird	0.000		0.000	
Red-winged blackbird	0.118	0.066	0.000	
Tricolored blackbird	0.073	0.040	0.000	
Western meadowlark	1.765	0.255	0.000	
Finch	0.153	0.066	0.000	
Goldfinch	0.122	0.040	0.000	
House finch	0.452	0.099	0.000	
Lesser goldfinch	0.118	0.040	0.000	
Bird	0.000		0.000	
Large bird	0.359	0.133	1.268	0.642

Species/Taxa	Fatalities/MW/Year			
	Selected turbines at Forebay		Santa Clara 95 KW Vestas	
	Mean	SE_P	Mean	SE_P
Medium bird	0.748	0.197	0.467	0.381
Small bird	5.174	0.379	1.661	0.532
Thayer's gull	0.101	0.066	0.000	
Northern oriole	0.084	0.040	0.000	
All bats	0.920	0.040	8.377	0.381
All raptors	4.247	1.066	0.965	0.762
All birds	44.747	6.571	6.562	3.841

(8.279 MW) that were selected for the BACI experiment (left columns) and 35 95-KW Vestas turbines (3.325 MW) searched for nearly one year at Santa Clara (right columns). Fatality estimates were adjusted for overall detection rates, D, and for search radius bias, d (Smallwood 2013). The wind turbines at Forebay were monitored as part of the Ogin study from 3 April 2012 through 16 February 2015, and those at Santa Clara were monitored 21 April 2014 through 16 February 2015 (and continuing through 31 March 2015). SEP was the predicted standard error based on body mass and SE of the unadjusted fatality finds.

Table 4: Comparison of Fatalities/MW/Year at Forebay Wind Turbines That Were Selected or Next to Selected Turbines for the BACI Experiment

Species/Taxa	Fatalities/MW/Year at Turbines with Operability Over Monitoring Period of:							
	0%		1%-33%		34%-64%		>64%	
	Mean	SE_P	Mean	SE_P	Mean	SE_P	Mean	SE_P
Mexican free-tailed bat	0.000		0.000		1.283	0.056	0.000	
Bat	0.000		0.000		0.000		0.000	
Grebe	0.000		0.000		0.000		0.621	0.379
American coot	1.073	0.943	0.000		0.108	0.093	0.000	
Killdeer	1.400	0.943	0.000		0.087	0.056	0.410	0.274
Spotted sandpiper	0.000		0.000		0.109	0.056	0.000	
Gull	0.000		0.448	0.397	0.330	0.126	0.622	0.379
California gull	0.000		0.000		0.066	0.056	0.000	
Glaucous-winged gull	0.000		0.000		0.065	0.056	0.000	
Herring gull	0.000		0.000		0.065	0.056	0.000	
Turkey vulture	0.000		0.000		0.063	0.056	0.000	
Golden eagle	0.000		0.000		0.000		0.000	
Ferruginous hawk	0.000		0.000		0.103	0.093	0.000	
Red-tailed hawk	2.532	1.567	0.000		0.210	0.132	0.000	
Large raptor	0.000		0.000		0.064	0.056	0.000	
American kestrel	0.000		0.786	0.379	0.868	0.219	0.393	0.274
Barn owl	0.585	0.497	0.791	0.472	0.138	0.080	0.324	0.274
Burrowing owl	5.288	2.722	3.478	1.353	2.101	0.486	0.703	0.354
Great-horned owl	0.000		0.000		0.063	0.056	0.297	0.274
Dove	0.698	0.497	0.944	0.472	0.764	0.203	0.387	0.274
Mourning dove	0.698	0.497	3.092	1.259	1.853	0.308	1.546	0.508
Rock pigeon	15.639	3.628	33.037	6.484	15.470	1.781	18.552	2.046
Common poorwill	0.000		0.000		0.154	0.082	0.000	
White-throated swift	0.000		0.000		0.121	0.056	0.000	
Acorn woodpecker	0.000		0.000		0.000		0.000	

Northern flicker	0.000		0.000		0.082	0.056	0.385	0.274
Ash-throated flycatcher	0.000		0.000		0.000		0.588	0.274
Black phoebe	0.000		0.000		0.244	0.093	0.000	
Pacific-slope flycatcher	0.000		0.000		0.324	0.093	0.940	0.274
Say's phoebe	0.000		0.000		0.229	0.093	0.000	
Horned lark	0.000		0.000		0.228	0.080	0.000	
Corvid	0.000		0.000		0.079	0.056	0.000	
Common raven	0.546	0.497	0.999	0.513	0.257	0.113	0.000	
American robin	0.000		0.000		0.091	0.056	0.000	
Loggerhead shrike	0.000		0.000		0.000		0.000	
European starling	5.029	1.676	7.859	1.312	4.758	0.559	2.612	0.815
Yellow-rumped warbler	0.000		2.432	0.548	0.000		0.000	
Sparrow	0.000		0.000		0.233	0.093	0.000	
Lazuli bunting	0.000		0.000		0.000		0.000	
Lincoln sparrow	0.000		0.000		0.131	0.048	0.000	
Rufous-crowned sparrow	1.263	0.497	0.000		0.000		0.000	
Song sparrow	0.000		0.568	0.274	0.000		0.000	
Blackbird	0.000		0.000		0.467	0.135	0.476	0.274
Brown-headed cowbird	0.000		0.000		0.000		0.000	
Red-winged blackbird	0.000		0.778	0.448	0.000		0.000	
Tricolored blackbird	0.000		0.000		0.102	0.056	0.000	
Western meadowlark	1.973	0.925	2.075	0.600	1.755	0.330	1.225	0.453
Finch	0.000		0.000		0.213	0.093	0.000	
Goldfinch	0.000		0.000		0.170	0.056	0.000	
House finch	0.000		0.000		0.438	0.111	0.000	
Lesser goldfinch	0.000		0.000		0.000		0.776	0.274
Bird	0.000		0.000		0.000		0.000	
Large bird	0.000		0.262	0.235	0.380	0.170	0.305	0.274
Medium bird	1.150	0.943	1.463	0.829	0.473	0.156	1.348	0.647
Small bird	5.846	1.518	7.821	1.227	4.326	0.393	5.397	1.027

Thayer's gull	0.000		0.667	0.448	0.000		0.000	
Northern oriole	0.000		0.000		0.117	0.056	0.000	
All bats	0.000	0.000	0.000	0.000	1.283	0.056	0.000	0.000
All raptors	8.405	4.786	5.056	2.205	3.609	1.178	1.717	1.177
All birds	43.719	17.351	67.501	17.250	37.900	7.005	37.909	9.627

Were operable for 0%, >0% to 33%, >33% to <65%, and ⩾65% of the monitoring period, including respectively, 10 turbines (0.563 MW), 21 turbines (1.341 MW). 99 turbines (5.611 MW), and 21 turbines (1.384 MW). Fatality estimates were adjusted for overall detection rates, D, and for search radius bias, d (Smallwood 2013). The wind turbines at Forebay were monitored as part of the Ogin study from 3 April 2012 through 16 February 2015. SEP was the predicted standard error based on body mass and SE of the unadjusted fatality finds.

Figure 15: Adjusted Fatality Rates of All Birds at Altech 1, Swamp, Viking, and Venture Winds Projects, Altamont Pass Wind Resource Area, 3 April 2012 – 16 February 2015

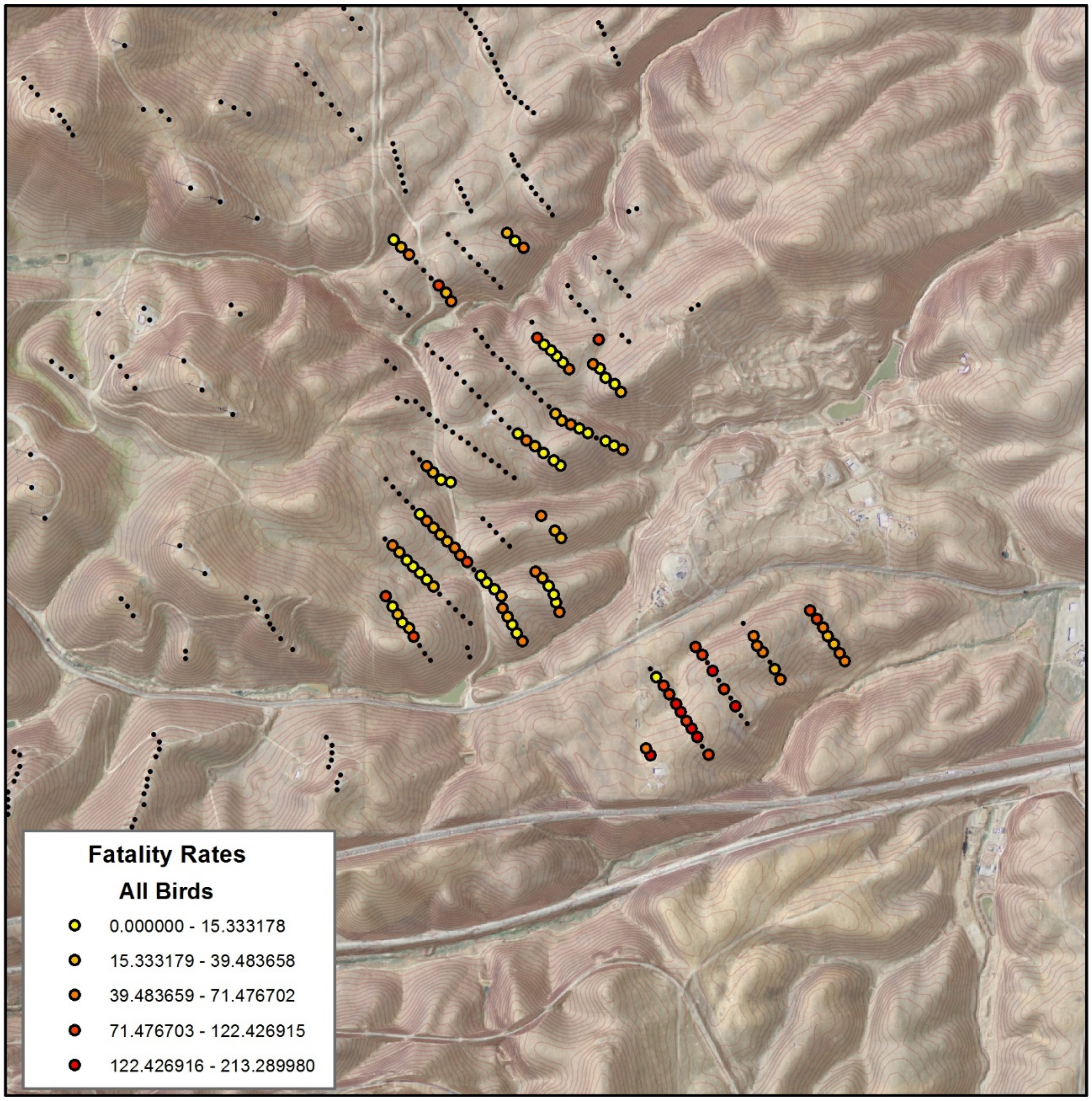

Figure 16: Adjusted Fatality Rates of All Birds at the Taxvest Project Near Mountain House, Altamont Pass Wind Resource Area, 3 April 2012 – 16 February 2015

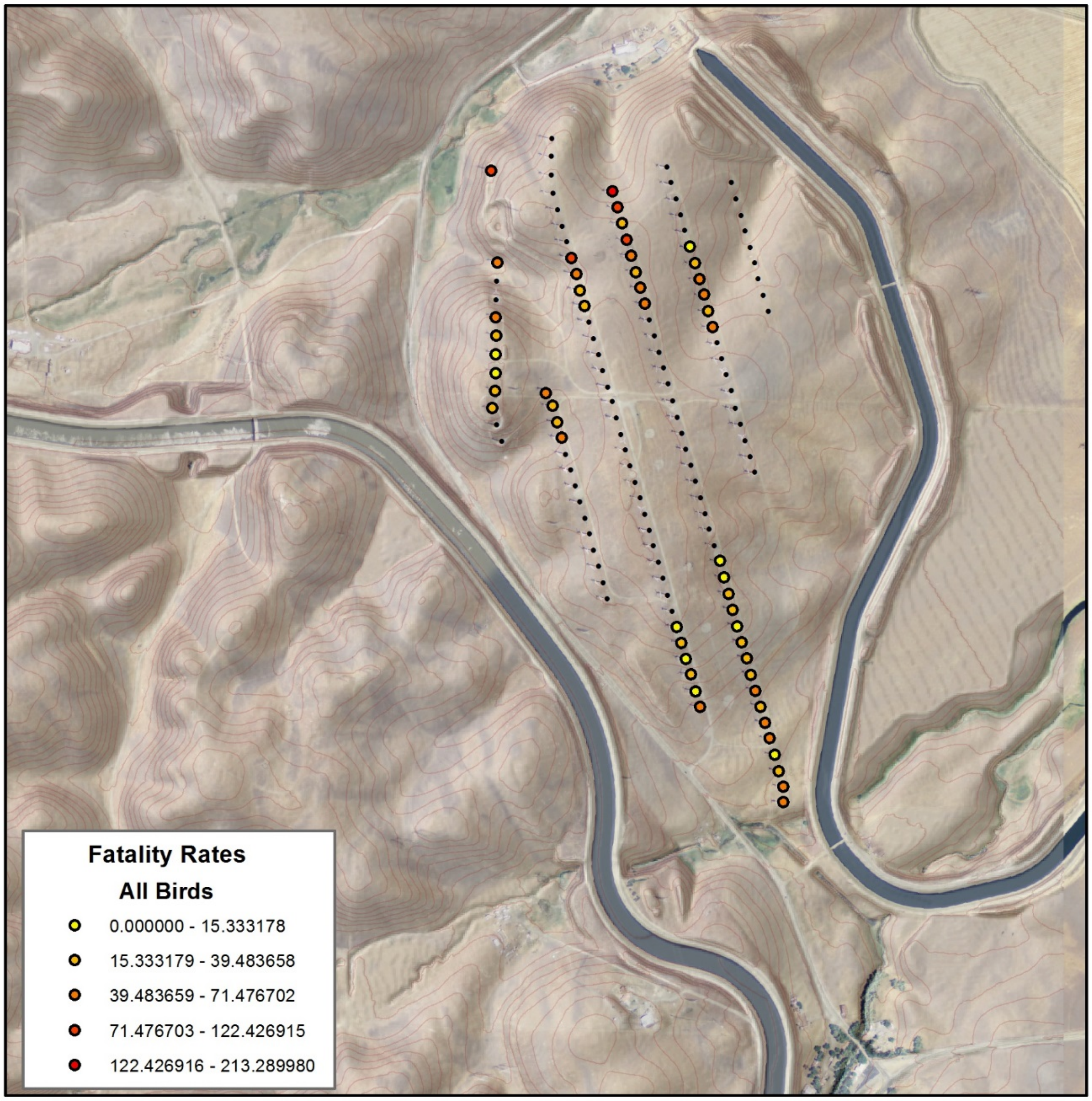

Figure 17: Adjusted Fatality Rates of All Birds at the Taxvest Project Off Midway Road, Altamont Pass Wind Resource Area, 3 April 2012 – 16 February 2015

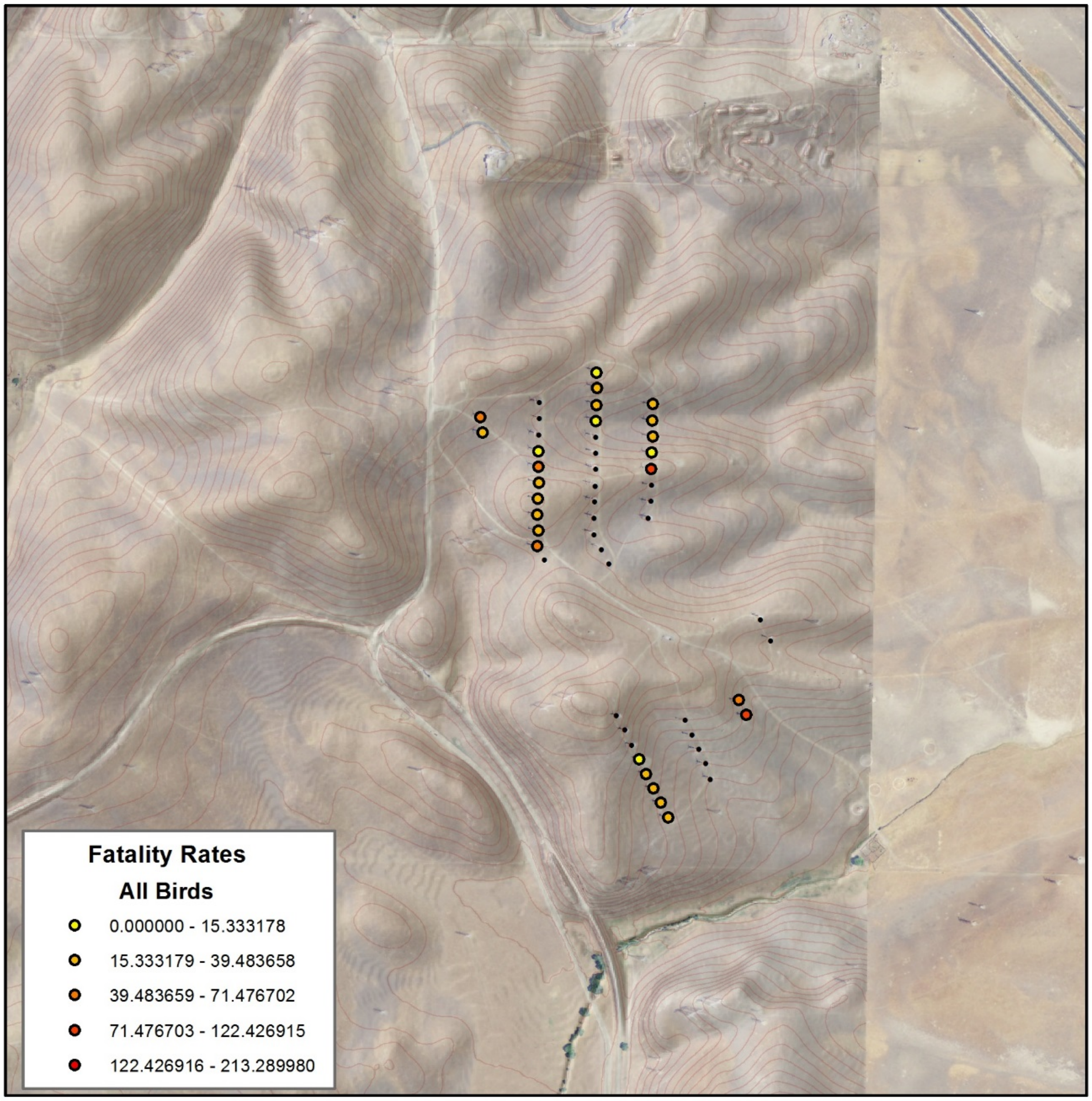

Figure 18: Adjusted Fatality Rates of All Birds at Rows 5-7, Santa Clara Project, Altamont Pass Wind Resource Area, 21 April 2014 – 16 February 2015

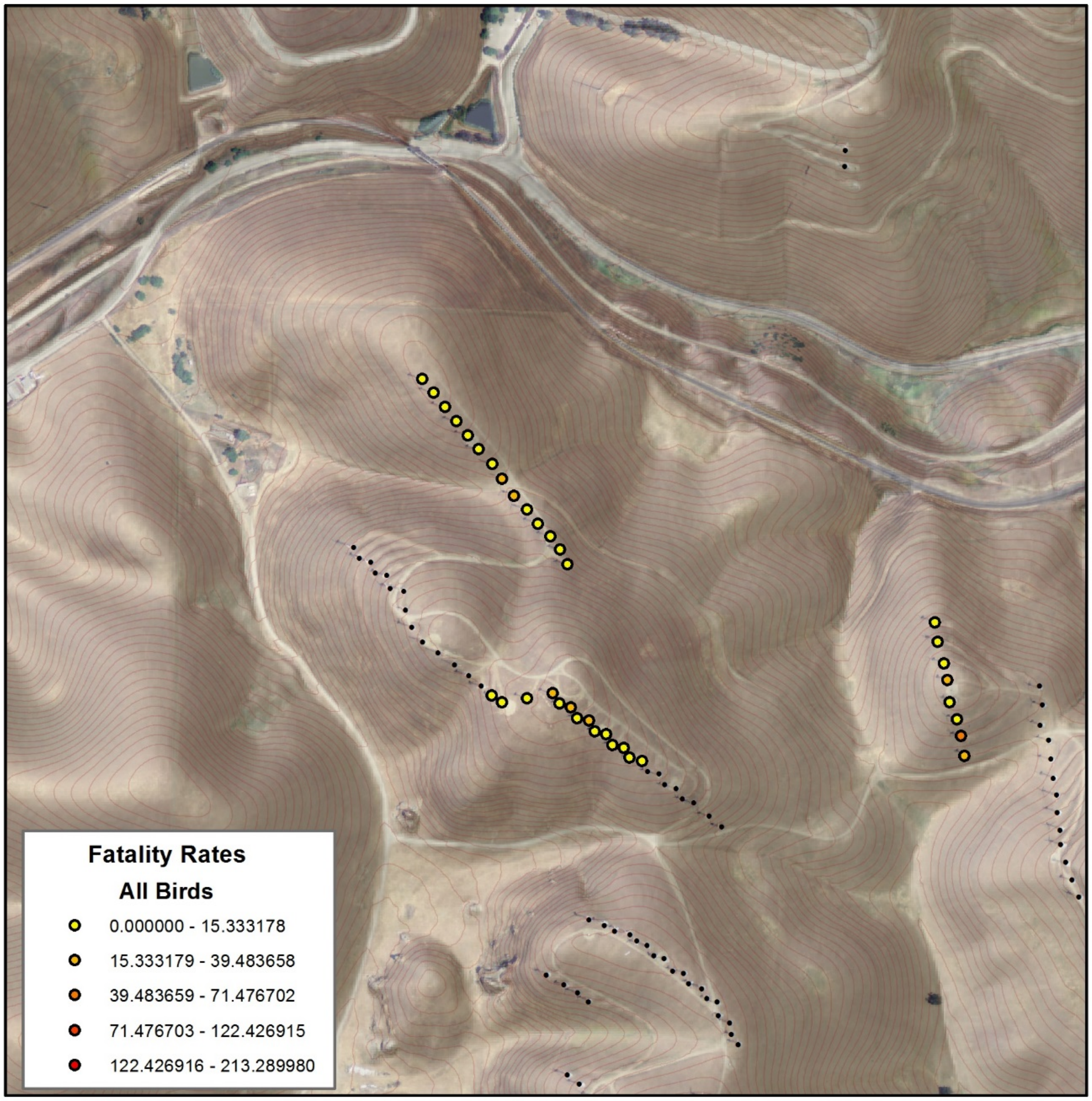

Figure 19: Adjusted Fatality Rates of All Native Birds at Altech 1, Swamp, Viking, and Venture Winds Projects, Altamont Pass Wind Resource Area, 3 April 2012–16 February, 2015

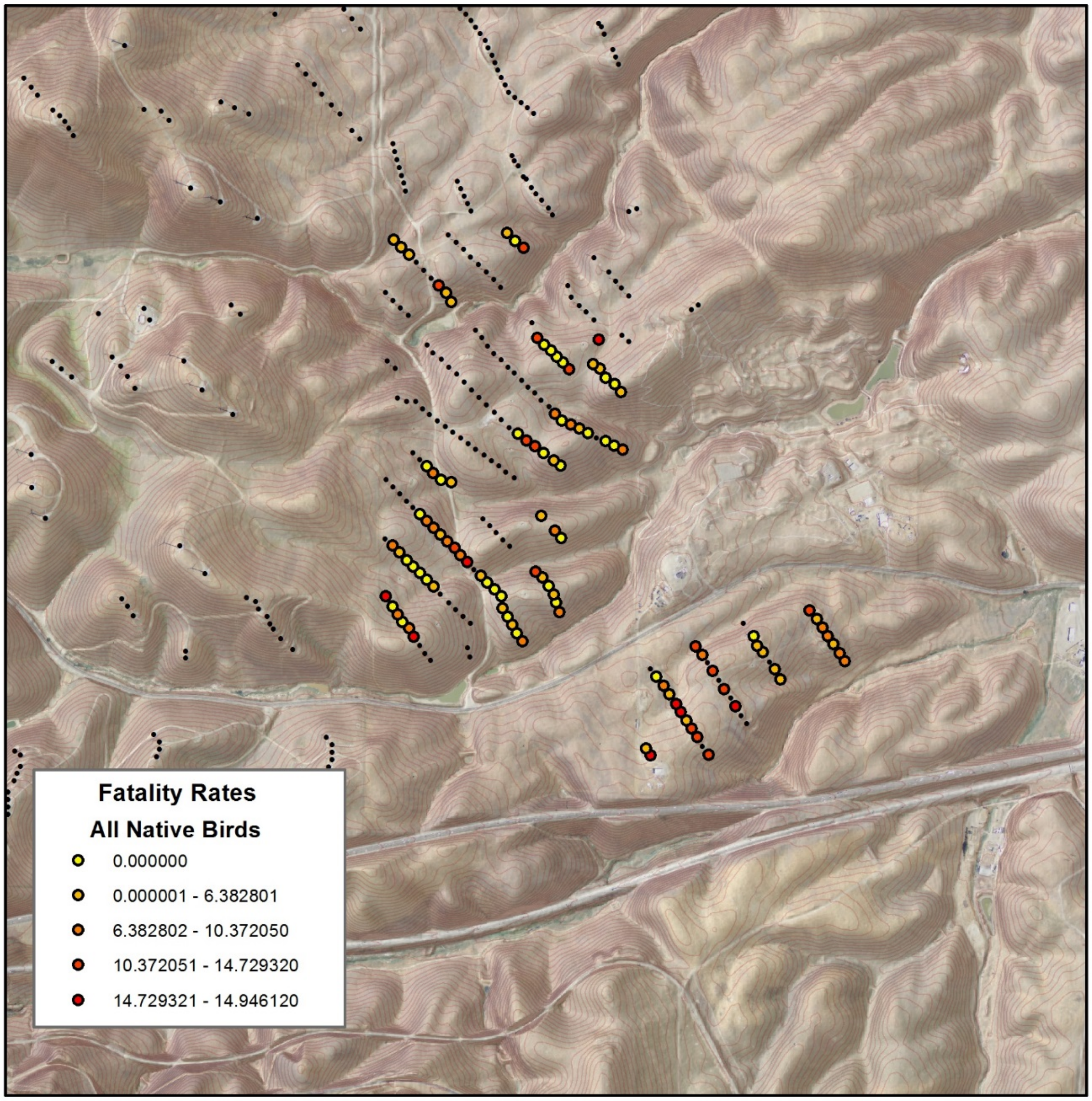

Figure 20: Adjusted Fatality Rates of All Native Birds at the Taxvest Project Near Mountain House, Altamont Pass Wind Resource Area, 3 April 2012 – 16 February 2015

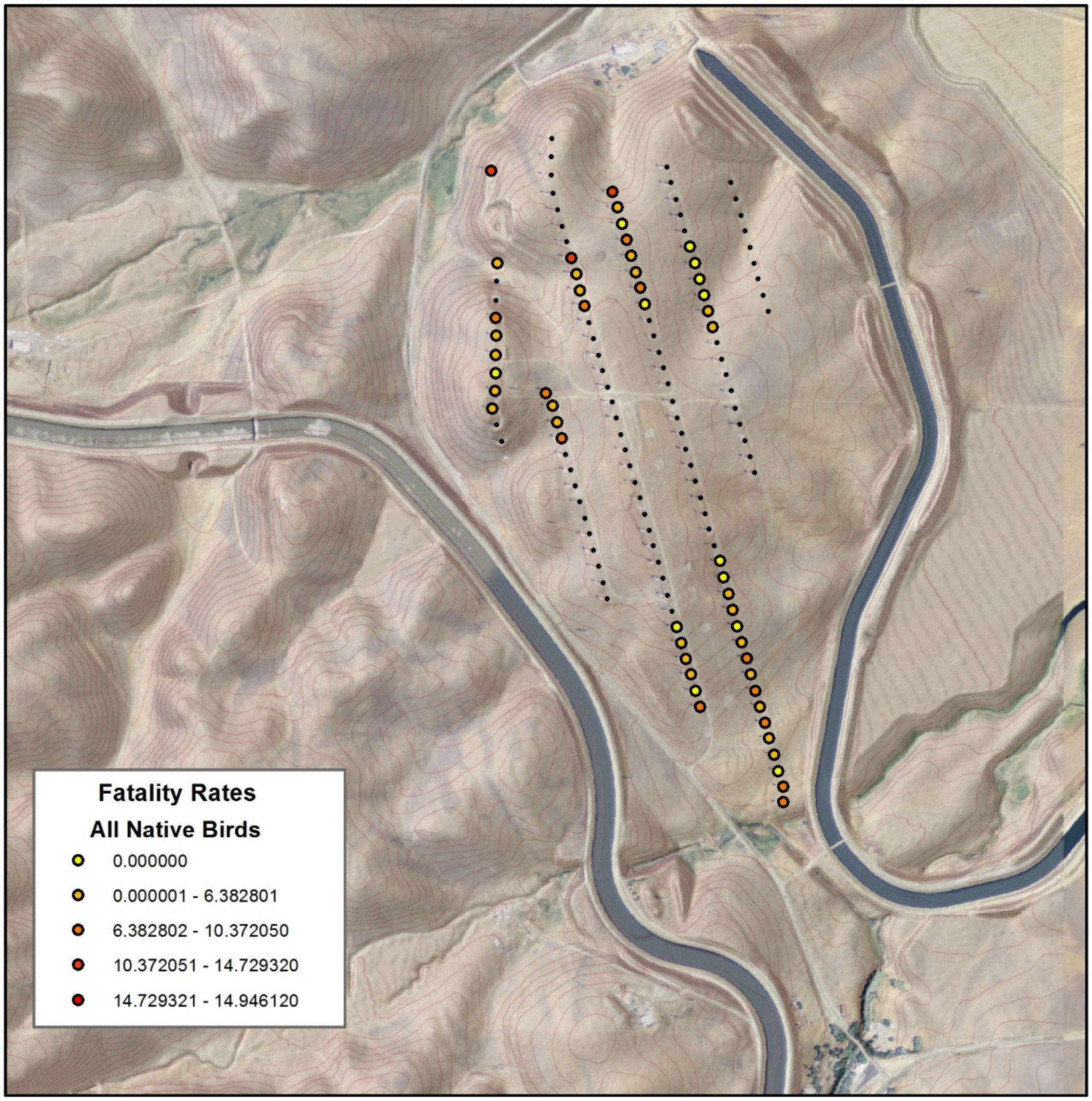

Figure 21: Adjusted Fatality Rates of All Native Birds at the Taxvest Project Off Midway Road, Altamont Pass Wind Resource Area, 3 April 2012 – 16 February 2015

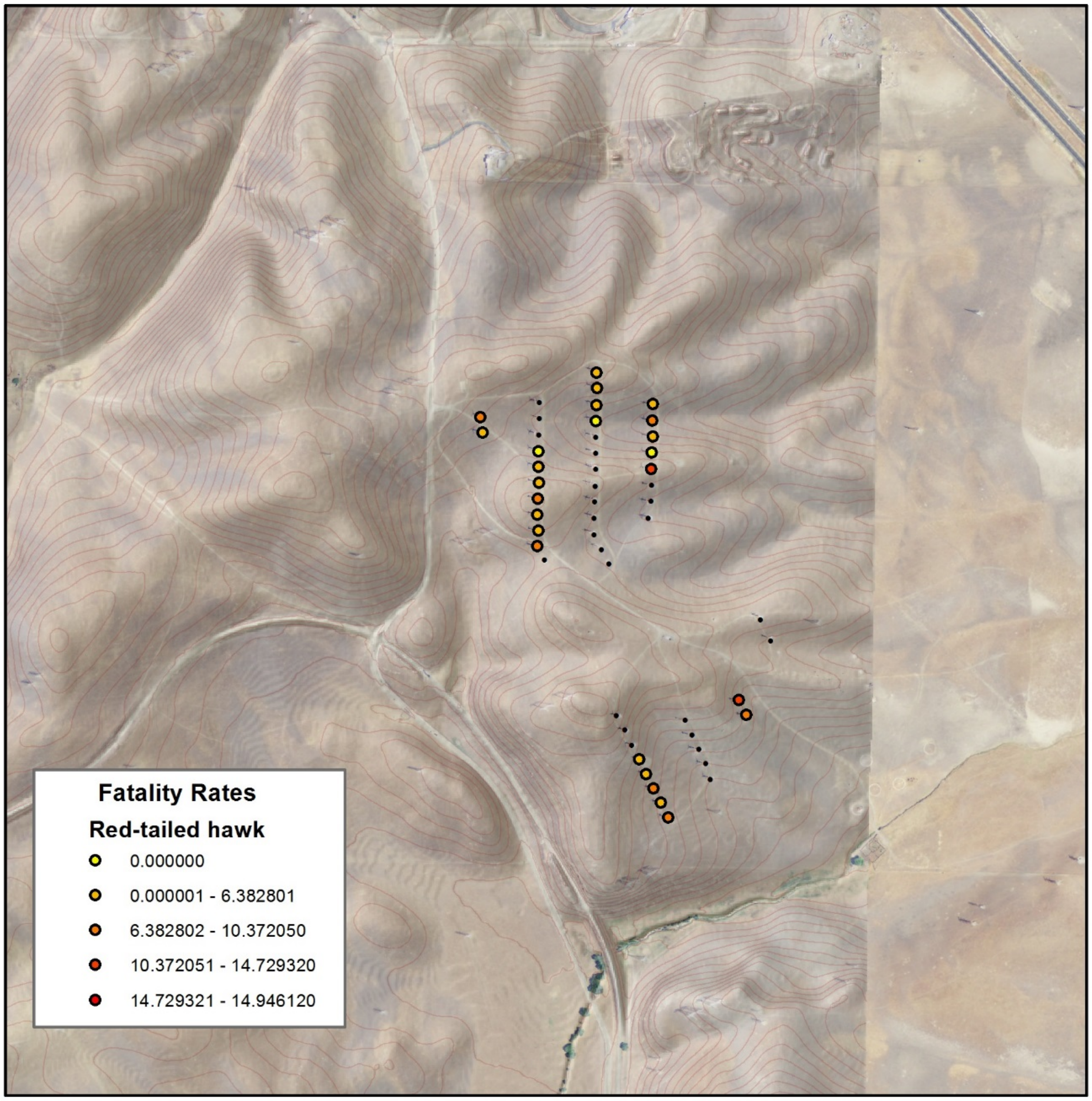

Figure 22: Adjusted Fatality Rates of All Native Birds at Rows 5-7, Santa Clara Project, Altamont Pass Wind Resource Area, 21 April 2012 – 16 February 2015

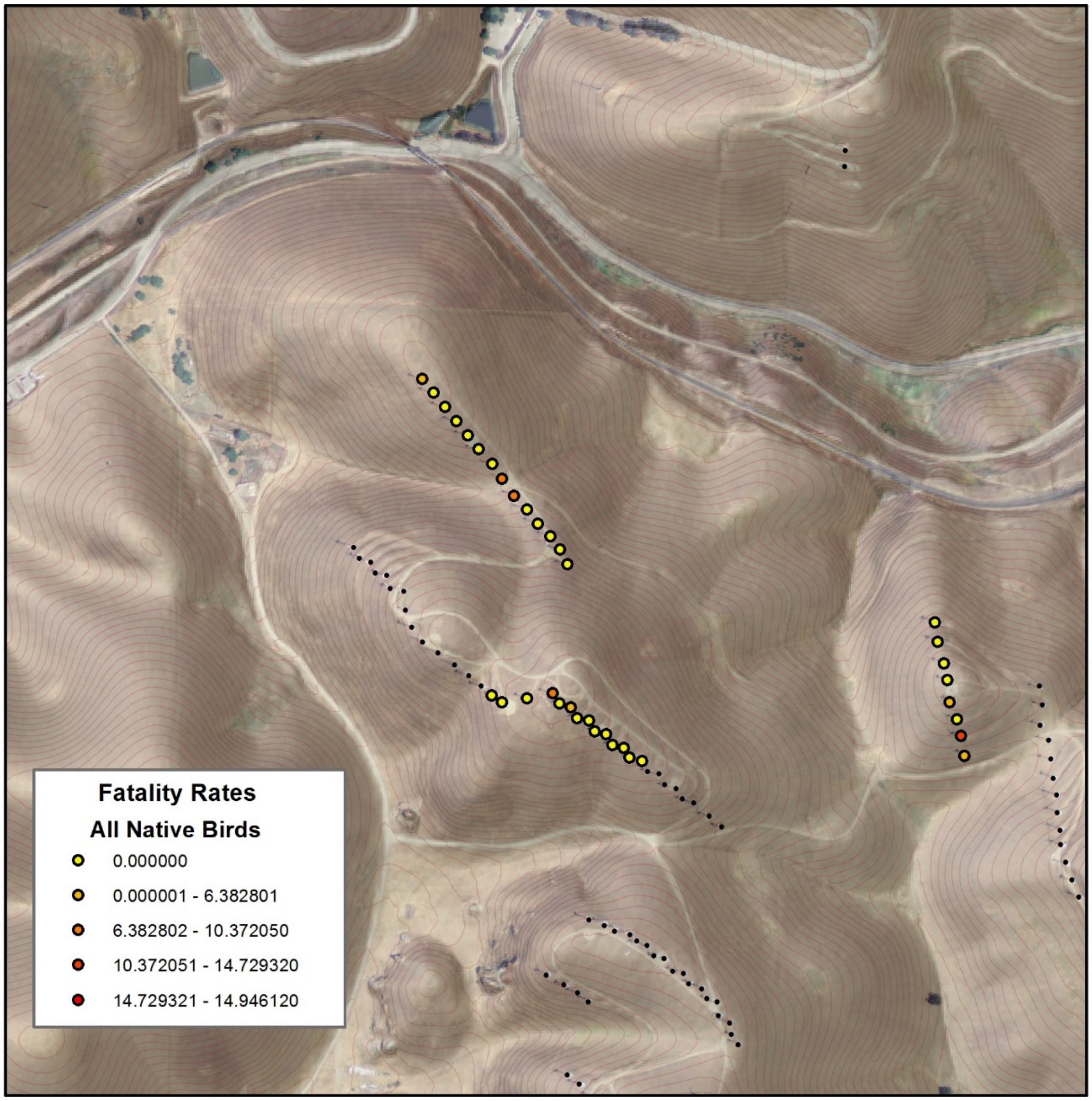

Figure 23: Adjusted Fatality Rates of Red-Tailed Hawks at Altech 1, Swamp, Viking, and Venture Winds Projects, Altamont Pass Wind Resource Area, 3 April 2012 – 16 February 2015

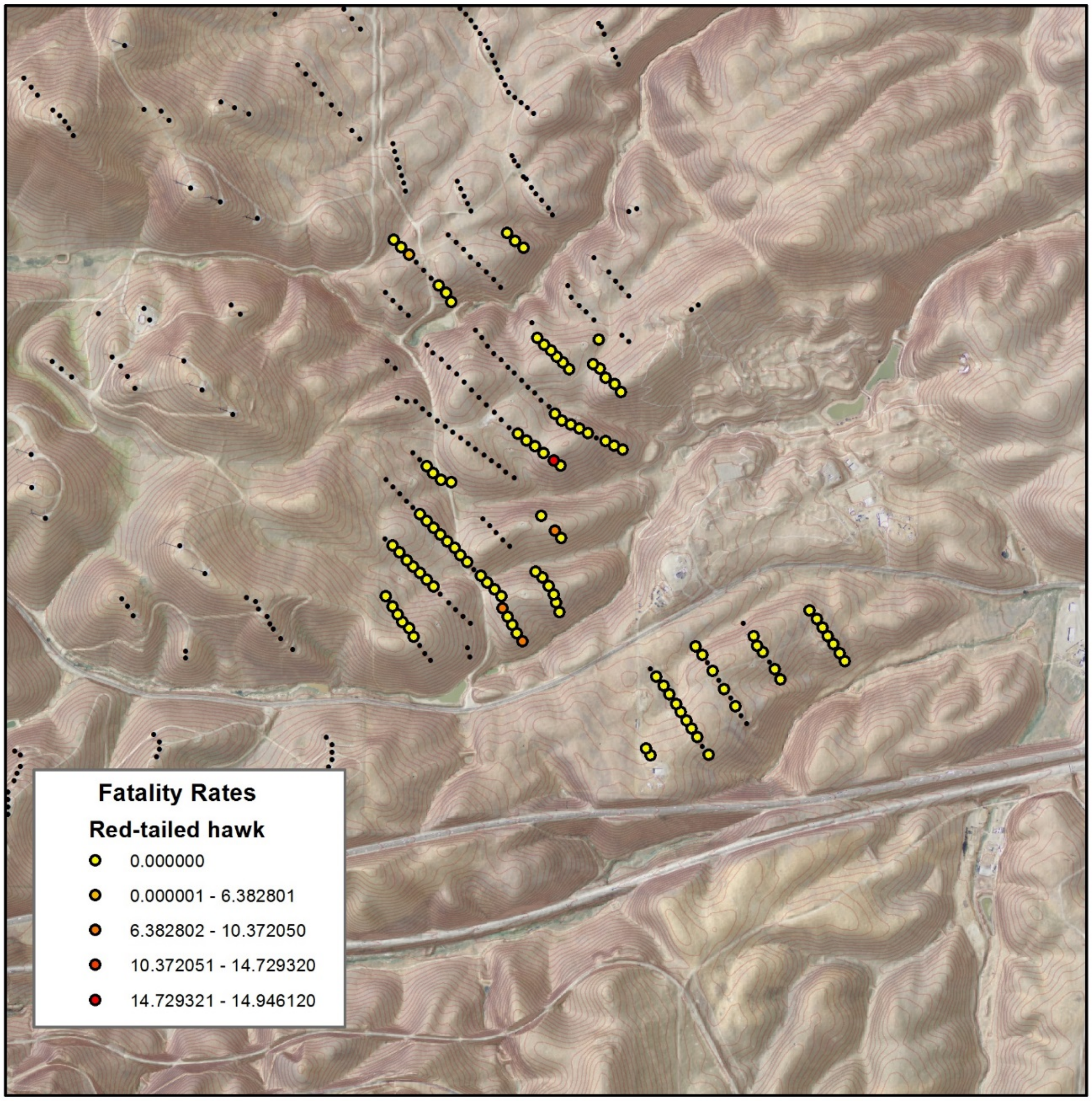

Figure 24: Adjusted Fatality Rates of Red-Tailed Hawks at the Taxvest Project Near Mountain House, Altamont Pass Wind Resource Area, 3 April 2012 – 16 February 2015

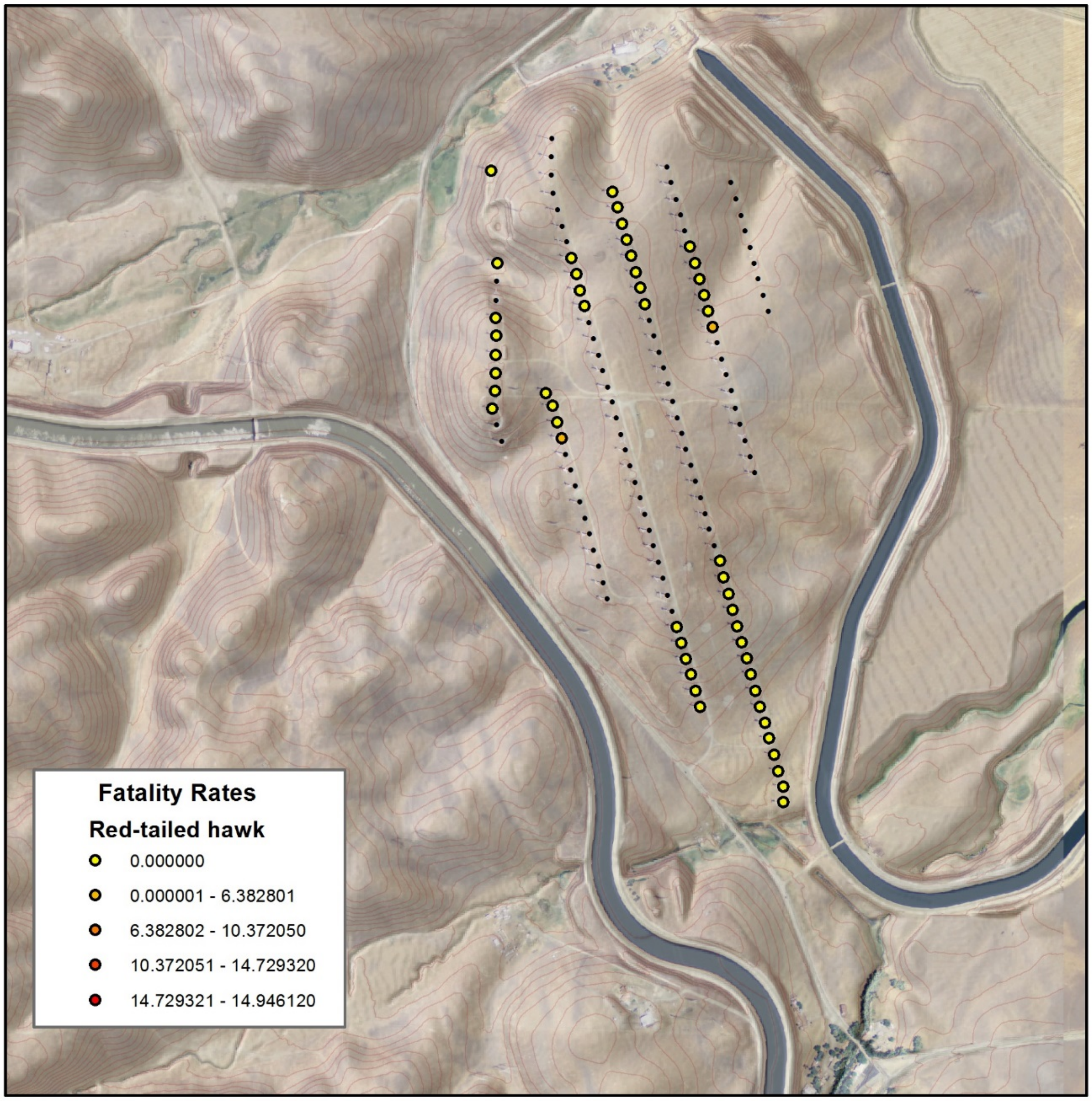

Figure 25: Adjusted Fatality Rates of Red-Tailed Hawks at the Taxvest Project Off Midway Road, Altamont Pass Wind Resource Area, 3 April 2012 – 16 February 2015

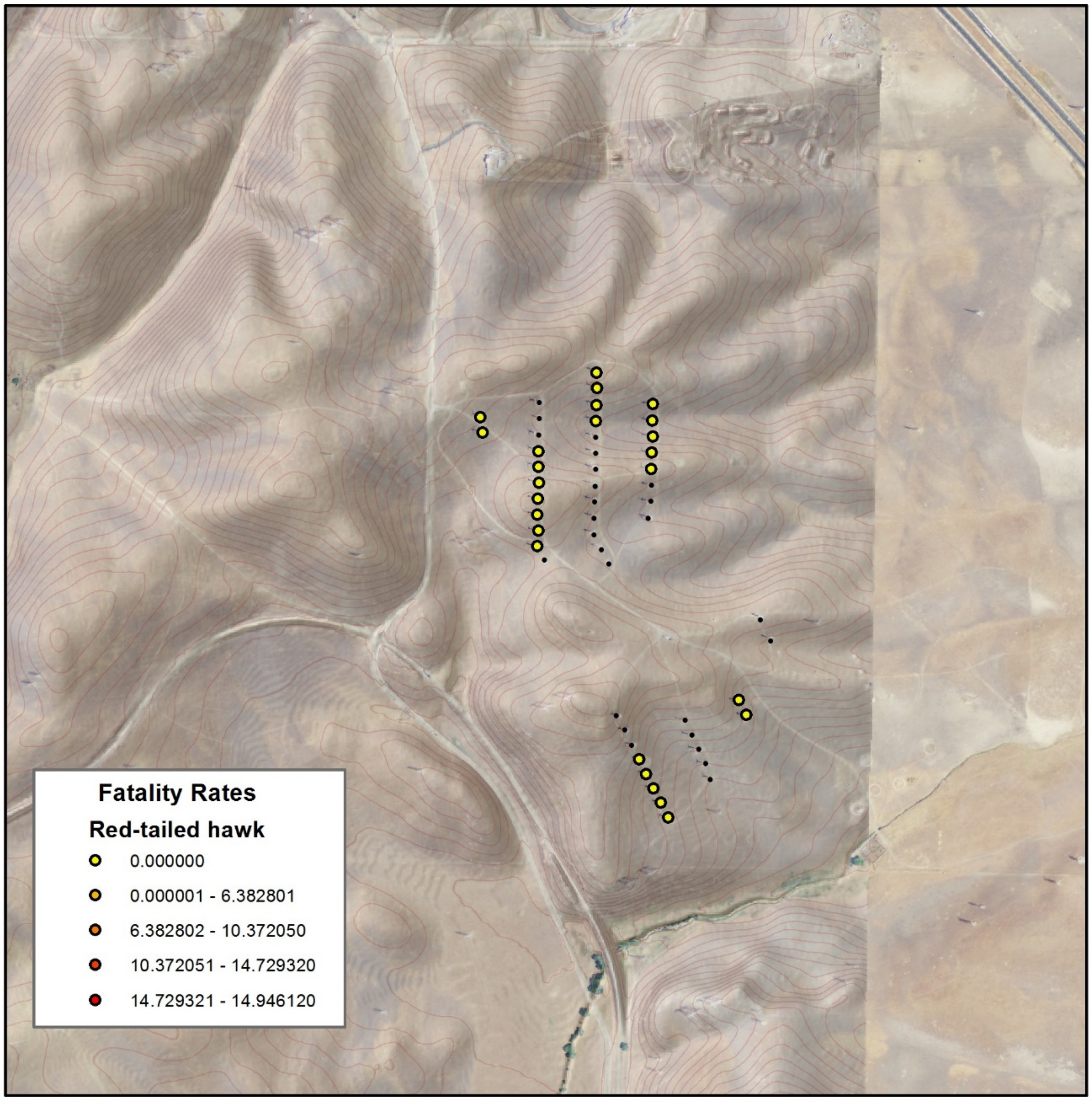

Figure 26: Adjusted Fatality Rates of Red-Tailed Hawks at Rows 5-7, Santa Clara Project, Altamont Pass Wind Resource Area, 21 April 2012 – 16 February 2015

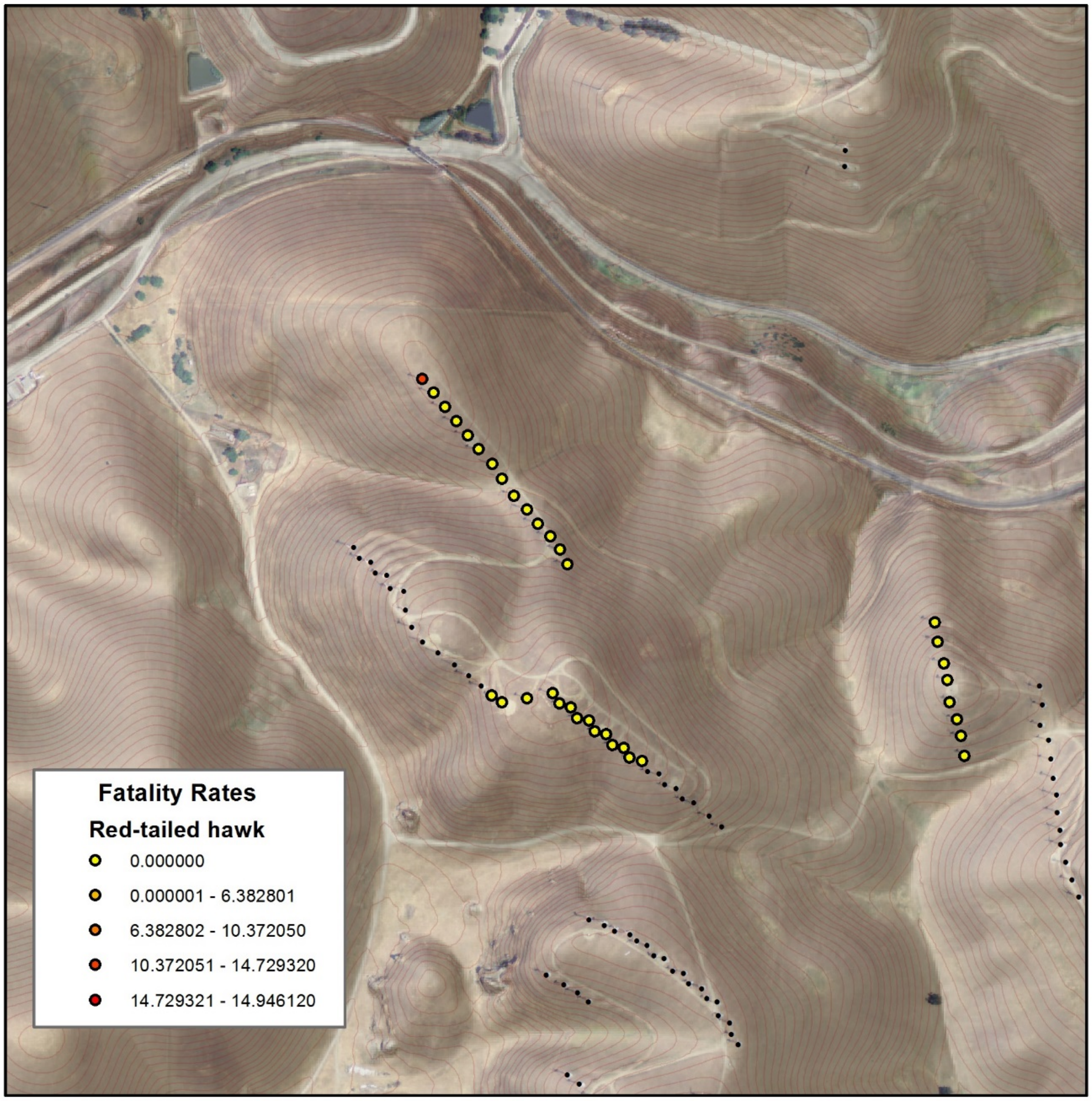

Figure 27: Adjusted Fatality Rates of American Kestrels at Altech 1, Swamp, Viking, and Venture Winds Projects, Altamont Pass Wind Resource Area, 3 April 2012 – 16 February 2015

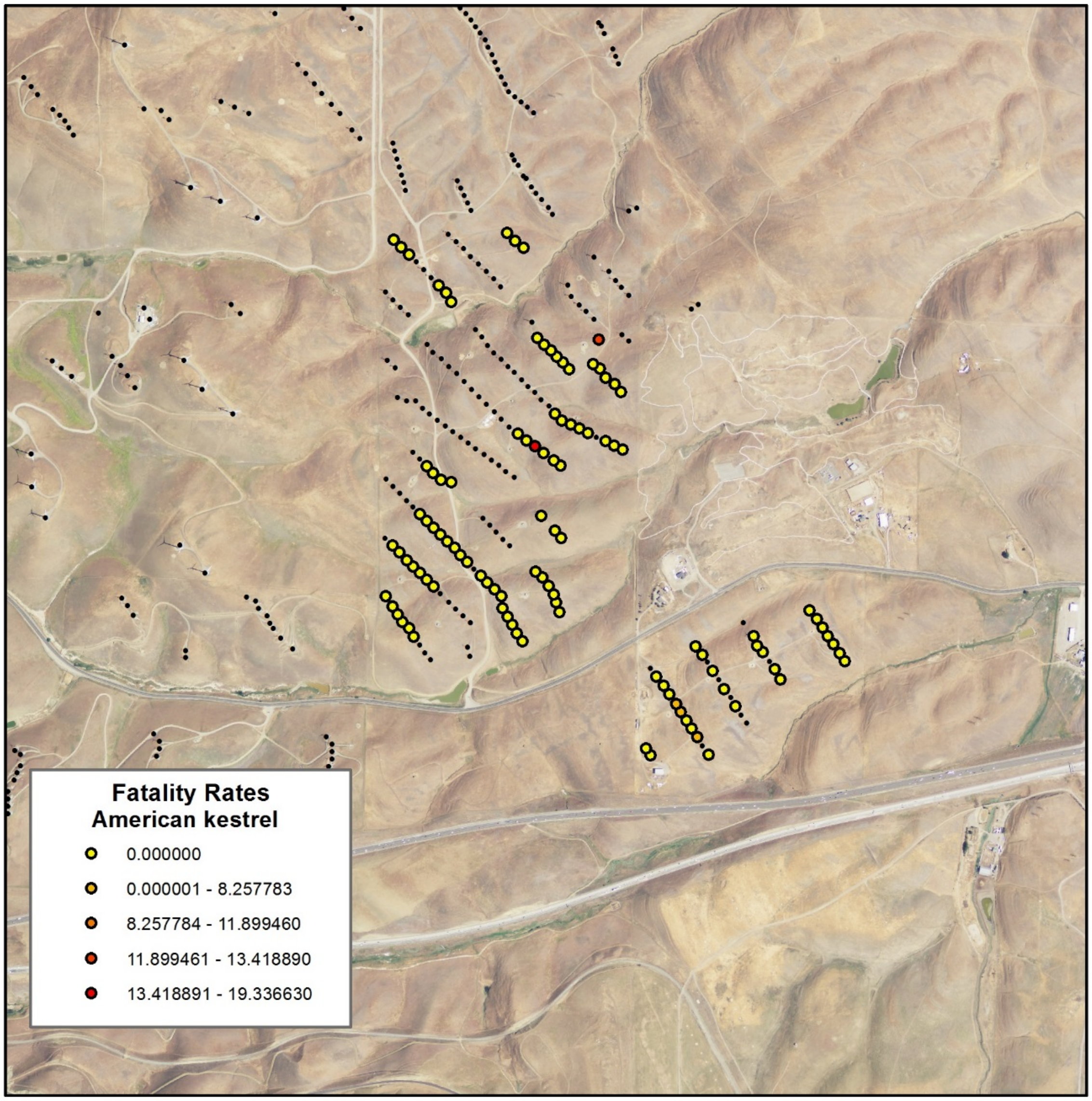

Figure 28: Adjusted Fatality Rates of American Kestrels at the Taxvest Project Near Mountain House, Altamont Pass Wind Resource Area, 3 April 2012 – 16 February 2015

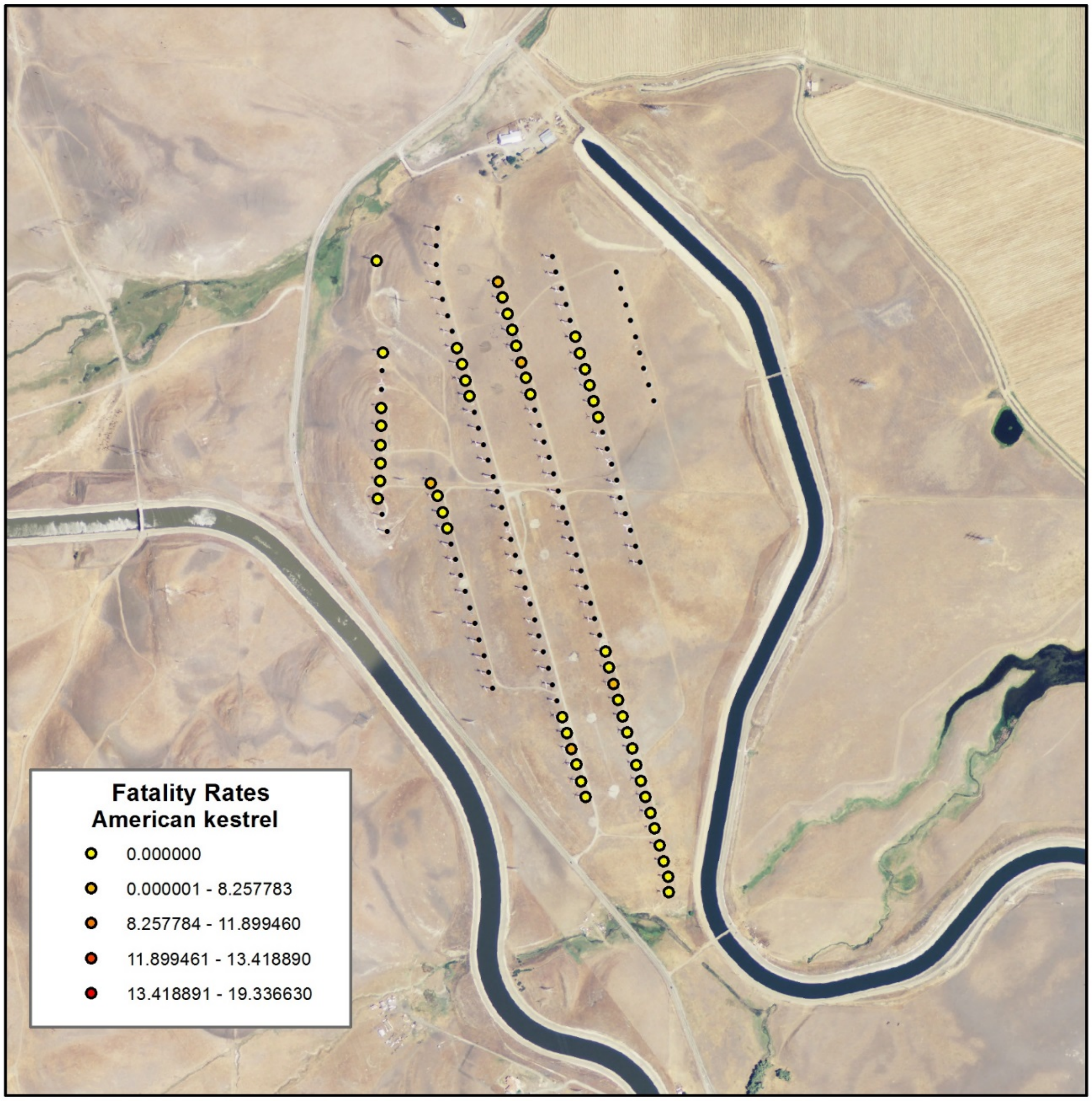

Figure 29: Adjusted Fatality Rates of American Kestrels at the Taxvest Project Off Midway Road, Altamont Pass Wind Resource Area, 3 April 2012 – 16 February 2015

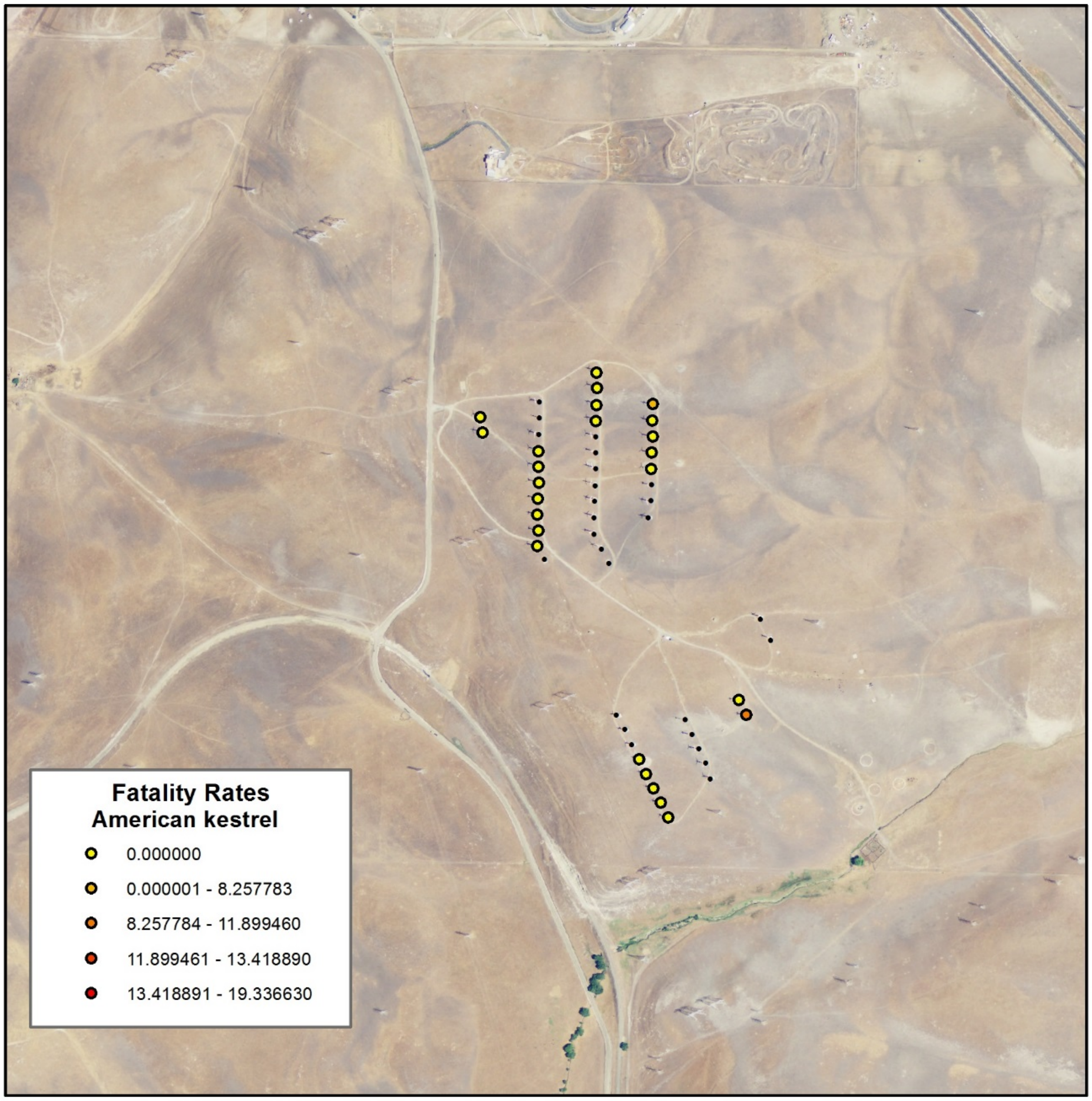

Figure 30: Adjusted Fatality Rates of Burrowing Owls at Altech 1, Swamp, Viking, and Venture Winds Projects, Altamont Pass Wind Resource Area, 3 April 2012 – 16 February 2015

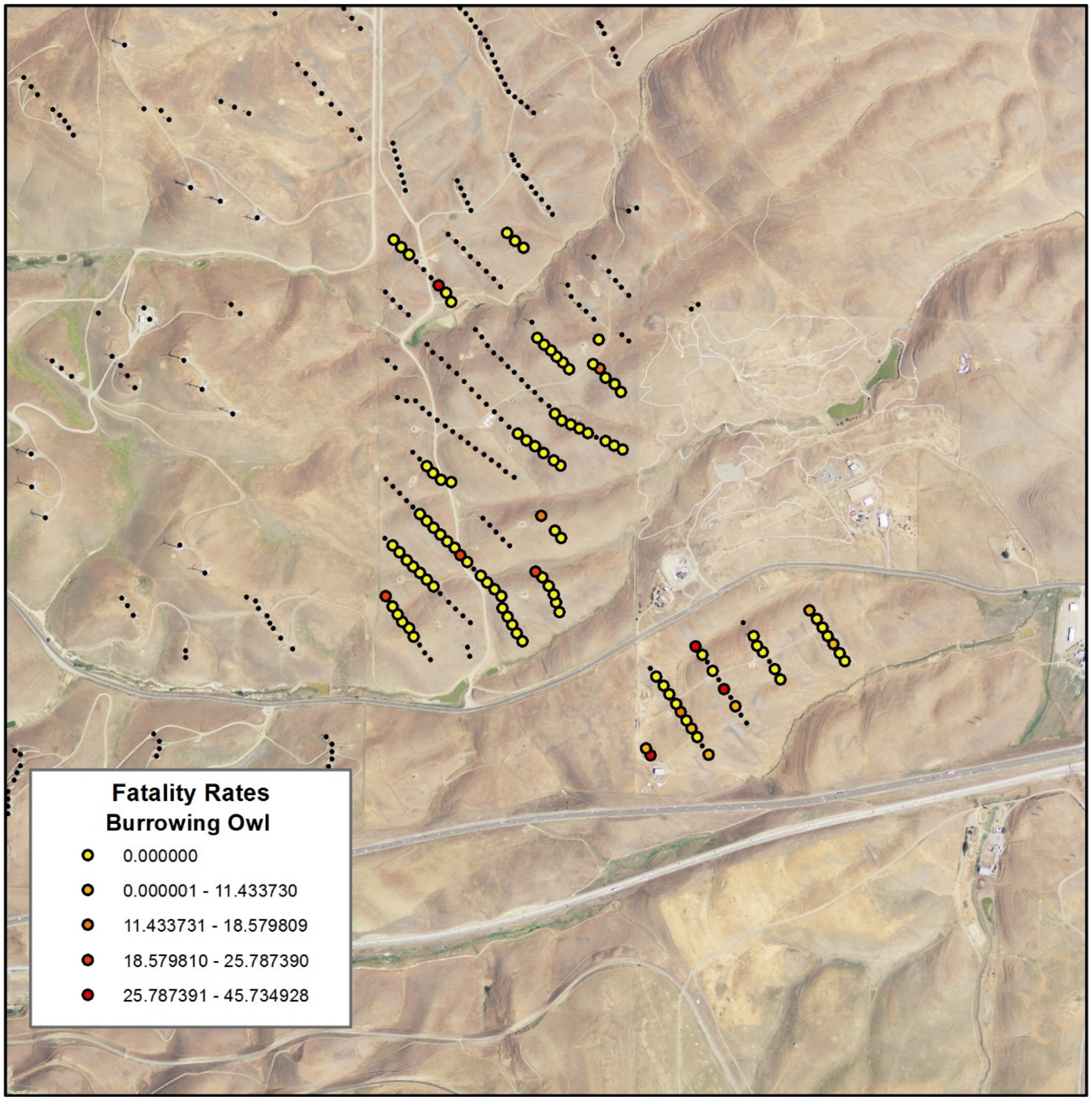

Figure 31: Adjusted Fatality Rates of Burrowing Owls at the Taxvest Project Near Mountain House, Altamont Pass Wind Resource Area, 3 April 2012 – 16 February 2015

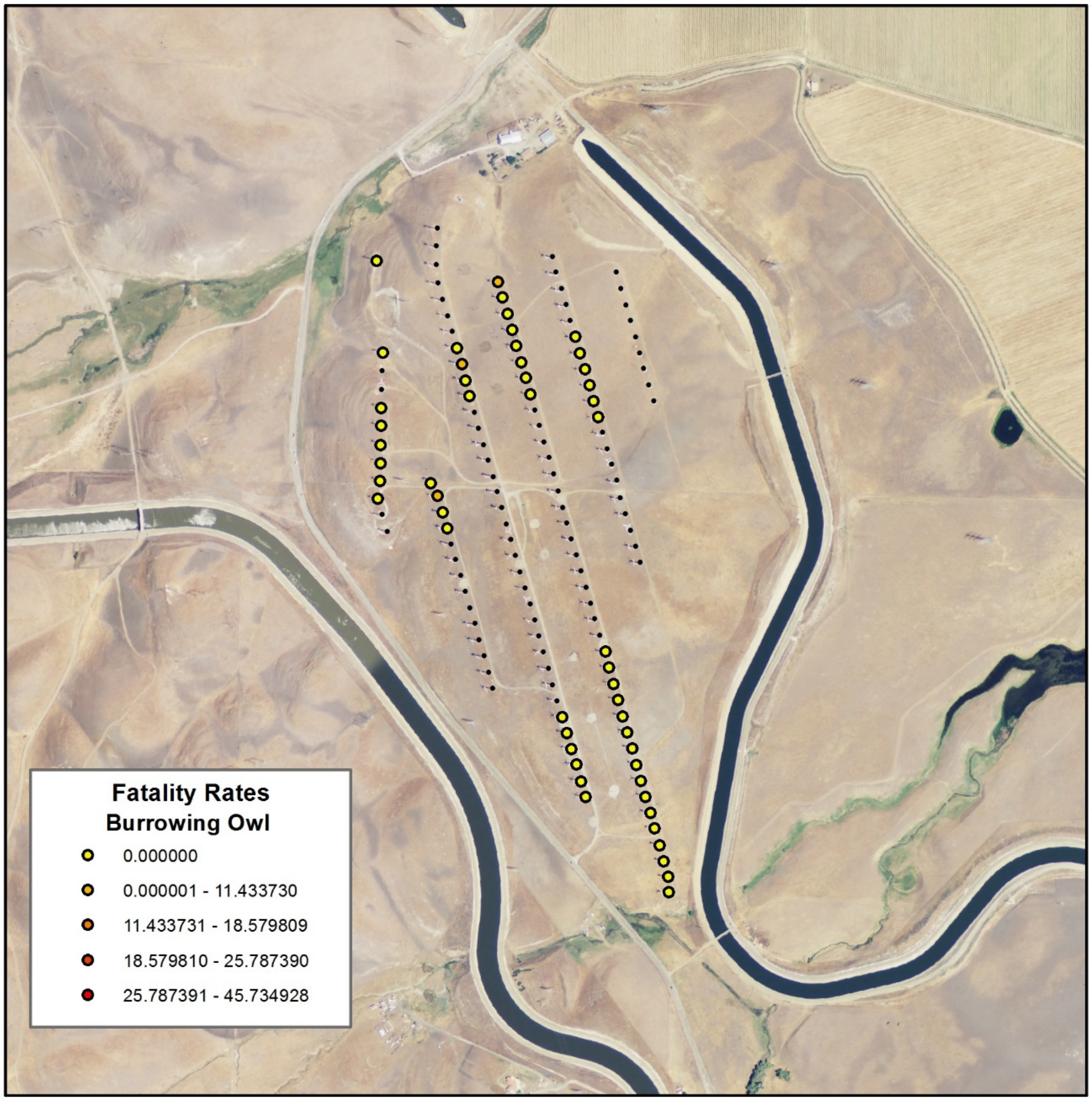

Figure 32: Adjusted Fatality Rates of Burrowing Owls at the Taxvest Project Off Midway Road, Altamont Pass Wind Resource Area, 3 April 2012 – 16 February 2015

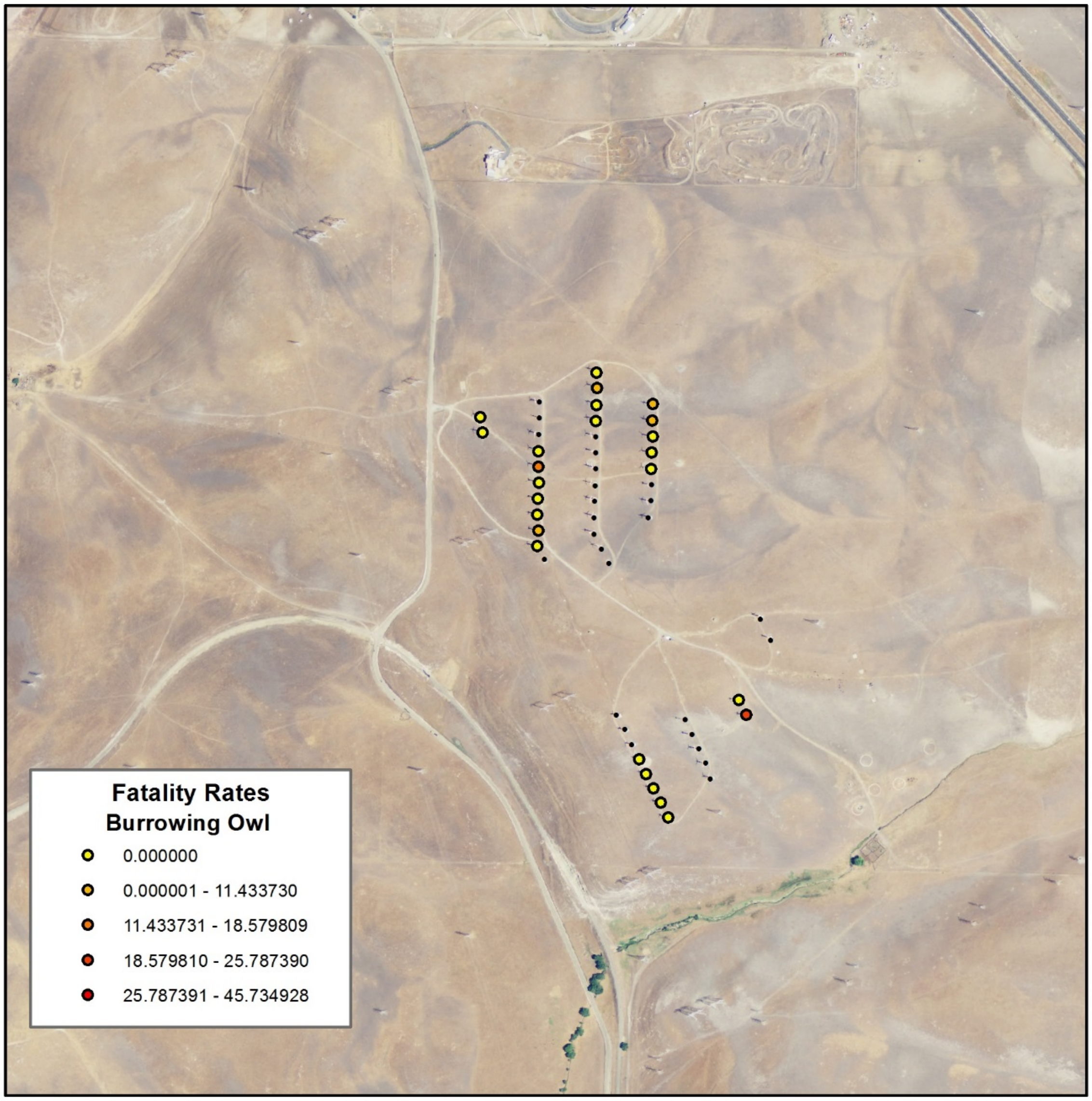

Figure 33: Adjusted Fatality Rates of Rock Pigeons at Altech 1, Swamp, Viking, and Venture Winds Projects, Altamont Pass Wind Resource Area, 3 April 2012 – 16 February 2015

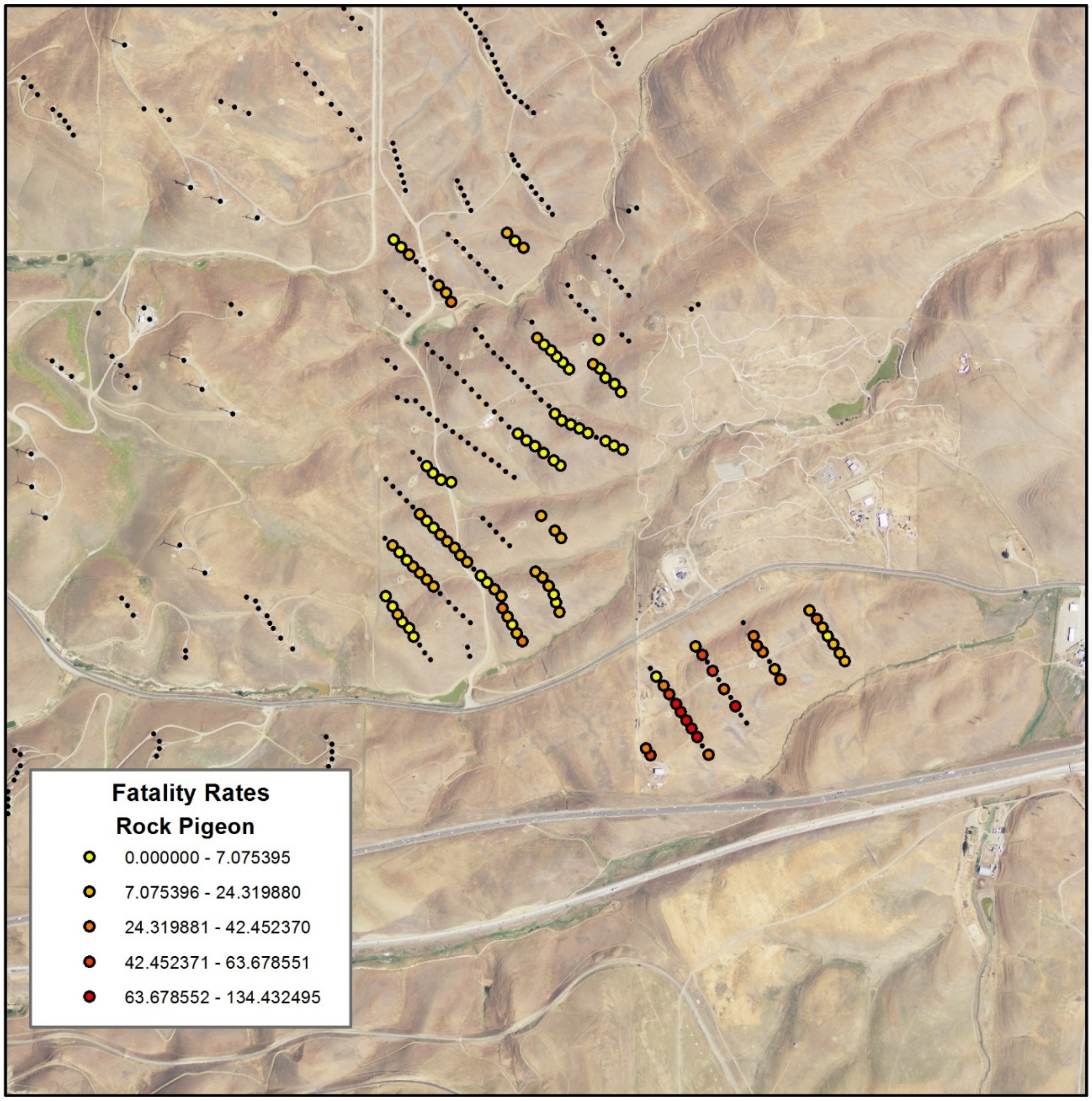

Figure 34: Adjusted Fatality Rates of Rock Pigeons at the Taxvest Project Near Mountain House, Altamont Pass Wind Resource Area, 3 April 2012 – 16 February 2015

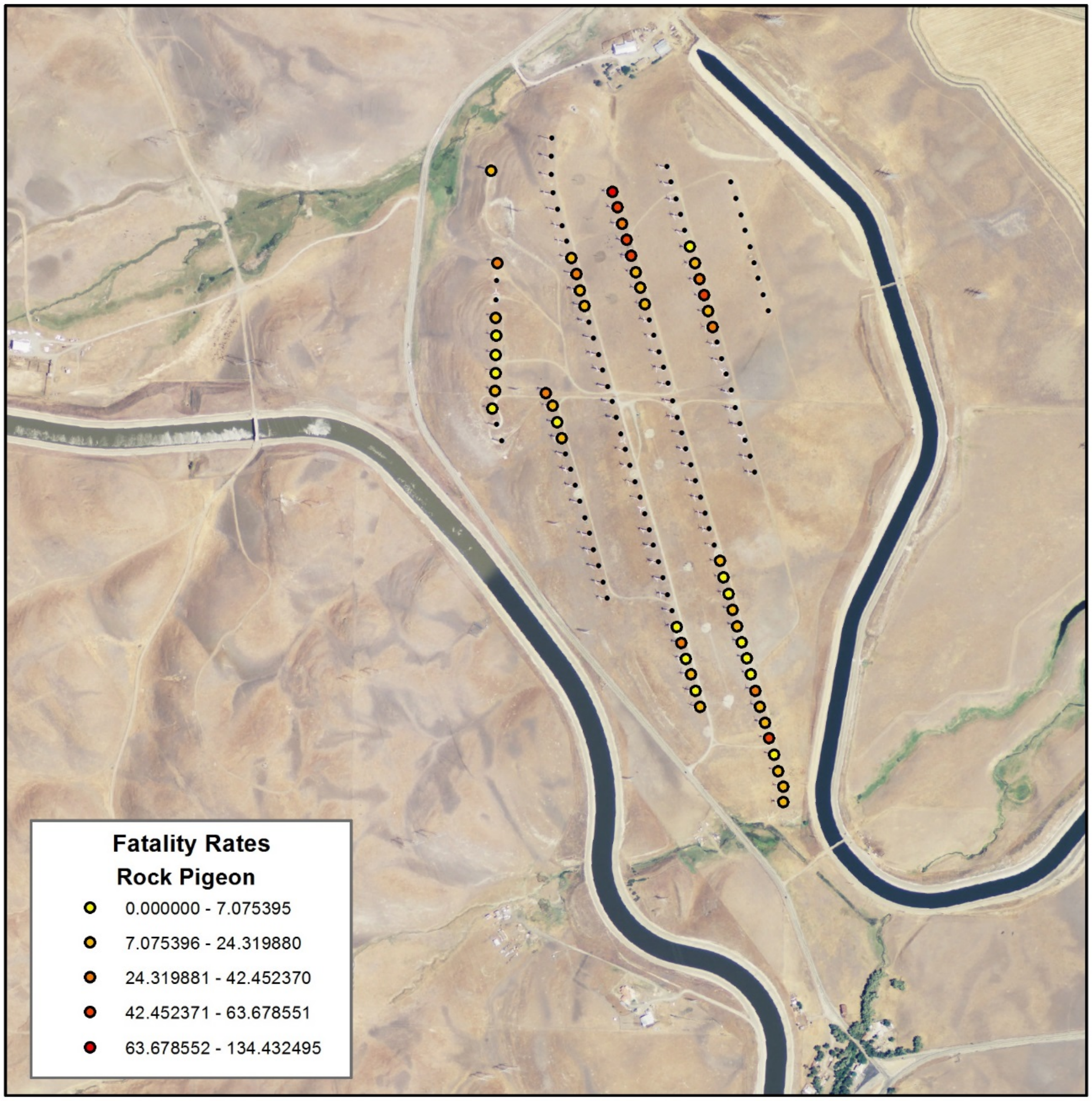

Figure 35: Adjusted Fatality Rates of Rock Pigeons at the Taxvest Project Off Midway Road, Altamont Pass Wind Resource Area, 3 April 2012 – 16 February 2015

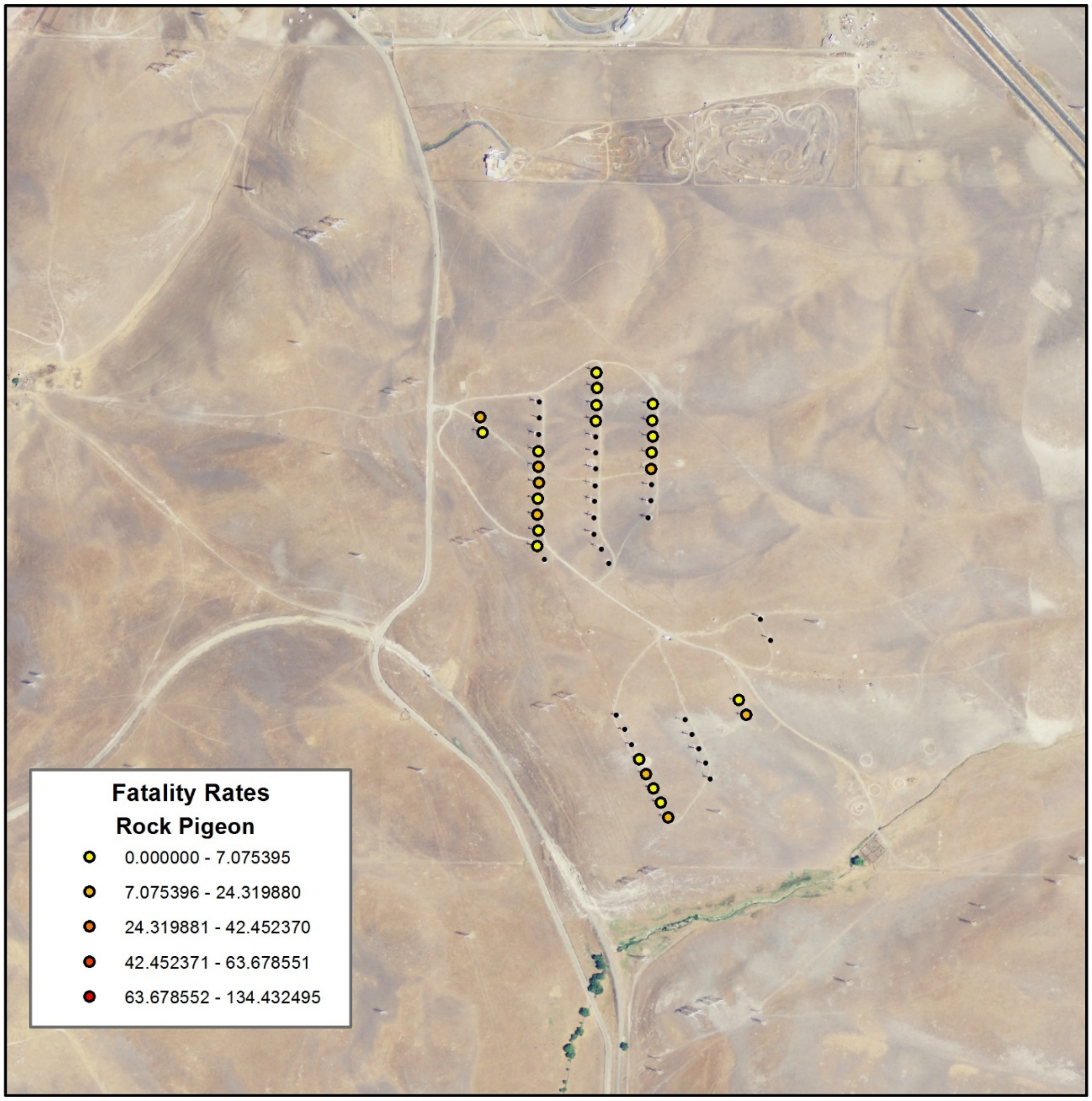

2.4 Discussion

2.4.1 Integrated Detection Trials

In a critical review of carcass persistence trials and searcher detection trials performed at wind projects, Smallwood (2007) listed potential sources of error and bias associated with these trials. The list was long, and for carcass persistence trials it included scavenger swamping (placing more carcasses than a scavenger can process relative to the typical carcass deposition rate), use of inappropriate species, use of carcasses that are too decayed to be attractive to scavengers, terminating trials too early or too late in the case of using mean days to removal, and seasonal and site variation in scavenger activity. Also, searcher detection trials consisting of one opportunity to find placed birds unrealistically simulate detection probabilities of periodic fatality searches, which can result in higher fatality rate estimates. And use of only two or three size classes can misrepresent the factor that explains most of the variation in detection rates, i.e., wide variation in body sizes found at wind turbines.

An easy way to overcome the majority of these shortfalls is to integrate the detection trials into routine monitoring, so that appropriate carcasses, i.e., fresh carcasses of species typically killed by wind turbines, are placed into the search areas in a manner that simulates both the patterns of carcass deposition from wind turbines and searcher detection probabilities. An additional way to more accurately simulate searcher detection probabilities is by not altering the population of carcasses deposited by wind turbines, or in other words, by leaving found carcasses where they were found and by not controlling wildlife deemed to be prey of raptors. It is unlikely that a new statistical treatment or improvements to fatality rate estimators can gain as much accuracy in fatality rate estimates as can improvements to field methods.

This study revealed that the accuracy of species identification declines the longer the time between carcass deposition and searcher detection of the carcass, and these inaccuracies propagate earlier the smaller the bird. The implication of these findings is that many species killed by wind turbines are likely missing from reports of fatality monitoring at wind projects worldwide, especially where the average search rotation was longer than 5 days and where searchers were not as experienced and skilled as the searchers selected for this study. It was also found in this study that many species were misidentified, and some species were reported to have been killed by Ogin wind turbines when in fact they were not the species identified by the searchers.

This study also revealed that estimates of time since death vary widely, and are biased high through discovery times that overlap typical fatality search intervals. The bias in estimating time since death might have resulted in too many birds being attributed to death prior to the last search, resulting in assignment to the wrong season, the wrong year, and in some cases omitted inappropriately from the fatalities contributing to fatality estimates. This bias also calls into question the usefulness of any fatality estimator that is based on estimates of time since death.

In this study, despite having used skilled fatality searchers within a search environment that provided relatively high ground visibility, multiple searches were often needed before available carcasses were detected. The smaller the carcass, the greater the average number of searches per first detection. Because available carcasses were often missed multiple times preceding detection, the “clearing searches” that are often used in fatality monitoring at wind projects likely discard valuable data while not truly clearing the search area of accumulated carcasses.

2.4.2 Fatality Estimates

The fatality rates estimated at wind turbines known a priori to be hazardous to birds were indeed extraordinarily high. The fatality rate for all birds was 45 fatalities/MW/year at the selected turbines, and it was 36 fatalities/MW/year including adjacent turbines to those that were selected for the BACI study. Most of the contribution to these high fatality rates was the detections of fatalities representing many species of small bird. Not only were these wind turbines likely the most hazardous at Forebay, but the shorter than usual search interval probably also managed to detect more of the available small bird fatalities.

The generally higher fatality rates at barely operational wind turbines tends to support the longstanding notion that birds might habituate to nonoperational wind turbines, and are surprised when the normally nonoperational turbines suddenly start operating (Smallwood and Thelander 2004). Birds might grow accustomed to wind turbines that do not operate over long time periods. After repairs are made to a broken turbine and it is reactivated, the habituated birds might fly through the rotor as usual, but this time with lethal consequence. A mitigation option might be to disallow the operations of turbines once their capacity factors fall below a certain threshold over a certain time period.

That the second highest fatality rates occurred at nonoperational wind turbines indicates that more of the collision hazard is in the structure than in the moving blades. There is no doubt that moving blades cause fatalities, as this has been seen numerous times and has been captured in videos from around the world. However, birds colliding with nonmoving wind turbine parts likely happen more often than previously believed. As will be described later in this report, a burrowing owl was seen to collide with a nonoperational wind turbine during a nocturnal survey. A mitigation option might be to remove broken turbines and vacant towers (Smallwood and Thelander 2004) once the turbine has been nonoperational over a threshold time period.

Despite the 5 day search interval, some mortally wounded birds did not contribute to fatality rate estimates because they could not be attributed to a particular wind turbine. For example, on 21 August 2013 Smallwood found an injured red-tailed hawk under the tower of turbine D-2 inside Gate 11. It's right foot and/or leg was injured, and could not hold any weight. The hawk flushed from the ground under the tower and flew low over the ground until it cleared the cattle fence to the west and vanished over the hill. Leyvas and Standish saw this hawk the day earlier near Gate 11. They watched it fly west and out of their sight. This bird was not captured and likely perished shortly after discovery. The bird's mobility prevented it from being attributed to turbine D-2; it is unknown which turbine caused the injury.

Another mobile but injured red-tailed hawk was discovered by the Ogin fatality searchers on 24 April 2013. This hawk was also found near Gate 11 amongst the Enertech wind turbines. It was captured and later euthanized at Lindsay Wildlife Hospital. It did not factor into fatality rate estimation in this study because its injury could not be attributed to a particular wind turbine.

On or the day prior to 10 August 2014 members of the Alameda County Avian Monitor flushed a golden eagle from the N-row in Gate 11. The golden eagle did not look right to the members of the Monitoring Team, but because it glided over to the Forebay field house the Alameda County Avian Monitor declined to report it. Later that day fatality searchers in the Ogin study found the eagle and determined that it was injured. They called Loan Tran of NextEra, and together they captured the eagle. It was taken to Lindsay Wildlife Hospital with a broken ulna and was found to be emaciated and suffering from Trichinosis. It was euthanized.

CHAPTER 3: Raptor Behavior

3.1 Introduction

Careful siting of wind turbines is one of the principal measures available to minimize raptor fatalities caused by collisions with the turbines (Smallwood and Thelander 2004, Smallwood and Karas 2009, Smallwood and Neher 2009). The objective of this approach is to carefully site new wind turbines to minimize the frequencies at which raptors of various species encounter the wind turbines while flying, but most especially while performing specific types of flight behaviors, such as low flights crossing ridge-like topographic features in the case of golden eagles and hovering or kiting in the cases of red-tailed hawks and American kestrels. This objective relies on learning how raptors and other birds react to wind turbines (Osborn et al. 1998, Hoover & Morrison 2005, Smallwood et al. 2009a,b, May et al. 2010, Garvin et al. 2011, Dahl et al. 2013, Hull & Muir 2013, Kitano & Shiraki 2013, Johnston et al. 2014), thus the need for focused behavior surveys. Other modeling approaches have been proposed for assisting with wind project or wind turbine siting decisions, such as migratory flights recorded using GSM telemetry (Katzner et al. 2012, Ainslie et al. 2013), but these data have so far been collected at a resolution too coarse for wind turbine siting. Another approach has been advocated using utilization data, or visual scans (New et al. 2015), but these have data that are prone to bias and error (Madders & Whitfield 2006) and are coarse in resolution and of poor relation to fatality rates (de Lucas et al. 2008, Ferrer et al. 2012). In this study, simple Fuzzy Logic (FL) models (Tanaka 1997) of raptor activity were developed from behavior data collected at the Forebay sites, as well as across Patterson Pass between 15 October 2013 and 24 September 2014 and from the remainder of the APWRA between 13 November 2012 and 11 November 2014.

The Fuzzy Logic approach is a rule-based system useful with noisy data or with zero-dominated data sets, and is applied to events occurring within classes that are assumed to have graduated rather than sharp boundaries (Tanaka 1997). The rules, in this case, consist of assigning likelihood values of an event occurring within a cell of an analytical grid laid over the project area. Likelihood values can range 0 to 1 for each predictor variable, depending on how far a value of the predictor variable differs from the mean where the event has been recorded. The magnitude of each deviation from the mean is assessed by the analyst based on error levels, data distribution, and the analyst's knowledge of the system. In the case of this study, the events were of birds flying over terrain characterized by suites of measured attributes.

The study goal was to accurately predict the locations where golden eagles, red-tailed hawks and American kestrels are most likely to perform flight behaviors putting these species at greater risk of collision with Forebay wind turbines, so that new wind turbines can be sited to avoid these locations. Achieving this goal depended on understanding how these species use terrain and wind, and how they perceive and react to wind turbines. It also depended on understanding patterns of fatality rates in the APWRA, so fatality rate models were also developed for golden eagle and red-tailed hawk (no model was predictive for American kestrel).

3.2. Methods

Multiple types of data were needed to develop collision hazard models. For developing collision hazard models golden eagle, red-tailed hawk, and American kestrel, flight behavior data were collected and then related to terrain. For burrowing owls, burrow locations were recorded and later related to terrain. For all four raptor species, fatality rates were estimated among individual wind turbines monitored throughout the APWRA and over various time periods since 1998. And of course the terrain needed to be measured, and this was done using imagery, digital elevation models, and geoprocessing steps to bring objectivity to decisions about where a slope transitions from trending towards concavity to trending towards convexity, as an example. All of these data and the steps used to integrate them are covered in the following paragraphs.

3.2.1 Behavioral Data

Culminating 14 years of behavior surveys and utilization surveys in the APWRA (Smallwood et al. 2004, 2005, 2009b, c; Smallwood 2013), a new methodology was developed for behavior monitoring to benefit the development of wind turbine collision hazard models. The earlier behavior surveys recorded avian behaviors that were unmapped (Smallwood and Thelander 2004, 2005; Hoover and Morrison 2005; Smallwood et al. 2009b), so no spatial analysis was possible. The mapping of bird locations emerged in 2002, but the 2002 approach was integrated with utilization surveys that were focused primarily on counting birds to estimate relative abundance. This mixing of objectives impinged on both objectives – on both the counting of birds and the mapping of their behavior patterns. On-the-minute mapping of bird locations and behaviors yielded only crude spatial patterns for only a few site-repetitive behaviors such as perching, kiting and hovering. After comparing use rates to fatality rates and seeing no significant spatial or inter-annual relationships between the two rates, it was decided to focus more on the behavior patterns to predict collision hazards. New methods were formulated to map flight behaviors.

Sixteen behavior observation stations were established among the Forebay sites (Figure 36), each location optimized to observe how golden eagles and other raptors behave in the airspace around Ogin's BACI experimental treatment plots. The data from these stations were supplemented with data gathered from 9 stations in Patterson Pass and 36 stations across the rest of the APWRA. Twenty-one of these stations across the APWRA were selected from those that had been ranked from 1st through 30th in order of the number of first observations per hour per km^3 of visible airspace out to the maximum survey radius at each station during use surveys performed by the Alameda County Avian Monitor from 2005 through 2009. Fifteen additional stations were added to Vasco Caves Regional Preserve, Northern Territories, Vasco Winds Energy Project, and the Buena Vista Wind Energy Project in Contra Costa County, where the Alameda County Avian Monitor did very little work.

Behavior sessions at Forebay lasted 30 minutes each and elsewhere they lasted 1 hour each. Between 30 April 2012 and 18 November 2014 there were 1,878 surveys completed for 939 hours. The maximum survey radius depended on the printed map image extent and how far the observer felt comfortable estimating the bird's spatial location and height above ground.

Map extents rarely permitted survey distances of >300 m. One of us (Smallwood) recorded all of the behavior data within Patterson Pass, and additional behavior data were collected across the APWRA by Smallwood, Erika Walther, Brian Karas, and Harvey Wilson.

The 9 Patterson Pass stations were surveyed 167 times (167 hours) from 15 October 2013 to 24 September 2014. The 36 APWRA stations were surveyed 636 times (636 hours) from 13 November 2012 through 11 November 2014. Between all three studies, 1,742 hours of behavior surveys provided the data used for developing collision hazard models reported herein.

Each bird was recorded onto image-based maps of the survey area as point features connected by vector lines depicting the bird's flight path. Height above ground, behavior, and time into the session was recorded into Tascam digital voice recorders fitted with windjammers designed to reduce noise buffeting by high winds. Point features were recorded as often as the observer could record attribute data into the voice recorder. One objective of the behavior sessions was to obtain high quality flight paths and summaries of flight behaviors of individual birds using the surveyed airspace, and it was notably not to count birds, although it was likely that just as many raptors were recorded as would have been counted based on the use survey protocols.

Another objective of the behavior surveys was to learn how birds interact with wind turbines when they approached the wind turbines. Special attention was given to the bird's flight whenever it flew within 50 m of a wind turbine and, in the opinion of the observer, faced the possibility of colliding with the wind turbine. During this time, the bird's approach angle to the turbine was recorded, as well as any changes in flight direction, flight height, behavior, interactions with other birds, and the wind turbine's operating status. Whenever special attention was directed to such flights, the flight observation was termed an "event," or a wind turbine interaction event.

At the start of each behavior session, the observer identified which wind turbines in the survey area were operating, as well as temperature, wind direction, average and maximum wind speed, and percentage cloud cover. Behavior data were transcribed to electronic spreadsheets within 24 hours of collection. Mapped bird location points and line features representing the bird's flight path were then digitized into the GIS.

3.2.2 Burrowing Owl Burrows

Burrowing owl burrows were mapped in sampling plots throughout the APWRA using a Trimble GeoXT GPS, both during the nesting season (Smallwood et al. 2013b) and throughout the year in 2011. Additional burrow mapping efforts were made in follow-up visits in 2012, 2013, and 2014. Most of the burrows that were mapped were nest burrows, but refuge burrows were also included in the data pool. No satellite burrows were used. The Forebay study sites hosted some of the highest densities of burrowing owls in the APWRA.

Figure 36: Locations of Avian Behavior Survey Stations

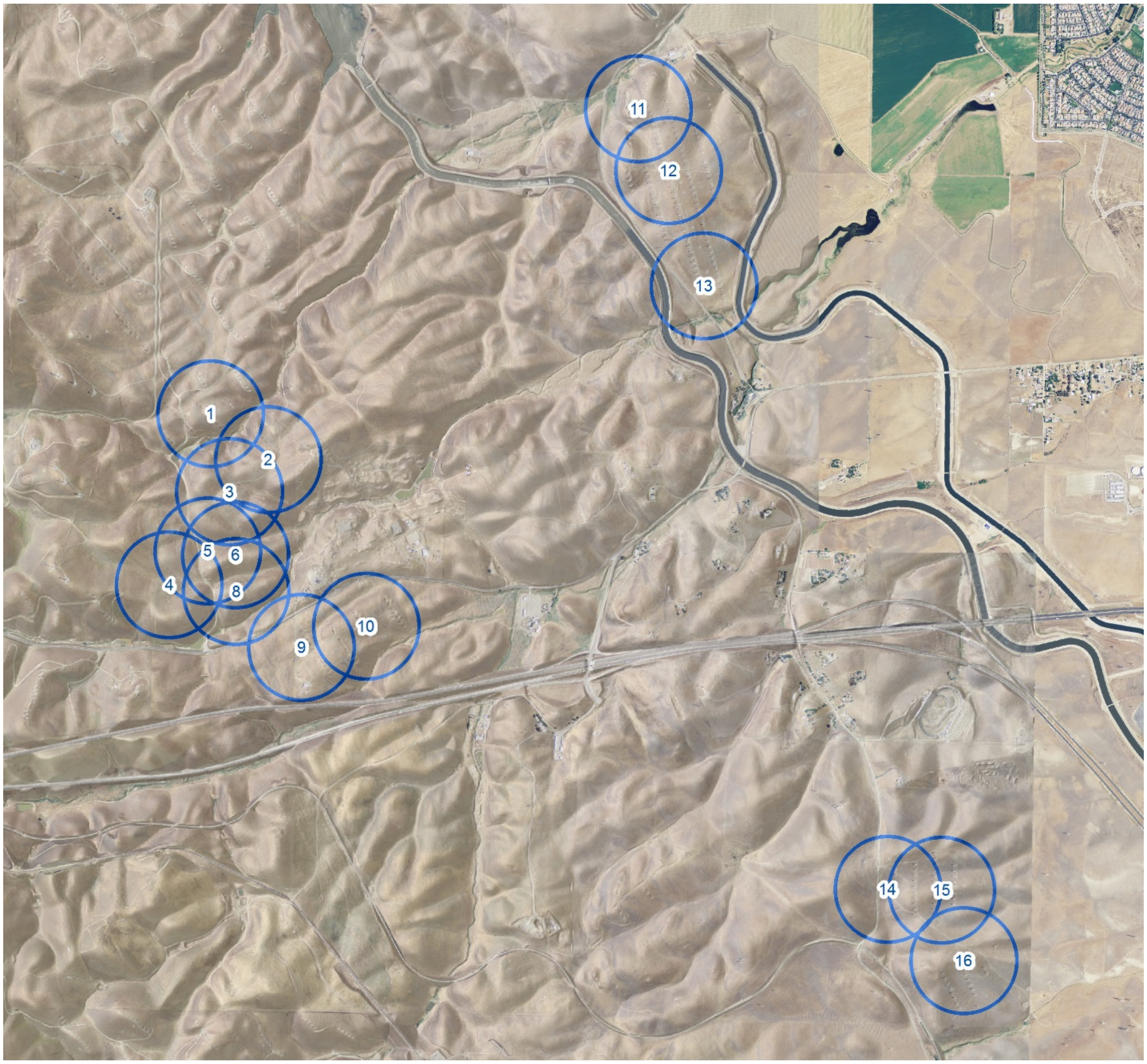

Locations of avian behavior survey stations, with stations 1 through 8 covering the Viking, Swamp, and Altech 1 projects inside Gate 11, stations 9 and 10 covering the Venture Winds project, stations 11 through 13 covering the Taxvest project near Mountain House, and stations 14 through 16 covering the Taxvest project off Midway Road.

3.2.3 Fatality Rates for Collision Hazard Models

Annual fatality rates were estimated at all wind turbines that were searched at least one year between the years 1998 through 2011 in the APWRA. All fatality rates were adjusted for search detection and carcass persistence rates that were averaged among wind projects where trials were performed in similar grassland environments as compared to the APWRA (see Smallwood 2013 and Chapter 1 of this report). Fatality rates were also adjusted for variation in the maximum search radius, based on the method used by Smallwood (2013). Finally, fatality rates were adjusted for monitoring duration to account for the bias warned about in Smallwood and Thelander (2004: App. A); that is, as the number of fatalities is averaged into more years of survey effort, the resulting ratio of fatalities to years will decrease inversely with increasing number of years (Figure 37). This bias, which reflects a relatively constant number of fatalities (numerator) relative to a continuously varying number of years (denominator), was corrected by fitting an inverse function to the data, and then multiplying the ratio of observed to predicted values by the predicted value at 10 years of monitoring (Figure 37). In other words, all fatality rates at individual wind turbines were adjusted to a common 10-year period of monitoring, even if they had been monitored only one year, 4 years, or 10 years, etc. Also, note that the fatality rate metric in this case excluded the turbine's rated capacity, MW.

An alternative source of fatality data for developing collision hazard models would have been data collected from fatality monitoring in the Ogin study, which would have provided more accurate burrowing owl and American kestrel fatality rates due to the 5 day search interval. However, the data set from the Ogin study would have provided only one golden eagle fatality and would not have been prepared in time to develop the models reported herein.

3.2.4 Digital Elevation Model and Terrain Measures

Two separate digital elevation model (DEM) grids were used for this project. The geoprocessing tasks were performed using a 10 foot cell size DEM created by combining DEMs obtained from Contra Costa and Alameda Counties. These data sets were produced using LIDAR data and ARC TIN software by Mapcon Mapping Inc. during 2007-2008. The border of the APWRA was used as a mask to produce the APWRA DEM composed of 25,440,000 10x10-foot cells. This DEM was then converted to a cell centroid point feature class and each point assigned a unique membership number.

Figure 37: Mean Annual Fatalities/Year

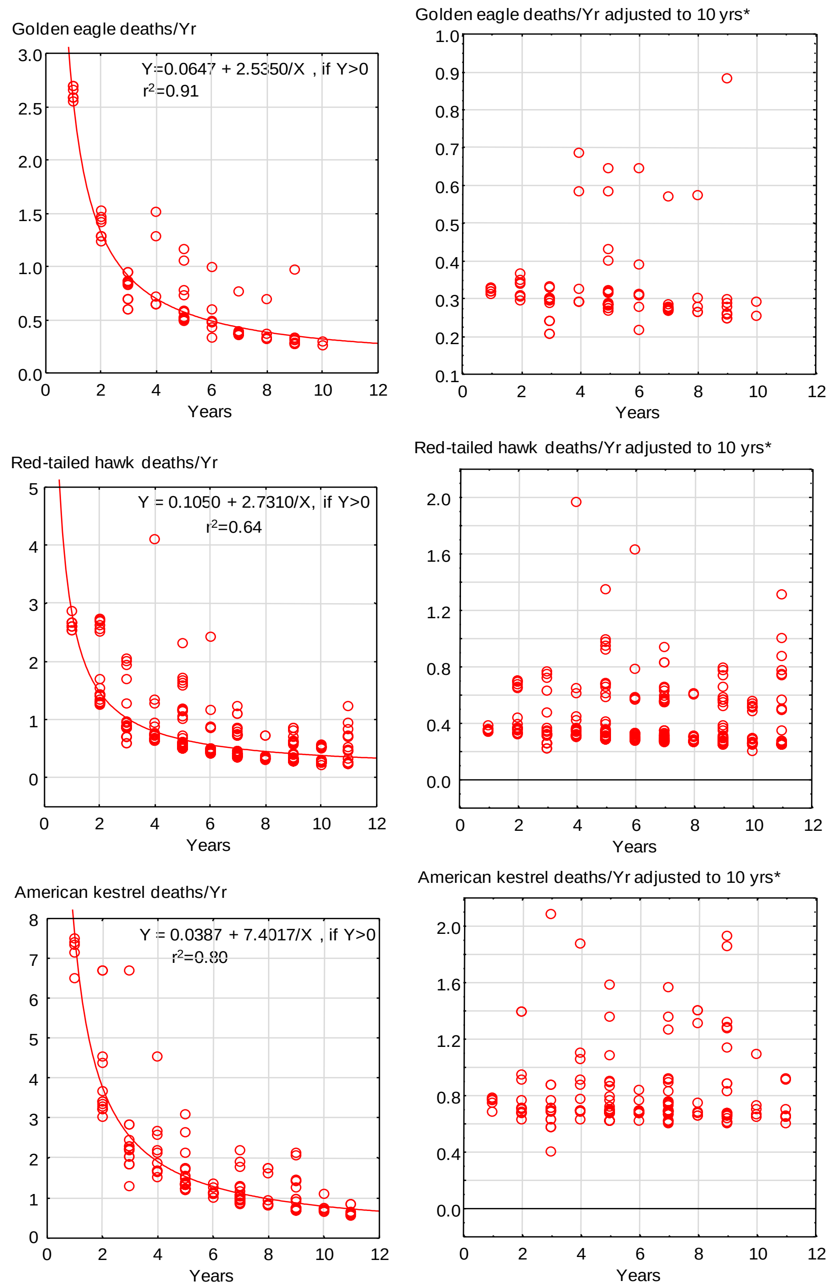

*(Obs/pred$_n$) x pred$_{10}$, where n = years, and pred$_{10}$ = predicted deaths/yr after 10 years, which was 0.3181 for golden eagles, 0.3781 for red-tailed hawks, and 0.7789 for American kestrels

Fatalities declined inversely with the number of years used in the denominator for Golden eagle, red-tailed hawk, and American kestrels (left graphs), so fitting inverse functions to the data removed the effect of number of years on the metric (right graphs).

All derived parameters were calculated for the entire APWRA DEM and attributed into the cell centroid point feature class. An aggregated 792-m buffer served as our mask (limit) for analyzing previously collected bird data against the DEM parameters. The 792-m radius was converted to a 2,600 foot radius and an additional 200 feet was added to buffer modeling data for geoprocessing and to ensure that all bird observations would be covered.

The statistical analyses within the APWRA were limited (masked) to data within the areas searched for raptors within the behavior study areas, bur burrowing owl burrows within the burrowing owl sampling plots, and for fatality rates among the wind turbines that were monitored at least one year (and the grid cells on which the turbines were located). The resulting analytical grids within the behavior survey areas were composed of a 7,548,578 (30%) subset of the 10x10-foot centroid point feature class serving as the study area for the behavior surveys, and a 393,555 subset serving as the study area for the behavior surveys restricted to 10-m buffered ridge-like features. These analytical grids were used to develop and test predictive models.

The same geoprocessing steps were used to characterize terrain attributes as reported in Smallwood and Neher (2010a,b). The Curvature function was used in the Spatial Analysis extension of ArcGIS 10.2 to calculate the curvature of a surface at each cell centroid. A positive curvature indicated the surface was upwardly convex at that cell, a negative curvature indicated the surface was upwardly concave, and a value of zero indicated the cell surface was flat. The curvature data (-51 to 38) were classified using the Natural Breaks (Jenks) function with 3 classes of curvature – convex, concave and mid-range. The break values were visually adjusted to minimize the size of the mid-range class. A series of geoprocessing steps was used, called 'expand,' 'shrink,' and 'region group,' as well as 'majority filter tools' to enhance the primary slope curvature trend of a location. The result was a surface almost exclusively defined as either convex or concave (expressed as 1 or 0, respectively, for the variable *Curve*, and 2 and 1 respectively, for the variable *RidgeValley*, which will appear in the models below). The convex surface areas consisted primarily of ridge crests and peaks, hereafter referred to as ridges, and the concave surface areas consisted primarily of valleys, ravines, ridge saddles and basins, hereafter referred to as valleys.

Line features representing the estimated average centers of ridge crests and valley bottoms were derived from the following steps. ESRI's Flow direction function was used to create a flow direction from each cell to its steepest down slope neighbor, and then the Flow accumulation function was used to create a grid of accumulated flow through each cell by accumulating the weight of all cells flowing into each down slope cell. A valley started where 50 upslope cells had contributed to it in the Flow accumulation function, and a ridge started where 55 cells contributed to it. The flow direction and flow accumulation functions were applied to the ridges by multiplying the DEM by -2 to reverse the flow. Line features that represented ridges and valley bottoms were derived from ESRI's gridline and thin functions, which feed a line through the centers of the cells composing the valley or ridge. Thinning put the line through the centers of groups of cells ≥40 in the case of valleys. Lines representing ridges and valleys were also clipped to identify the major valleys and major ridges, or the topographic features dominating the local skyline and local drainage systems.

The two-foot slope analysis grid was used to create polygons with a relatively gentle slope. A Standard Deviation classification was used to identify areas with < 7.4 % slope. These areas were then converted to polygons and intersected with the ridge/valley lines to determine polygons associated with either ridge or valley descriptions. The borders of these polygons were converted to lines and combined with the ridge/valley line datasets, respectively, and polygons in valley features were termed *valley polygons* and polygons on ridge tops were termed *ridge polygons*.

Horizontal distances (m) were then measured between each DEM grid cell and the nearest valley bottom boundary (in the valley line combined data set) and the nearest ridge top boundary or ridgeline (in the ridgeline combined data set), referred to as *distance to valley* and *distance to ridge*, respectively. These distances were measured from the DEM grid cell to the closest grid cell of a valley bottom or ridgeline, respectively, not including vertical differences in position. The *total slope distance* was the sum of *distance to valley* and *distance to ridge*, and expressed the size of the slope. The DEM grid cell's position in the slope was also expressed as the ratio of *distance to valley* and *distance to ridge*, referred to as the *distance ratio*. This expression of the grid cell's position on the slope removed the size of the slope as a factor. The same measurements were made to major valleys and major ridges.

The vertical differences between each DEM grid cell and the nearest valley bottom boundary and nearest ridge top boundary or ridgeline were referred to as *elevation difference*, and this measure also expressed the size of the slope. In addition to the trend in slope grade at each DEM grid cell, the *gross slope* was measured as the ratio of *elevation difference* and *total slope distance*. The DEM grid cell's position on the slope was also expressed as the ratio of the elevation differences between the grid cell and the nearest valley and between the grid cell and the nearest ridge, referred to as *elevation ratio*. Additionally, the grid cell's position on the slope was measured as the average of the percentage distance and the percentage elevation to the ridge top. This mean percentage was named *percent up slope*, and provided a more robust expression of the grid cell's position on the slope. The same measurements were made to major valleys and major ridges; leading to the variable we named *percent up major terrain slope*. Thus, on a small hill adjacent to a major hill in the area, a grid cell could be 90% under *percent up slope* and only 30% under *percent up major terrain slope*.

Percent up slope did not distinguish a grid cell's position between slopes on large hills versus medium or small-sized hills, so the local topographic influence of the feature where each cell was located was expressed by the variable *hill size*, which was the elevation difference between the nearest valley bottom polygon and nearest prominent ridge top polygon. *Major hill size* was the elevation difference between the nearest major valley bottom and nearest major ridge top.

Breaks in slope were characterized with the ratio of *slope to gross slope*, and the ratio *gross slope to major gross slope* was also calculated. Additional ratios included *local to major hill size*, *local to major ridge elevation*, and *local to major valley elevation*.

Each DEM grid cell was classified by *aspect* according to whether it faced north, northeast, east, southeast, south, southwest, west, northwest, or if it was on flat terrain. Each grid cell was also categorized as to whether its center on the landscape was windward, leeward or perpendicular to the prevailing southwest and northwest wind directions as recorded during the behavior observation sessions.

The study area was divided into smaller polygons of land with like aspect, creating a predictor variable termed *Subwatershed Orientation*. Existing sub-watershed polygons already had been created between ridgelines and valley bottom lines. These watershed polygons were further divided by reviewing the existing 2-foot hypsography (contour) data and then dividing them into orientation polygons where the overall orientation of the contours changed. An orientation line feature layer was digitized with a line for each new polygon following the best observed orientation of that polygon's contours. Python scripts attributed the new line with its compass orientation, e.g., N, NNE, NE. These lines were non-directional, so a compass value could be either the returned value or the direction 180 degrees opposite. These same scripts calculated a perpendicular compass direction to the returned orientation line direction. The perpendicular orientation direction had two possible values, differing by 180 degrees based on which side of the ridge the line described. A reference point within each orientation polygon was georeferenced by scripts to a generalized aspect grid of the study area. The scripts determined the correct perpendicular orientation and calculated the compass direction of the orientation polygon.

Using similar steps, a predictor variable termed *Ridge Orientation* was created. Ridgelines were buffered by 10 m and the resulting ridgeline polygons classified by orientation: north to south, north-northwest to south-southeast, northwest to southeast, west-northwest to east-southeast, west to east, west-southwest to east-northeast, southwest to northeast, and south-southwest to north-northeast. Flight paths crossing ridgelines were related to these Ridge Orientation polygons in use and availability analysis.

3.2.5 Steps to Identify Saddles, Notches, and Benches

Because a large amount of evidence links disproportionate numbers of raptor fatalities to wind turbines located on aspects of the landscape that are lower than immediately surrounding terrain or that represent sudden changes in elevation, a special effort was directed toward identifying ridge saddles, notches in ridges, and benches of slopes. Benches of slopes are where ridge features emerge from hill slopes that extend above the emerging ridge. These types of locations are where winds often compress by the landscape to create stronger force, and where raptors typically cross hilly terrain or spend more time to forage for prey. Compared to surrounding terrain, these types of features are often relatively flatter or shallower in slope and sometimes include lower elevations (e.g., saddles). Geoprocessing steps were used to provide some objectively to the identification of these features, but judgment was also required because conditions varied widely in how such features were formed and situated.

The same procedures were used as used in the ridge/valley selection. The two foot slope analysis grid was used to create polygons with a relatively gentle slope. A Standard Deviation classification was used to identify areas with < 7.4 % slope. These areas were then converted to polygons. Those polygons not associated with ridge or valley polygons were examined manually. Where these polygons were visually associated with saddle and or step features, they were identified as *hazard sites* representing saddles, notches, or benches. Maps depicting contours of the variable *percent up slope* were also examined, because these contours readily revealed sudden breaks in slope typical of saddles, notches, and benches, which were then also represented with polygons.

3.2.6 Associations between Bird Behaviors and Terrain Attributes

The location of each raptor was characterized by aspect, slope, rate of change in slope, direction of change in slope, and elevation. These variables were also used to generate raster layers of the study area, one raster expressing the aspect of the corresponding slope (hereafter referred to as *aspect*), and the other expressing whether the landscape feature was tending toward convex versus concave orientation (expressed in a variable named *curve*). These features were defined using geoprocessing.

Fuzzy logic (FL) modeling (Tanaka 1997) was used to predict the likelihood each grid cell would be used by golden eagle, red-tailed hawk, and American kestrel. FL likelihood surfaces were first created by each selected predictor variable. The mean, standard deviation, and standard error were calculated for each predictor variable among the grid cells where each targeted bird species was observed during standard observation sessions. These statistics formed the basis from which FL membership was assigned to grid cells. Depending on the pattern in the data, FL membership was assigned values of 1 whenever the value of the predictor variable was within a certain prescribed distance in value from the mean, oftentimes within 1 SD, but sometimes within 1 or 2 SE. FL membership values of 1 expressed confidence that grid cells with the corresponding value range for the predictor variable are likely to be visited by the target species. FL membership values of 0 were assigned to grid cells that were far from the mean value, usually defined by prescribed distances from the mean such as >2 SD from the mean. FL membership values of 0 expressed confidence that grid cells with the corresponding value range for the predictor variable are unlikely to be visited by the target species. All other grid cells were assigned FL membership values according to the following formulae, assuming that the likelihood of occurrence of each species will grade gradually rather than abruptly across grid cells that vary in value of the predictor variable (Y):

$$0.5 \times (1 - \cos(\pi \times (Y - V_c) \div (V_f - V_c))) \text{ below the mean}$$

$$0.5 \times (1 + \cos(\pi \times (Y - V_c) \div (V_f - V_c))) \text{ above the mean,}$$

where V_c represented the variance term (SD or SE) closer to the mean and V_f represented the variance term farther from the mean.

FL likelihood values were then summed across predictor variables contributing to a species-specific model. In earlier efforts to develop FL models for golden eagle, red-tailed hawk, American kestrel and burrowing owl in other parts of the APWRA, natural breaks were used to divide the summed values into 4 classes, but the percentages of study area composing these classes remained consistent despite use of natural breaks. Therefore, this time the class divides were established at 63.5%, 83.5%, and 95.5%. Class 1, including FL likelihood values <63.5% (i.e., 63.5% of the study area), represented the suite of grid cells including fewer bird observations other than expected. Class 2, including FL likelihood values between 63.5% and 83.5% (i.e., 20% of the study area), represented the suite of grid cells including about equal or slightly greater than equal bird observations other than expected. Class 3, including FL likelihood values between 83.5% and 95.5% (i.e., 12% of the study area), represented the suite of grid cells including more bird observations other than expected. And class 4, including the upper 4.5% of FL likelihood values, represented the suite of grid cells including substantially more bird observations other than expected.

The performance of each model was assessed by the magnitude of the ratio of the observed number to the expected number of observations representing a dependent variable and occurring within the suite of conditions specified by each FL surface class. Dependent variables included fatality rates (golden eagles only), flights <180 m above ground, flights across ridge features and <180 m above ground, and wind turbine interaction events. FL surface models were later projected across the Forebay sites and intervening areas.

Because burrowing owls tend to nest low on the slope, it would be rare for a predictive model of burrowing owl burrow locations to correspond with terrain where burrowing owls are killed by wind turbines. Therefore, we developed a burrowing owl fatality model and relied on hazard classes 3 and 4 of this model wherever the cell centroids were located within 60 m of class 4 predicted by the burrow model. Otherwise, all class values of the burrow model remained unchanged.

3.3 Results

3.3.1 Surveys

The number of grid cells that included bird points recorded during behavior surveys totaled 7,023 for golden eagle, 11,486 for red-tailed hawk, 2,430 for American kestrel, and 79,720 for all birds. During the surveys at Forebay, the number of bird observations recorded totaled 404 golden eagles, 1,008 red-tailed hawks, and 497 American kestrels. Additional flights were recorded for 2 white-tailed kites, 2 bald eagles, 88 ferruginous hawks, 3 rough-legged hawks, 97 Swainson’s hawks, 1 osprey, 40 prairie falcons, 2 peregrine falcons, 51 northern harriers, 1,268 turkey vultures, 1,789 common ravens, 37 double-crested cormorants, 62 mourning doves, 1,065 rock pigeons, 35 barn swallows, 11 Say’s phoebes, 3,883 European starlings, 111 loggerhead shrikes, 62 horned larks, 392 tricolored blackbirds, 8,060 Brewer’s blackbirds, 129 western meadowlarks, 86 killdeer, 307 California gulls, 5,152 gulls. No birds or their behaviors were recorded in 228 surveys, or 114 hours of the total survey time.

During the surveys at Patterson Pass the rest of the APWRA, the number of bird observations recorded totaled 842 golden eagles, 1,585 red-tailed hawks, 262 American kestrels. Among all three studies the behaviors and locations of 29,755 birds were recorded. Rates of bird detections, or birds per hour, were 0.43 golden eagles, 1.07 red-tailed hawks, 0.53 American kestrels at Forebay, and 1.05 golden eagles, 1.97 red-tailed hawks, and 0.33 American kestrels among the stations throughout the rest of the APWRA. Among all three studies, the detection rates during behavior surveys totaled 0.72 golden eagles per hour, 1.49 red-tailed hawks per hour, and 0.44 American kestrels per hour.

Many thousands of bird flight paths were recorded during the behavior surveys at Forebay (Figures 38 through 40). The flight path data were so dense in these figures that little meaningful pattern could be discerned until data were depicted for one bird species at a time. One meaningful pattern that could be discerned through careful examination was the greater densities of flight paths over concave valley-like topographic features and relatively lower terrain.

Golden eagle flight paths no higher than 160 m followed concave terrain features, but not as a rule (Figures 41 through 43). Nevertheless, the concentration of golden eagle flights was through the deepest ravines and around the bases of the largest hills.

The flight paths of red-tailed hawks under 160 m, on the other hand, were more concentrated over slopes facing southwest, west, or northwest (Figures 44 through 46). But they also often traversed the relatively low terrain.

Those flight paths of American kestrels less than 160 m appeared to be concentrated along the rows of wind turbines and along electric distribution lines (Figures 47 through 49). However, American kestrels also flew over concave valley-like structures and over relatively low terrain.

Burrowing owl flight paths were relatively short and happened to be seen where nocturnal activity was concentrated (see Chapter 3) and fatality rates were high (see Chapter 1) (Figure 50).

There were 1,325 wind turbine events recorded during the behavior surveys at Forebay (Table 5). There were 27 golden eagle events, 14 of which occurred at nonoperating wind turbines during maximum wind speeds of 11.7 km/hr (SD = 4.0) and 13 at operating wind turbines during maximum wind speeds of 17.9 km/hr (SD = 3.7). There were 105 red-tailed hawk events, 83 of which occurred at nonoperating wind turbines during maximum wind speeds of 12.1 km/hr (SD = 7.0) and 22 at operating wind turbines during maximum wind speeds of 21.3 km/hr (SD = 6.2). There were 99 American kestrel events, 73 of which occurred at nonoperating wind turbines during maximum wind speeds of 9.2 km/hr (SD = 6.6) and 26 at operating wind turbines during maximum wind speeds of 18.0 km/hr (SD = 6.8). Many of the events happened when birds were distracted by other birds, such as during courtship or harassment (mobbing). Many others occurred when birds of prey were distracted by foraging, such as while diving on prey or chasing or approaching prey.

Figure 38: Flight Patterns of All Birds During Behavior Surveys at Altech 1, Swamp, Viking, and Venture Winds Projects, Altamont Pass Wind Resource Area

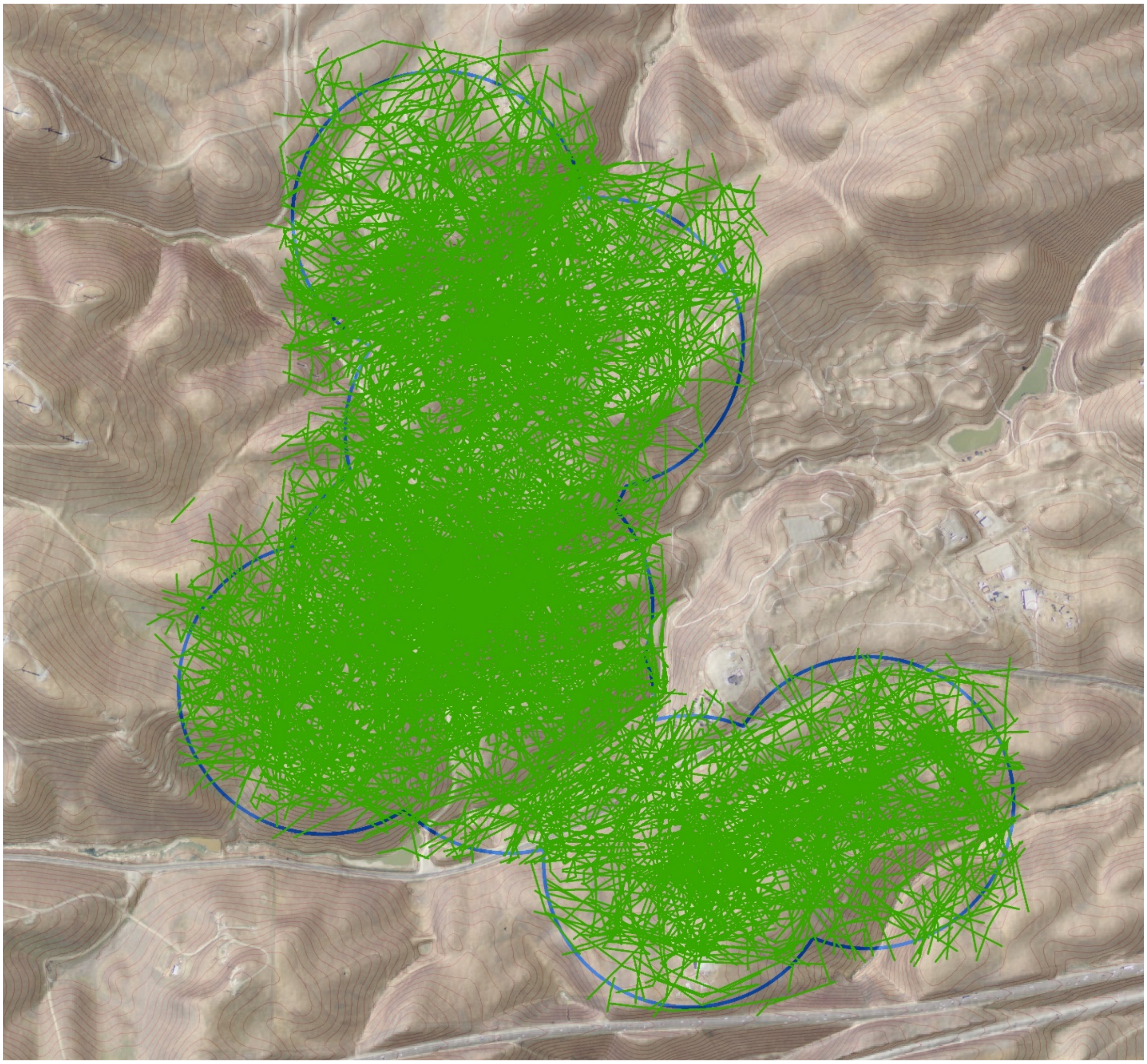

Figure 39: Flight Patterns of All Birds During Behavior Surveys at the Taxvest Project Near Mountain House, Altamont Pass Wind Resource Area

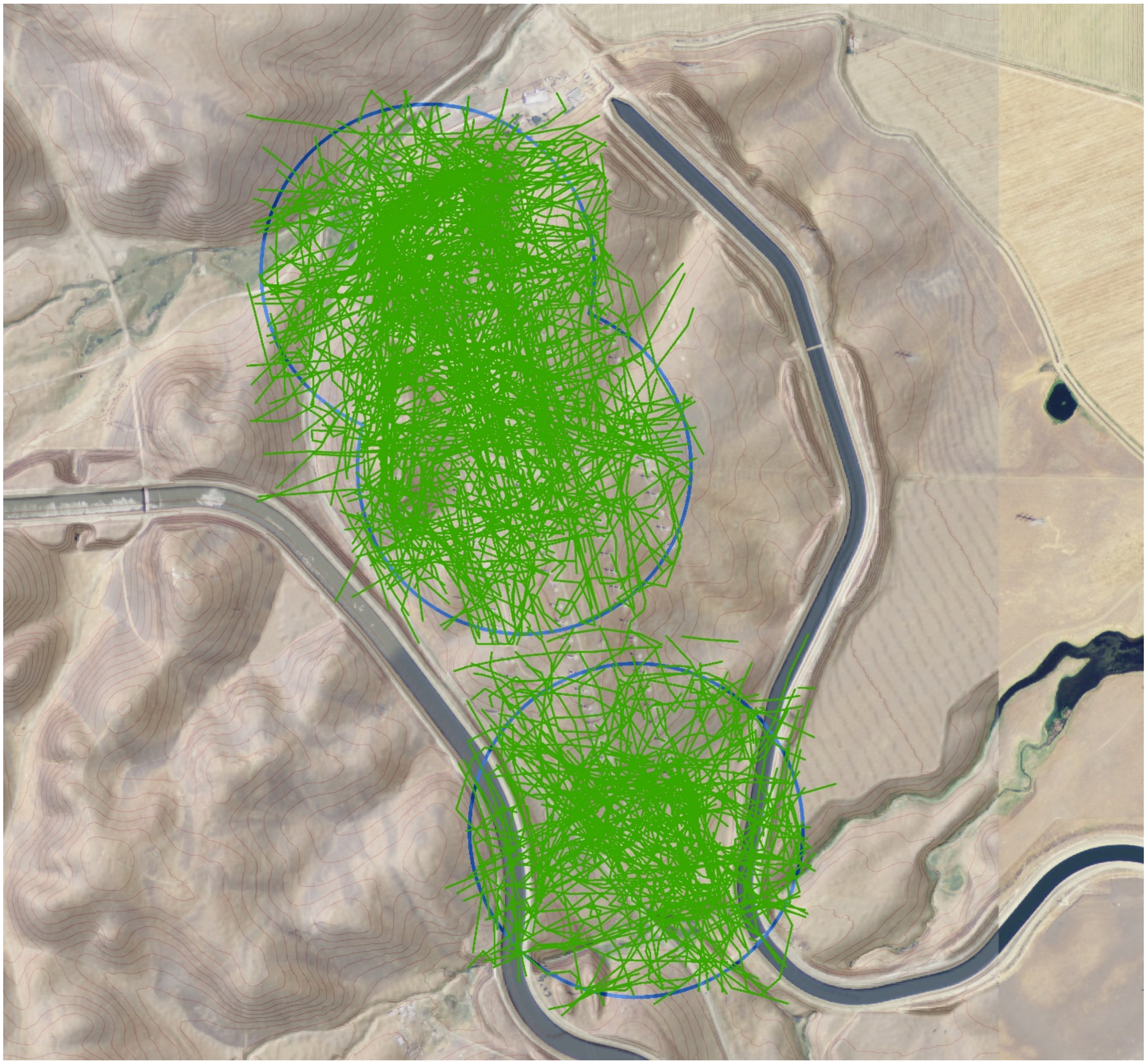

Figure 40: Flight Patterns of All Birds During Behavior Surveys at the Taxvest Project Off Midway Road, Altamont Pass Wind Resource Area

Figure 41: Flight Patterns of Golden Eagles During Behavior Surveys at Altech 1, Swamp, Viking, and Venture Winds Projects, Altamont Pass Wind Resource Area

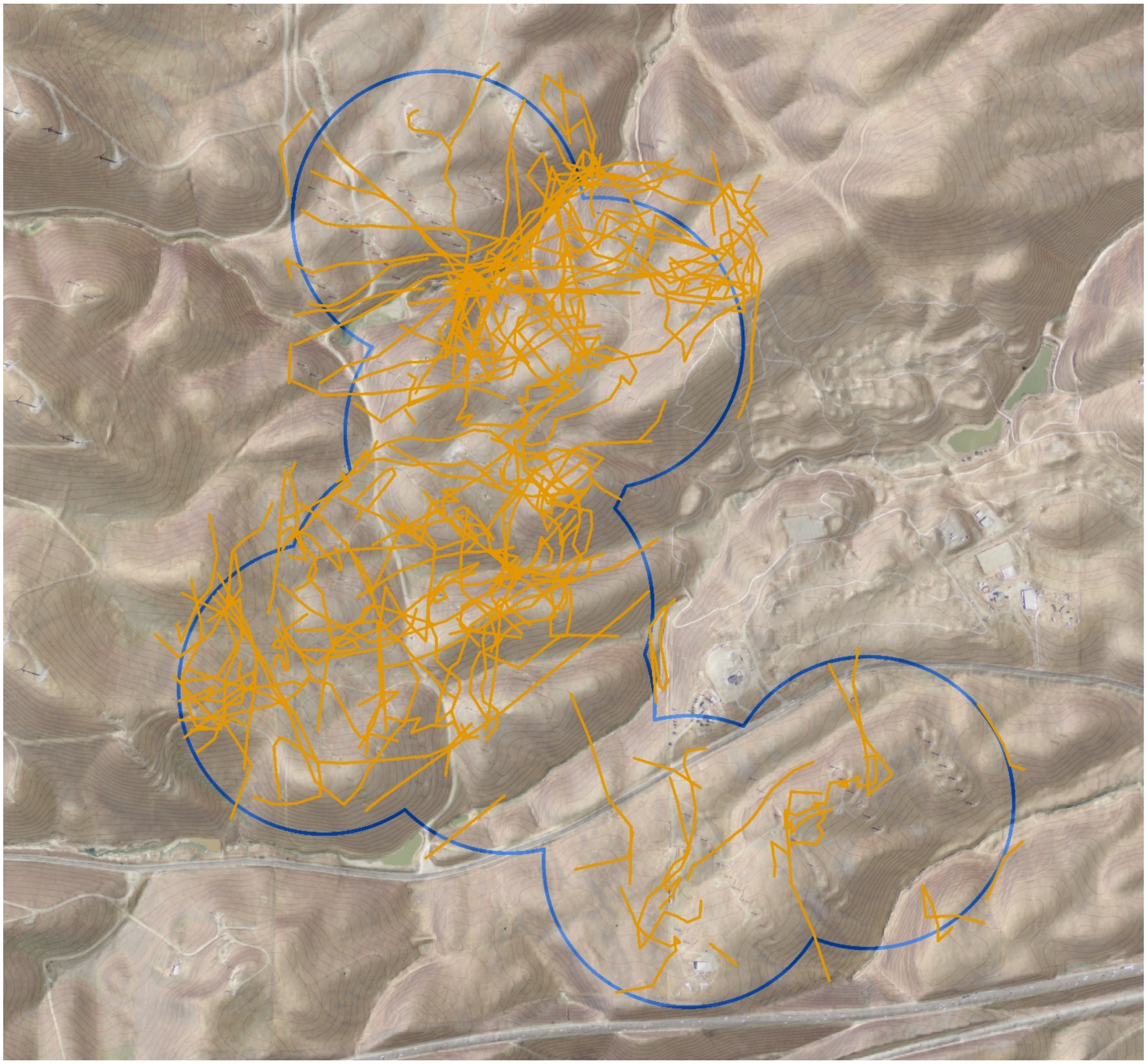

Figure 42: Flight Patterns of Golden Eagles During Behavior Surveys at the Taxvest Project Near Mountain House, Altamont Pass Wind Resource Area

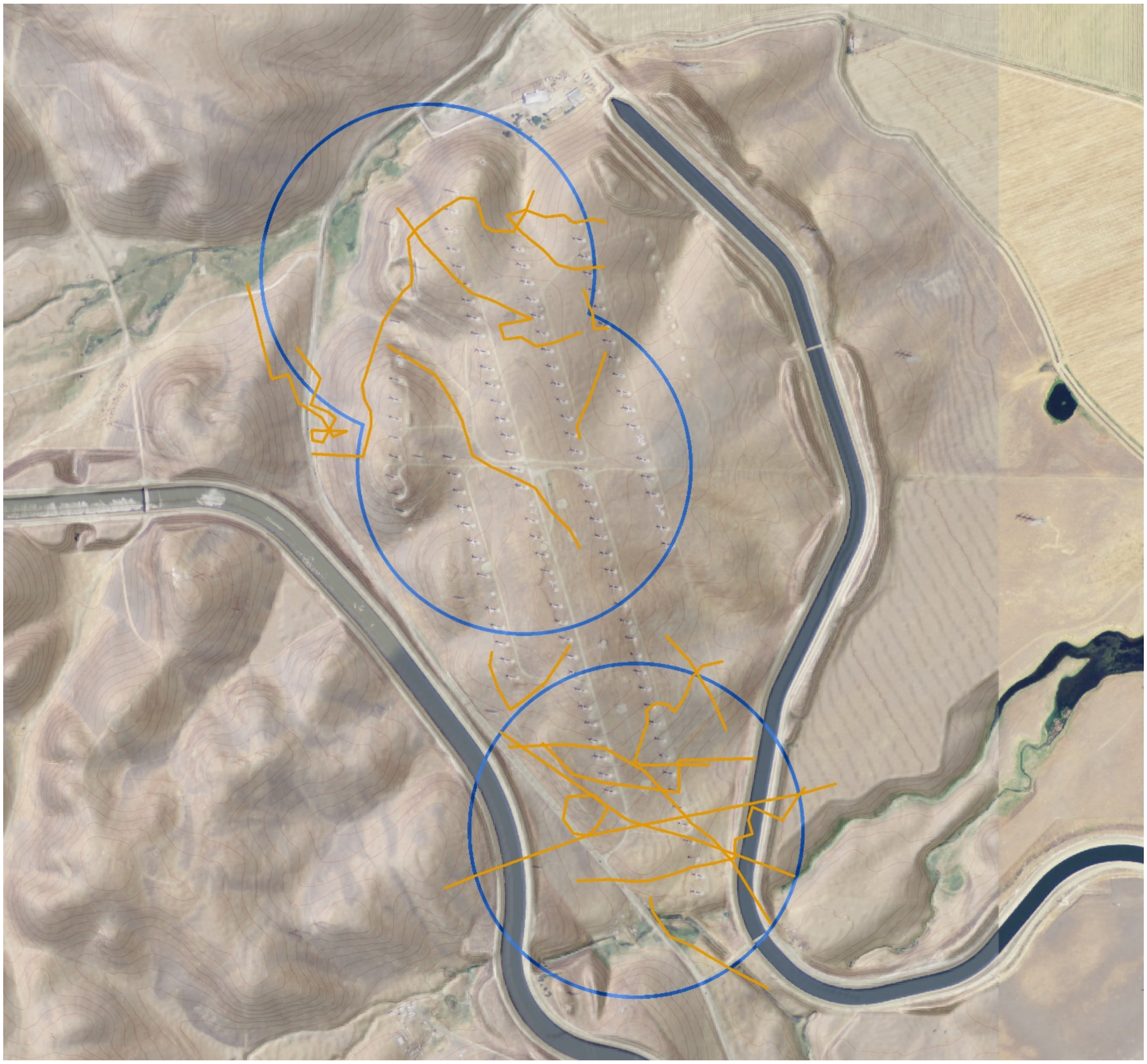

Figure 43: Flight Patterns of Golden Eagles During Behavior Surveys at the Taxvest Project off Midway Road, Altamont Pass Wind Resource Area

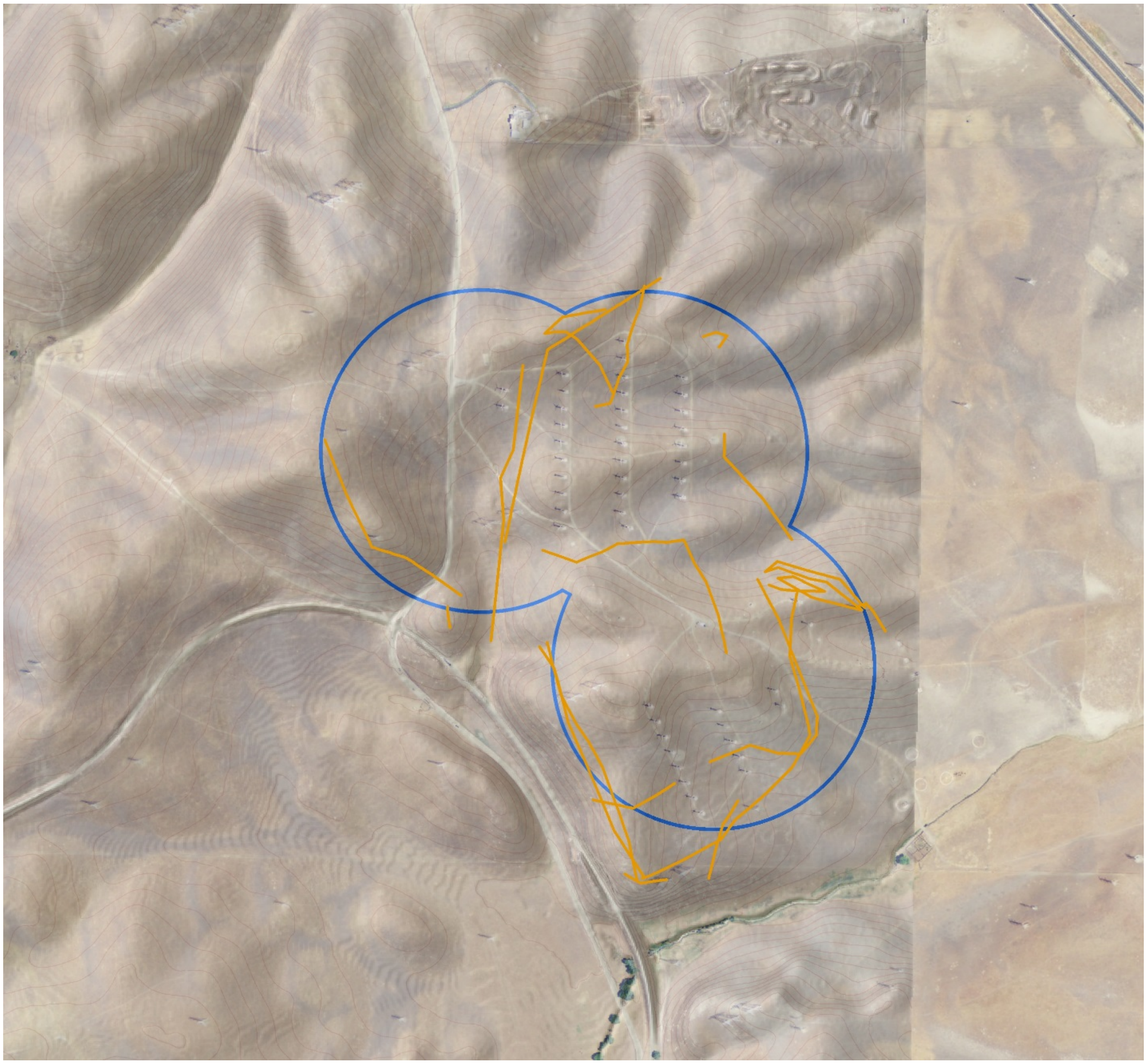

Figure 44: Flight Patterns of Red-Tailed Hawks During Behavior Surveys at Altech 1, Swamp, Viking, and Venture Winds Projects, Altamont Pass Wind Resource Area

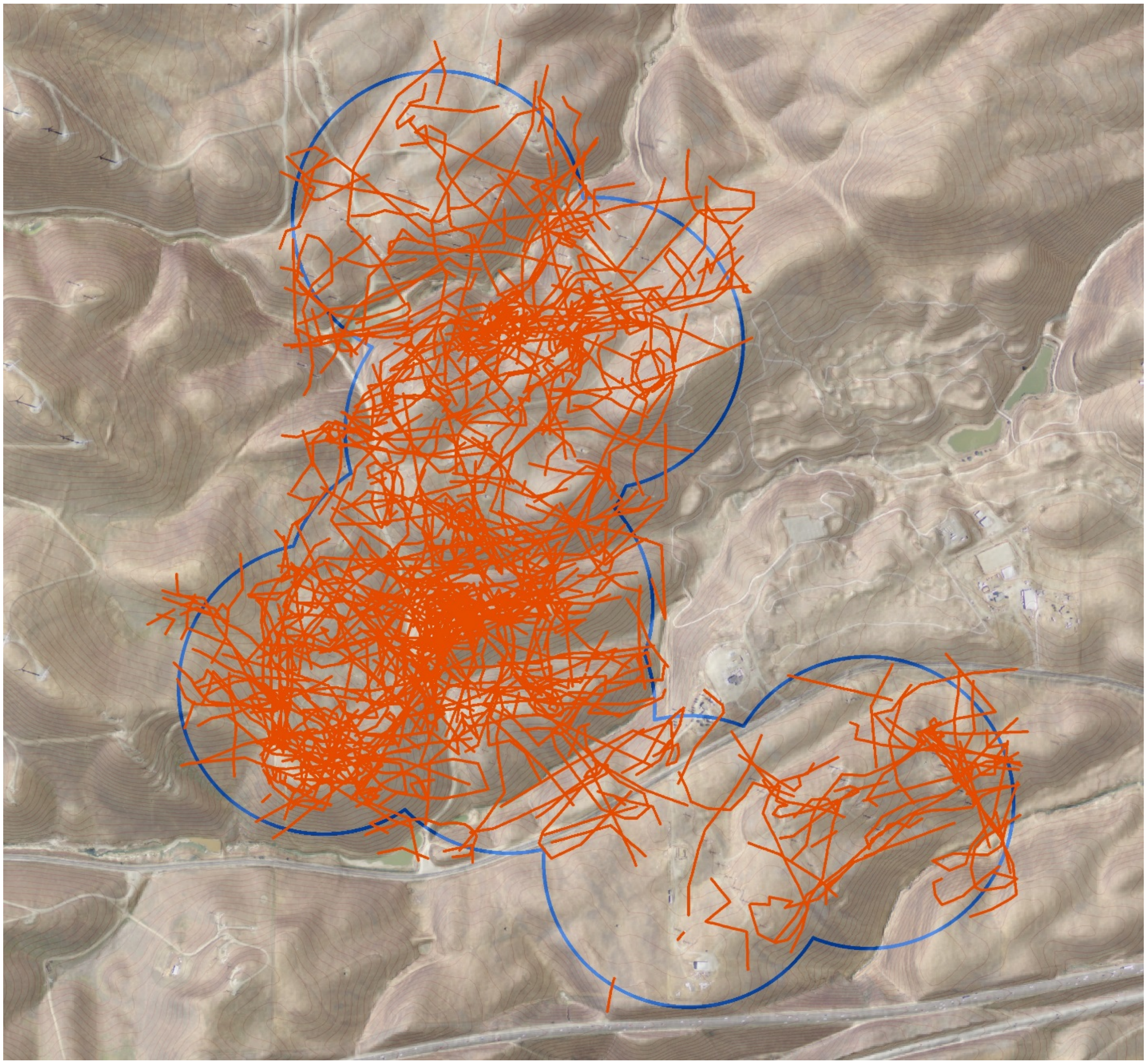

Figure 45: Flight Patterns of Red-Tailed Hawks During Behavior Surveys at the Taxvest Project Near Mountain House, Altamont Pass Wind Resource Area

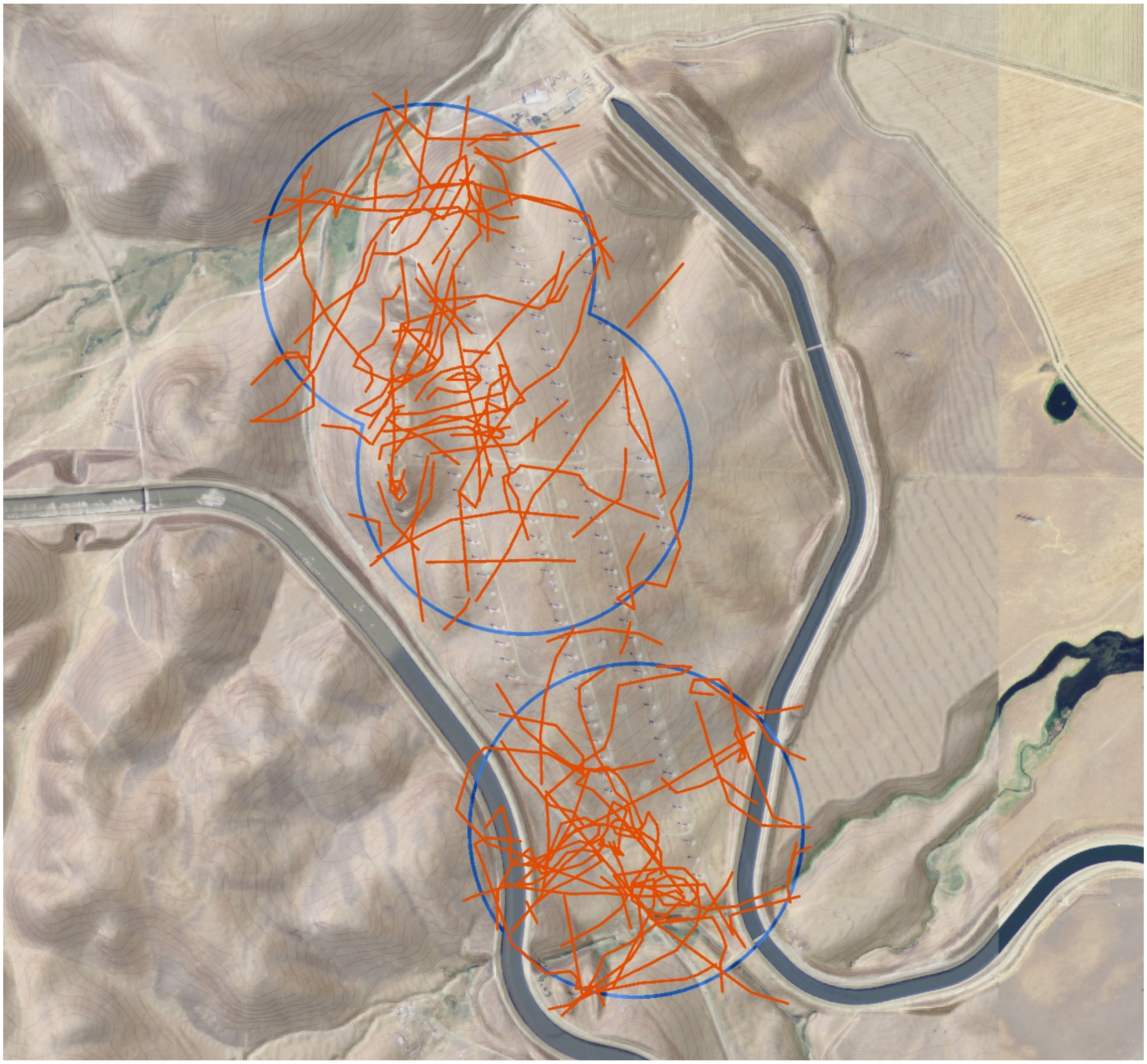

Figure 46: Flight Patterns of Red-Tailed Hawks during Behavior Surveys at the Taxvest Project Off Midway Road, Altamont Pass Wind Resource Area

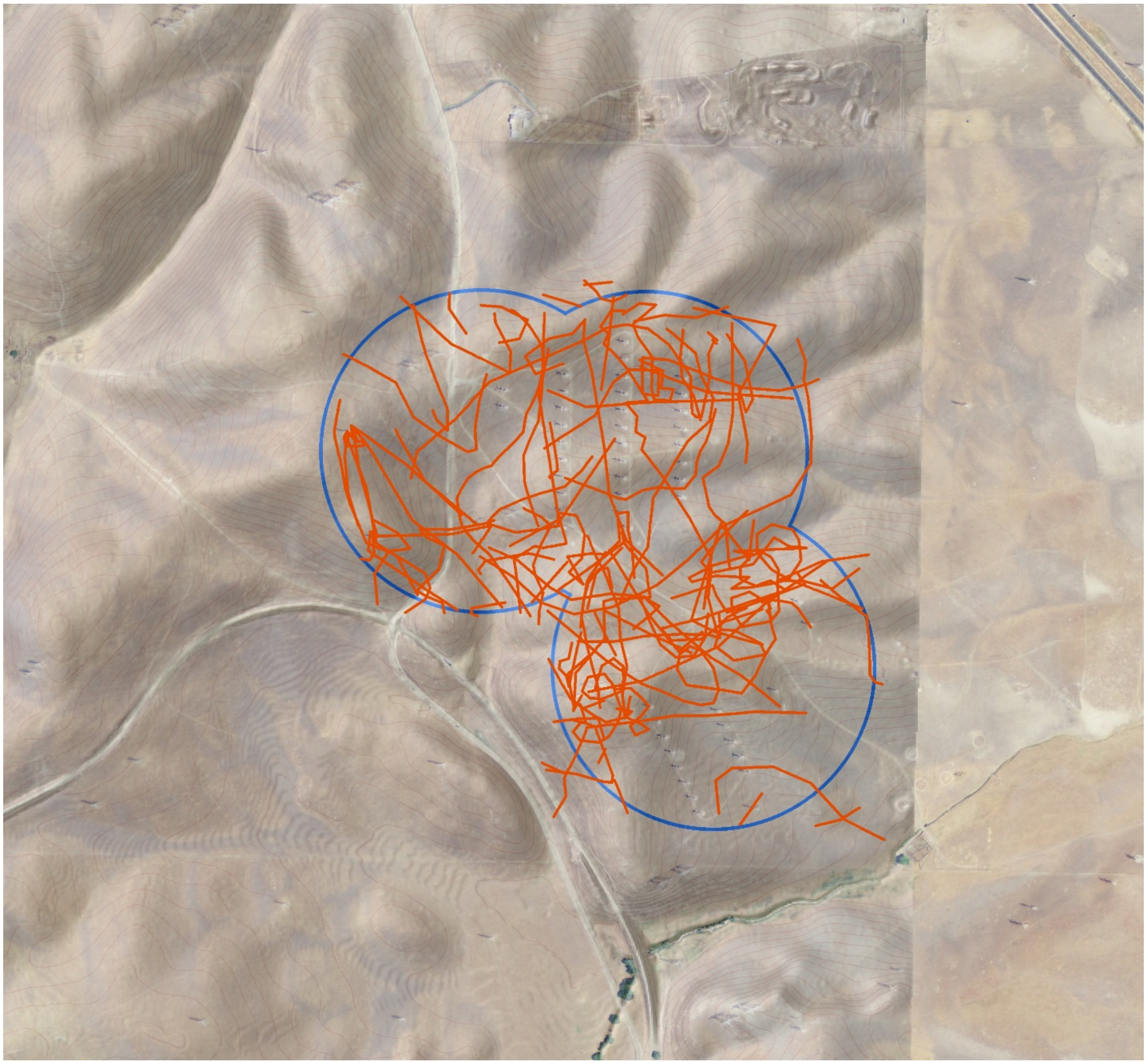

Figure 47: Flight Patterns of American Kestrels During Behavior Surveys at Altech 1, Swamp, Viking, and Venture Winds Projects, Altamont Pass Wind Resource Area

Figure 48: Flight Patterns of American Kestrels During Behavior Surveys at the Taxvest Project Near Mountain House, Altamont Pass Wind Resource Area

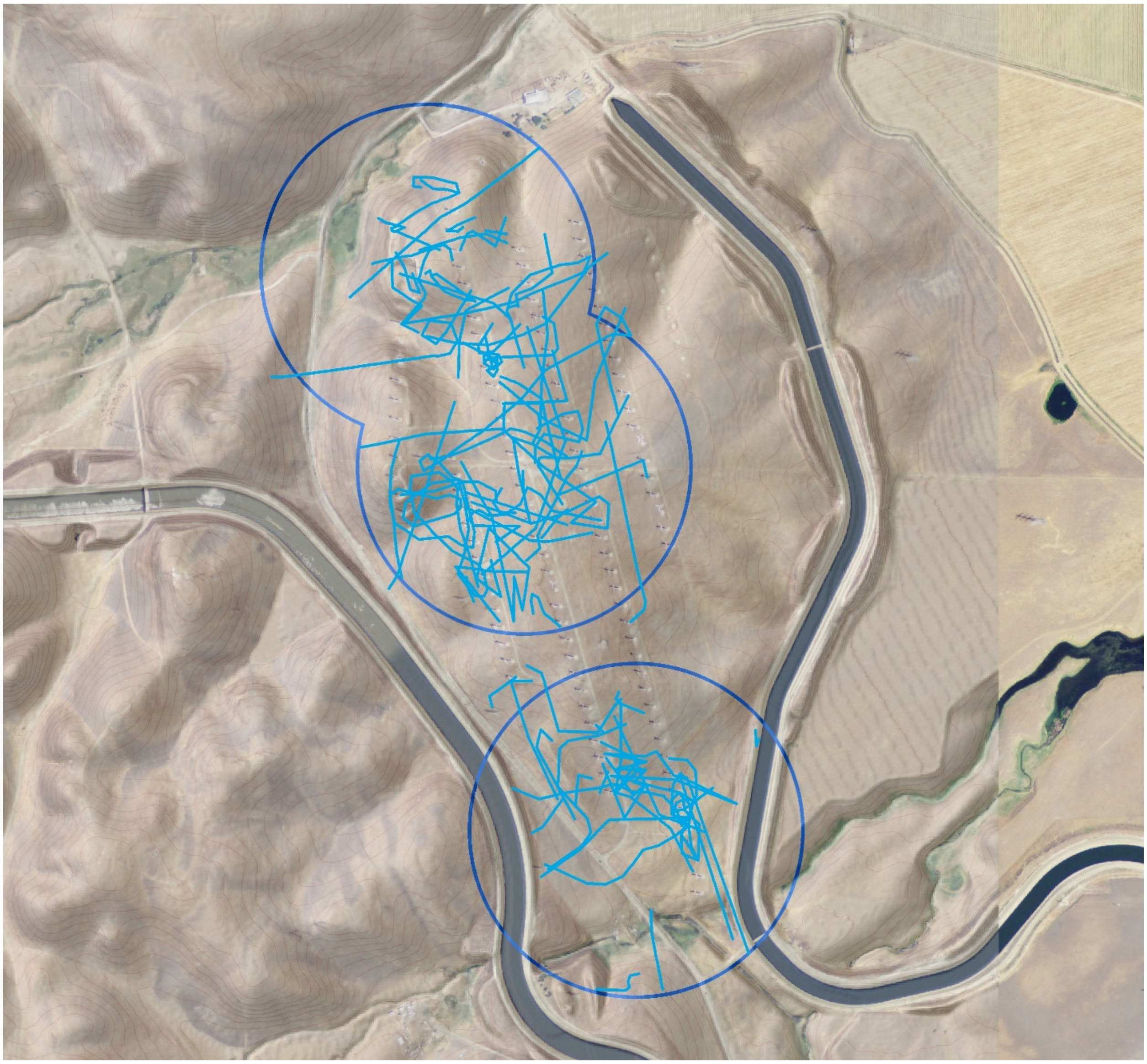

Figure 49: Flight Patterns of American Kestrels During Behavior Surveys at the Taxvest Project Off Midway Road, Altamont Pass Wind Resource Area

Figure 50: Flight Patterns of Burrowing Owls During Behavior Surveys at Altech 1, Swamp, Viking, and Venture Winds Projects, Altamont Pass Wind Resource Area

Table 5: Wind Turbine Events Involving Predatory Raptor Species During Behavior Surveys at Forebay

Date	AOU	N	Behavior	Turbine status	Angle (°) & approach to rotor plane		Reaction to turbine	Near hazard (m)	Impact	Max wind	Note
04/30/2012	GOEA	1	Forward flight	On	90	Wake	Descended			14	
09/13/2012	GOEA	1	Gliding	Off	90		Between turbines			9	
09/13/2012	GOEA	1	Stooping	Off			Ascended			9	Ascending & diving 5 m
09/13/2012	GOEA	1	Stooping	Off			Ascended			9	Ascending & diving 5 m
09/13/2012	GOEA	1	Stooping	Off			Ascended			9	Ascending & diving 5 m
09/13/2012	GOEA	1	Gliding	Off			None reported			9	
09/13/2012	GOEA	1	Gliding	Off			None reported			9	
11/26/2012	GOEA	1	Gliding	Off	45	Wind	None	4		5	
02/23/2013	GOEA	1	Fleeing	On	90	90	Descended	5		17	Flapped hard between two spinning turbines
02/28/2013	GOEA	1	Gliding	Off	90	Wind	Distracted	10		9	Mobbed
03/04/2013	GOEA	1	Gliding	Off	90	Wake	None	1	Near miss	15	
03/15/2013	GOEA	1	Forward flight	On	90	Wake	Banked from rotor	3		13	
04/23/2013	GOEA	1	Gliding	On	0	90	None	5	Near miss	20	Very dangerous!
07/17/2013	GOEA	1	Gliding	On	90	Wake	None	10		17	

Date	AOU	N	Behavior	Turbine status	Angle (°) & approach to rotor plane		Reaction to turbine	Near hazard (m)	Impact	Max wind	Note
07/17/2013	GOEA	1	Gliding	Off	0	Wake	Targeted gap in turbines	7		17	
08/21/2013	GOEA	1	Forward flight	On	45	Wake	Close maneuver to avoid collision	0.33	Near miss	15	
09/05/2013	GOEA	1	Banking	Feather	90	Wake	Banked from rotor	15		26	
09/05/2013	GOEA	1	Flap & glide	On	90	Wake	Flapped to ascend	10		26	
10/28/2013	GOEA	1	Gliding	On	90	Wake		5		22	R leg hanging down
01/09/2014	GOEA	1	Contouring	Fence					Near miss	12	Barely cleared fence
01/09/2014	GOEA	1	Gliding	Fence					Near miss	12	Barely cleared fence
01/31/2014	GOEA	1	Avoidance	Off	0		Close maneuver to avoid collision	1	Near miss	16	
01/31/2014	GOEA	1	Flap & glide	Off	0			1		16	
01/31/2014	GOEA	1	Flap & glide	Off	0			5		16	
01/31/2014	GOEA	1	Flap & glide	Off	90			1		16	
04/28/2014	GOEA	1	Gliding	On	90	Wake		10		19	
04/28/2014	GOEA	1	Gliding	On	90	Wake		10		19	
04/28/2014	GOEA	1	Flap & glide	On	90	Wake		10		19	
04/28/2014	GOEA	1	Gliding	On	0	Wake		5		19	
06/19/2014	GOEA	1	Gliding	On	90	Wind	Descended	5		13	

Date	AOU	N	Behavior	Turbine status	Angle (°) & approach to rotor plane		Reaction to turbine	Near hazard (m)	Impact	Max wind	Note
07/28/2014	GOEA	1	Mobbed or chased							15	Transmission lines; distracted
09/24/2012	NOHA	1	Gliding	On	90	Wake	None			14	
10/23/2012	NOHA	1	Gliding	Off	90	90	Targeted operating rotor	0		6	Slowed to enter rotor plane and flushed ROPIs from turbine nacelle
10/30/2012	NOHA	1	Forward flight	Off	90	Wake	None			21	
10/30/2012	NOHA	1	Contouring	Off	90	Wake	None	6		21	
02/22/2013	NOHA	1	Soaring	Off	0		None	12		9	
02/22/2013	NOHA	1	Gliding	Off	45	Wind	None	10		9	
02/22/2013	NOHA	1	Soaring	Off	90	Wake	None	5		9	
03/26/2013	NOHA	1	Forward flight	Off	90	Wake		10		15	
05/24/2013	NOHA	1	Contouring	On	90	Wake	None	15		22	
06/05/2013	NOHA	1	Forward flight	On	90	Wake	Ascended	1		26	
06/05/2013	NOHA	1	Forward flight	Off	90	Wake	None reported	4		26	
07/18/2013	NOHA	1	Flap & glide			Wake	Ascended			24	Transmission lines
03/28/2014	NOHA	1	Flap & glide	Off	90	90	None	0		9	
12/27/2012	FEHA	1	Flap & glide	Off	90	90	None	3		10	
01/08/2013	FEHA	1	Diving	Off	90	90	Between turbines	15		5	

Date	AOU	N	Behavior	Turbine status	Angle (°) & approach to rotor plane		Reaction to turbine	Near hazard (m)	Impact	Max wind	Note
01/08/2013	FEHA	1	Gliding	Off	90	Wake	None	12		6	
01/17/2013	FEHA	1	Gliding	Off	90		Ascended	10		0	
01/17/2013	FEHA	1	Gliding							0	Transmission lines
01/17/2013	FEHA	1	Gliding				Ascended over			0	Transmission lines
01/17/2013	FEHA	1	Flap & glide	Off	90	Wind	Targeted operational gap in turbines	3		4	
01/21/2013	FEHA	1	Flap & glide	Off	90	Wake	Targeted gap in turbines	1		8	
02/22/2013	FEHA	1	Gliding	Off	90	Wake	None	5		10	
11/06/2013	FEHA	1	Flap & glide	Off	0	Wind	Ascended over nacelle	1		9	Turbine not facing wind
03/17/2014	FEHA	1	Avoidance	On	90	Wake	Close maneuver to avoid collision	1	Near miss	17	Dipped right wing as it passed over blades, then flapped hard
07/03/2012	RTHA	1	Gliding	Off	90	Wind	None	1		14	
08/06/2012	RTHA	1	Forward flight	On	90	Wind	Shifted path from rotor			30	
08/06/2012	RTHA	1	Forward flight	On	45	Wind	Shifted path from rotor			30	

Date	AOU	N	Behavior	Turbine status	Angle (°) & approach to rotor plane		Reaction to turbine	Near hazard (m)	Impact	Max wind	Note
08/30/2012	RTHA	1	Circling	Off	0	Both	Circled around rotor	2		10	With 2 TUVUs
08/30/2012	RTHA	1	Forward flight	Off			None			10	
09/05/2012	RTHA	1	Forward flight	Off	90	Wake	Descended	4		10	
09/05/2012	RTHA	1	Forward flight	Off	90	Wake	Ascended	4		10	
09/20/2012	RTHA	1	Flap & glide	On	45	Wind	None	15		25	
09/20/2012	RTHA	1	Flap & glide	On	90	Wake	None	15		25	Went through a gap
10/01/2012	RTHA	1	Perched	Off	90	Wind	None	0		5	Flushed RTHA, LOSH & CORA upon arrival
10/01/2012	RTHA	1	Soaring	Off	90	Wind	None	3		5	
10/01/2012	RTHA	1	Flap & glide	Off	90	Wind	None	3		5	
10/02/2012	RTHA	1	Forward flight	Off	90	Wake	Aborted landing	2		6	
10/08/2012	RTHA	1	Flap & glide	On	90	Wind	None	3		20	
10/19/2012	RTHA	1	Perched	Off	0	Wind		1		12	Mobbed by 3 ROPI, but never left blade next to spinning turbine
10/25/2012	RTHA	1	Diving	Off	0	Wake		1		7	After prey on ground
10/29/2012	RTHA	1	Forward flight	Off	90	Wake	Flew between	0		5	Flew over hub

Date	AOU	N	Behavior	Turbine status	Angle (°) & approach to rotor plane		Reaction to turbine	Near hazard (m)	Impact	Max wind	Note
							turbines				
10/29/2012	RTHA	1	Forward flight	Off	45	Wake		1		5	Flew over hub
11/06/2012	RTHA	1	Landing	Off	90	Wind	Aborted landing	0		9	
11/06/2012	RTHA	1	Landing	Off	90	Wake		0		9	
11/06/2012	RTHA	1	Gliding	Off	90	Wake	None	5		9	
11/08/2012	RTHA	1	Gliding	Off	90	Wake	Between turbines	12		25	
11/12/2012	RTHA	1	Forward flight	Off	0		None			6	
11/12/2012	RTHA	1	Circling	Off	90	90	None reported	15		11	
11/13/2012	RTHA	1	Perched	Off	90	90	None	1		5	
11/20/2012	RTHA	1	Flap & glide	Off	90	Wake	Between turbines	10		8	
11/26/2012	RTHA	1	Flap & glide	Off	0	90	None	2		2	
11/26/2012	RTHA	1	Flap & glide	Off	90	Wake	Between turbines	10		8	
11/26/2012	RTHA	1	Flap & glide	Off	90	Wake	Between turbines	10		8	
11/26/2012	RTHA	1	Flap & glide	Off	90	Wake	Banked away from rotor	6		8	
01/09/2013	RTHA	1	Surfing	Off	90	Wake	None	5		17	
01/22/2013	RTHA	1	Gliding	Off	90	Wake	None	5		9	
02/13/2013	RTHA	1	Flap & glide	Off	0	Wind	None	5		8	
02/21/2013	RTHA	1	Gliding	Off	90	Wake	None	0		13	
02/21/2013	RTHA	1	Soaring	On	90	Wake	Banked from rotor	15		13	

Date	AOU	N	Behavior	Turbine status	Angle (°) & approach to rotor plane		Reaction to turbine	Near hazard (m)	Impact	Max wind	Note
02/28/2013	RTHA	1	Forward flight	Off	90	Wake	Distracted	5		9	Diving on GOEA
03/18/2013	RTHA	1	Soaring	Off	90	Wind	None	1		11	
03/22/2013	RTHA	1	Surfing	Off	90	90	None	10		27	
03/22/2013	RTHA	1	Gliding	Off	0	90	None	5		27	
04/17/2013	RTHA	1	Forward flight	on/off	0	Wind	None reported			30	
04/25/2013	RTHA	1	Gliding	On	90	Wind		4		32	
05/16/2013	RTHA	1	Flap & glide	On	90	Wind	Targeted gap in turbines	10		24	
06/25/2013	RTHA	1	Gliding	Off	90	NO WIND	None	5		11	Soared/circled over turbines
07/30/2013	RTHA	1	Forward flight				Hard flapping			22	Transmission line
08/02/2013	RTHA	1	Forward flight	On	45	Wind	Banked from rotor	1		15	
08/09/2013	RTHA	1	Soaring	On	90	Wind	None	4		25	
09/13/2013	RTHA	1	Gliding	On	90	Wake	None	12		16	
09/18/2013	RTHA	1	Flap & glide	On	90	90	Descended	5		26	
09/18/2013	RTHA	1	Flap & glide	Off	90	90	None	5		26	
09/19/2013	RTHA	1	Avoidance	Off	90	Wind	Aborted landing	0.5		10	Flapped hard & flared tail to change flight path

Date	AOU	N	Behavior	Turbine status	Angle (°) & approach to rotor plane		Reaction to turbine	Near hazard (m)	Impact	Max wind	Note
09/24/2013	RTHA	2	Gliding	Off	90	Wind	None	7		19	
10/14/2013	RTHA	1	Flap & glide	On	0	Wake	Timed passage	1	Jostled by wake	20	
10/22/2013	RTHA	1	Diving	Off	90	Wind	Timed passage	0		13	Tucked wings for shallow dive
10/22/2013	RTHA	1	Gliding	On	0	Wake		10		13	
10/22/2013	RTHA	1	Landing	Off	90	Wake	Landing	0		13	Landed on back of RTHA on catwalk. Both tumbled off catwalk & flew off
10/28/2013	RTHA	1	Diving	On	90	Wake	Descended	5		17	Long shallow dive
11/01/2013	RTHA	1	Flap & glide	Off	90			1		6	No wind
11/04/2013	RTHA	1	Hovering	Off	90	0	None	1		36	
11/05/2013	RTHA	1	Gliding	Off	90	Wake		10		9	Weaving in and out
11/05/2013	RTHA	1	Gliding	Off	90	Wind		10		9	Weaving in and out
11/05/2013	RTHA	1	Gliding	Off	90	Wake		10		9	Weaving in and out
11/05/2013	RTHA	1	Circling	Off	90	Wind		3		9	
11/06/2013	RTHA	1	Gliding	Off	90	Wind		5		11	

Date	AOU	N	Behavior	Turbine status	Angle (°) & approach to rotor plane		Reaction to turbine	Near hazard (m)	Impact	Max wind	Note
11/06/2013	RTHA	1	Ascending glide	Off	0	Wake	Timed passage	10		11	Ascended
11/06/2013	RTHA	1	Landing	Off	90	Wake		1		11	
11/07/2013	RTHA	1	Forward flight	Off	90	Wind	None	1		5	
11/11/2013	RTHA	1	Diving	Off	90	Wake	Distracted	5		5	
11/11/2013	RTHA	1	Gliding	Off	90	Wake		5		5	
11/11/2013	RTHA	1	Gliding	Off	90	Wake		5		5	
11/12/2013	RTHA	1	Gliding	Off	90	90	Distracted	0		20	
11/12/2013	RTHA	1	Gliding	Off	45	90	None	3		20	
11/13/2013	RTHA	1	Mobbing	Off	90	Wind	Braked/slowed	1		8	Attacked RTHA
11/15/2013	RTHA	1	Flap & glide	Off	90	90	None	7		16	
11/15/2013	RTHA	1	Mobbed or chased	Off	0	90	Close maneuver to avoid collision	3		16	
11/18/2013	RTHA	1	Forward flight	Off	90	Wind	None	1		14	
11/18/2013	RTHA	1	Forward flight	Off	90	Wind	Distracted	1		14	
11/22/2013	RTHA	1	Flapping	Off	90	Wake	Braked/slowed	0		22	Attempted to land on blade tip
11/22/2013	RTHA	1	Gliding	Off	0	90	None	3		34	
11/25/2013	RTHA	1	Forward flight	Off	45	Wind	Landing			4	
12/04/2013	RTHA	1	Soaring	Off	90	0	None	5		15	

Date	AOU	N	Behavior	Turbine status	Angle (°) & approach to rotor plane		Reaction to turbine	Near hazard (m)	Impact	Max wind	Note
12/04/2013	RTHA	1	Flap & glide	Off	90	90	None			24	
12/04/2013	RTHA	1	Gliding	Off	90	0	None	5		15	
12/04/2013	RTHA	1	Gliding	Off	90	90	None			24	
12/11/2013	RTHA	1	Forward flight	Off	90	Wind	None	1		6	
12/11/2013	RTHA	1	Forward flight	Off	90	Wind	None	1		6	
12/12/2013	RTHA	1	Flap & glide	Off	90	90		10		9	
12/12/2013	RTHA	1	Flap & glide	Off	90	90				9	
01/09/2014	RTHA	1	Landing	Off	90	Wind	Landing	0		12	Lost balance on wobbly blade tip, so jumped off
01/20/2014	RTHA	1	Flap & glide	Off	0	Wake	None	5		8	
01/29/2014	RTHA	1	Flap & glide	Off	0	90	Descended	2		11	
02/12/2014	RTHA	1	Forward flight	Off	90	Wake	Taking off	0		7	From perch, flew through rotor above hub
03/12/2014	RTHA	1	Gliding	Off	0	90	None	7		16	
03/12/2014	RTHA	1	Soaring	Off	90	90	None	7		16	
04/09/2014	RTHA	1	Forward flight	On	45	Wake	Banked from rotor	1		18	
04/29/2014	RTHA	1	Gliding	Off	90	45	None	7		21	
05/06/2014	RTHA	1	Gliding	Off	90	Wake	Circled around turbine	0		21	Focused on ground squirrel

Date	AOU	N	Behavior	Turbine status	Angle (°) & approach to rotor plane		Reaction to turbine	Near hazard (m)	Impact	Max wind	Note
											burrows
05/06/2014	RTHA	1	Forward flight	On	90	Wind	Braked/slowed & banked	8		23	Flew toward turbines, turned along row into crosswind that pushed it toward turbines
05/06/2014	RTHA	1	Forward flight	On	90	Wind	None reported	2		23	
05/07/2014	RTHA	1	Soaring	On	90	Wind		10		18	
06/10/2014	RTHA	1	Gliding	On	90	Wake	Flew over short turbine	3		13	
06/10/2014	RTHA	1	Gliding	On	90	Wind		3		13	
10/16/2014	RTHA	1	Flap & glide	Off	90	Wake	Timed passage	0		8	Quick flutter of wings
10/16/2014	RTHA	1	Flap & glide	Off	90	Wake	Timed passage			8	Quick flutter of wings
10/21/2014	RTHA	1	Gliding	Off	0	90		1		19	
10/21/2014	RTHA	1	Gliding	Off	0	90		10		19	
11/18/2014	RTHA	1	Soaring	Off	90	Wake		0		8	
05/10/2013	SWHA	1	Soaring	On	90	Wind	None	25		21	
05/23/2013	SWHA	1	Gliding	Off	90	Wind	None			22	
05/24/2013	SWHA	1	Gliding	On	90	Wind	None			29	
06/13/2013	SWHA	1	Forward flight	On	90	90		5		18	

Date	AOU	N	Behavior	Turbine status	Angle (°) & approach to rotor plane		Reaction to turbine	Near hazard (m)	Impact	Max wind	Note
06/13/2013	SWHA	1	Gliding	On	90	Wind		5		18	
06/13/2013	SWHA	3	Gliding	Off	90	Wind		4		18	
05/06/2014	SWHA	1	Gliding	Off	90	90	None	6		24	
07/21/2014	SWHA	1	Gliding	On	45	Wind	Targeted nonop turbine	5		25	Chose nonop from row of spinning turbines
07/21/2014	SWHA	1	Gliding	On	45	Wake		5		25	
06/25/2012	AMKE	1	Forward flight	Off	90	Wake	None	0	Struggled with wind	18	
07/09/2012	AMKE	1	Forward flight	On	90	Wind	None	2		24	
08/06/2012	AMKE	1	Landing	Off	90	Wake	Landing	0	Struggled with wind	30	
08/13/2012	AMKE	1	Circling	Off			Circled around rotor			13	
08/13/2012	AMKE	1	Flying	Off	90	Wake	None reported			18	
08/13/2012	AMKE	1	Gliding	Off			None reported			13	
08/15/2012	AMKE	1	Perched	Off	90	Wind	Landing			33	Inside hub cone
08/16/2012	AMKE	1	Landing	On	90	Wake	Landing			36	
08/28/2012	AMKE	1	Forward flight	Off	90	Wind	Turned 90° to parallel with rotor			12	

Date	AOU	N	Behavior	Turbine status	Angle (°) & approach to rotor plane		Reaction to turbine	Near hazard (m)	Impact	Max wind	Note
08/29/2012	AMKE	1	Perched	On		Wake	Taking off			14	
08/30/2012	AMKE	1	Forward flight	Off	0		None reported			11	
08/30/2012	AMKE	1	Landing	Off	90		Landing			11	
09/05/2012	AMKE	1	Forward flight	On	90	Wind	None	1		14	
09/11/2012	AMKE	1	Forward flight	Off	45	Wake	Timed passage	0		9	
09/11/2012	AMKE	1	Flapping							6	
09/11/2012	AMKE	1	Flapping							6	
09/11/2012	AMKE	1	Flapping							6	
09/13/2012	AMKE	1	Forward flight	Off	0		Targeted operational gap in turbines			9	
09/13/2012	AMKE	1	Forward flight	Off	0		Between turbines			9	
09/13/2012	AMKE	1	Forward flight	Off	90	Wake	None reported	0		3	
09/13/2012	AMKE	1	Gliding	Off	0		Between turbines			9	
09/20/2012	AMKE	1	Forward flight	On	90	Wind	None	3		18	
09/20/2012	AMKE	1	Banking	On	0	Wake	Banked from rotor	30		18	
09/20/2012	AMKE	1	Banking	On	90	Wake	Banked from rotor	30		18	
09/20/2012	AMKE	1	Landing	Off	90	Wake	Landed in hole where of missing rotor cone			18	Turbine facing opposite way
09/27/2012	AMKE	1	Landing	Off	90	Wind	None	1		12	

Date	AOU	N	Behavior	Turbine status	Angle (°) & approach to rotor plane		Reaction to turbine	Near hazard (m)	Impact	Max wind	Note
09/27/2012	AMKE	1	Forward flight	Off	0	Wake	None	2		5	
09/27/2012	AMKE	1	Landing	Off	0	90	None	0		12	Turbine may be broken
09/28/2012	AMKE	1	Forward flight	Off	90	Wind		1			
10/01/2012	AMKE	1	Landing	Off	90	Wake	None	10		5	
10/01/2012	AMKE	1	Chasing prey	Off	90	Wake	Distracted	0		2	Chasing ROPI
10/01/2012	AMKE	1	Landing	Off	90	Wake	Landing	0		2	Onto fiberglass pieces at base of blade
10/01/2012	AMKE	1	Landing	Off	0			0		2	Flew from broken blade to intact blade
10/01/2012	AMKE	1	Chasing prey	Off	0	Wind	Distracted	0		2	Chasing ROPI
10/01/2012	AMKE	1	Taking off	Off				0		2	
10/01/2012	AMKE	1	Landing	Off	90	Wake	None reported	0		2	
10/01/2012	AMKE	1	Diving	Off	90	Wake	None reported	0		2	
10/01/2012	AMKE	1	Landing	Off	90	Wake	Landing	0		2	
10/01/2012	AMKE	1	Landing	Off	90	Wind	Landing	0		2	
10/02/2012	AMKE	1	Landing	Off	90	90	Landing	1		7	Squeezed through bottom gap of nacelle
10/02/2012	AMKE	1	Forward flight	Off	90	Wind	None	15		5	

Date	AOU	N	Behavior	Turbine status	Angle (°) & approach to rotor plane		Reaction to turbine	Near hazard (m)	Impact	Max wind	Note
10/02/2012	AMKE	1	Forward flight	Off	90	Wind	None	15		5	
10/05/2012	AMKE	1	Forward flight	off/on	90	Wake		1		12	
10/05/2012	AMKE	1	Forward flight	off/on	90	Wake		1		12	
10/09/2012	AMKE	1	Forward flight	Feather	90	90	Banked from rotor	3		7	
10/09/2012	AMKE	1	Forward flight	On	0	Wind	Distracted	1		9	En route to attack EUST
10/09/2012	AMKE	1	Attack	Off	0	Wind	Distracted	0		9	Failed attack on EUST
10/09/2012	AMKE	1	Forward flight	Off	0	90	Banked from rotor	1		9	
10/09/2012	AMKE	1	Gliding	Off	0	90	Between turbines	11		9	
10/09/2012	AMKE	1	Gliding	On	0	90	Between turbines	11		9	
10/30/2012	AMKE	1	Forward flight	Off	90	Wind	Circled around rotor	1		7	Interaction with AMKE
10/30/2012	AMKE	1	Forward flight	On	0	90	Banked from rotor	2		11	
10/30/2012	AMKE	1	Forward flight	Off	0	90	Circled through rotor	0		7	
10/30/2012	AMKE	1	Perched	Off	0	90	Timed passage	0.2	Near miss	11	Noticed blade last second
11/07/2012	AMKE	1	Forward flight	Off	90	Wind	None	1		29	
11/07/2012	AMKE	1	Forward flight	Off	0	Wind	None	1		29	
11/07/2012	AMKE	1	Forward flight	Off	90	Wind	Banked from rotor	15		4	Turned along row

Date	AOU	N	Behavior	Turbine status	Angle (°) & approach to rotor plane		Reaction to turbine	Near hazard (m)	Impact	Max wind	Note
11/10/2012	AMKE	1	Forward flight	Off	90	Wind		0		11	
11/12/2012	AMKE	1	Mobbing	Off	90	90	Distracted	0		3	Mobbing RTHA
11/12/2012	AMKE	1	Mobbing	Off	90	Wind	Distracted	0		11	
11/20/2012	AMKE	1	Forward flight		90	Wake	Flapped to ascend			9	Transmission lines
11/20/2012	AMKE	1	Forward flight	Off	90	Wind	Between turbines	10		8	
11/26/2012	AMKE	1	Diving attack	Off	90	Wind	Targeted operating rotor	0		8	Ambushed/flushed 2 EUST from rotor
12/04/2012	AMKE	1	Perched	Off	90	Wind	Distracted			3	
12/04/2012	AMKE	1	Perched	Off	90	Wind	Distracted			3	
12/17/2012	AMKE	1	Forward flight	Off	90	Wind	Aborted landing			8	
01/22/2013	AMKE	1	Forward flight				None			0	Vacant tower
01/22/2013	AMKE	1	Forward flight	Off	90		None	0		1	
01/23/2013	AMKE	1	Forward flight	Off	90	90	None reported	3		4	
01/23/2013	AMKE	1	Forward flight	Off	90	Wake	Banked from rotor	5		4	
01/23/2013	AMKE	1	Forward flight	Off	0	90	None	2		4	
02/06/2013	AMKE	2	Landing	Off	90	Wind	Braked/slowed	2		9	Flew into hole at rear of nacelle
03/07/2013	AMKE	1	Displaying	Off	0	90	Distracted	0		8	Stooping while calling in front

Date	AOU	N	Behavior	Turbine status	Angle (°) & approach to rotor plane		Reaction to turbine	Near hazard (m)	Impact	Max wind	Note
											of rotor hub
03/15/2013	AMKE	1	Forward flight	On	90	Wake	None	7		13	
03/19/2013	AMKE	1	Forward flight	Off	90	Wake	None reported	0		7	
03/19/2013	AMKE	1	Forward flight	Off	90	90	None	2		7	
03/19/2013	AMKE	1	Landing	Off	90	Wake	Aborted landing	0		7	Aborted landing
03/25/2013	AMKE	1	Forward flight	Off	90	Wake	Targeted operational gap in turbines	5		15	
03/26/2013	AMKE	1	Forward flight	On	90	45	None	10		13	
04/02/2013	AMKE	2	Landing	Feather	90	90	Aborted landing	0		11	Broken turbine
06/03/2013	AMKE	1	Hovering	On	90	Wind	Hovered near rotor	10		22	
06/03/2013	AMKE	1	Hovering	On	90	Wind	Hovered near rotor	10		22	
06/03/2013	AMKE	1	Hovering	On	45	Wind	None reported	5		22	
06/06/2013	AMKE	1	Forward flight	Off	0	90	Ascended	2		5	
07/13/2013	AMKE	1	Diving	On	45	Wake	Taking off			10	
07/18/2013	AMKE	1	Forward flight	Off	90	Wake		0		16	
09/03/2013	AMKE	1	Forward flight	On	90	Wake	None	7		29	
09/04/2013	AMKE	1	Forward flight	On	90	Wake	Timed passage	1		25	Veered wide of rotor
09/04/2013	AMKE	1	Forward flight	On	90	Wake	Flapped to ascend	1		25	
10/01/2013	AMKE	1	Forward flight	Off	0	Wind	None	1			Under repair

Date	AOU	N	Behavior	Turbine status	Angle (°) & approach to rotor plane		Reaction to turbine	Near hazard (m)	Impact	Max wind	Note
12/10/2013	AMKE	1	Forward flight	Off	45	Wind		1		9	
01/16/2014	AMKE	1	Avoidance	Off	90	90	Descended	5		9	Quickly turned right shoulder down
02/18/2014	AMKE	1	Mobbing	Off	45	Wake	Distracted	1		6	Mobbing CORA
03/05/2014	AMKE	1	Forward flight	Off	90	Wake	None	0		10	
03/05/2014	AMKE	1	Forward flight	Off	90	Wake	None	3		9	
03/05/2014	AMKE	1	Stooping	Off	0	90	None	1		10	
03/05/2014	AMKE	1	Flap & glide	Off	90	Wake	None	3		9	
03/05/2014	AMKE	1	Forward flight	Off	90	Wake	None	3		9	
03/07/2014	AMKE	1	Hovering	Off	90	Wind	Hovered near rotor	1		14	
04/02/2014	AMKE	1	Forward flight	Off	90	Wake	None	1		11	
04/08/2014	AMKE	1	Forward flight	Off	90	Wake		0		10	
04/14/2014	AMKE	1	Forward flight	Off	90	Wake	None	3		14	Carrying nest material
04/22/2014	AMKE	1	Forward flight	On	90	Wind		2		27	Flew in front of rotor
05/05/2014	AMKE	1	Forward flight	On	45	90	None	7		17	
05/05/2014	AMKE	1	Forward flight	On	0	90	None	5		17	
06/18/2014	AMKE	1	Forward flight	On	90	Wind		5		15	
07/28/2014	AMKE	1	Forward flight	On	90	Wake	Timed passage	5		15	Veered wide of

Date	AOU	N	Behavior	Turbine status	Angle (°) & approach to rotor plane		Reaction to turbine	Near hazard (m)	Impact	Max wind	Note
											rotor
07/28/2014	AMKE	1	Hovering	Off	0	Wind	Braked/slowed	5		13	
10/17/2012	PEFA	1	Forward flight	Off	0	Wind	Ascended	0		22	
10/14/2014	PEFA	1	Gliding	Off	90	Wake	None	1		29	
08/16/2012	PRFA	1	Contouring	On		Wake	None reported			29	
08/16/2012	PRFA	1	Contouring	Off		Wake	None reported			29	
08/30/2012	PRFA	1	Forward flight	Off	90	Wake	None reported			7	
08/30/2012	PRFA	1	Forward flight	Off	90	Wake	None reported			13	
08/30/2012	PRFA	1	Forward flight	Off	90	Wake	Targeted operational gap in turbines			7	
08/30/2012	PRFA	1	Forward flight	Off	90	Wake	None reported			13	
10/02/2012	PRFA	1	Forward flight	Off	90	Wake	None	15		5	
10/02/2012	PRFA	1	Gliding	Off	90	Wind	None	10		5	
10/02/2012	PRFA	1	Landing	Off	0	Wake	Landing	0		5	
10/02/2012	PRFA	2	Forward flight	Off	90	Wind	Banked from rotor	2		6	Chased PRFA
10/02/2012	PRFA	1	Forward flight	Off	90	Wake	None	20		5	
10/02/2012	PRFA	1	Gliding	Off	90	Wind	Descended	25		5	
10/02/2012	PRFA	1	Forward flight	Off	90	Wake	None	15		5	
10/02/2012	PRFA	1	Gliding	Off	90	Wake	Descended	50		5	

Date	AOU	N	Behavior	Turbine status	Angle (°) & approach to rotor plane		Reaction to turbine	Near hazard (m)	Impact	Max wind	Note
10/02/2012	PRFA	1	Forward flight	Off	90	Wake	None	15		5	
10/02/2012	PRFA	1	Landing	Off	90	Wake	Descended	30		5	
10/02/2012	PRFA	1	Gliding	Off	90	Wake	Ascended	30		5	
10/02/2012	PRFA	1	Landing	Off	90	Wake	Landing	0		5	
10/02/2012	PRFA	1	Chasing prey	Off	0	Wake	Turned 90° to parallel with rotor	0	Contact blade	5	Feet touched blade but didn't land; continued to chase ROPI
10/02/2012	PRFA	1	Landing	Off	0	Wake	Landing	0		5	
10/02/2012	PRFA	1	Forward flight	Off	90	Wind	None reported	3		5	
10/02/2012	PRFA	1	Forward flight	Off	0	Wake	Ascended	10		5	
10/02/2012	PRFA	1	Landing	Off	0	Wake	Landing	0		5	
10/02/2012	PRFA	1	Gliding	Off	0	Wind	Shifted path from rotor	25		5	Looking at me
10/02/2012	PRFA	1	Gliding	Off	90	Wake	Descended	30		5	Circled me
10/02/2012	PRFA	1	Forward flight	Off	90	Wind	Ascended	20		5	
10/02/2012	PRFA	1	Forward flight	Off	90	Wind	None reported	45		5	
10/02/2012	PRFA	1	Forward flight	Off	90	Wind	None	0		5	
12/20/2012	PRFA	1	Forward flight	Off	90	Wind	None	0.5		13	
05/28/2013	PRFA	1	Gliding	On	90	Wake	Ascended	10		23	Glided over turbine

Date	AOU	N	Behavior	Turbine status	Angle (°) & approach to rotor plane		Reaction to turbine	Near hazard (m)	Impact	Max wind	Note
05/28/2013	PRFA	1	Forward flight	On	90	Wind	Ascended	10		23	
07/27/2013	PRFA	1	Forward flight	On	90	Wake	Ascended	10		19	Facing wind
07/27/2013	PRFA	1	Forward flight	On	90	Wind		10		19	Facing wind
07/27/2013	PRFA	1	Forward flight	On	90	Wind		2		19	Facing wind
10/23/2013	PRFA	1	Forward flight	Off	0	Wake		2		8	
10/28/2013	PRFA	1	Forward flight	On	90	Wind		5		22	
12/12/2013	PRFA	1	Avoidance	Off	90	90	Banked from rotor	1		9	Flew straight to blade, veered from blade tip & from turbine
03/12/2014	PRFA	1	Forward flight	Feather	90	90		1		11	

GOEA = golden eagle, AMKE = American kestrel, RTHA = red-tailed hawk, PRFA = prairie falcon, PEFA = peregrine falcon, NOHA = northern harrier, FEHA = ferruginous hawk, and SWHA = Swainson’s hawk.

3.3.2 Hazard Models

The golden eagle FL model was composed of 8 predictor variables, 3 of which were categorical in nature and the other 5 included fuzzy boundaries (Tables 6 and 7). Five variables contributed to an FL model of golden eagle flights, ridge crossings, and interaction events at wind turbines (Table 6), and 4 variables contributed to an FL model of golden eagle fatality rates (Table 7). These two models were subsequently normalized and combined with an equally weighted contribution from the variable *Hazard site* (Table 13).

Golden eagle flights and wind turbine interactions occurred disproportionately over ridges oriented generally west-east. Associations were also strong with subwatershed slopes facing westerly directions, especially west-southwest. Eagles also flew and interacted with wind turbines disproportionately over breaks in slope, as indicated by grid cells that were relatively shallow compared to the overall slope from valley bottom to ridge top (*slope to gross slope ratio*). Golden eagles flew and interacted with wind turbines disproportionately at 84% to 100% up the slope, and at 55% to 100% up the slope of major terrain features.

The red-tailed hawk model was composed of 7 predictor variables, 3 of which were categorical in nature and the other 4 included fuzzy boundaries (Tables 8 and 9). Red-tailed hawks hovered and kited disproportionately over ridges oriented west to east and north-northwest to south-southeast. They hovered and kited disproportionately over slopes oriented southwest, west-southwest and west. Red-tailed hawks hovered and kited disproportionately over ground that was between 87% and 95% to the top of the slope. Red-tailed hawk kiting and hovering was broader across major terrain features, with peak activity ranging between 78% and 93% to the top of the feature. The weightings applied to the variables appear in Table 13.

The American kestrel model was composed of 4 predictor variables, 2 of which were categorical in nature and the other 2 included fuzzy boundaries (Table 10). American kestrels flew most disproportionately over ridges oriented west-east and west-northwest to east-southeast. American kestrels flew disproportionately over slopes oriented west and west-southwest, ranging mostly between three-quarters to the peak of the slope and midway to just below the peaks of major terrain features. The weightings applied to the variables appear in Table 13.

The burrowing owl model was composed of 6 predictor variables 2 of which were categorical in nature and the other 4 included fuzzy boundaries (Tables 11 and 12). Burrowing owl burrows were located disproportionately between 5% and 30% of the way up south-facing slopes. Burrowing owl fatality rates were disproportionately higher at low to moderate elevations and between 35% and 42% of the way up the slopes of major terrain features and in hazard sites. The weightings applied to the variables appear in Table 13.

Table 6: Golden Eagle Fuzzy Logic Membership Functions of DEM Grid Cells Based on Flights Involving Ridge Crossings, Interactions with Other Birds, and Wind Turbine Interaction Events

Value of variable Y for *i*th grid cell	Basis of membership function about $\bar{x}$	Membership function of grid cell (Values >1 include weightings)
Y = Ridge Orientation (Ridge crossings)		
Y = WSW-ENE	Not applicable	5
Y = W-E	Not applicable	5
Y = WNW-ESE	Not applicable	3
Y = N-S	Not applicable	0.5
Y = NE-SW	Not applicable	0.5
Y = NW-SE	Not applicable	0.5
Y = WNNW-SSE	Not applicable	0.5
Y = NNE-SSW	Not applicable	0
Y = Subwatershed Orientation (events)		
Y = WSW	Not applicable	2
Y = W	Not applicable	2
Y = NW	Not applicable	2
Y = WNW	Not applicable	1
Y = Other orientation	Not applicable	0
Y = Percent up slope (events)		
84.29 < Y < 100.33	Within 3 SE of $\bar{x}$	1
60.23 < Y < 84.29	Within 12 & 3 SE < $\bar{x}$	0.5 × (1 - COS(π × (Y – 60.23) / (84.29 – 60.23)))
100.33 < Y < 124.4	Within 3 & 12 SE > $\bar{x}$	0.5 × (1 + COS(π × (Y – 100.33) / (124.4 – 100.33)))
Y < 60.23 or Y> 124.4	< > $\bar{x}$ ± 12 SE	0
Y = Percent up major terrain slope (events)		
55.66 < Y < 100.62	Within 0.25 SD < $\bar{x}$ & 1.6 SD > $\bar{x}$	1
42.30 < Y < 55.66	Within 1 SE & 0.5 SD < $\bar{x}$	0.5 × (1 - COS(π × (Y –42.3) / (55.66 – 42.3)))
Y < 42.3	< ($\bar{x}$ - 0.25 SD)	0

Y = Hill Size (interactions)		
78.34 < Y < 82.58	Within 1 SE of $\bar{x}$	1
54.98 < Y < 78.34	Within 12 & 1 SE < $\bar{x}$	0.5 × (1 - COS(π × (Y – 54.98) / (78.34 – 54.98)))
82.58 < Y < 105.94	Within 1 & 12 SE > $\bar{x}$	0.5 × (1 + COS(π × (Y – 82.58) / (105.94 – 82.58)))
Y < 78.34 or Y > 105.94	< > $\bar{x}$ ± 12 SE	0

Table 7: Golden Eagle Fuzzy Logic Membership Functions of DEM Grid Cells Based on Fatality Rates

Value of variable Y for *i*th grid cell	Basis of membership function about $\bar{x}$	Membership function of grid cell (Values >1 include weightings)
Y = Ridge elevation (if slope convex)		
219.84 < Y < 273.88	Within 5 SE of $\bar{x}$	1
70.60 < Y < 219.84	Within 2 SD & 5 SE < $\bar{x}$	0.5 × (1 - COS(π × (Y – 70.60) / (219.84 – 70.60)))
273.88 < Y < 423.12	Within 5 SE & 2 SD > $\bar{x}$	0.5 × (1 + COS(π × (Y – 273.88) / (423.12 – 273.88)))
Y < 70.60 or Y> 423.12	>2 SD from $\bar{x}$	0
Y = Major valley elevation (if slope convex)		
160.36 < Y< 211.41	Within 5 SE of $\bar{x}$	1
102.62 < Y < 160.36	Within 1 SD & 5 SE < $\bar{x}$	0.5 × (1 - COS(π × (Y – 102.62) / (160.36 – 102.62)))
211.41< Y < 269.16	Within 5 SE & 1 SD > $\bar{x}$	0.5 × (1 + COS(π × (Y – 211.41) / (269.16 – 211.41)))
Y < 102.62 or Y> 269.16	>1 SD from $\bar{x}$	0
Y = Slope to gross slope ratio (if slope convex)		
0.36 <Y< 0.49	Within 3 SE of $\bar{x}$	1
0.08 < Y < 0.36	Within 1 SD & 3 SE < $\bar{x}$	0.5 × (1 - COS(π × (Y –0.08) / (0.36 – 0.08)))
0.49 < Y < 0.77	Within 3 SE & 1 SD > $\bar{x}$	0.5 × (1 + COS(π × (Y – 0.49) / (0.77 – 0.49)))
Y < 0.08 or Y > 0.77	>1 SD from $\bar{x}$	0
Y = Hazard site		
Y = Within polygon	Not applicable	8

Table 8: Red-Tailed Hawk Fuzzy Logic Membership Functions of DEM Grid Cells Based on Kiting, Hovering, and Surfing Flights

Value of variable Y for *i*th grid cell	Basis of membership function about $\overline{x}$	Membership function of grid cell (Values >1 include weightings)
Y = Ridge Orientation		
Y = W-E	Not applicable	2
Y = NNW-SSE	Not applicable	2
Y = WSW-ENE	Not applicable	1
Y = N-S	Not applicable	1
Y = WNW-ESE	Not applicable	1
Y= NW-SE	Not applicable	1
Y = Other orientation	Not applicable	0
Y = Subwatershed Orientation		
Y = SW, WSW, W	Not applicable	3
Y = WNW	Not applicable	2
Y = N, NNW	Not applicable	1
Y = Other orientation	Not applicable	0
Y = Percent up slope		
86.76 <Y< 95.24	Within $\overline{x}$ ± 5 SE	1
65.53 < Y < 86.76	Within 30 & 5 SE < $\overline{x}$	0.5 × (1 - COS(π × (Y – 65.53) / (86.76 – 65.53)))
95.24 < Y < 101.19	Within 5 & 12 SE > $\overline{x}$	0.5 × (1 + COS(π × (Y – 95.24) / (101.19 – 95.24)))
Y < 95.24 or Y > 101.19	<($\overline{x}$ - 30 SE) or >($\overline{x}$ + 12 SE)	0
Y = Percent up major terrain slope		
77.72 <Y< 92.28	Within $\overline{x}$ ± 10 SE	1
63.16 < Y < 77.72	Within 30 & 10 SE < $\overline{x}$	0.5 × (1 - COS(π × (Y –63.16) / (77.72 – 63.16)))
92.28< Y < 106.84	Within 10 & 30 SE > $\overline{x}$	0.5 × (1 + COS(π × (Y – 92.28) / (106.84 – 92.28)))
Y < 63.16 or Y > 106.84	Outside 30 SE of $\overline{x}$	0

Table 9: Red-Tailed Hawk Fuzzy Logic Membership Functions of DEM Grid Cells Based on Fatality Rates

Value of variable Y for *i*th grid cell	**Basis of membership function about $\bar{x}$**	**Membership function of grid cell (Values >1 include weightings)**
Y = Elevation		
166.42 <Y< 291.07	Within $\bar{x}$ ± 5 SE	1
131.39 <Y< 166.42	Within 1 SD & 5 SE < $\bar{x}$	0.5 × (1 - COS(π × (Y – 131.39) / (166.42 – 131.39)))
291.07 <Y< 326.1	Within 5 SE & 1 SD > $\bar{x}$	0.5 × (1 + COS(π × (Y – 291.07) / (326.1 – 291.07)))
Y < 131.39 or Y > 326.1	Outside 1 SD of $\bar{x}$	0
Y = Ridge elevation		
199.06 <Y< 273.62	Within $\bar{x}$ ± 3 SE	1
139.28 <Y< 199.06	Within 1 SD & 3 SE < $\bar{x}$	0.5 × (1 - COS(π × (Y – 139.28) / (199.06 – 139.28)))
273.62 <Y< 333.4	Within 3 SE & 1 SD > $\bar{x}$	0.5 × (1 + COS(π × (Y – 273.62) / (333.4 – 273.62)))
Y < 139.28 or Y > 333.4	Outside 1 SD of $\bar{x}$	0
Y = Percent up major terrain slope		
45.34 <Y< 67.16	Within $\bar{x}$ ± 3 SE	1
27.85 < Y < 45.34	Within 1 SD & 3 SE < $\bar{x}$	0.5 × (1 - COS(π × (Y – 27.85) / (45.34 – 27.85)))
67.16 < Y < 84.65	Within 3 SE & 1 SD > $\bar{x}$	0.5 × (1 + COS(π × (Y – 67.16) / (84.65 – 67.16)))
Y < 27.85 or Y > 84.65	Outside 1 SD of $\bar{x}$	0
Y = Hazard site		
Y = Within polygon	Not applicable	3

Table 10: American Kestrel Fuzzy Logic Membership Functions of DEM Grid Cells Based on Kiting, Hovering, and Surfing Flights

Value of variable Y for *i*th grid cell	**Basis of membership function about $\bar{x}$**	**Membership function of grid cell (Values >1 include weightings)**
Y = Ridge orientation		
Y = W-E	Not applicable	3
Y = WNW-ESE	Not applicable	3
Y = SSW-NNE	Not applicable	1
Y = Other orientation	Not applicable	0
Y = Subwatershed orientation		
Y = W	Not applicable	4
Y = WSW	Not applicable	3
Y = NW, SE	Not applicable	2
Y = SSE, SSW	Not applicable	1
Y = WNW, NNW	Not applicable	1
Y = Other orientation	Not applicable	0
Y = Percent up slope		
71.27 < Y < 99.22	Within ($\bar{x}$ -2 SE) & ($\bar{x}$ + 13 SE)	1
48.92 < Y < 71.27	Within 14 & 2 SE < $\bar{x}$	0.5 × (1 - COS(π × (Y – 48.92) / (71.27 – 48.92)))
99.22 < Y < 101.08	Within 13 & 14 SE > $\bar{x}$	0.5 × (1 + COS(π × (Y – 99.22) / (101.08 – 99.22)))
Y < 48.92 or Y > 101.08	Outside $\bar{x}$ ± 14 SE	0
Y = Percent up major terrain slope		
63.7 <Y< 96.9	Within 5 SE < $\bar{x}$ & 15 SE > $\bar{x}$	1
42.12 < Y < 63.7	Within 18 & 5 SE < $\bar{x}$	0.5 × (1 - COS(π × (Y –42.12) / (63.7 – 42.12)))
96.7 < Y < 101.88	Within 15 & 18 SE > $\bar{x}$	0.5 × (1 + COS(π × (Y – 96.7) / (101.88 – 96.7)))
Y < 42.12 or Y > 101.88	Outside $\bar{x}$ ± 18 SE	0

Table 11: Burrowing Owl Fuzzy Logic Membership Functions of DEM Grid Cells Based on Burrow Locations

Value of variable Y for *i*th grid cell	Basis of membership function about $\bar{x}$	Membership function of grid cell (Values >1 include weightings)
Y = Subwatershed orientation		
Y = S	Not applicable	2.5
Y = ESE, SE	Not applicable	1.5
Y = ENE, E, SSE	Not applicable	1
Y = Other orientation	Not applicable	0
Y = Percent up slope		
5.56 < Y < 20.83	Within ($\bar{x}$ -0.25 SD) & ($\bar{x}$ + 0.5 SD)	1
0.47 < Y < 5.56	Within 0.5 & 0.25 SD < $\bar{x}$	0.5 × (1 - COS(π × (Y – 0.47) / (5.56 – 0.47)))
20.83 < Y < 51.37	Within 0.5 & 2 SD > $\bar{x}$	0.5 × (1 + COS(π × (Y – 20.83) / (51.37 – 20.83)))
Y < 0.47 or Y > 51.37	Outside ($\bar{x}$ -0.5 SD) & ($\bar{x}$ + 2 SD)	0

3.3.3 Collision Hazard Maps

Based on flight behaviors, the collision hazard predicted for golden eagle was distributed along the crests of ridge structures that were oriented east-west (Figure 51). East-west oriented ridge structures are common on the east slope of the APWRA. However, based on fatality rates, the collision hazard was more sparsely distributed within and around Forebay sites, mostly restricted to hazard sites consisting of ridge saddles and breaks in slope (Figure 52). The collision hazard model developed from both behaviors and fatality rates identified east-west ridge crests and ridge saddles as most hazardous within the Forebay sites (Figure 53). However, it should be remembered that the collision hazard modeling approach used herein assumed that relatively low terrain would be avoided for future wind turbine siting; it was assumed that low-lying terrain is inherently hazardous to golden eagle and other birds. The only golden eagle that was killed on a Forebay site and that could be attributed to a particular turbine was in a ravine bottom between two east-west stretches of FL class 4 hazard polygons.

Based on flight behaviors, the collision hazard predicted for red-tailed hawk was distributed on generally west-facing slopes, with two spots highlighted in Venture and Altech project areas, and larger areas along the western aspects of the Taxvest project near Mountain House and off Midway Road (Figure 54). The behavior model predictions corresponded well with the spatial distribution of fatality rates (Figures 23 and 24). Based on fatality rates, the collision hazard was very sparsely distributed within the Forebay sites, and was within ridge saddles and relatively low terrain typically used for travel (Figure 55). The collision hazard model developed from both behaviors and fatality rates emphasized the ridge saddles and low terrain, or the *Hazard sites* (Figure 56).

Table 12: Burrowing Owl Fuzzy Logic Membership Functions of DEM Grid Cells Based on Burrow Locations

Value of variable Y for *i*th grid cell	Basis of membership function about $\bar{x}$	Membership function of grid cell (Values >1 include weightings)
Y = Elevation		
168.78 < Y < 193	Within $\bar{x}$ ± 2 SE	1
120.36 < Y < 168.78	Within 10 & 2 SE < $\bar{x}$	0.5 × (1 - COS(π × (Y – 120.36) / (168.78 – 120.36)))
193 < Y < 241.42	Within 2 & 10 SE > $\bar{x}$	0.5 × (1 + COS(π × (Y – 193) / (241.42 – 193)))
Y < 120.36 or Y > 241.42	Outside $\bar{x}$ ± 10 SE	0
Y = Valley elevation		
138.42 < Y < 155.09	Within $\bar{x}$ ± 1.5 SE	1
113.41 < Y < 138.42	Within 6 & 1.5 SE < $\bar{x}$	0.5 × (1 - COS(π × (Y – 113.41) / (138.42 – 113.41)))
155.09 < Y < 180.1	Within 1.5 & 6 SE > $\bar{x}$	0.5 × (1 + COS(π × (Y – 155.09) / (180.1 – 155.09)))
Y < 113.41 or Y > 180.1	Outside $\bar{x}$ ± 6 SE	0
Y = Percent up major terrain slope		
35.51 < Y < 42.49	Within $\bar{x}$ ± 2 SE	1
25.05 < Y < 35.51	Within 8 & 2 SE < $\bar{x}$	0.5 × (1 - COS(π × (Y – 25.05) / (35.51 – 25.05)))
42.49 < Y < 52.95	Within 2 & 8 SE > $\bar{x}$	0.5 × (1 + COS(π × (Y – 42.49) / (52.95 – 42.49)))
Y < 25.05 or Y > 52.95	Outside $\bar{x}$ ± 8 SE	0
Y = Hazard site		
Y = Within polygon	Not applicable	2

Table 13: Fuzzy Logic Models Developed for Forebay

Dependent variable	Model	Max score possible
Golden eagle flights	2×Ridge orientation + 2×Subwatershed orientation + 0.5×(Percent up slope + Percent up major terrain slope) + 0.75×Hill size	15.75
Golden eagle fatalities	Hazard site + (Ridge elevation + Major valley elevation)×RidgeValley + Slope to gross slope×RidgeValley	11
Golden eagle combined	GOEA flights/15.75 + GOEA fatalities/11 + Hazard site	3
Red-tailed hawk kiting	2×(Percent up slope + Percent up major terrain slope) + Ridge orientation + 2×Subwatershed orientation	12
Red-tailed hawk fatalities	Hazard site + 2×Elevation + Percent up major terrain slope	7
Red-tailed hawk combined	(Red-tailed hawk kiting/12 + Red-tailed hawk fatalities/7)/2 + Hazard site	2
American kestrel kiting	2×Subwatershed orientation + Ridge orientation + 4×(Percent up slope + Percent up major terrain slope)	19
Burrowing owl burrows	2.5×Percent up slope + Subwatershed orientation	3.5
Burrowing owl fatalities	Hazard site + Elevation + 2×Valley elevation + Percent up major terrain slope	6
Burrowing owl combined	Burrowing owl fatalities + 2×Burrowing owl burrows	13

Based on flight behaviors, the collision hazard predicted for American kestrel was distributed among western and southern slopes (Figure 57). The most hazardous site according to the model was the Taxvest project near Mountain House. The model predictions corresponded well with the spatial distribution of fatality rates at Forebay sites (Figures 27 through 29).

Based on burrow locations, the collision hazard predicted for burrowing owl was distributed along long reaches of south-facing slopes, forming east-west bands of areas relatively high in collision hazard wherever wind turbines happen to be present (Figure 58). The collision hard map based on fatality rates depicted a broader portion of the Altech and Venture project areas as hazardous, as well as the western portion of the site along Midway Road (Figure 59). The collision hazard model developed from both burrow locations and fatality rates emphasized low-lying terrain and the lower reaches of south-facing slopes (Figure 60). The collision hazard predictions from this combined model corresponded well with the spatial distribution of burrowing owl fatality rates at the Altech and Venture sites (Figure 30) and at the Taxvest project along Midway Road (Figure 32).

Figure 51: Fuzzy Logic Likelihood Surface Classes of Golden Eagle Collision Hazard

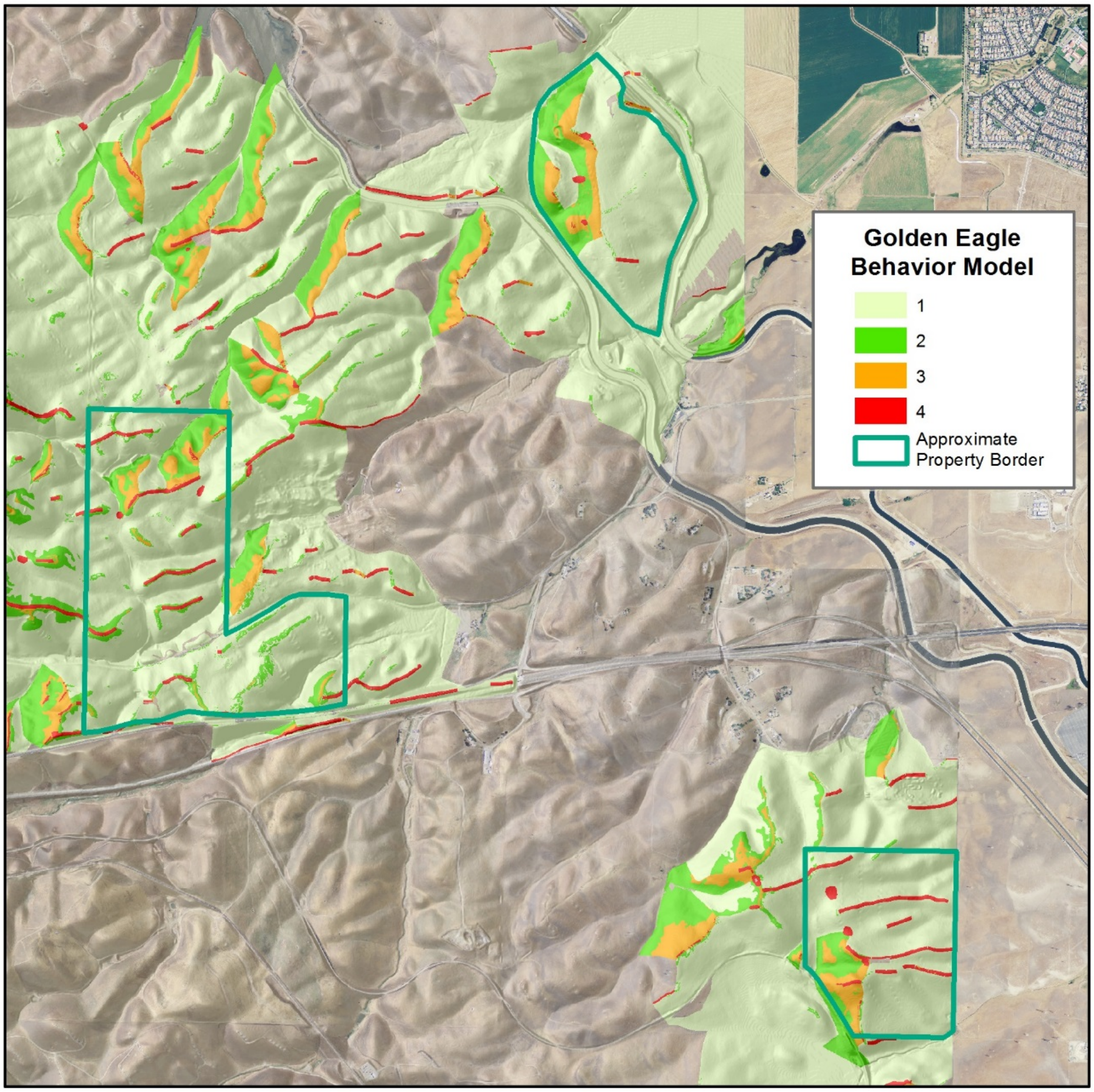

Based on ridge crossings, wind turbine interaction events, and interactions with other birds (behaviors), where collision likelihood grades from red as the highest, orange, as second highest, dark green as third highest, and light green as least.

Figure 52: Fuzzy Logic Likelihood Surface Classes of Golden Eagle Collision

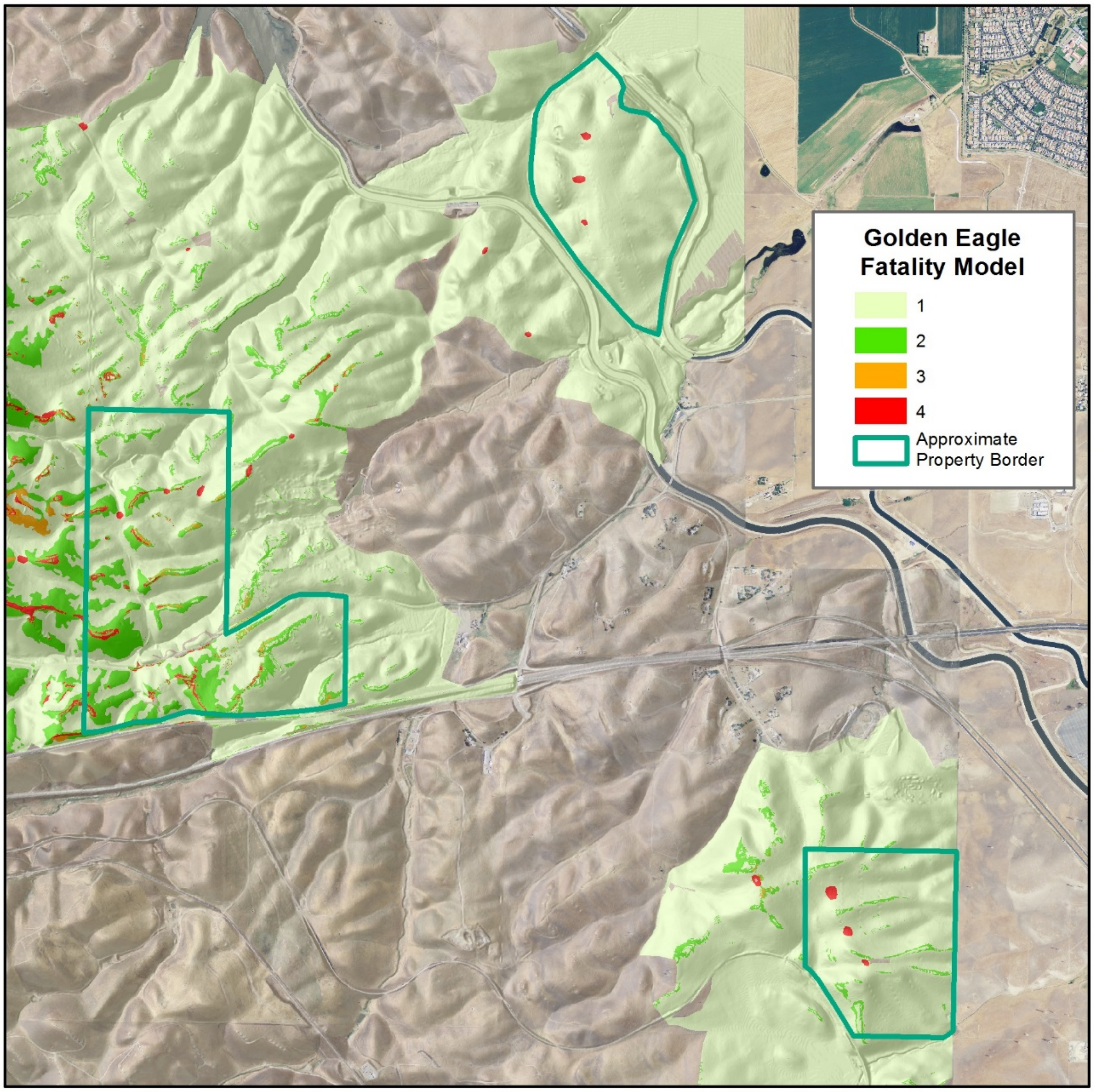

Hazard based on fatality rates among wind turbines monitored since 1998, where collision likelihood grades from red as the highest, orange, as second highest, dark green as third highest, and light green as least.

Figure 53: Fuzzy Logic Likelihood Surface Classes of Golden Eagle Collision Hazard

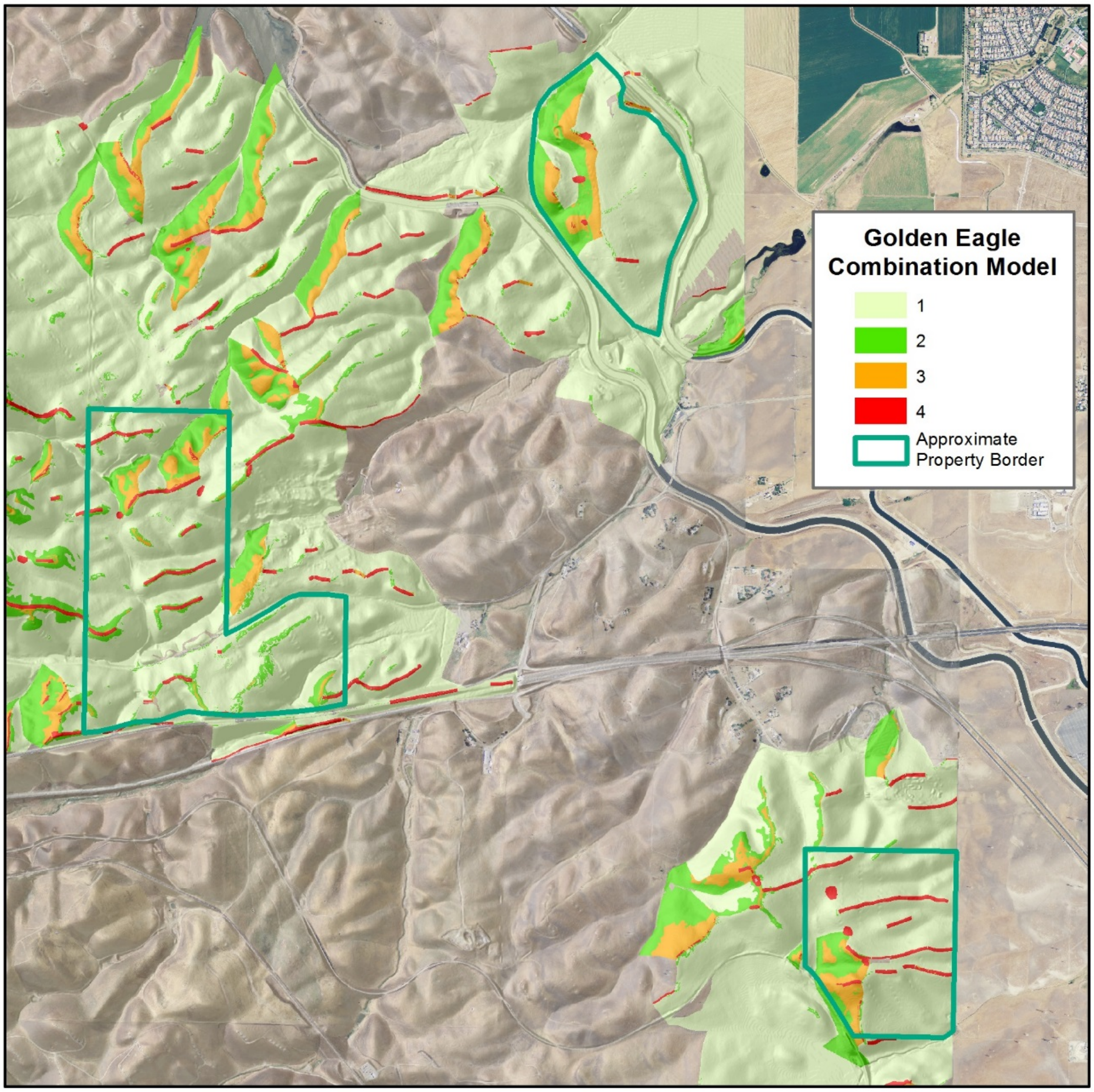

Based on both behaviors and fatality rates, where collision likelihood grades from red as the highest, orange, as second highest, dark green as third highest, and light green as least.

Figure 54: Fuzzy Logic Likelihood Surface Classes of Red-Tailed Hawk Collision Hazard

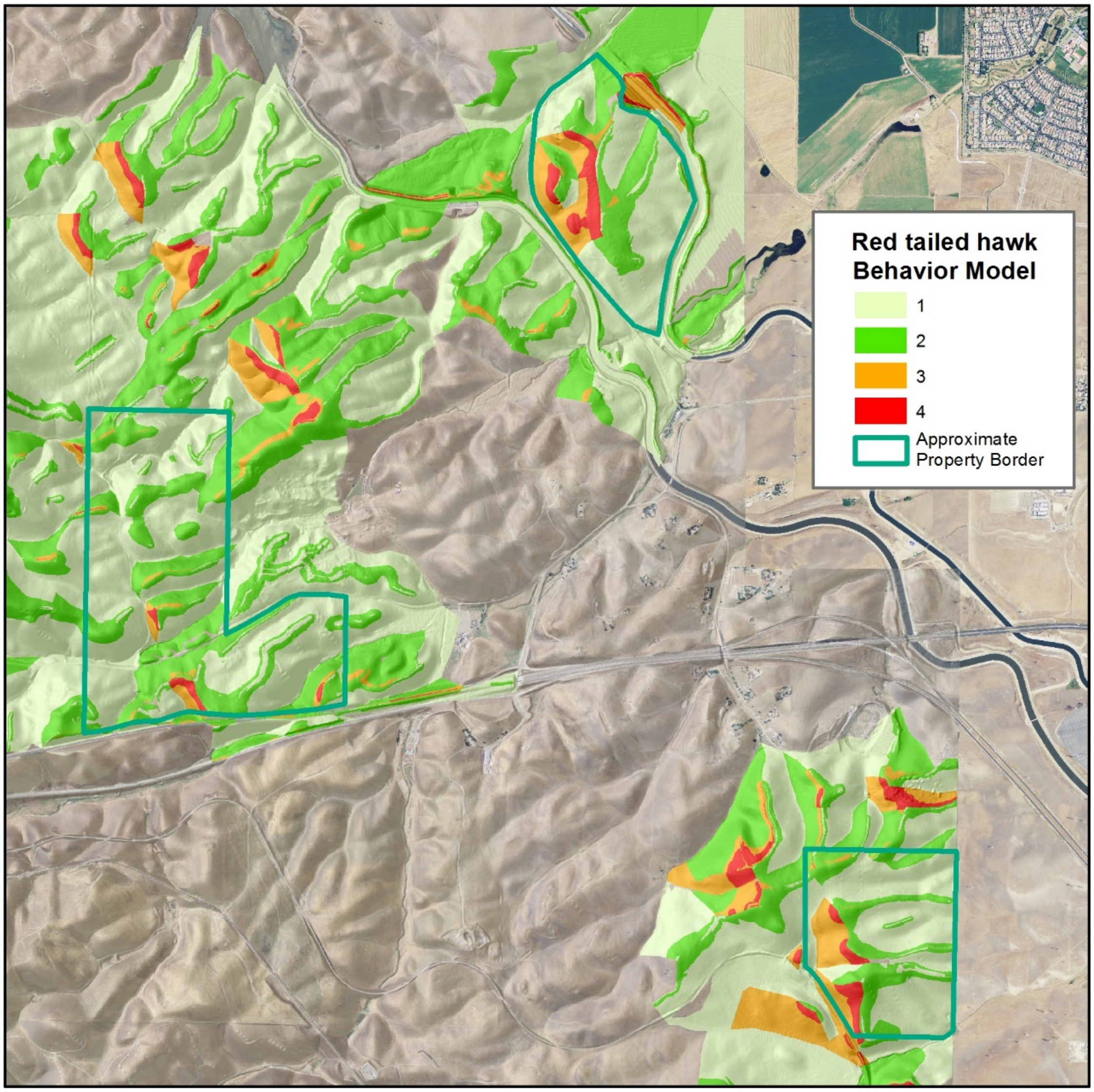

Based on kiting, hovering, and surfing (behaviors), where collision likelihood grades from red as the highest, orange, as second highest, dark green as third highest, and light green as least.

Figure 55: Fuzzy Logic Likelihood Surface Classes of Red-Tailed Hawk Collision Hazard

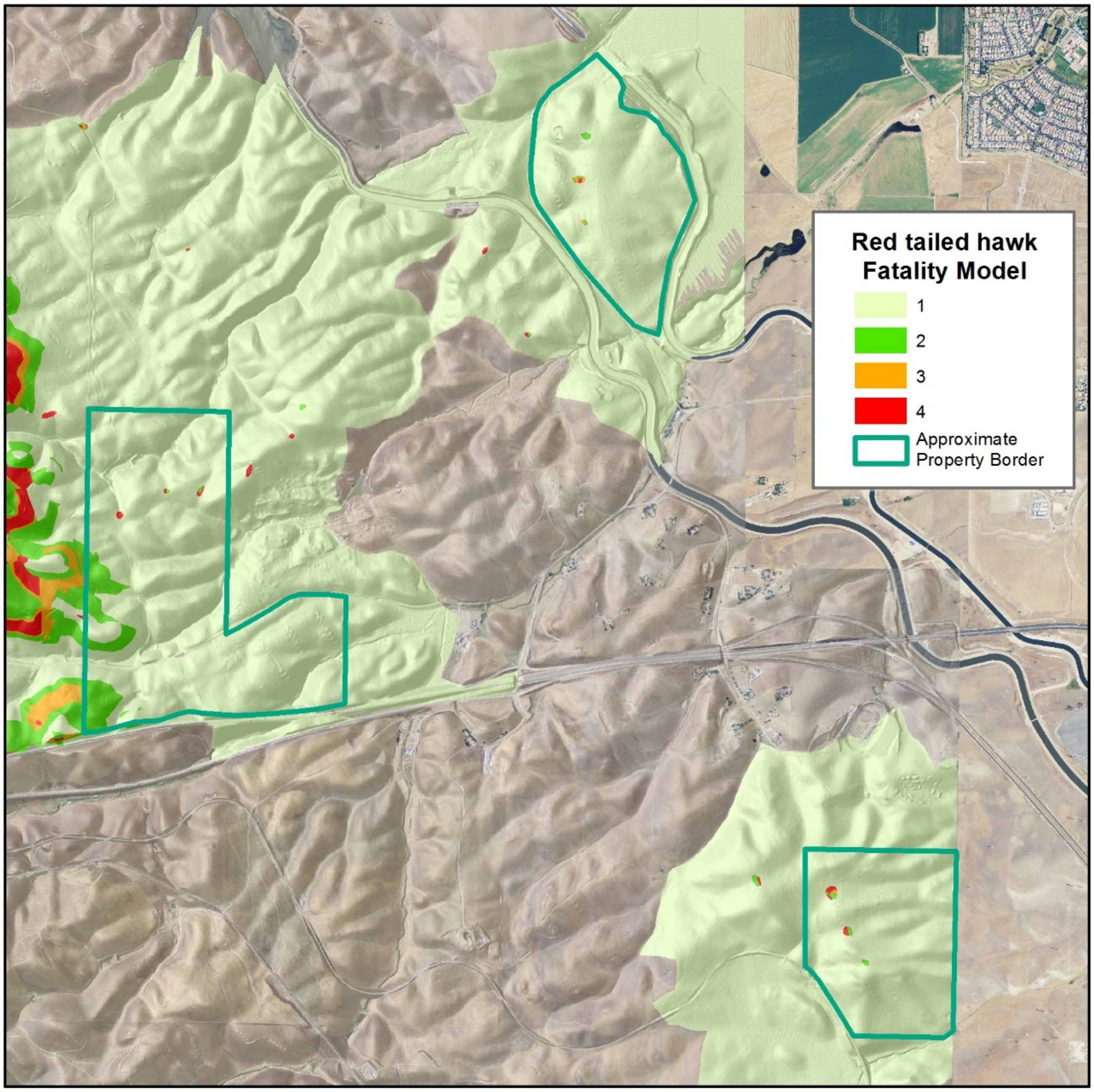

Based on fatality rates among wind turbines monitored since 1998, where collision likelihood grades from red as the highest, orange, as second highest, dark green as third highest, and light green as least.

Figure 56: Fuzzy Logic Likelihood Surface Classes of Red-Tailed Hawk Collision Hazard

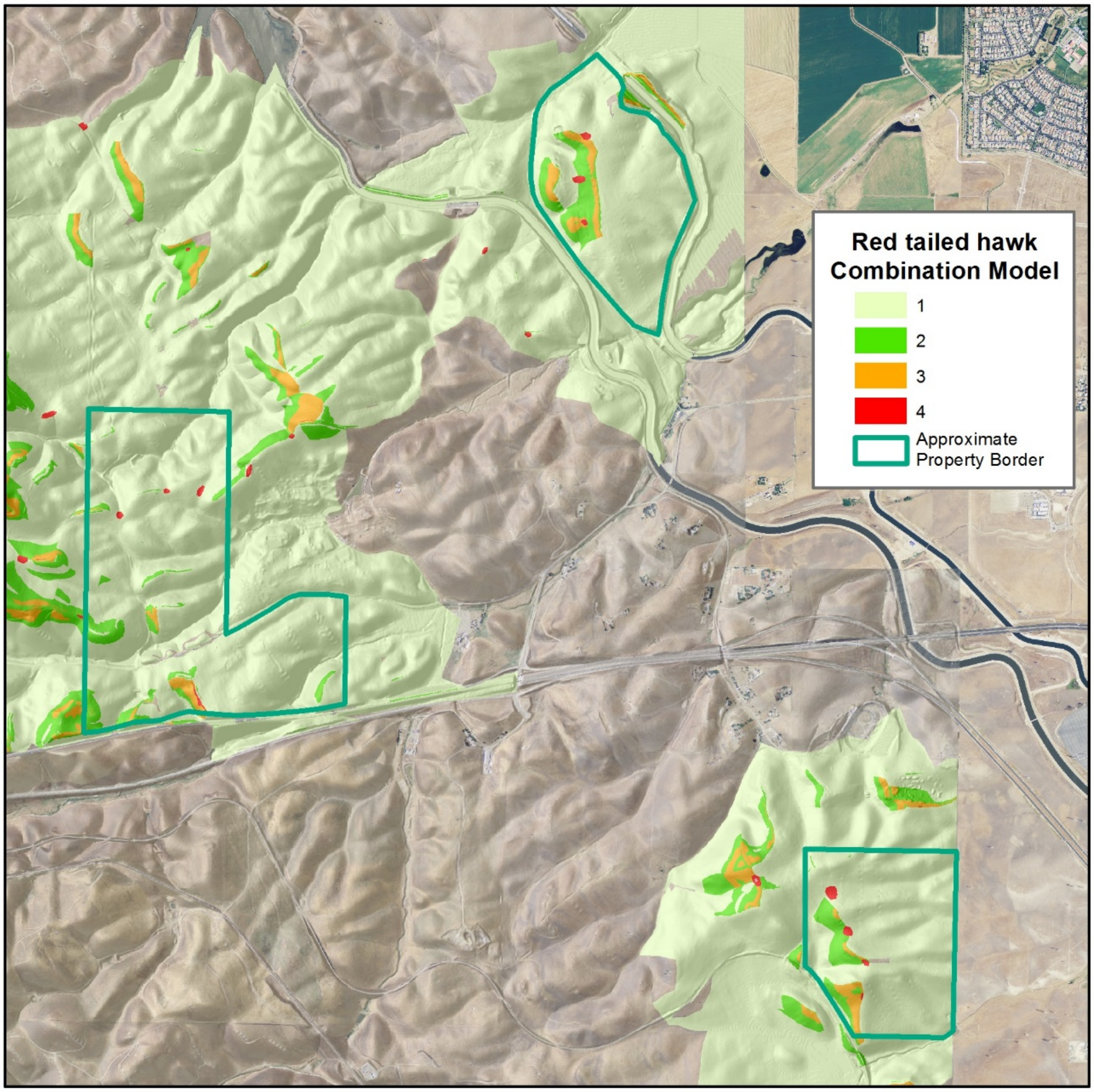

Based on both behaviors and fatality rates, where collision likelihood grades from red as the highest, orange, as second highest, dark green as third highest, and light green as least.

Figure 57: Fuzzy Logic Likelihood Surface Classes of American Kestrel Collision Hazard

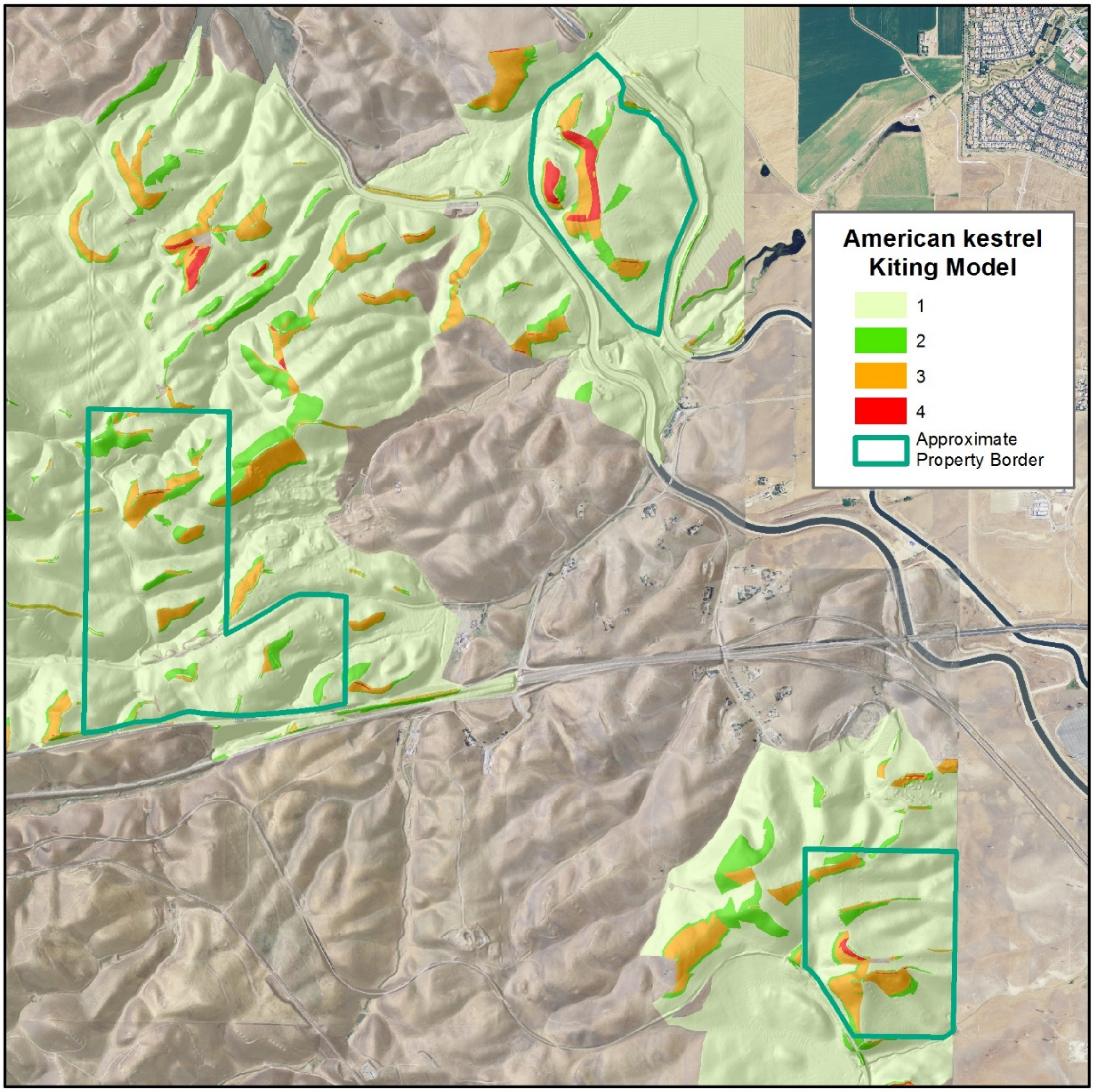

Based on kiting, hovering, and surfing (behaviors), where collision likelihood grades from red as the highest, orange, as second highest, dark green as third highest, and light green as least.

Figure 58: Fuzzy Logic Likelihood Surface Classes of Burrowing Owl Collision Hazard

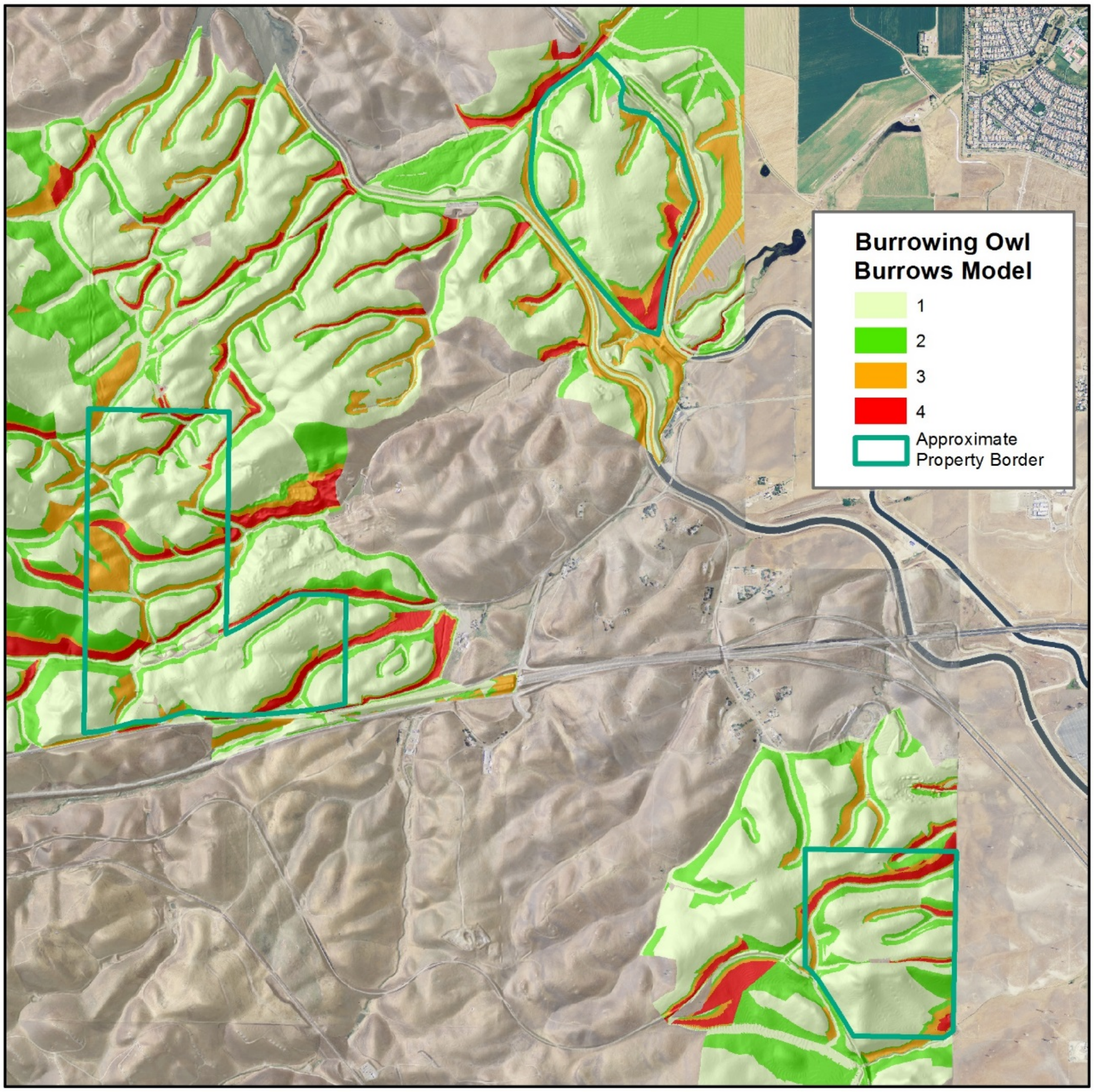

Based on burrow locations, where collision likelihood grades from red as the highest, orange, as second highest, dark green as third highest, and light green as least.

Figure 59: Fuzzy Logic Likelihood Surface Classes of Burrowing Owl Collision Hazard

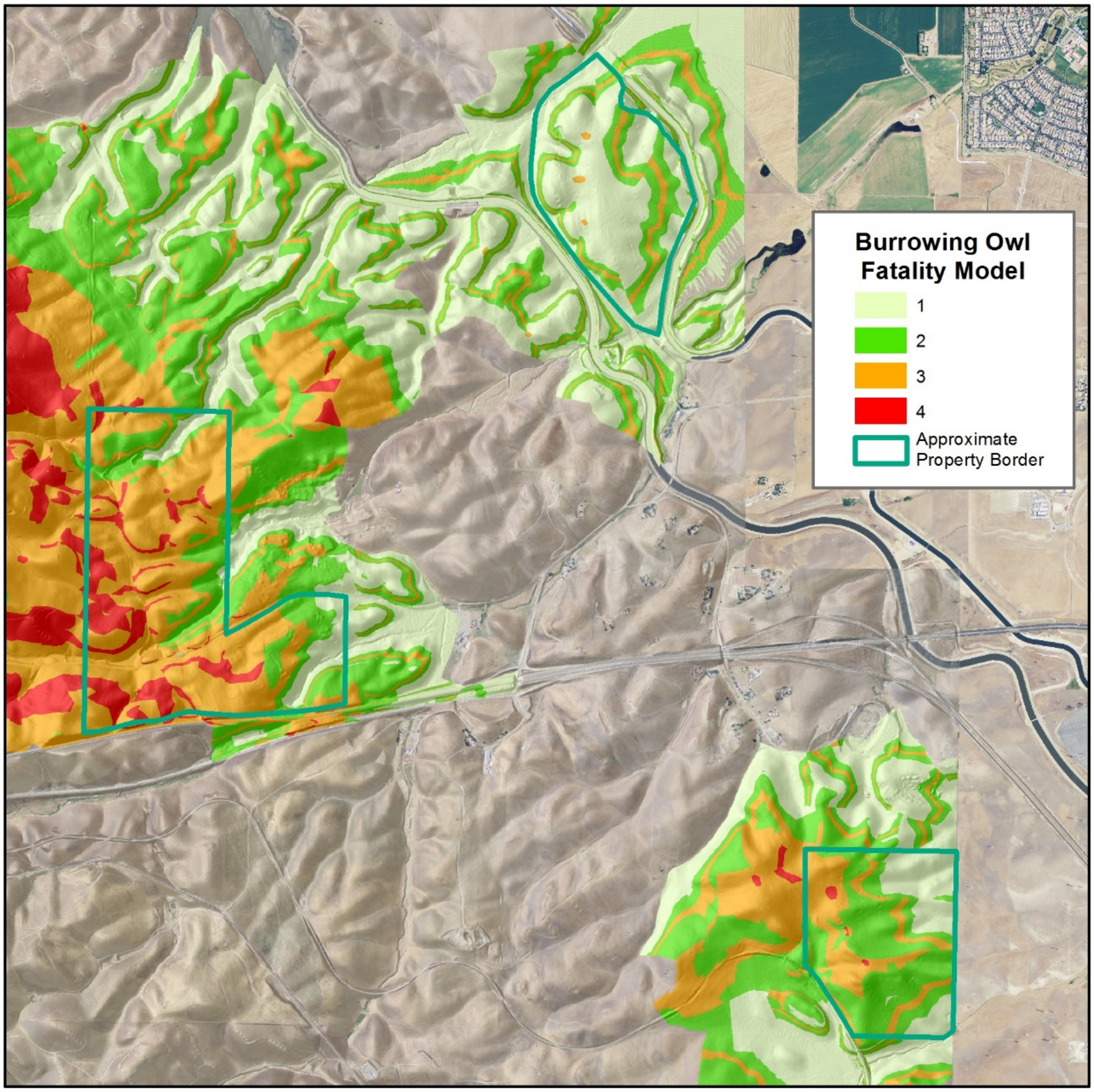

Based on fatality rates among wind turbines monitored since 1998, where collision likelihood grades from red as the highest, orange, as second highest, dark green as third highest, and light green as least.

Figure 60: Fuzzy Logic Likelihood Surface Classes of Burrowing Owl Collision Hazard

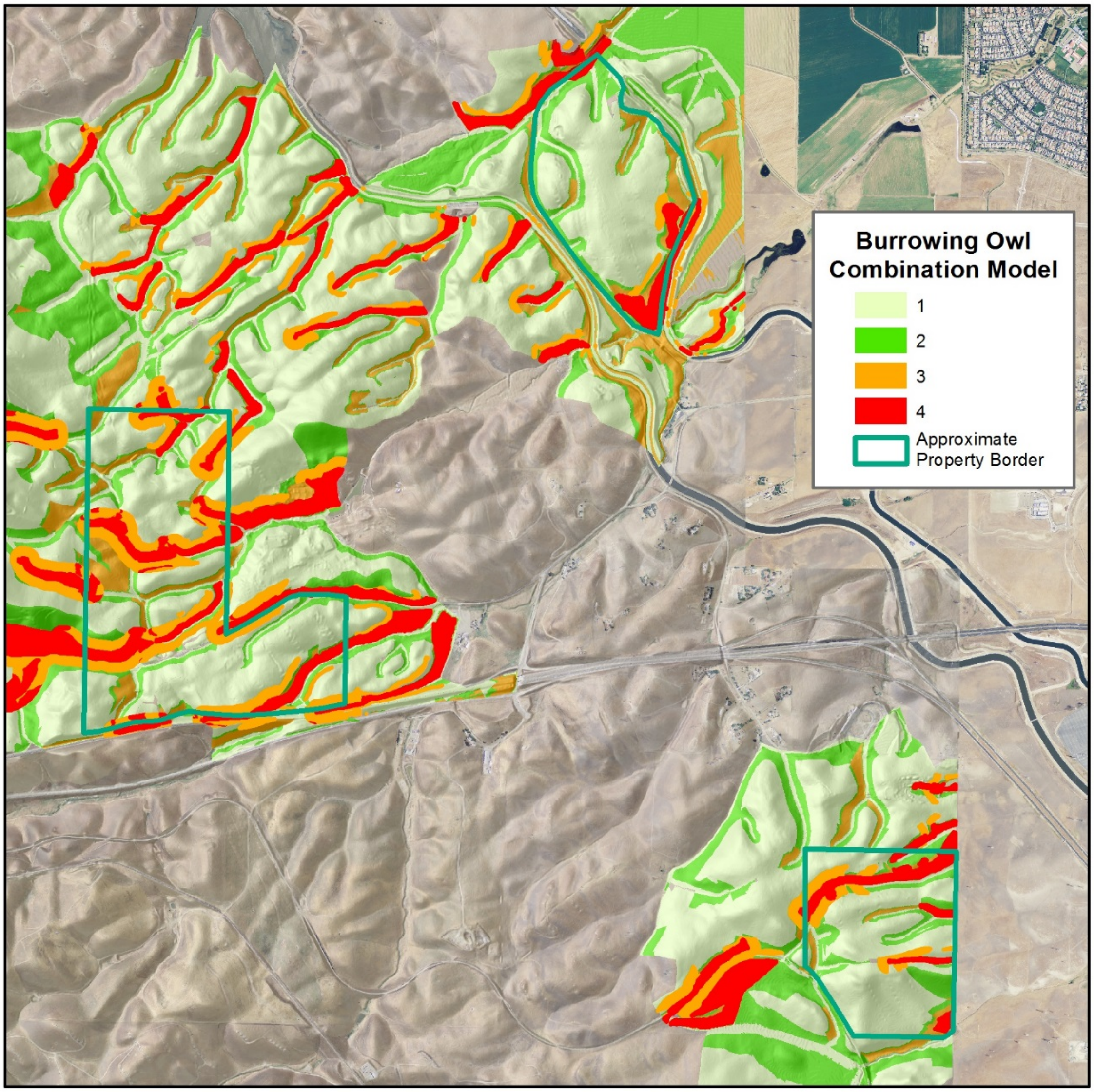

Based on both burrow locations and fatality rates, where collision likelihood grades from red as the highest, orange, as second highest, dark green as third highest, and light green as least.

3.4. Discussion

The large number of red-tailed hawk interaction events with nonoperating wind turbines was consistent with the finding in Chapter 1 of all red-tailed hawk fatalities occurring at nonoperational wind turbines. The total number of near misses and obvious last-second reactions to avoid wind turbines and blades indicated the level of hazard posed to birds by the wind turbines in the APWRA. Dedicated surveys to observe wind turbine events make sense in this environment. Without too much time invested, many observations of dangerous flights around wind turbines can be accumulated.

Simple collision risk models were derived from golden eagle and red-tailed hawk flight behaviors and wind turbine fatalities, as well as from American kestrel hovering and kiting flights and from burrowing owl burrow locations and fatalities at the Altamont Pass Wind Resource Area, including the Forebay sites. After the first two years of operations at the repowered Vasco Winds Energy Project, and compared to the old-generation wind project that preceded it, Brown et al. (2014) estimated fatality rate reductions of 90% for golden eagle, 68% for red-tailed hawk, and 59% for American kestrel. If modern wind turbines are installed at Forebay, it is hoped that the collision hazard models provided herein will help guide siting so that fatality rates can be minimized.

The collision hazard maps in this chapter will need to be interpreted carefully, however. For example, these maps did not account for grading that will be necessary for access roads and wind turbine pads. Grading can change the landscape upon which terrain attributes were measured, so the hazard maps will not translate perfectly to a revised landscape to suit large wind turbines. To install a wind turbine, the underlying ridge might be cut for a level pad area, and the resulting break in slope, had it been anticipated, might have been regarded as a hazard site. At the time of this report, no consideration had been given to the level and location of grading needed for new wind turbines, and so grading had not factored into the collision hazard map predictions.

The behavior data collected at Forebay and throughout the APWRA provide the opportunity to quantify behavior responses of raptors to changes in wind turbine models and layouts, along with the changes to the landscape due to grading for repowered projects. The thousands of flight paths and flight behaviors recorded during behavior surveys can serve as the baseline against which future flight paths and behaviors can be compared of birds using a landscape with new, repowered wind projects. Against these data, one can test whether the large wind turbines displace raptors (Garvin et al. 2011), or whether raptors alter their flight paths (Hull and Muir 2013), or whether the flight paths remain unchanged and to what degree the new turbine layout reduced collision risk or the larger turbines altered avoidance measures that affect collision risk (Band et al. 2005, Chamberlain et al. 2006, Smales et al. 2013).

As repowering proceeds, an experimental design opportunity arises, akin to a before-after, control-impact (BACI) design. Thousands of behavior survey observations were collected from locations where old-generation wind turbines are being replaced with modern turbines in carefully sited projects. These data were from locations representing the “before” phase of the opportune experimental design, and going forward many of these data could represent the "after" phase as well as the "control" and "impact" portions of the design. The impact portions would be wherever repowered turbines occur within the surveyed airspace of behavior stations. Follow-up surveys within these areas of overlap would be comparable to the survey data from areas of non-overlap, so the effects of repowering can be quantifiable.

CHAPTER 4: Nocturnal Behaviors

4.1 Introduction

The nocturnal surveys were originally intended to measure changes, if any, in nocturnal flight paths of owls and bats due to the installation of Ogin's shrouded wind turbine. The original goal and associated objectives changed after Ogin determined that it could no longer install its turbine. However, the nocturnal surveys were also exploratory in nature right from the start, because it was the first time that systematic surveys had been performed in a wind project at night using a high-end thermal imaging camera. Until the surveys were well underway, it remained unknown whether sufficient animals would be seen or whether risky behaviors might be quantified. Furthermore, there was no formal plan to observe the activities of mammalian scavengers, which turned out to be one of the most interesting outcomes of the surveys.

Before this study, observations of volant nocturnal wildlife around wind turbines were made mostly using radar and acoustic detectors. Using radar, Harmata et al. (1998) reported 7 to 17 times greater detection rates of flying birds compared to using visual scans, although radar requires clear weather (Hanowski & Hawrot 2000), and in many cases is unable to help investigators identify targets to species. Mabee et al. (2006) used radar to evaluate avian passage rates and flight heights of nocturnal migrants over a proposed wind project area, but their passage rates were incomparable to passage rates measured elsewhere and it was unclear whether the study results influenced wind turbine siting. May et al. (2009) also used radar to detect diurnal flights of white-tailed eagles (*Haliaeetus albicilla*), including those killed by wind turbines, leading to some useful inference regarding times of day when visual surveys might be more effective (early morning and late evening). Acoustic detectors have often been used to identify species of bats flying within the rotor zone of wind turbines, to quantify passage rates, and to quantify temporal patterns of bat activity near wind turbines. However, passage rates measured by acoustic detectors have yet to correlate significantly with bat fatality rates (Hein et al. 2012). Thermal cameras have also been used to view volant nocturnal wildlife, principally bats (Horn et al. 2008), but no precedent existed for watching nocturnal birds or mammalian scavengers using thermal cameras. Cooper et al. (2005) used a combination of night vision goggles and radar to quantify bat passage rates at night.

The revised goal of the nocturnal surveys was to explore nocturnal flight patterns of birds and bats and mammalian scavenger activities that might bear on fatality rate estimation. The revised objectives were the following:

1. Provide field-tested behavior survey methods and data that inform avoidance rates in collision risk models and map-based collision hazard models to guide wind turbine siting;
2. Quantify mammalian scavenger activities during nocturnal surveys and characterize movement patterns; and,

3. Quantify owl and bat activities and describe flight patterns and reactions to wind turbines.

4.2 Methods

Nocturnal surveys began as the sky grew dark, and each session lasted three hours. The surveys were performed by one person viewing the monitor on the back of a tripod-mounted FLIR T620 thermal imaging camera fitted with an FLIR IR 88.9 mm lens. The tripod was weighted by a 5 pound sandbag hung from the center pole of the tripod to stabilize the tripod against wind force.

The camera was moved to pan the ground and airspace 360° for all signs of wildlife, pausing at intervals to examine candidate targets emitting sufficient heat to represent an animal. As the surveys progressed it became apparent that the feathers of some bird species effectively dampened heat emission, so live targets of scans also were identified by detecting dark silhouettes formed by the animal's body occluding background heat emissions from grassland, wind turbines, transmission towers, and any other emitter of ambient or physiological heat. Great-horned owls emitted enough heat to be detected by the camera only when facing the camera and barn owls did so when facing the camera or flying high enough for the underwings to be viewed by the camera. Burrowing owls also emitted little heat when facing away from the camera, but heat emission could be detected while burrowing owls faced the camera or were in flight in most directions and orientations relative to the camera. Bats were highly visible and could be seen to great distances, even as distant as 1.6 km.

Weather measurements were made into a voice recorder at the start and end of each session, as well as at one hours and two hours into the session. Weather measurements included air temperature, average and maximum wind speeds, and wind direction. The moon phase was recorded at the start of sessions, and the time of moonrise was recorded. All wildlife data were recorded onto handheld images of the survey area either as line or point features, as appropriate. Mapped wildlife locations were labeled and the labels used to record attributes of the observation into the voice recorder.

4.3 Results

4.3.1 Mammalian Scavengers

As nocturnal surveys got underway each night, darkness had just descended and the first animals often seen were striped skunks running up slopes towards the wind turbines. These skunks usually numbered between one and six, although the numbers reduced greatly during the last year of the study probably due to drought. Joining the skunks at various times during the survey sessions were coyotes, foxes, American badgers, and occasionally house cats and bobcats. Long-tailed weasels were rarely seen, and these only briefly.

During the surveys, the numbers of terrestrial mammal observations made were 2 of bobcat, 7 of house cat, 37 of foxes, 64 of coyote, 24 of American badger, 2 of long-tailed weasel, 4 of raccoon, 1 of opossum, and 84 of striped skunk. Rates of observations included 0.39 striped skunks per hour, 0.3 coyotes per hour, 0.17 foxes per hour, and 1.05 terrestrial mammals per hour, not including lagomorphs and rodents. Together, mammalian scavenger activity levels varied seasonally (Figure 61). Intriguingly, adjusted fatality rates correlated negatively with increasing numbers of mammalian scavengers observed per hour among nocturnal survey stations (Figure 62). The outlier in Figure 61 was likely due to a disproportionate number of rock pigeon fatalities on the west side of the Venture Winds project; feathers of rock pigeons are liberally shed from carcasses found by scavengers, so evidence of rock pigeon fatalities is often detectable even after the carcass was removed.

Except for long-tailed weasels, mammalian Carnivores typically searched the ground around wind turbines, and usually on the downwind aspect relative to the pr evailing wind direction (Figures 63 through 65). Foxes and coyotes also trotted or walked straight transects, often parallel to the wind turbine row and about 30 m downwind of the row. These locations would have been optimal for finding birds and bats that had been killed or wounded by wind turbines.

Figure 61: The Number of Nocturnal Scavengers per Hour at Forebay

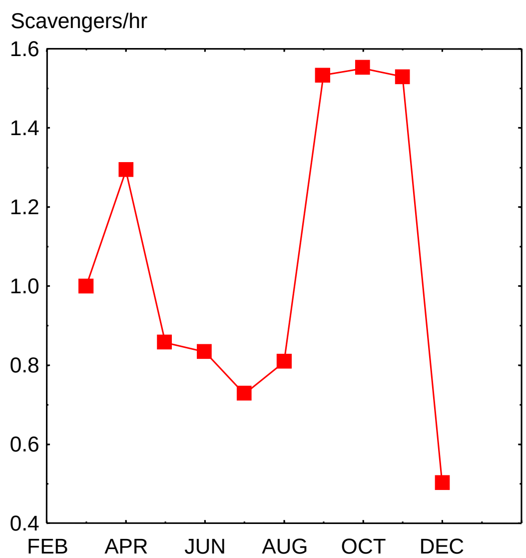

Peaked in April and September through November.

Figure 62: After Removing Outlier (Left Graph)

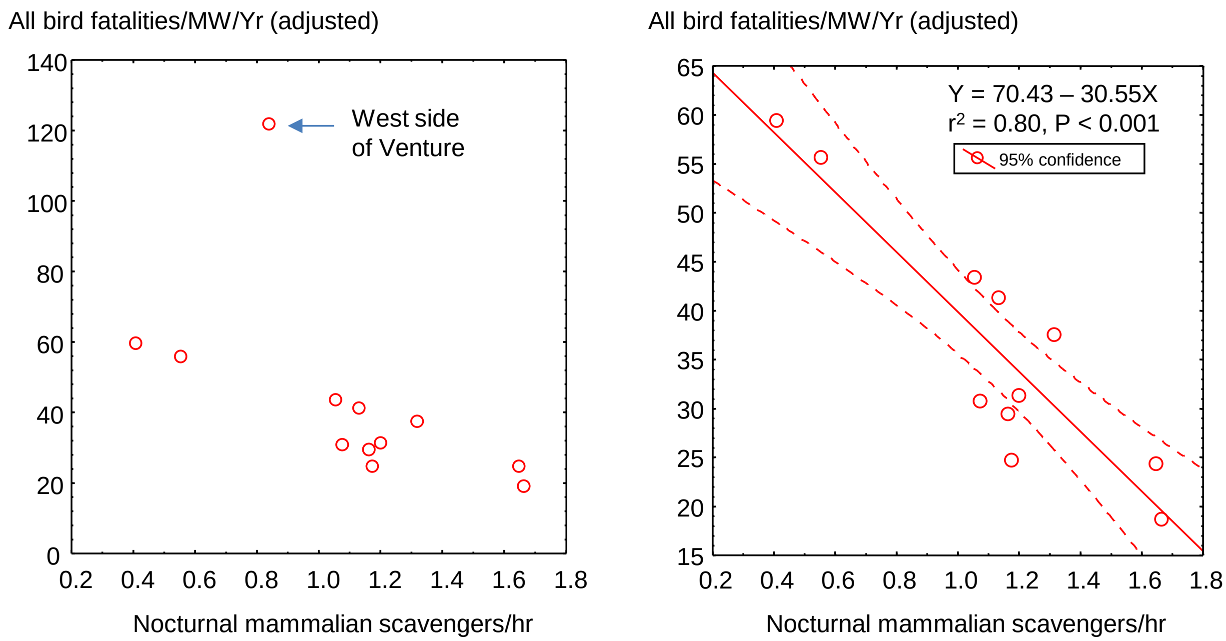

Bird fatalities/MW/year declined with increasing numbers of nocturnal mammalian scavengers/hour among nocturnal survey plots.

4.3.2 Flying Birds and Bats

During nocturnal surveys at Forebay sites, observations were made of 99 burrowing owls, 38 barn owls, 25 great-horned owls, 8 ducks, 1 heron, 16 medium-sized birds, 36 small birds, 10 large birds, and 120 bats. (These observations could have included repeat observations on some of the same individuals.) The rate of observations was 0.46 burrowing owls per hour, 0.18 barn owls per hour, 0.12 great-horned owls per hour, and 0.56 bats per hour. Maps of flight paths are depicted in Figures 66 through 71.

Burrowing owl flight activity was much greater at night than during the day (compare maps of flight paths between Figures 66 and 50 and between Figures 67 and 50). Also, contrary to diurnal surveys, nocturnal surveys revealed that burrowing owls spend much of their flight time very close to wind turbines. The flight behaviors also consisted of hovering near wind turbines, which was not seen during diurnal behavior surveys.

Barn owls also flew close to wind turbines, often crisscrossing the sky just upwind of wind turbines (Figures 67 and 68). On the other hand, great-horned owl flights more often followed terrain features, such as ravines (Figures 66-68), although at Mountain House many of the flights were made between wind turbines, which were used for still-hunting (Figure 67).

Bat flight patterns were strongly influenced by terrain (Figures 69 through 71). Most bat flights followed low terrain such as ravines and crossed ridge saddles and break in slope, much the same as most birds.

Seasonally, bat activity peaked in May, declined rapidly through August, and steadily increased again from September (Figure 71). Burrowing owl activity peaked in May and June and September and October, and barn owl and great-horned owl activity was seasonally sporadic (Figure 72).

Figure 63: Locations and Movement Patterns of Mammalian Carnivores During Nocturnal Surveys at Altech 1, Swamp, Viking, and Venture Winds Projects, Altamont Pass Wind Resource Area

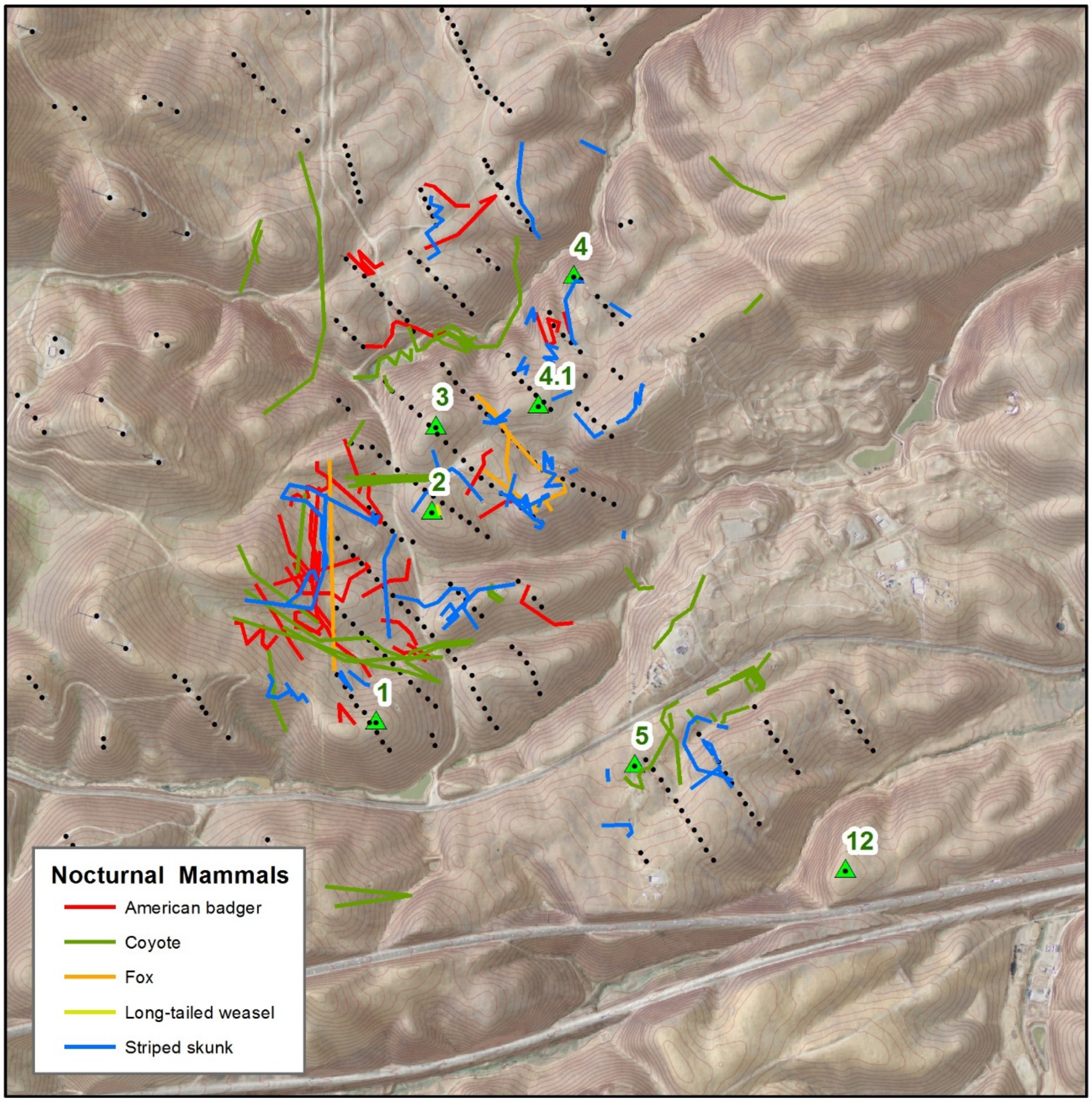

Figure 64: Locations and Movement Patterns of Mammalian Carnivores During Nocturnal Surveys at the Taxvest Project near Mountain House, Altamont Pass Wind Resource Area

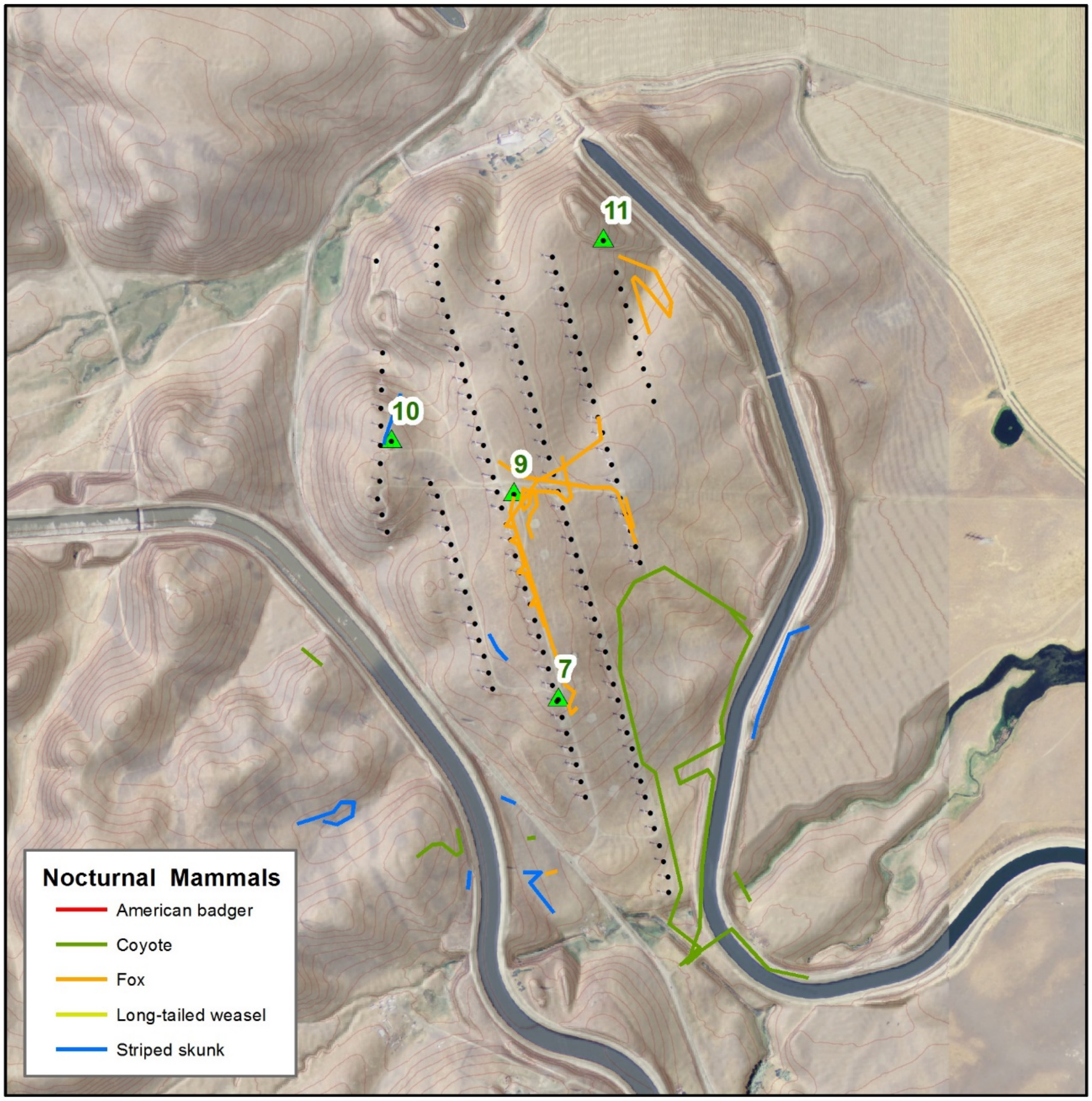

Figure 65: Locations and Movement Patterns of Mammalian Carnivores During Nocturnal Surveys at the Taxvest Project off Midway Road, Altamont Pass Wind Resource Area

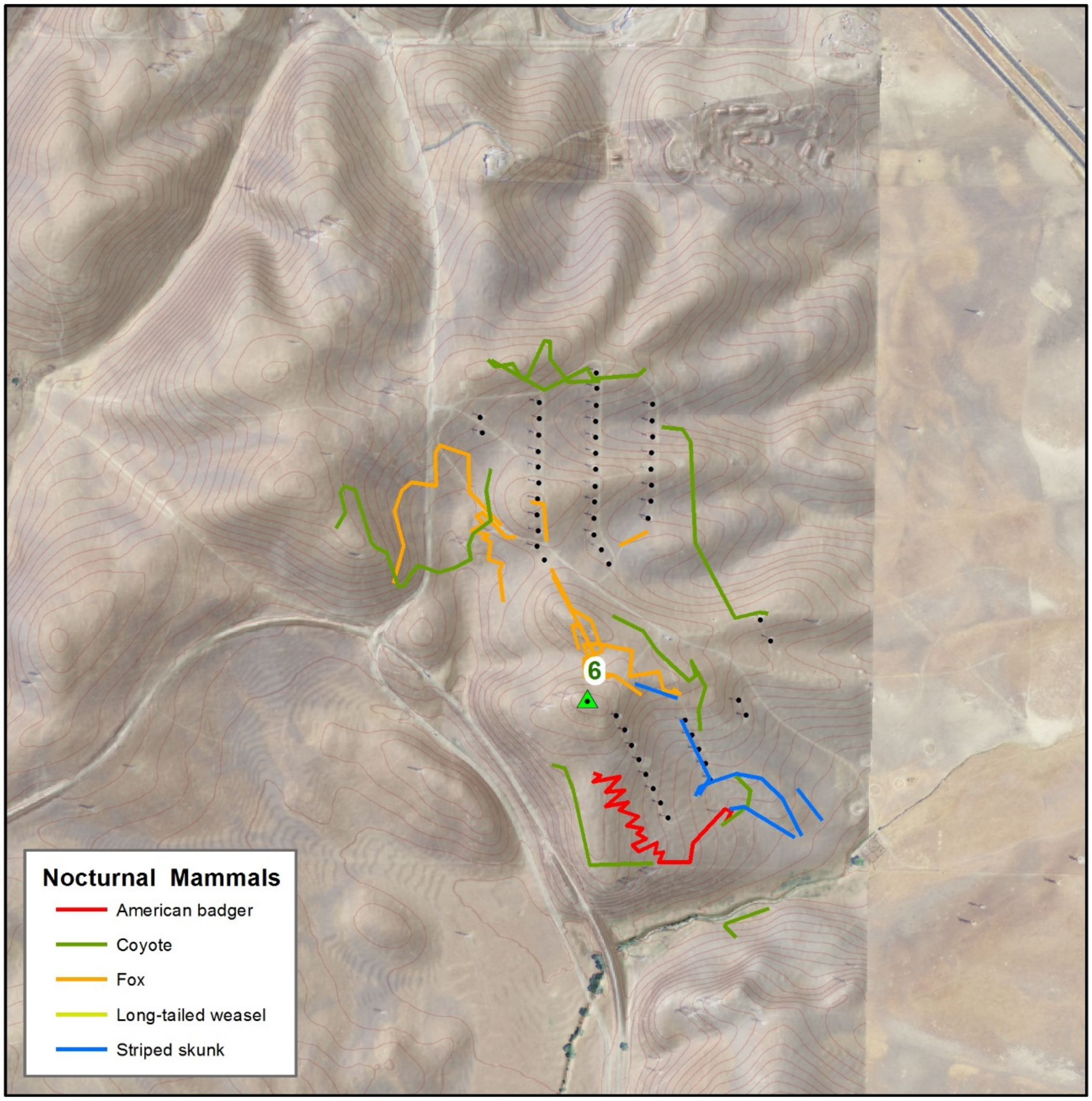

Figure 66: Flight Patterns of Owls During Nocturnal Surveys at Altech 1, Swamp, Viking, and Venture Winds Projects, Altamont Pass Wind Resource Area

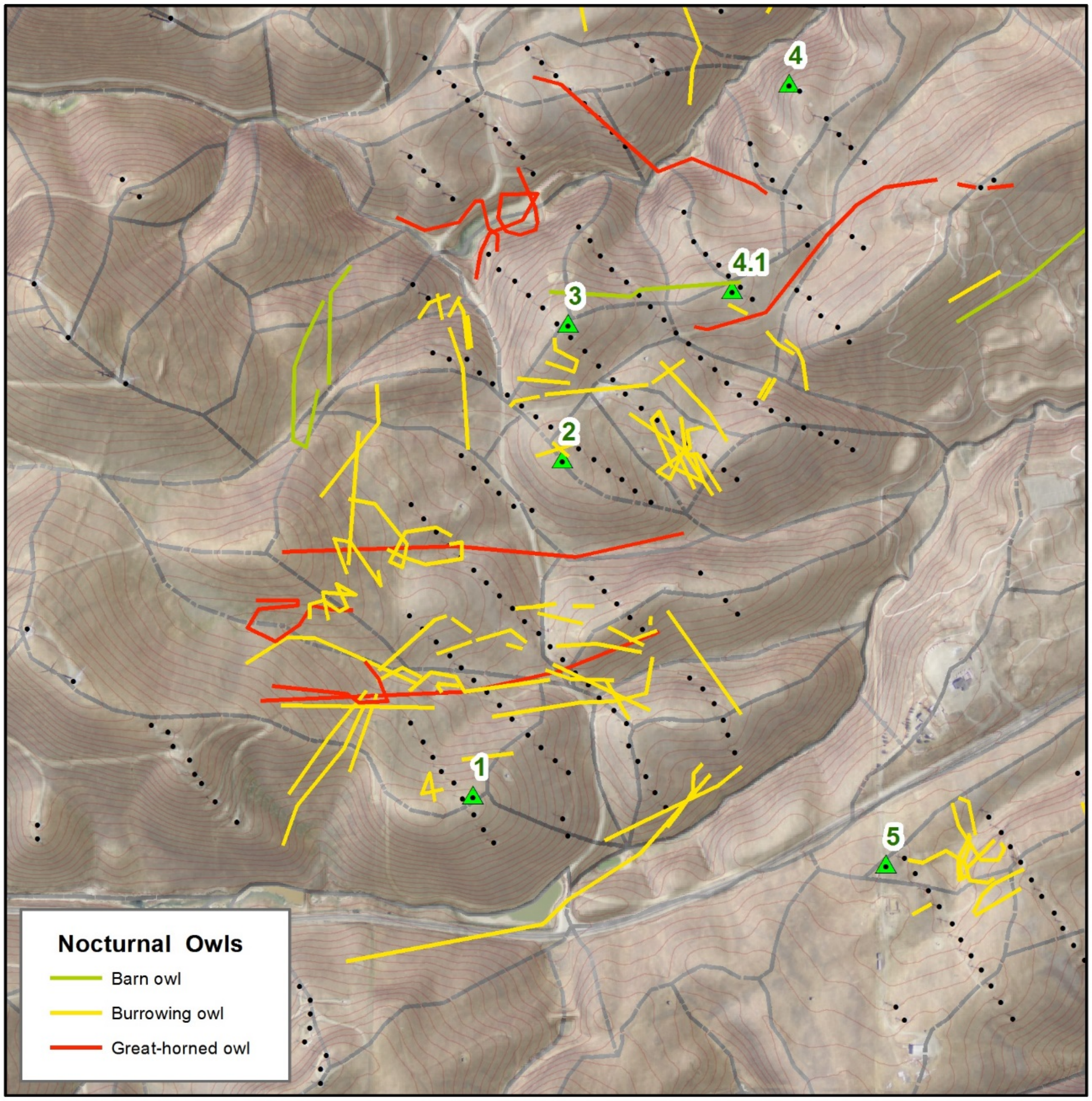

Figure 67: Flight Patterns of Bats During Nocturnal Surveys at the Taxvest Project Near Mountain House, Altamont Pass Wind Resource Area

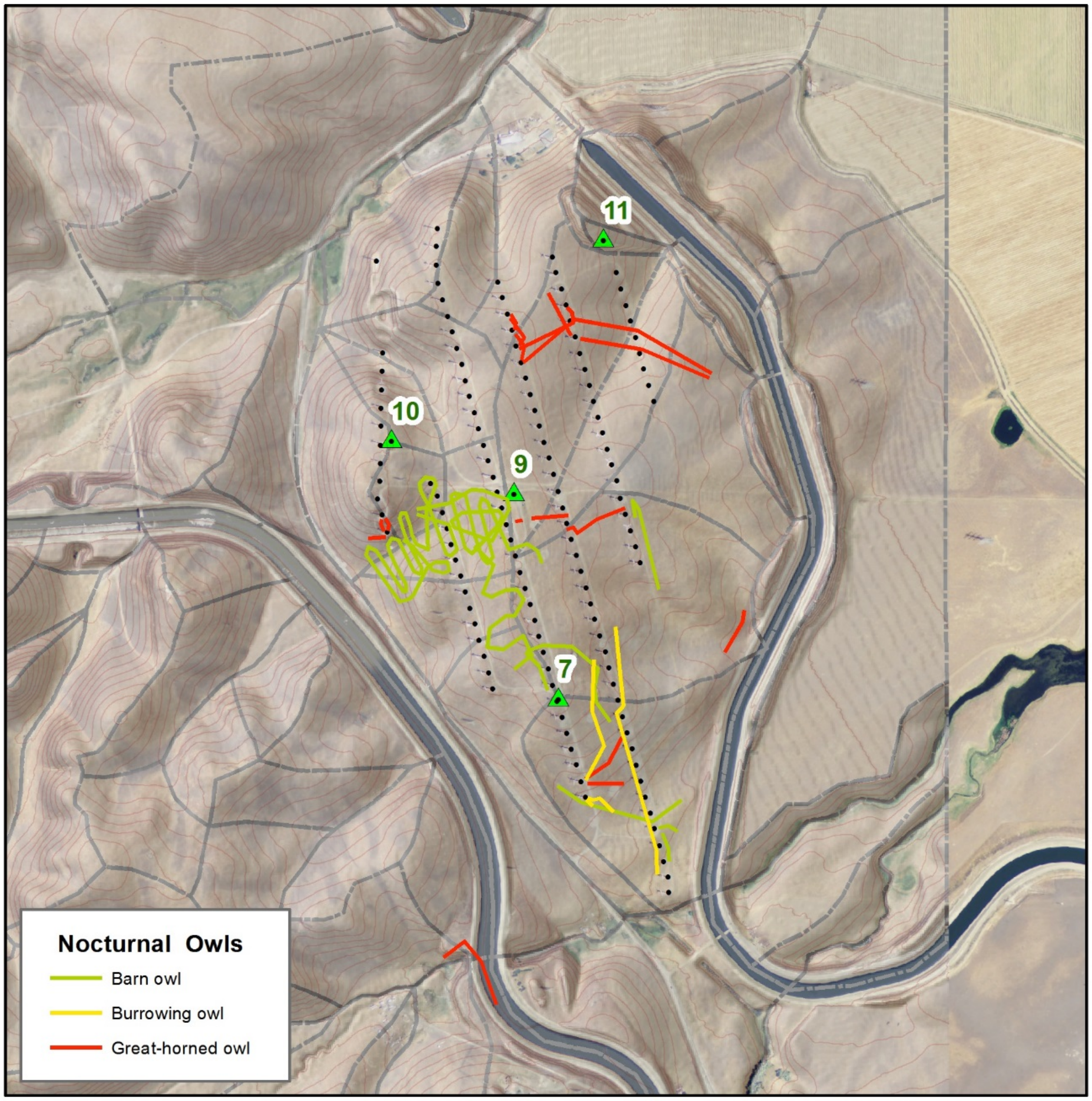

Figure 68: Flight Patterns of Bats During Nocturnal Surveys at the Taxvest Project Off Midway Road, Altamont Pass Wind Resource Area

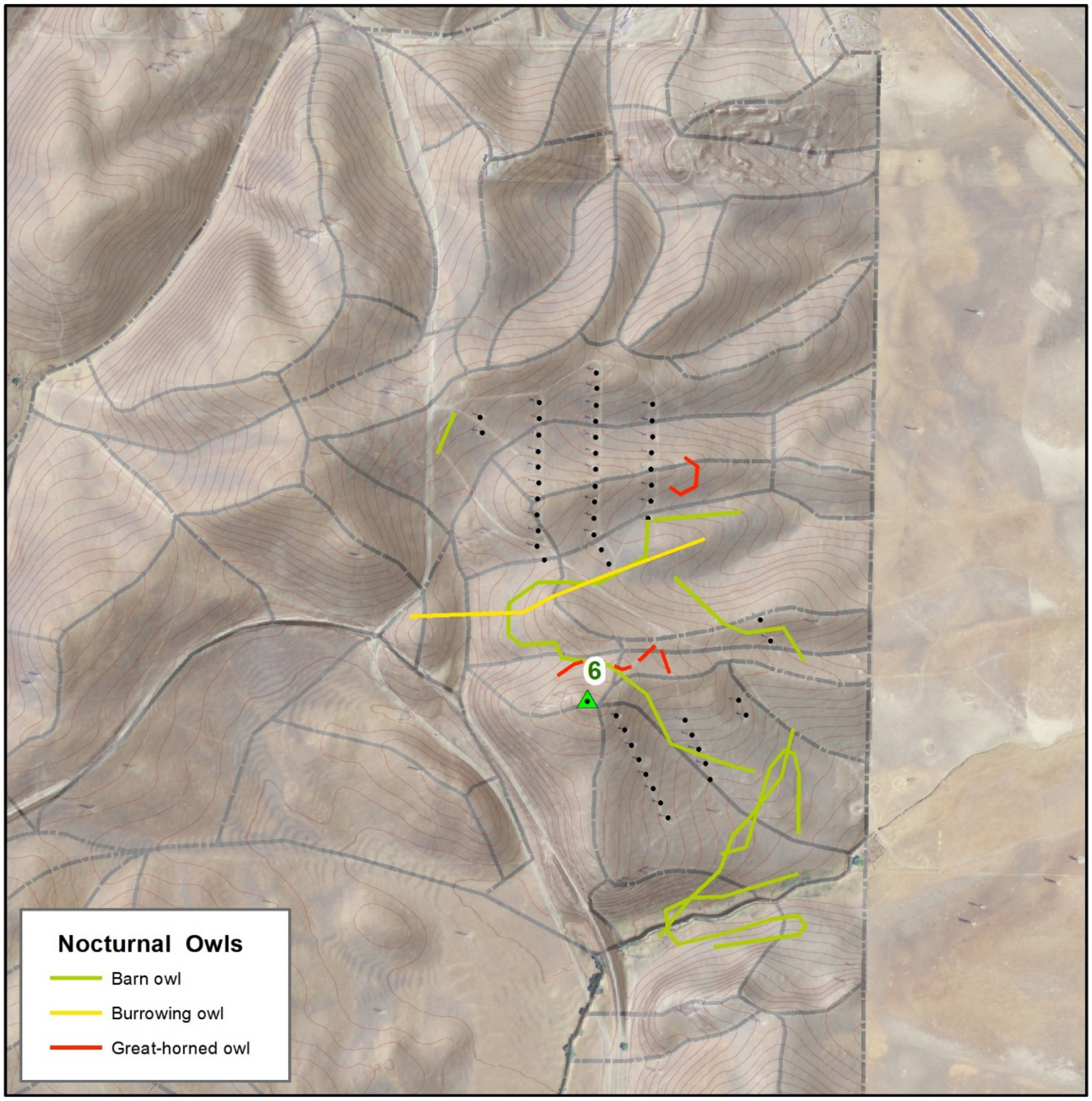

Figure 69: Flight Patterns of Bats During Nocturnal Surveys at Altech 1, Swamp, Viking, and Venture Winds Projects, Altamont Pass Wind Resource Area

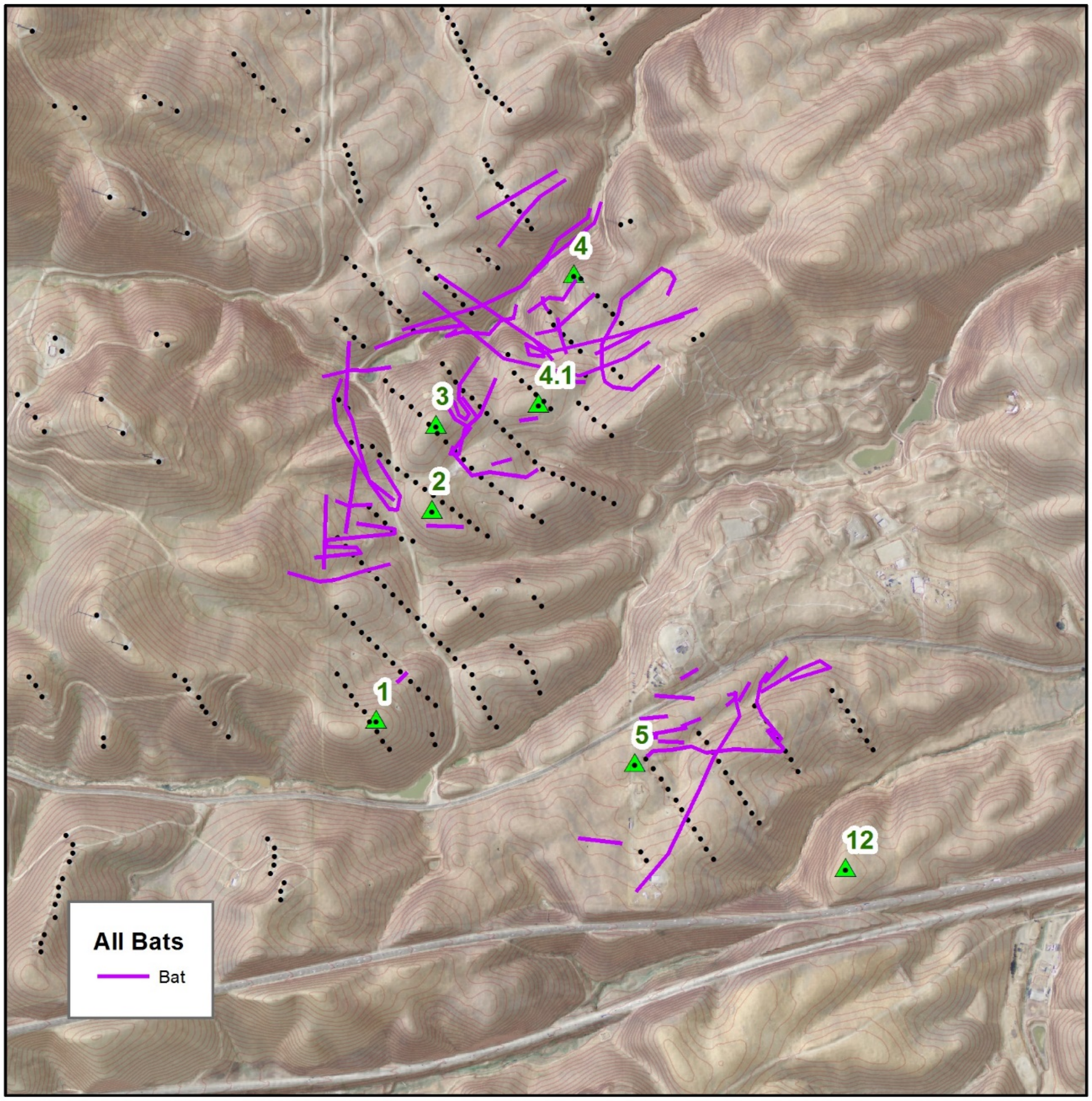

Figure 70: Flight Patterns of Bats During Nocturnal Surveys at the Taxvest Project Near Mountain House, Altamont Pass Wind Resource Area

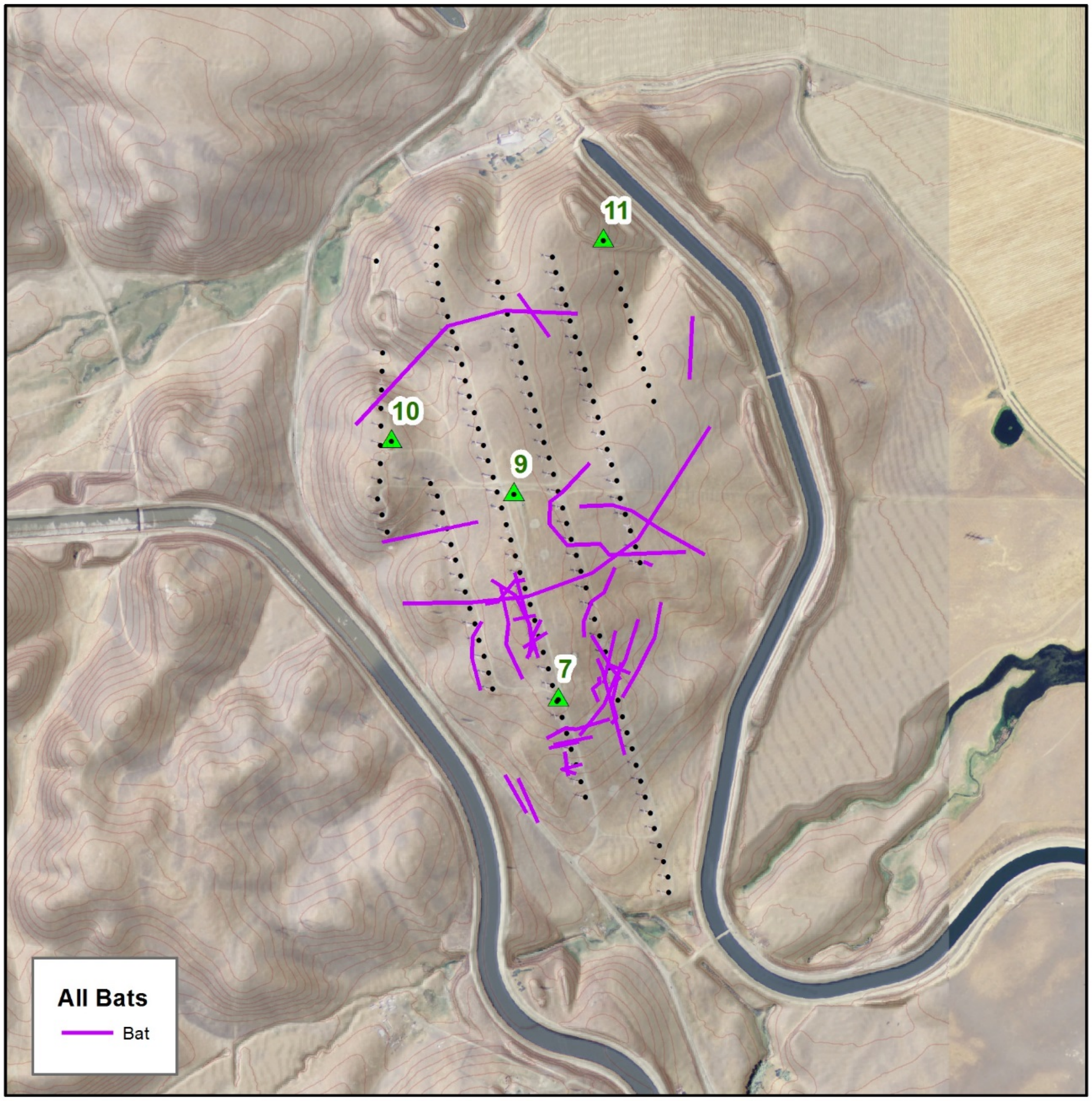

Figure 71: Flight Patterns of Bats During Nocturnal Surveys at the Taxvest Project off Midway Road, Altamont Pass Wind Resource Area

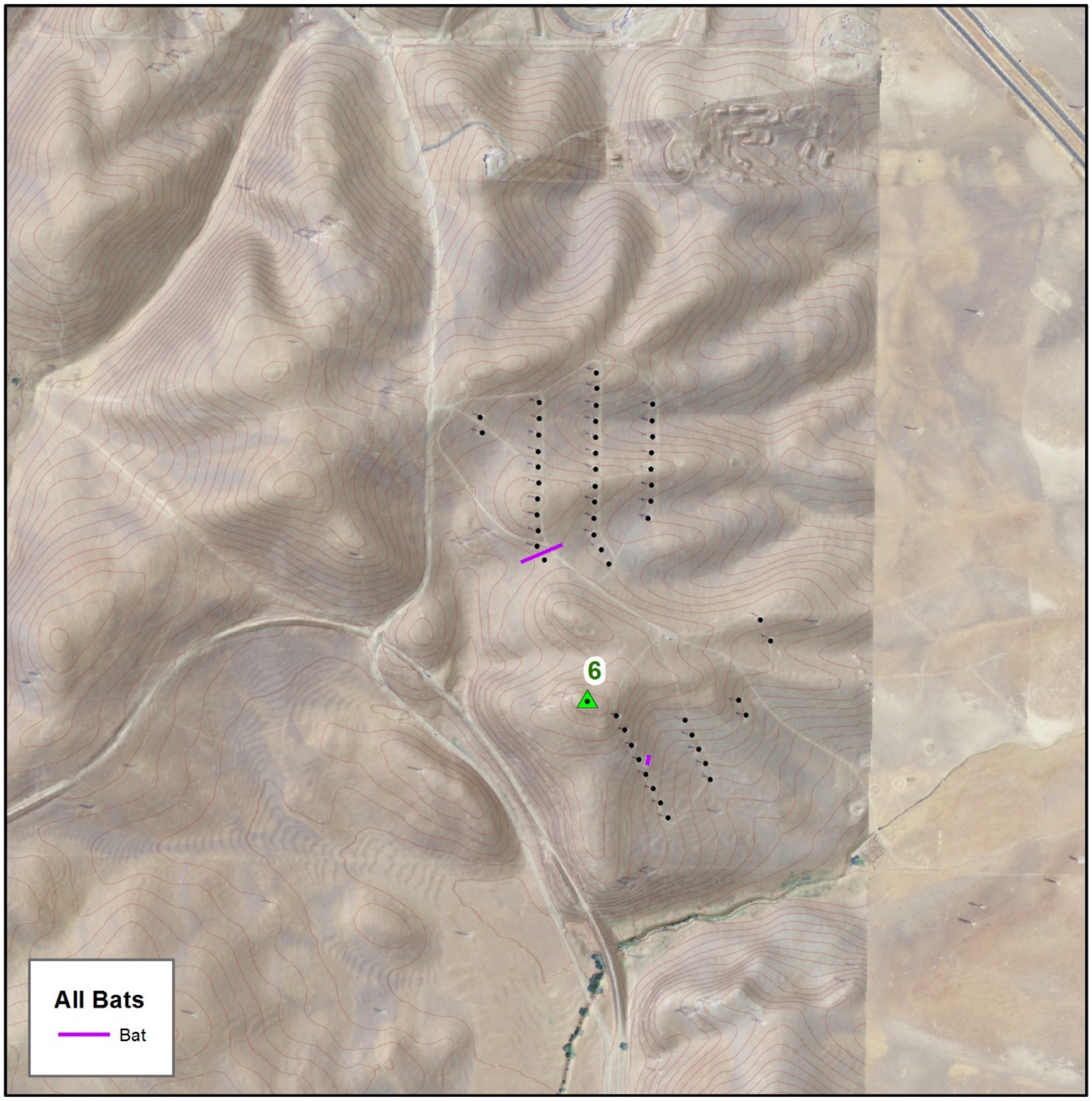

Figure 72: Seasonal Variation in Hourly Rates of Bats (Top Left), Burrowing Owls (Top Right), Barn Owls (Bottom Left), and Great-Horned Owls Bottom Right) Observed During Nocturnal Surveys at Forebay

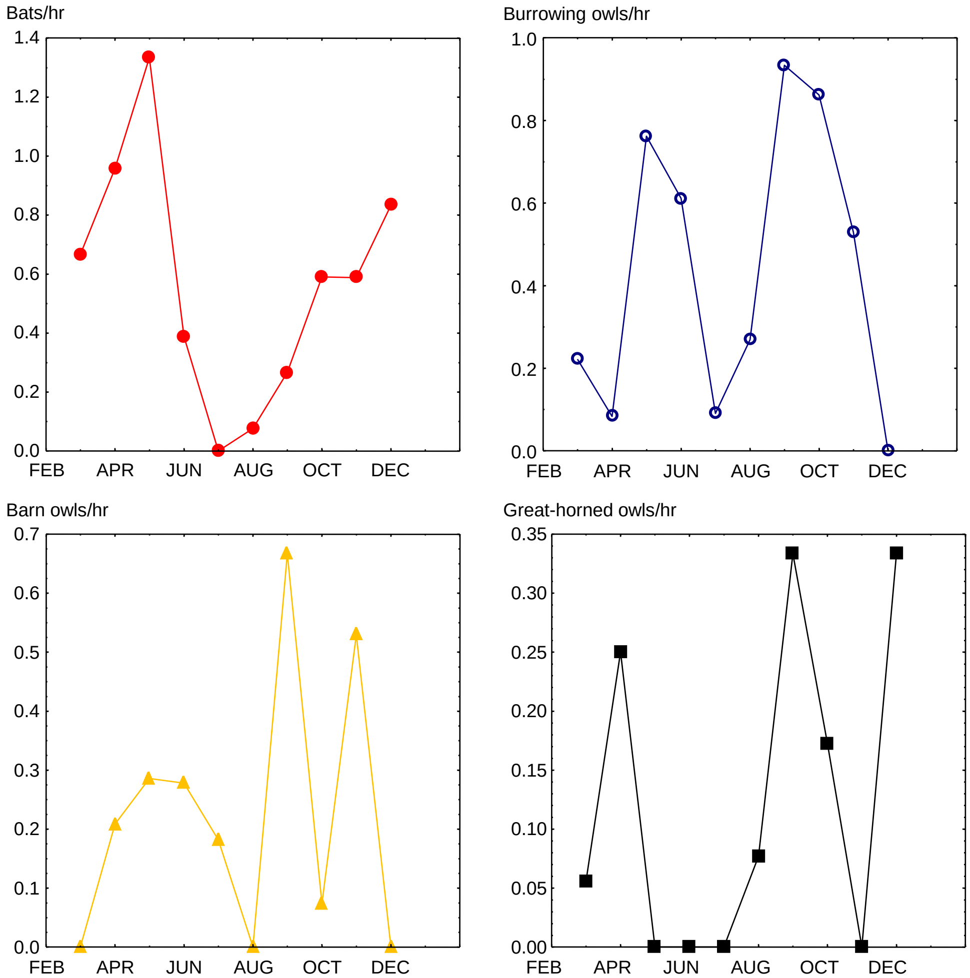

During nearly 214 hours of nocturnal surveys using a FLIR T620 thermal imaging camera, 52 near-collision events were observed between wildlife and wind turbines (Table 14). Five events involved 6 barn owls, one of which ascended over transmission lines and four of which flew within 1 to 3 m of wind turbine rotors. Only one barn owl flew near an operating wind turbine, approaching from a parallel angle to the rotor plane and from the wake aspect of the turbine; this owl ascended to land on the nacelle of the operating turbine.

Two great-horned owls were observed in summer flying near operating wind turbines. One of these owls flew along the turbine row, just above the concrete pads and very near the tubular towers, as if it was scanning the ground for food. The other great-horned owl was seen flying with the wind passed a non-operational wind turbine and then proceeding to within a meter of an operating turbine rotor; no evasive action was evident.

Eleven burrowing owls were seen flying dangerously close to wind turbines and a transmission line (n = 1), and one collided with a broken, non-operating wind turbine during strong winds on 10 September 2013. The burrowing owl that collided with a wind turbine had twice flown downslope between two rows of 65 KW Micon wind turbines at the Mountain House site during the 30 minutes prior to the event. Upon the third observation of this owl, it had veered west-southwest near the toe of the slope and across the site occupied by turbine AC-20. This turbine was broken at the time, and had a nacelle but no blades. The owl struggled against the wind until it reached airspace that the turbine protected from the wind. As the burrowing owl entered this wind-protected airspace, it surged forward and struck the rear of the nacelle with force. The owl stopped flapping and fell freely at least 33% of the distance to the ground before recovering itself and resuming its flight. The burrowing owl flapped its wings hard and flew away from the turbine to the southeast until it disappeared from view in about 3 seconds.

Four of the burrowing owl events occurred in fall, and 7 occurred in spring. Six of the burrowing owl events involved hovering behavior, and the other 5 were of burrowing owls encountering wind turbines and in one case a transmission line during forward flapping flight. Half of the hovering flights were upwind of the turbine, and 2 were downwind on the wake side of the rotor (Figure 73). In one event, a burrowing owl flew a course that encountered 17 wind turbines in a row, 14 of which were operating in strong wind. Flying parallel to the axis of the rotor planes, this owl repeatedly flapped hard to ascend and dove down to descend about the rotors, but mostly just upwind of the rotors and not always achieving heights that were below or above the blade reach. It was unclear whether the burrowing owl was reacting to the rotors or simply struggling to fly across a strong wind.

Three medium-sized birds that were thought to be grebes flew over a non-operating wind turbine on 4 December 2013 at a site where grebes were found dead during fatality monitoring. These birds flew toward the turbine at a parallel angle to the rotor plane, and ascended to twice the tower height before passing over the rotor.

On the 9th of December 2013, a coyote was seen walking parallel to a row of wind turbines and flushing groups of a small bird that behaved like horned larks. The escaping horned larks nearly missed the tubular towers of the turbines multiple times, and one horned lark that separated from the flock nearly collided with the towers of 6 or 7 wind turbines as it continued flying southeast along the turbine row.

Although not resulting in near collisions with wind turbines, two burrowing owls were also seen to have been flushed by a fox that was trotting in a direction parallel to a long row of wind turbines. On 5 September 2013, the fox was trotting through the grassland when a burrowing owl flushed up and flew southeast, parallel to the rows of wind turbines. This owl disappeared from view before it could be seen whether it encountered a wind turbine. The fox subsequently started running in the directing that the owl escaped when a second burrowing owl flushed and flew to two-thirds the height of the nearby turbine towers before disappearing from view.

Another burrowing owl was flushed by a passing barn owl on 5 September 2013. The barn owl was flying along and suddenly dove toward the ground. A burrowing owl flew up and away without encountering a wind turbine.

Similarly, on 25 November 2013, a fox flushed a great-horned owl. The fox was trotting through grassland when it discovered a great-horned owl perched on the ground. The fox rushed the owl, which flew up and perched on a utility line. Another great-horned owl was flushed from a ground perch on 28 August 2013, but this great-horned owl was flushed by another great-horned owl that dove down on it. Both owls flew down the slope, with the flushed owl pursued by the aggressor.

Thirty-five 35 bats were recorded in 32 wind turbine events, 21 of which happened during spring and 11 during fall. Twenty of the events (25 bats) involved operating wind turbines, and 11 were non-operating wind turbines. The operating wind turbines were approached from the direction of the wind by 13 bats, from the wake direction by 4 bats, and across the wind and parallel to the rotor axis by 5 bats. One bat approached an operating wind turbine from both the wind and wake sides of the rotor, making repeat passes. Non-operating wind turbines were approached from the direction of the wind by 8 bats, from the wake direction by 2 bats, and across the wind and parallel to the rotor axis by 1 bat. Bats often were seen to change altitudes or flight direction to approach the wind turbines, sometimes deviating far from their original course. Bats approaching wind turbines also made repeat passes, and usually flew through the plane of the rotor.

The majority of bat flight behavior was flapping forward flight. However, two bats hovered near the rotors of operating wind turbines, and two paused briefly before continuing flights, once just upwind of an active rotor, and once above the rear of a nacelle. Bats often exhibited vertical flight directions, either descending sharply through the rotor plane, or ascending steeply through it.

On 3 October 2013 a large bat – likely a hoary bat -- was seen to be making multiple passes through the rotor of an operating Windmatic wind turbine very near to the observer. In tracking the bat, the observer noticed a burrowing owl fly off of a ground perch about 60 m away from the turbine. The owl flew directly to the turbine, ascending gradually along the way. When the owl arrived at the turbine it was at a height just below the low reach of the blades in the 6:00 position, when it ascended rapidly in pursuit of the bat. Both the bat and the burrowing owl flew straight up into the rotor, but the observer was unable to move the thermal camera fast enough to see the rest of the encounter. However, shortly after the burrowing owl returned to its ground perch and the bat flew to a non-operating Polenko turbine to the east, where it flew a tight 360° circle around the blade positioned in the 12:00 position before flying northward and away.

Table 14: Nocturnal Wildlife Flight Events Involving Close Approaches or Near Misses With Wind Turbines (Unless Otherwise Stated) or Transmission Lines During the Ogin Study in the Altamont Pass WRA, September 2012 Through November 2014

Date	Species	No.	Behavior	Turbine status	Approach angle & aspect to rotor plane	Event change in flight behavior, height, direction, speed	Distance (m) at which flight changed	Nearest approach (m) to rotor plane	Note
10/25/2012	Barn owl	1	Forward flight	Off	90°, wake	None		1	Close to turbine in second row it passed
11/06/2012	Barn owl	1	Forward flight	Off	90°, wind	Flapped hard to ascend	2	1	
04/11/2013	Barn owl	2	Forward flight	Off	From wake	One owl flapped hard to ascend, then descended after overflying transmission lines	3	1	One owl flew ahead of the other; both owls entered nacelle of turbine
05/02/2013	Barn owl	1	Forward flight	On	0°, wake	None		3	Ascended to nacelle of operating turbine
05/02/2013	Barn owl	1	Flap & glide	Off	0°, wake	None		3	Passed active rotors to utility pole, then landed
08/15/2013	Great-horned owl	1	Forward flight	On	0°, across wind	None		8	Flew 1-13 m above ground and right over pads of multiple turbines
08/21/2013	Great-horned owl	1	Flap & glide	On	90°, wind	None		1	Passed non-op turbine within 4 m at half tower height, then flew to operating turbine.
11/20/2012	Burrowing owl	1	Forward flight	Off	90°, wake	Turned left and bypassed turbine tower	2	2	

Date	Species	No.	Behavior	Turbine status	Approach angle & aspect to rotor plane	Event change in flight behavior, height, direction, speed	Distance (m) at which flight changed	Nearest approach (m) to rotor plane	Note
05/31/2013	Burrowing owl	1	Hovering	On	Windward	None		4	
05/31/2013	Burrowing owl	1	Hovering	On	Windward	None		4	
05/31/2013	Burrowing owl	1	Hovering	On	Windward	None		4	Dove to ground after hovering
06/27/2013	Burrowing owl	1	Hovering	Off	90°, wake	None		2	
06/27/2013	Burrowing owl	1	Hovering	On	90°, wake	None		2	Lots of very close hovering to operating rotors
09/10/2013	Burrowing owl	1	Forward flight	On	0°, across wind	Alternately descended under and ascended over 14 of 17 operating turbines, but mostly slightly upwind of the rotors		3	Turbines not operating during this flight were AD-17, AD-13, AD-11, AD-8. This owl was same owl that struck turbine in the following event.
09/10/2013	Burrowing owl	1	Forward flight	Broken	90°, wake	None, except for surging forward after entering airspace that the turbine protected from strong wind	0	0	Struggling against wind, the owl surged forward and collided with rear of nacelle. It fell freely for 33% of tower height before regaining flight.
10/03/2013	Burrowing	1	Forward	On	90	Unknown		1	Chased bat that was flying repeatedly through

Date	Species	No.	Behavior	Turbine status	Approach angle & aspect to rotor plane	Event change in flight behavior, height, direction, speed	Distance (m) at which flight changed	Nearest approach (m) to rotor plane	Note
	owl		flight						rotor, but bat escaped and flew east to Polenko
04/08/2014	Burrowing owl	1	Flap and glide, then hovered	On	0°, across wind	Stopped flap and glide, and began hovering	4	4	
05/06/2014	Burrowing owl	1	Forward flight		From wake	Flapped harder to ascend over transmission lines, then descended			
12/04/2013	Medium bird	3	Forward flight	Off	0°, across wind	Ascended to 2 tower heights	0	10	Probable grebes
12/09/2013	Small bird	20	Flushed by coyotes	Off	0°, across wind	None		1	Probable horned larks; several nearly collided with towers, and 1 nearly collided with 6 or 7 towers
10/25/2012	Bat	2	Forward flight	On	90°, wind	None		0	Flew through rotor plane, then last-second ascent over transmission line downwind of turbines (near miss)
10/25/2012	Bat	2	Forward flight	On	90°, wind	None			Distance and angle occluded my view
10/25/2012	Bat	1	Forward	Off	90°, wind	None		2	Large bat

Date	Species	No.	Behavior	Turbine status	Approach angle & aspect to rotor plane	Event change in flight behavior, height, direction, speed	Distance (m) at which flight changed	Nearest approach (m) to rotor plane	Note
			flight						
11/06/2012	Bat	1	Forward flight	Off	90°, wind	Thrice ascended straight up through rotor plane	0	0	AC-16
11/06/2012	Bat	1	Forward flight	Off	90°, wind	None		0	
11/06/2012	Bat	1	Forward flight	Off	90°, wind	Flew straight up through rotor plane		0	
04/11/2013	Bat	1	Forward flight	Off	90°, wind	None		5	
05/02/2013	Bat	1	Forward flight	On	90°, wake	Redirected flight path to engage turbine rotor	10	0	
05/02/2013	Bat	2	Forward flight	On	90°, wind	None		0	
05/02/2013	Bat	1	Forward flight	Off	90°, wind	None			Higher-altitude bat activity dropped after 2nd hour, when wind slowed down
05/02/2013	Bat	1	Forward flight	On	90°, wind	None		0	
05/02/2013	Bat	1	Forward flight	On	0°, wind	None		3	

Date	Species	No.	Behavior	Turbine status	Approach angle & aspect to rotor plane	Event change in flight behavior, height, direction, speed	Distance (m) at which flight changed	Nearest approach (m) to rotor plane	Note
05/02/2013	Bat	1	Forward flight	On	90°, wake	Intentional flight into active rotor	10	0	
05/02/2013	Bat	1	Forward flight	On	90°, wind	Intentional flight into active rotor	10	0	
05/02/2013	Bat	1	Diving	Off	90°, wake	Dove toward turbine and into operating rotor plane		0	Definite change in flight path
05/02/2013	Bat	1	Forward flight	On	90°, wind	Dove toward turbine		4	Dropped to rotor height in front of turbines
05/16/2013	Bat	1	Forward flight	On	90°, wind	Paused and changed direction away from turbine	2	2	Hovered next to another turbine rotor
05/16/2013	Bat	1	Hovering	On	90°, wake	Descended to bottom of rotor plane and flew away from turbine	1	1	
05/16/2013	Bat	1	Forward flight	On	90°, wind	None		10	Descended to rotor
09/10/2013	Bat	1	Forward flight	On	90°, wind	Descended into rotor wake to just above nacelle, paused briefly, and continued east		1	
10/03/2013	Bat	1	Forward flight	On	90°, across	None		0	Flew tight 360° circle around blade of

Date	Species	No.	Behavior	Turbine status	Approach angle & aspect to rotor plane	Event change in flight behavior, height, direction, speed	Distance (m) at which flight changed	Nearest approach (m) to rotor plane	Note
					wind				feathering Polenko after flying away from chasing burrowing owl
10/15/2013	Bat	1	Forward flight	Off	0°, across wind	Flew tight 360° turn around blade in 12:00 position	0.5	0	
12/02/2013	Bat	1	Forward flight	Off	90°, wake	Descended sharply to approach blade	4	4	Investigated blade, then descended to 5 m above ground
12/02/2013	Bat	1	Forward flight	Off	90°, wind	None		8	Split distance between turbines
04/09/2014	Bat	1	Forward flight	On	0°, across wind	Zigzagged left & right, ascended to avoid blades	0	0	Went out of way to pass through rotor, then closely dodged blades, coming within 0.5 m of moving blades
04/09/2014	Bat	1	Forward flight	Off	90°, wind	None		0	
04/16/2014	Bat	1	Forward flight	On	0°, across wind	Bolted forward from rotor hub		1	Flew right in front of 2 turbine rotors after going out of way to approach turbines
04/30/2014	Bat	1	Forward flight	On	90°, wind	Accelerated and descended through rotor	2	0	Flew through the only operating turbine rotor in the row; intentional

Date	Species	No.	Behavior	Turbine status	Approach angle & aspect to rotor plane	Event change in flight behavior, height, direction, speed	Distance (m) at which flight changed	Nearest approach (m) to rotor plane	Note
04/30/2014	Bat	1	Forward flight	On	0°, across wind	Zigzag around turbine nacelle	1	2	
04/30/2014	Bat	1	Forward flight	On	0°, across wind	Ascended rapidly and veered right to avoid blade collision	0.5	0	
04/30/2014	Bat	1	Forward flight	On	90°, wind	Paused in front of turbine, then turned away	3	3	Large bat
05/14/2014	Bat	1	Forward flight	Off	From both wind and wake	Approached 2 blades of 2 turbines, or 4 blades total, including vertical flights	2	0.05	

Figure 73: A Photograph of a Burrowing Owl (White Arrow) Hovering at Twilight Just Downwind of Operating Enertech Wind Turbines in the Altech Project, Altamont Pass Wind Resource Area, Alameda County, California

4.4 Discussion

4.4.1 Mammalian Scavengers

The study achieved its goal of exploring nocturnal flight patterns of birds and bats and mammalian scavenger activities that might bear on fatality rate estimation. The nocturnal surveys revealed some patterns that could not have been anticipated prior to the surveys because there was not precedent for nocturnal surveys in the Altamont Pass. For example, it was not known that mammalian carnivores patrol the ground in search patterns similar to the search patterns used by human fatality searchers. It was not known the degree to which mammalian scavengers target wind turbines, especially the prevailing downwind areas next to wind turbines.

The surveys also confirmed that birds are flushed by mammalian carnivores during the night, including birds that are normally active during daylight hours. Not only were birds flushed by carnivores, but they were flushed in close proximity to wind turbines, which increased the collision risk significantly. Horned larks were flushed by coyotes. Burrowing owls were flushed by foxes.

One of the most important findings in the nocturnal surveys was the negative correlation between adjusted fatality rates and numbers of mammalian scavengers observed per hour among nocturnal survey stations. An intriguing question related to this correlation is whether fatality rates are a function of nocturnal scavenger activity levels even after the fatality rates were adjusted for carcass persistence. That such a strong relationship exists even after fatalities were adjusted by overall detection, *D*, suggests that mammalian scavengers exert a greater impact on detection rates than has so far been adjusted by the integrated detection trial (or that would be adjusted by any other type of trial used to date). The implication of this bias is that fatality rate estimates are still biased low, even with the use of integrated detection trials.

However, because correlation does not equal causation, the regression relationship between adjusted fatality rates and mammalian scavenger activity might or might not mean that a strong bias remains in fatality rate estimation due to spatial variation in scavenger activity. Additional research needs to be directed towards this question. A likely productive question to pursue would be the rate at which carcasses are removed by scavengers within the first 12 hours of deposition. It might be that with greater levels of scavenger activity, a larger proportion of fatalities are discovered and removed within the first few hours of death than was simulated by the integrated detection trial. The integrated trial might more effectively simulate this possible early removal rate by depositing more trial carcasses at dusk or after dark, or by making a greater effort to minimize human scent on carcasses or along routes taken to place carcasses.

Another way to more effectively simulate the ecological processes that affect detection probabilities would be to tailor trial carcass placements to the scavenger community. It might be that random carcass placement throughout the fatality search areas ends up placing many or even most of the carcasses where wind turbine-killed birds do not normally fall, and where mammalian scavengers spend less of their time searching during the night. If the scavengers search only a fourth of the fatality search areas used by humans, and if those scavenger searches are where the majority of wind turbine-killed birds actually land, then a purely random placement of trial carcasses would put three-fourths of the trial carcasses in areas less traveled by mammalian scavengers. Even if only half of these "misplaced" carcasses were missed by scavengers during the first night, the result might substantially bias detection rates high and fatality rates low.

Tailoring the placement of trial carcasses to simulate ecological processes at night would consist of performing nocturnal surveys to quantify nocturnal scavenger activity. Once the patterns of carcass searches performed by scavengers have been characterized, a randomized placement schedule can be spatially weighted by levels of scavenger activity. If one portion of the fatality search area receives 10 times the attention from mammalian scavengers than does another portion of the search area, then that area should receive 10 times the number of placed trial carcasses.

The amount of attention devoted to a portion of the fatality search area should be decided not only by the travel paths as depicted in Figures 61 through 63, but also by the amount of time spent by the scavengers in the area, and by the behaviors. Time budgets were recorded in this study, but they were not analyzed in time for inclusion in this report. However, it can be reported that the scavengers -- whose paths appear on Figures 61 through 63 – spent considerable time at the locations near wind turbines. Often, a striped skunk would search an area near wind turbines for an hour or during the entire three hour survey period.

4.4.2 Flying Birds and Bats

Without nocturnal surveys, there is no means to observe flight behaviors of owls and bats other than the occasional short flights made by burrowing owls during daylight hours. However, even the flights made by burrowing owls during the day fail to represent the types of behaviors seen at night with use of a thermal imaging camera. Without thermal surveys, it would remain anecdotally known that burrowing owls hover in the wind at night. Now it is known that not only do burrowing owls hover at night, but they perform this behavior in much the same way that red-tailed hawks and American kestrels do during daylight. Burrowing owl hovering behavior can be even more dangerous, though, because the nocturnal observations made during this study witnessed burrowing owls hovering just under the blade tips of spinning rotors and in the wake just downwind of the rotor. Burrowing owls were even seen hovering within the lattice towers of operating wind turbines. The nocturnal surveys also revealed the dangerous habit of burrowing owls breaking away from their hovering activity and dive-gliding downhill to their burrows. These dive-glides can easily take the owls through the rotors of operating wind turbines.

A burrowing owl was seen to collide with a broken turbine, after it struggled against a strong wind and then surged forward into the turbine after it reached a pocket of airspace that was protected from the wind by the turbine. This collision did not appear to be fatal, but the owl appeared to have been briefly knocked unconscious. This collision mechanism might be common, as the fatality rate of burrowing owls in this study was found to increase with decreasing operability of the wind turbines. An implication is that the impact on burrowing owls might be effectively reduced by removing vacant towers and broken turbines.

Barn owls spent a lot of time flying near and around wind turbines, often landing inside gaps of the nacelles of turbines. Barn owls radically change altitude as they fly, often dropping toward the ground and surging upward toward the sky. Lateral shifts are also often made suddenly and quickly. This erratic flight path behavior might represent a foraging strategy, a predator avoidance strategy (from great-horned owls, for example), or both. It probably increases the risk of collision with wind turbines, transmission lines, and electric distribution lines, however. More time is needed on nocturnal surveys to better understand this behavior and the risk it poses to barn owls.

Great-horned owls still-hunt from wind turbines and any other tall structure on the landscape. They often fly from turbine to turbine, and their perch time on each structure is fairly predictable at 2 to 3 minutes. Great-horned owls were also seen to fly low over the ground, including right over turbine pads. It might be that great-horned owls search for turbine victims. Smallwood et al. (2010), using event-triggered cameras, recorded a great-horned owl removing another great-horned owl that had been placed in a carcass trial. It is possible that wind turbine collisions feed back on additional wind turbine collision as some birds forage for victims.

Just as the landscape strongly influenced the flight paths of owls, so too did it influence bat flight paths. An implication of bats following ravines and crossing over saddles is that wind turbines might be placed carefully on the landscape to minimize the encounter rates between bats and wind turbines, just as careful siting has been directed toward raptors in repowering projects in the APWRA. A complicating factor, however, is the obvious attraction that bats have for operating wind turbines. During the nocturnal surveys performed in this study, many of the bats that were observed had convincingly gone out of their way to approach and investigate wind turbines. Bats even hovered near operating rotors, much like burrowing owls did. When bats visited wind turbines, they often repeat passes through the rotor plane, and they often flew by the nacelle.

Another finding of the bat surveys was that bat activity was not confined to the late summer or fall, as often reported in fatality monitoring reports and bat acoustic detection monitoring at many wind projects. In this study bat activity spanned much of the year.

The two years of nocturnal surveys performed in this study revealed possible opportunities and improvements in nocturnal survey methods. For example, the camera and lens used in this study was suitable for viewing bats at great distances, so bats could be tracked over relatively long periods to discern behavior and flight paths. One type of nocturnal survey can consist of tracking individual animals. Another type of survey can consist of training the camera on a particular turbine or set of turbines and counting bats or birds flying by or through the rotor plane to obtain passage rates. An advantage of this approach over use of acoustic detectors is that with the thermal imaging camera the entire rotor can be viewed at once, whereas acoustic detectors can cover only a portion of the rotor plane unless many detectors are placed on the turbine to collectively cover the rotor plane. Another advantage over acoustic detectors is that the thermal imager can see what the bat or bird actually did as it passed through or by the rotor. The imager cannot discern the type of call being emitted by a bat, but it can see the flight path. It can also see interactions between bats, which are common but not reported in this report for lack of time. During bat migration it would be helpful to deploy multiple thermal imagers with appropriate lenses so that multiple wind turbines can be covered per night and per similar wind and temperature conditions.

GLOSSARY

Term	Definition
APWRA	Altamony Pass Wind Resource Area
BACI	Before-after control impact
DEM	Digital elevation model
FL	Fuzzly Logic Modeling; computing based on degrees of truth, rather than “true’ or “false”.
g	Grams
GIS	Geographical Information System
km	kilometers
KW	Kilowatts
LIDAR	Light Detection and Ranging; surveying technology that measures distance using a laser light.
m	Meters
MEWT	Mixer-ejecter wind turbine
MW	Megawatts
Orgin	Origin Inc.
RMSE	Root-mean square error
SRC	Science Review Committee

REFERENCES

Ainslie, B., Alexander, N. Johnston, N. Bradley, J. Pomeroy, A.C. Jackson, P.L. & Otter, K.A. (2013) Predicting spatial patterns of Eagle migration using a mesoscale atmospheric model: a case study associated with a mountain-ridge wind development. International Journal of Biometeorology 58(1). DOI: 10.1007/s00484-012-0620-0.

Anderson, R., M., Morrison, K. Sinclair, D. Strickland. 1999. Studying wind energy and bird interactions: A guidance document. National Wind Coordinating Committee. Washington, D.C.

Arnett, E. B., Huso, M. M. P., Schirmacher, M. R. & Hayes, J. P. 2011. Altering turbine speed reduces bat mortality at wind-energy facilities. Frontiers in Ecology and the Environment 9:209-214. DOI:10.1890/100103

Baerwald, E. F., Edworthy, J. Holder, M., and Barclay, R. M. R. 2009. A Large-Scale Mitigation Experiment to Reduce Bat Fatalities at Wind Energy Facilities. Journal of Wildlife Management 73:1077-1081.

Band, W., M. Madders, and D. P. Whitfield. 2005. Developing field and analytical methods to assess avian collision risk at wind farms. In De Lucas, M., G. Janss, and M. Ferrer, eds. Birds and Wind Power. Barcelona., Spain: Lynx Edicions.

Bispo, R., J. Bernardino, T. A. Marques, and D. Pestana. 2010. Modeling carcass removal time and estimation of a scavenging correction factor for avian mortality assessment in wind farms using parametric survival analysis. Presented at Wind Wildlife Research Meeting VIII, http://www.nationalwind.org/assets/research_meetings/Research_Meeting_VIII_Bispo.pdf

Brown, K., K. S. Smallwood, J. Szewczak, and B. Karas. 2015. Final 2012-2015 Annual Report Avian and Bat Monitoring Project Vasco Winds, LLC. Prepared for NextEra Energy Resources, Livermore, California.

Brown, K., K. S. Smallwood, J. Szewczak, and B. Karas. 2014. Final 2013-2014 Annual Report Avian and Bat Monitoring Project Vasco Winds, LLC. Prepared for NextEra Energy Resources, Livermore, California.

Brown, K., K. S. Smallwood, and B. Karas. 2013. Final 2012-2013 Annual Report Avian and Bat Monitoring Project Vasco Winds, LLC. Prepared for NextEra Energy Resources, Livermore, California. http://www.altamontsrc.org/alt_doc/p274_ventus_vasco_winds_2012_ 13_avian_bat_monitoring_report_year_1.pdf

Chamberlain, D. E., M. R. Fehfisch, A. D. Fox, M. Desholm, and S. J. Anthony. 2006. The effects of avoidance rates on bird mortality predictions made by wind turbine collision risk models. Ibis 148:198-202.

Cole, S.G. and E. L. Dahl. 2013. Compensating White-Tailed Eagle Mortality at the Smøla Wind-Power Plant Using Electrocution Prevention Measures. Wildlife Society Bulletin 37:84-93.

Cooper, B. 2005. Preliminary comparison of nocturnal passage rates and bat fatalities in Pennsylvania and West Virginia. Pages 21-22 in Proceedings: Onshore wildlife interactions with wind developments: Research meeting V. The National Wind Coordinating Committee, Resolve, Inc., Washington, D.C.

Dahl, E. L., R. May, P. L. Hoel, K. Bevanger, H. C. Pedersen, E. Røskaft, and B. G. Stokke. 2013. White-Tailed Eagles (Haliaeetus albicilla) at the Smøla Wind-Power Plant, Central Norway, Lack Behavioral Flight Responses to Wind Turbines. Wildlife Society Bulletin 37:66-74.

de Lucas, M., G. F. E. Janss, D. B. Whitfield, and M. Ferrer. 2008. Collision fatality of raptors in wind farms does not depend on raptor abundance. J. Applied Ecology 45:1695-1703.

de Lucas, M., M. Ferrer, M. J. Bechard, and A. R. Muñoz. 2012. Griffon vulture mortality at wind farms in southern Spain: Distribution of fatalities and active mitigation measures. Biological Conservation 147:184-189.

Ferrer, M., M. de Lucas, G. F. E. Janss, E. Casado, A. R. Munoz, M. J. Bechard, and C. P. Calabuig. 2012. Weak relationship between risk assessment studies and recorded mortality in wind farms. J. Applied Ecology 49:38–46.

Garvin, J. C., C. S. Jennelle, D. Drake and S. M. Grodsky. 2011. Response of raptors to a windfarm. Journal of Applied Ecology 48:199-209.

Gauthreaux, S. A. 1995. Suggested practices for monitoring bird populations, movements and mortality in wind resource areas. In: Proceedings of National Avian-Wind Power Planning Meeting II. Palm Springs, California, 20-22 Sept. 1995. Prepared for the Avian Subcommittee of the National Wind Coordination Committee by RESOLVE Inc., Washington, DC, and LGL Ltd., King City, Ont. Hodos, W. 2003. Minimization of motion smear: Reducing avian collisions with wind turbines. Period of Performance July 12, 1999 – August 31, 2002. NREL/SR-500-33249, National Renewable Energy Laboratory, Golden, Colorado.

Hanowski, J. M., and R. Y. Hawrot. 2000. Avian issues in the development of wind energy in western Minnesota. Pages 80-87 in Proceedings of National Avian-Wind Power Planning Meeting III, San Diego, California, May 1998. Prepared for the Avian Subcommittee of the National Wind Coordinating Committee by LGL Ltd., King City, Ontario. 202 pp.

Harmata, A., K. Podruzny, and J. Zelenak. 1998. Avian use of Norris Hill Wind Resource Area, Montana. NREL/SR-500-23822, National Renewable Energy Laboratory, Golden, CO.

Hein, C., W. Erickson, J. Gruver, K. Bay, and E. B. Arnett. 2012. Relating pre-construction bat activity and post-construction fatality to predict risk at wind energy facilities. PNWWRM IX. 2013. Proceedings of the Wind-Wildlife Research Meeting IX. Broomfield, CO. November 28-30, 2012. Prepared for the Wildlife Workgroup of the National Wind Coordinating Collaborative by the American Wind Wildlife Institute, Washington, DC, Susan Savitt Schwartz, ed.

Hoover, S. L. and M. L. Morrison. 2005. Behavior of red-tailed hawks in a wind turbine development. Journal of Wildlife Management 69:150-159.

Horn, J. W., E. B. Arnett, and T. H. Kunz. 2008. Behavioral responses of bats to operating wind turbines. Journal of Wildlife Management 72:123-132.

Horvitz, D. G. and D. J. Thompson. 1952. A generalization of sampling without replacement from a finite universe. Journal of American Statistical Association 47:663-685.

Howe, R., and R. Atwater. 1999. The potential effects of wind power facilities on resident and migratory birds in Eastern Wisconsin. Unpublished Report to Wisconsin Department of Natural Resources, Monona, USA.

Hull, C. L., and S. Muir. 2013. Behavior and Turbine Avoidance Rates of Eagles at Two Wind Farms in Tasmania, Australia. Wildlife Society Bulletin 37:49-58.

Huso, M. M. P. 2010. An estimator of wildlife fatality from observed carcasses. Environmetrics 22:318-329.

Huso, M. M. P., D. Dalthorp, D. Dail, and L. Madsen. 2015. Estimating wind-turbine-caused bird and bat fatality when zero carcasses are observed. Ecological Applications, 25:1213–1225.

ICF International. 2015. Altamont Pass Wind Resource Area Bird Fatality Study, Monitoring Years 2005–2013. December. Sacramento, CA. Prepared for Alameda County Community Development Agency, Hayward, CA. http://altamontsrc.org/alt_doc/m107_apwra_bird_fatality_report_fy2013_draft_final.pdf

Johnston, N. N., J. E. Bradley, K. A. Otter. 2014. Increased flight altitudes among migrating golden eagles suggest turbine avoidance at a Rocky Mountain wind installation. PLoS ONE 9(3): e93030. doi:10.1371/journal.pone.0093030.

Katzner, T. E., D. Brandes, T. Miller, M. Lanzone, C. Maisonneuve, J. A. Tremblay, R. Mulvihill, and G. T. Merovich, Jr. 2012. Topography drives migratory flight altitude of golden eagles: implications for on-shore wind energy development. Journal of Applied Ecology 49:1178-1186.

Kitano, M. and S. Shiraki. 2013. Estimation of bird fatalities at wind farms with complex topography and vegetation in Hokkaido, Japan. Wildlife Society Bulletin 37:41-48.

Korner-Nievergelt, F., P. Korner-Nievergelt, O. Behr, I. Niermann, R. Brinkmann, and B. Hellriegel. 2011. A new method to determine bird and bat fatality at wind energy turbines from carcass searches. Wildlife Biology 17:350-363.

Mabee, T. J., B. A. Cooper, J. A. Plissner, and D. P. Young. 2006. Nocturnal bird migration over an Appalachian ridge at a proposed wind power project. Wildlife Society Bulletin 34:682-690.

Madders, M., and D. P. Whitfield. 2006. Upland raptors and the assessment of wind farm impacts. Ibis 148:43-56.

May, R., Y. Steinheim, F. Hansen, R. Vang, K. Bevanger, E. L. Dahl, S. Clausen, T. Nygård and A. Smith. 2009. Radar studies on White-tailed Sea Eagle at an onshore wind farm on the island of Smøla. Pages 50-53 in H. Hötker (Ed.), Birds of Prey and Wind Farms. Documentation of an International Workshop in Berlin, 21st and 22nd October 2008. http://bergenhusen.nabu.de/forschung/greifvoegel/ .

May, R., P. L. Hoel, R. Langston, E. L. Dahl, K. Bevanger, O. Reitan, T. Nygård, H. C. Pedersen, E. Røskaft, B. G. Stokke. 2010. Collision risk in white-tailed eagles Modelling collision risk using vantage point observations in Smøla wind-power plant. NINA Report 639, Trondheim, Norway.

May, R., O. Reitan, K. Bevanger, S.-H. Lorensten, and T. Nygård. 2015. Mitigating wind-turbine induced avian mortality: Sensory, aerodynamic and cognitive constraints and options. Renewable and sustainable energy reviews 42:170-181.

Morrison, M. L. 1998. Avian risk and fatality protocol. National Renewable Energy Laboratory, NREL/SR-500-24997, Golden Colorado.

New, L., Bjerre, E., Millsap, B., Otto, M.C. & Runge M.C. (2015) A collision risk model to predict avian fatalities at wind facilities: an example using Golden Eagles, Aquila chrysaetos. PLoS ONE 10(7):e0130978. doi:10.1371/journal.pone.0130978.

Orloff, S., and A. Flannery. 1992. Wind turbine effects on avian activity, habitat use, and mortality in Altamont Pass and Solano County Wind Resource Areas: 1989-1991. Report to California Energy Commission, Sacramento, California.

Osborn, R. G., C. D. Dieter, K. F. Higgins, and R. E. Usgaard. 1998. Bird flight characteristics near wind turbines in Minnesota. American Midland Naturalist 139:29-38.

Péron, G., J. E. Hines, J. D. Nichols, W. L. Kendall, K. A. Peters, and D. S. Mizrahi. 2013. Estimation of bird and bat mortality at wind-power farms with superpopulation models. Journal of Applied Ecology 50:902-911.

Shoenfeld, P. 2004. Suggestions regarding avian mortality extrapolation. Report to West Virginia Highlands Conservancy, Davis, West Virginia. 6 pp.

Smales, I., S. Muir, C. Meredith, and R. Baird. 2013. A Description of the Biosis Model to Assess Risk of Bird Collisions With Wind Turbines. Wildlife Society Bulletin 37:59-65.

Smallwood, K.S. 2001. The allometry of density within the space used by populations of Mammalian Carnivores. Canadian Journal of Zoology 79:1634-1640.

Smallwood, K. S. 2007. Estimating wind turbine-caused bird mortality. Journal of Wildlife Management 71:2781-2791.

Smallwood, K. S. 2008. Wind power company compliance with mitigation plans in the Altamont Pass Wind Resource Area. Environmental & Energy Law Policy Journal 2(2):229-285.

Smallwood, K. S. 2009. Mitigation in U.S. Wind Farms. Pages 68-76 in H. Hötker (Ed.), Birds of Prey and Wind Farms. Documentation of an International Workshop in Berlin, 21st and 22nd October 2008. http://bergenhusen.nabu.de/forschung/greifvoegel/ .

Smallwood, K.S. 2013. Comparing bird and bat fatality-rate estimates among North American wind-energy projects. Wildlife Society Bulletin 37: 19-33.

Smallwood, K. S. and C. Thelander. 2004. Developing methods to reduce bird mortality in the Altamont Pass Wind Resource Area. Final Report to the California Energy Commission, Public Interest Energy Research – Environmental Area, Contract No. 500-01-019. Sacramento, California. 531 pp.

Smallwood, K. S. and C. Thelander. 2005. Bird mortality in the Altamont Pass Wind Resource Area, March 1998 – September 2001 Final Report. National Renewable Energy Laboratory, NREL/SR-500-36973. Golden, Colorado.

Smallwood, K. S. and B. Karas. 2009. Avian and Bat Fatality Rates at Old-Generation and Repowered Wind Turbines in California. Journal of Wildlife Management 73:1062-1071.

Smallwood, K. S., and L. Neher. 2009. Map-Based Repowering of the Altamont Pass Wind Resource Area Based on Burrowing Owl Burrows, Raptor Flights, and Collisions with Wind Turbines. Final Report to the California Energy Commission, Public Interest Energy Research – Environmental Area, Contract No. CEC-500-2009-065. Sacramento, California. 63 pp. http://www.energy.ca.gov/2009publications/CEC-500-2009-065/CEC-500-2009-065.PDF

Smallwood, K. S. and L. Neher. 2010a. Siting Repowered Wind Turbines to Minimize Raptor Collisions at the Tres Vaqueros Wind Project, Contra Costa County, California. Draft Report to the East Bay Regional Park District, Oakland, California.

Smallwood, K. S. and L. Neher. 2010b. Siting Repowered Wind Turbines to Minimize Raptor Collisions at Vasco Winds. Unpublished report to NextEra Energy Resources, LLC, Livermore, California.

Smallwood, K. S., L. Neher, and D. A. Bell. 2009a. Map-based repowering and reorganization of a wind resource area to minimize burrowing owl and other bird fatalities. Energies 2009(2):915-943. http://www.mdpi.com/1996-1073/2/4/915

Smallwood, K. S., L. Rugge, and M. L. Morrison. 2009b. Influence of Behavior on Bird Mortality in Wind Energy Developments: The Altamont Pass Wind Resource Area, California. Journal of Wildlife Management 73:1082-1098.

Smallwood, K. S., L. Neher, D. Bell, J. DiDonato, B. Karas, S. Snyder, and S. Lopez. 2009c. Range Management Practices to Reduce Wind Turbine Impacts on Burrowing Owls and Other Raptors in the Altamont Pass Wind Resource Area, California. Final Report to the California Energy Commission, Public Interest Energy Research – Environmental Area, Contract No. CEC-500-2008-080. Sacramento, California. 183 pp. http://www.energy.ca.gov/ 2008publications/CEC-500-2008-080/CEC-500-2008-080.PDF

Smallwood, K. S., D. A. Bell, S. A. Snyder, and J. E. DiDonato. 2010. Novel scavenger removal trials increase estimates of wind turbine-caused avian fatality rates. Journal of Wildlife Management 74: 1089-1097 + Online Supplemental Material.

Smallwood, K. S., D. A. Bell, B. Karas, and S. A. Snyder. 2013a. Response to Huso and Erickson Comments on Novel Scavenger Removal Trials. Journal of Wildlife Management 77: 216-225.

Smallwood, K. S., L. Neher, J. Mount, and R. C. E. Culver. 2013. Nesting Burrowing Owl Abundance in the Altamont Pass Wind Resource Area, California. Wildlife Society Bulletin 37:787-795.

Tanaka, K. 1997. An Introduction to Fuzzy Logic for Practical Applications. Springer-Verlag, New York.

Tucker, V.A, 1996a. A mathematical model of bird collisions with wind turbine rotors. J. Solar Energy & Engineer. 118: 253-262.

Tucker, V.A, 1996b. Using a collision model to design safer turbine rotors for birds. J. Solar Energy & Engineer. 118: 263-269.

Warren-Hicks, W., J. Newman, R. Wolpert, B. Karas, L. Tran. (California Wind Energy Association.) 2013. Improving Methods for Estimating Fatality of Birds and Bats at Wind Energy Facilities. California Energy Commission. Publication Number: CEC-500-2012-086.

Winkelman, J. E. 1989. Birds and the wind park near Urk: collision victims and disturbance of ducks, geese, and swans. RIN Rep. 89/15. Rijksinstitut voor Natuurbeheer, Arnhem, The Netherlands. (c.f., in English summary reported on pages 122-126 in S. S. Schwartz, ed., Proceedings of the National Avian-Wind Power Planning Meeting IV. Avian Subcommittee of the National Wind Coordinating Committee, Washington, D.C.)

APPENDIX A:
Trial Carcass Placement Sheet

Figure A-1: Trial Carcass Placement Sheet

Date_______ Time_______ Trial ID #______ Turbine______Distance (m) _____ Bearing to turbine ______

Species________ Sex: M__ F__ U__ Age: A__ S__ J__ U__ Dessicated: None__ Slight__ Mod__

Carcass source_________________ Intermediary/Transporter________ Placed by: ____________

Occlusion: None__ Partial__ High__ Upward-facing aspect: Ventral __ Dorsal __ Lateral__

Distance (m) not visible (cap = 70 m): Toward turbine___ Transect ___ Transect ___

Cover: Grassland__ Gravel Road__ Gravel Pad__ Reclaimed pad__ Concrete pad__ Reclaimed grass__

Cut bank__ Rock ditch__ Other: Mass (g): _____

Notes:

Date_______ Time_______ Trial ID #______ Turbine______Distance (m) _____ Bearing to turbine ______

Species________ Sex: M__ F__ U__ Age: A__ S__ J__ U__ Dessicated: None__ Slight__ Mod__

Carcass source_________________ Intermediary/Transporter________ Placed by: ____________

Occlusion: None__ Partial__ High__ Upward-facing aspect: Ventral __ Dorsal __ Lateral__

Distance (m) not visible (cap = 70 m): Toward turbine___ Transect ___ Transect ___

Cover: Grassland__ Gravel Road__ Gravel Pad__ Reclaimed pad__ Concrete pad__ Reclaimed grass__

Cut bank__ Rock ditch__ Other: Mass (g): _____

Notes:

Date_______ Time_______ Trial ID #______ Turbine______Distance (m) _____ Bearing to turbine ______

Species________ Sex: M__ F__ U__ Age: A__ S__ J__ U__ Dessicated: None__ Slight__ Mod__

Carcass source_________________ Intermediary/Transporter________ Placed by: ____________

Occlusion: None__ Partial__ High__ Upward-facing aspect: Ventral __ Dorsal __ Lateral__

Distance (m) not visible (cap = 70 m): Toward turbine___ Transect ___ Transect ___

Cover: Grassland__ Gravel Road__ Gravel Pad__ Reclaimed pad__ Concrete pad__ Reclaimed grass__

Cut bank__ Rock ditch__ Other: Mass (g): _____

Notes:

Date_______ Time_______ Trial ID #______ Turbine______Distance (m) _____ Bearing to turbine ______

Species________ Sex: M__ F__ U__ Age: A__ S__ J__ U__ Dessicated: None__ Slight__ Mod__

Carcass source_________________ Intermediary/Transporter________ Placed by: ____________

Occlusion: None__ Partial__ High__ Upward-facing aspect: Ventral __ Dorsal __ Lateral__

Distance (m) not visible (cap = 70 m): Toward turbine___ Transect ___ Transect ___

Cover: Grassland__ Gravel Road__ Gravel Pad__ Reclaimed pad__ Concrete pad__ Reclaimed grass__

Cut bank__ Rock ditch__ Other: Mass (g): _____

Notes:

Appendix B:
Trial Carcass Check Sheet

Table B-1: Trial Carcass Status Check Sheet

Date											
Time											
Trial carcass ID											
Turbine											
Meters to turbine											
Bearing to turbine											
Species											
Flight feathers:											
Edged											
Tattered											
Body fluffy											
Body matted											
Original color											
Intermediate color											
Feathers bleached											
Maggots											

Beetles											
Ants											
Flies											
Grasshoppers											
Remains											
Notes											

Each status check was recorded in a column on the sheet, and carcass diagnostics were recorded with check marks.

Figure B-1: Example Diurnal Behavior Sheet Used in the Ogin Study

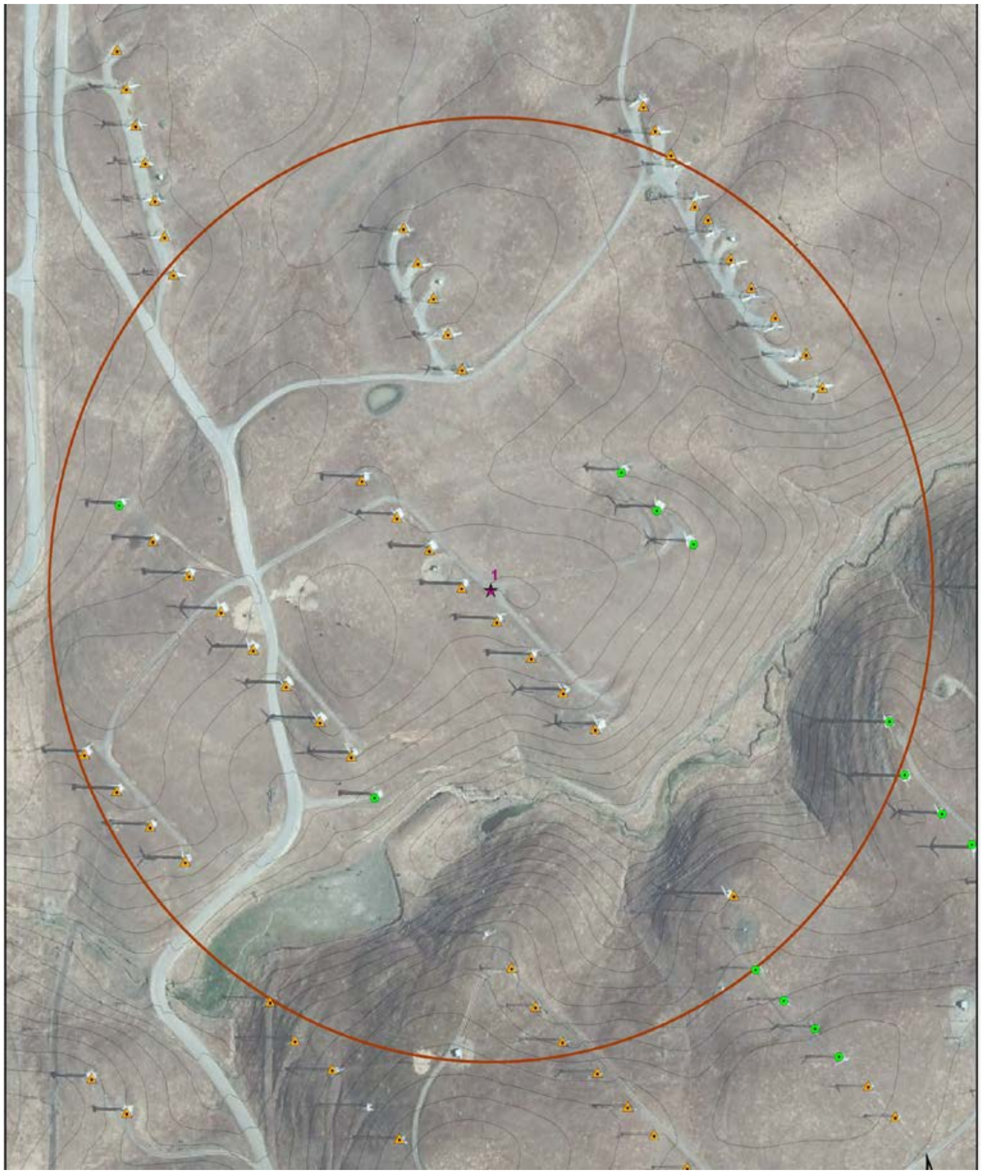

Date ________ Start time ________ Investigator _______

FloDesign (1)

	Temperature	Max wind	Avg wind	Wind direction	% overcast	Note
Start						
End						

A B C D E F G H I J

In this case at station 1, where green circles depict study turbines, orange triangles depict other wind turbines, the red circle represents a 200 m radius that served as a distance aid to the observer. Letters at bottom were assigned by observer to each observed bird in sequential order, corresponding with data entered into digital voice recorder.

APPENDIX C:
Nocturnal Survey

Figure C-1: Examle Data Sheet Used in Nocturnal Survey During the Ogin Survey, September 2012 Through November 2014

FD Nocturnal Survey Plot 3
Date:
Time:
Observer:

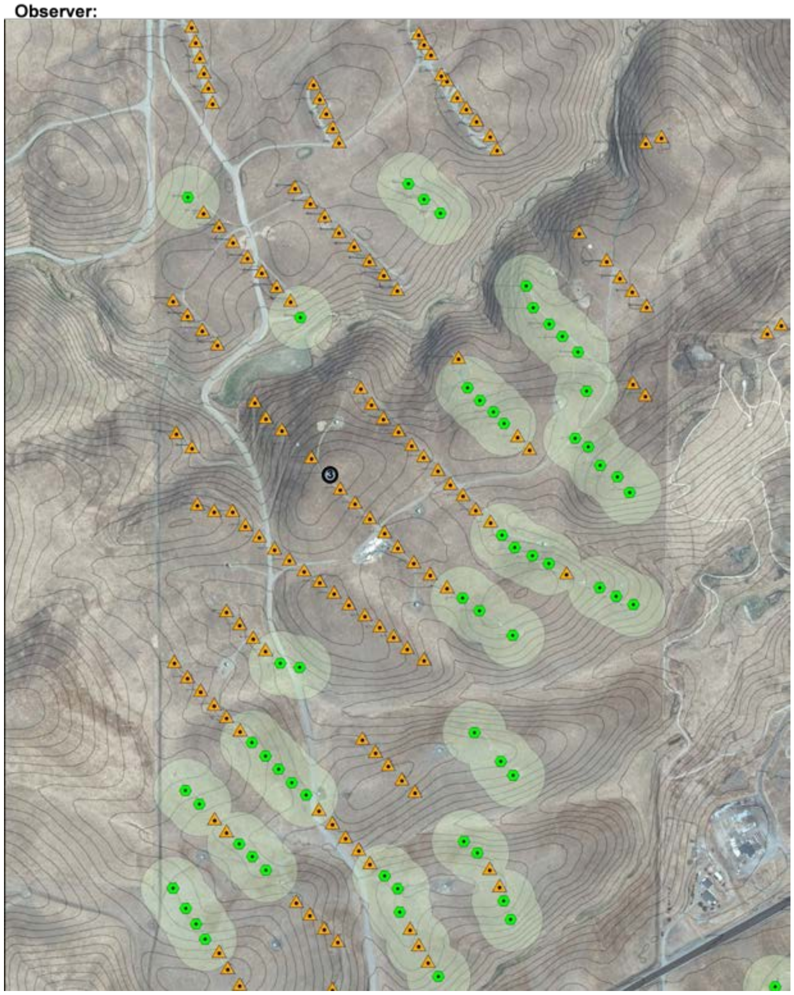

Orange triangles and green circles denote wind turbines, and highlighted polygons represent fatality search areas; these were intended to help the observer prioritize survey focus whenever too many animals present at once divided attention.